

NASA TECHNICAL
REPORT



NASA TR R-324

2.1

NASA TR R-324



LOAN COPY: RETURN TO
AFWL (WOL-2)
KIRTLAND AFB, N MEX

A SIMPLIFIED MOLECULAR MODEL FOR
STUDYING VIBRATION-DISSOCIATION
COUPLING IN FLUID FLOWS

by *Walter Albert Reinhardt*

Ames Research Center

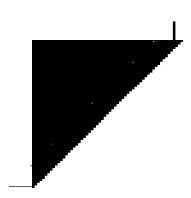
Moffett Field, Calif.



0068388

1. Report No. NASA TR R-324		2. Government Accession No.		3. Recipient's Catalog No.	
4. Title and Subtitle A SIMPLIFIED MOLECULAR MODEL FOR STUDYING VIBRATION- DISSOCIATION COUPLING IN FLUID FLOW		5. Report Date September 1969		6. Performing Organization Code	
		7. Author(s) Walter Albert Reinhardt		8. Performing Organization Report No. A-3277	
9. Performing Organization Name and Address NASA Ames Research Center Stanford University Moffett Field, Calif. 94035 and Stanford, Calif. 94303		10. Work Unit No. 129-01-01-05		11. Contract or Grant No.	
		12. Sponsoring Agency Name and Address National Aeronautics and Space Administration Washington, D.C. 20546		13. Type of Report and Period Covered Technical Report	
15. Supplementary Notes		14. Sponsoring Agency Code			
16. Abstract <p>A simplified mathematical model is derived that is useful for studying the effects of vibration-dissociation coupling in fluid flows. The derivation is based on an energy-moment procedure for simplifying the master equations. To obtain the model equations it is assumed that the vibrational energy can be approximated by the introduction of two vibrational temperatures. The effects of molecular anharmonicity are also accounted for in an approximate manner. The parameters contained within the equations are evaluated by making comparisons with experimental data. It is shown that the model contains the minimum required structure allowing favorable agreement with existing experimental data. Numerical solutions are given for the quasi-steady zone behind a normal shock wave, for the complete structure of a shock wave, and for nozzle flow. The results provide the appropriate pre-exponential temperature dependence of the effective dissociation rate, yield an induction time before dissociation is observed, and, in the case of expanding flow, yield one-fourth less effective relaxation time than the Landau-Teller theory. The thermodynamic quantities for the vibrational mode (partition function, internal energy, and specific heat) agree accurately with like quantities evaluated from spectroscopic data. By the introduction of appropriate assumptions it is shown that the equations reduce to a form identical to the Marrone-Treanor model except for a "truncation factor." When the vibrational temperatures are not large, the model is identical to that of Landau and Teller. The numerical procedure used to integrate the system of rate and flow equations is also described.</p>					
17. Key Words Suggested by Author(s) Molecular relaxation Vibration-dissociation coupling Nonequilibrium flow Collision rates Oxygen			18. Distribution Statement Unclassified - Unlimited		
19. Security Classif. (of this report) Unclassified	20. Security Classif. (of this page) Unclassified	21. No. of Pages 336	22. Price* \$3.00		

*For sale by the Clearinghouse for Federal Scientific and Technical Information
Springfield, Virginia 22151



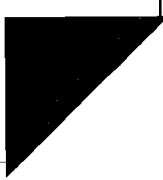
11/11/2020

SUMMARY

A simplified mathematical model is derived that is useful for studying the effects of vibration-dissociation coupling in fluid flows. The derivation is based on an energy-moment procedure for simplifying the master equations. The formalism yields a final set of rate equations that are similar in many respects to those of Marrone and Treanor. Instead of a single temperature for the vibrational energy mode, however, two vibrational temperatures are defined, one for the distribution in the lower vibrational states and one for the upper states. In this way the perturbing effect of dissociation and recombination on the vibrational energy states is approximately accounted for. Also included are the effects of molecular anharmonicity, both as regards the energy-level spacing and the collisional transition rates. Such effects require determination of the "rate of quantum transfer" occurring as a result of molecular collisions, which is approximated by means of linear relations. The rate equations that result contain the necessary modification of the Landau-Teller theory to account for anharmonic effects. The effects of dissociation and recombination are treated by a procedure similar to that used by Marrone and Treanor, except that only vibrationally excited molecules are allowed to dissociate. The thermodynamic quantities associated with the vibrational energy mode are derived, and it is shown that the procedure for considering the effects of anharmonicity results in relations that agree favorably with the more accurate quantities obtained from spectroscopically determined values of the vibrational energies.

The parameters of the model equations are evaluated by comparison of the pre-exponential temperature dependence of the effective dissociation rate with experimental results. For this comparison, analytical solutions are obtained that apply in the quasi-steady zone behind a normal shock wave. The effect of altering certain parameters is also discussed.

Complete numerical solutions of the model equations are then given for the flow behind a steady-shock wave and for nozzle flow. The shock structure is discussed in detail including the effects of the various terms that comprise the



rate equations. The transient, quasi-steady, and final relaxation zones, that have been described by previous researchers, are displayed; and the relaxation effects peculiar to the different zones are pointed out. Values of the induction time, during which the effects of dissociation are not observed, are found and compared with experimentally obtained delay times. The values obtained from the calculations are an order of magnitude too large, and the readjustments of the assigned parameters that would improve the agreement are indicated.

The nozzle solution is discussed in detail, and the effects of the various terms in the model rate equations are again described. It is shown that the characteristic vibrational relaxation time that results in the case of near equilibrium flow is about $1/4$ of that given by Landau-Teller theory and is in qualitative agreement with recent experimental data. However, such reductions of the vibrational relaxation time, resulting from consideration of molecular anharmonicity effects, are realized only if freezing occurs near the throat when the translational and vibrational temperatures are large.

The equations introduced in this paper contain the minimum structure allowing agreement with presently available experimental data. The formalism is sufficiently general that additional structure can be included as more refined experimental measurements become available.

The numerical procedure used to integrate the system of rate and flow equations is also described.

FOREWORD

This report is based on a dissertation submitted to the Department of Aeronautics and Astronautics, Stanford University in May 1969 as partial fulfillment of the requirements for the Ph.D. degree. The author was a member of the staff of Ames Research Center while working at Stanford and gratefully appreciates the valuable guidance and encouragement furnished by his faculty advisor, Professor Walter G. Vincenti, during the investigation covering this report. The author is also grateful to Dr. Charles E. Treanor, formerly a Visiting Professor at Stanford and presently head of the Aerodynamic Research Department, Cornell Aeronautical Laboratory, Inc., Buffalo, N.Y., for suggesting the research problem and for continued interest and helpful consultation. The work was further assisted by discussions with Dr. Barrett S. Baldwin, Jr., of Ames Research Center regarding the basic theory and with Harvard Lomax and Dr. Harry E. Bailey, also from Ames, regarding the numerical integration. Valuable criticism resulted from a review of the manuscript by Professor Morton Mitchner of Stanford. The work also benefited from the author's participation in a graduate research seminar supported at Stanford University by the U.S. Air Force Office of Scientific Research under Contracts AF49(638)-1280 and F44620-69-C-0006.

In view of the extensive nature of the thesis the version being published by NASA is substantially in the original form even though some deviation from the standard NASA format occurs.

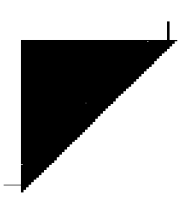


TABLE OF CONTENTS

	Page
LIST OF TABLES	vii
LIST OF ILLUSTRATIONS	viii
NOMENCLATURE	xv
I INTRODUCTION	1
II DERIVATION OF THE VIBRATION-DISSOCIATION MODEL EQUATIONS	11
II-A. Introductory Comments	11
II-B. Development of the Equations	18
II-B-1. T-V Energy Interchange, Multiple Transitions	19
II-B-1a. Zeroth Moment Equations	19
II-B-1b. First Energy Moment Equations	23
II-B-1c. Vibrational Temperatures	27
II-B-2. T-V Energy Interchange, Stepwise Transitions	32
II-B-3. Dissociation	53
II-B-4. Combined Effect of Vibrational Excitation and Dissociation	57
II-C. The Rate Equations Applicable to Fluid-Flow Problems	65
III SPECIAL SOLUTIONS OF THE MODEL EQUATIONS	73
III-A. Introductory Comments	74
III-B. Quasi-Steady State in a Dissociation Experiment	76
IV COMPLETE SOLUTIONS OF THE MODEL EQUATIONS	114
IV-A. Introductory Comments	114
IV-B. Normal-Shock Wave Solutions	116
IV-B-1. Shock Wave Structure	118
IV-B-2. The Incubation Time	167
IV-C. Nozzle Flow	173
IV-C-1. Example Solution	173
IV-C-2. Estimate of the Characteristic Vibrational Relaxation Time Applicable for Nozzle Flows	192
V RÉSUMÉ	197
APPENDIX A. THERMODYNAMIC QUANTITIES	199
A-1. General Relations	199
A-2. Derivation of the Relations for the Vibrational Mode	203
A-2a. Partial Vibrational Partition Functions	208
A-2b. Partial Vibrational Energy Functions	212
A-2c. Partial Vibrational Specific Heats	219

TABLE OF CONTENTS (Continued)

	Page
APPENDIX B. VIBRATIONAL TRANSITION RATES	223
B-1. Transition Rates, Analytical Form	223
B-2. Approximating the Transition Rates	230
APPENDIX C. PREFERENTIAL DISSOCIATION MODEL OF MARRONE AND TREANOR	251
APPENDIX D. A STUDY OF THE EFFECT OF THE TRUNCATION FACTOR; PROBLEM OF UNCOUPLED VIBRATIONAL RELAXATION	257
APPENDIX E. DEVELOPMENT OF THE NUMERICAL PROCEDURE FOR SOLVING THE MODEL AND FLUID-FLOW EQUATIONS	266
E-1. Introductory Comments	266
E-2. Fluid-Flow Equations.	267
E-3. Review of the Numerical Integration Methods	271
APPENDIX F. EXPLICIT FORMULATION OF THE FLOW EQUATIONS.	291
APPENDIX G. PHYSICAL CONSTANTS AND OTHER REQUIRED PARAMETERS.	300
REFERENCES.	303

LIST OF TABLES

Number		Page
II-1	Table of Formula Numbers of Quantities Contained in the Rate Equations.	69
III-1	Parameters Associated with the Quasi-Steady Solutions, Figures III-1 through III-12	86
IV-1	Parameters Associated with Complete Solutions, Figures IV-1 through IV-7.	117
D-1	Comparison of Characteristic 90 Percent Relaxation Time . . .	259
D-2	Comparison of Characteristic 90 Percent Relaxation Time . . .	260
G-1	Energy Units Conversion Factors	302

LIST OF ILLUSTRATIONS

Figure		Page
II-1	Schematic representation of the intermolecular potential of an anharmonic oscillator molecule	13
II-2	Diagram of the molecular distribution of energy states at some point behind a normal-shock wave	15
II-3	Diagram showing mesh points in a two-dimensional coordinate space where one coordinate is the vibrational quantum number and the other coordinate is the number of steps involved during a vibrational transition	21
III-1	Variables obtained from quasi-steady solution versus temperature (associated parameters are listed along first row table III-1)	
III-1a	Dimensionless vibrational temperatures	91
III-1b	Vibrational coupling factor	91
III-1c	Pre-exponential factor	92
III-2	Variables obtained from quasi-steady solution versus temperature (associated parameters are listed along second row of table III-1)	
III-2a	Dimensionless vibrational temperatures	93
III-2b	Vibrational coupling factor	93
III-2c	Pre-exponential factor	94
III-3	Variables obtained from quasi-steady solution versus temperature (associated parameters are listed along third row of table III-1)	
III-3a	Dimensionless vibrational temperatures	95
III-3b	Vibrational coupling factor	95
III-3c	Pre-exponential factor	96
III-4	Variables obtained from quasi-steady solution versus temperature (associated parameters are listed along fourth row of table III-1)	
III-4a	Dimensionless vibrational temperatures	97
III-4b	Vibrational coupling factor	97
III-4c	Pre-exponential factor	98

LIST OF ILLUSTRATIONS (Continued)

Figure		Page
III-5	Variables obtained from quasi-steady solution versus temperature (associated parameters are listed along fifth row of table III-1)	
III-5a	Dimensionless vibrational temperatures	99
III-5b	Vibrational coupling factor	99
III-5c	Pre-exponential factor	100
III-6	Variables obtained from quasi-steady solution versus temperature (associated parameters are listed along sixth row of table III-1)	
III-6a	Dimensionless vibrational temperatures	101
III-6b	Vibrational coupling factor	101
III-6c	Pre-exponential factor	102
III-7	Variables obtained from quasi-steady solution versus temperature (associated parameters are listed along seventh row of table III-1)	
III-7a	Dimensionless vibrational temperatures	103
III-7b	Vibrational coupling factor	103
III-7c	Pre-exponential factor	104
III-8	Variables obtained from quasi-steady solution versus temperature (associated parameters are listed along eighth row of table III-1)	
III-8a	Dimensionless vibrational temperatures	105
III-8b	Vibrational coupling factor	105
III-8c	Pre-exponential factor	106
III-9	Variables obtained from quasi-steady solution versus temperature (associated parameters are listed along ninth row of table III-1)	
III-9a	Dimensionless vibrational temperatures	107
III-9b	Vibrational coupling factor	107
III-9c	Pre-exponential factor	108

LIST OF ILLUSTRATIONS (Continued)

Figure		Page
III-10	Variables obtained from quasi-steady solution versus temperature (associated parameters are listed along tenth row of table III-1)	
III-10a	Dimensionless vibrational temperatures	109
III-10b	Vibrational coupling factor	109
III-10c	Pre-exponential factor	110
III-11	Vibrational coupling factor obtained from quasi-steady solution versus temperature T_U (associated parameters are listed along eleventh row of table III-1)	
III-11a	Relatively rapid vibrational relaxation time	111
III-11b	"Correct" characteristic vibrational relaxation time	111
III-12	Variables obtained from quasi-steady solution versus temperature (associated parameters are listed along twelfth row of table III-1)	
III-12a	Dimensionless vibrational temperatures	112
III-12b	Vibrational coupling factor	112
III-12c	Pre-exponential factor	113
IV-1	Variables obtained from shock solution versus adjusted laboratory time (associated parameters are listed along first row of table IV-1)	
IV-1a	Temperatures	119
IV-1b	Concentrations	120
IV-1c	Concentration, lower states and molecular	121
IV-1d	Vibrational coupling factor	122
IV-1e	Derivative, $Q^{\bar{y}A}$, and component terms, $Q_i^{\bar{y}A}$	127
IV-1f	Derivative, $Q^{\bar{y}a}$, and component terms, $Q_i^{\bar{y}a}$	129
IV-1g	Derivative, $Q^{\bar{y}B}$, and component terms, $Q_i^{\bar{y}B}$	130
IV-1h	Derivative, Q^{TA} , and component terms, Q_i^{TA}	132
IV-1i	Derivative, Q^{TB} , and component terms, Q_i^{TB}	135

LIST OF ILLUSTRATIONS (Continued)

Figure		Page
IV-2	Variables obtained from shock solution versus adjusted laboratory time (associated parameters are listed along second row of table IV-1)	
IV-2a	Temperatures.	138
IV-2b	Concentrations	139
IV-2c	Concentration, lower states.	140
IV-3	Variables obtained from shock solution versus adjusted laboratory time (associated parameters are listed along third row of table IV-1)	
IV-3a	Temperatures.	142
IV-3b	Concentrations	143
IV-3c	Concentration, lower states and molecular.	144
IV-3d	Vibrational coupling factor	145
IV-4	Variables obtained from shock solution versus adjusted laboratory time (associated parameters are listed along fourth row of table IV-1)	
IV-4a	Temperatures.	146
IV-4b	Concentrations	147
IV-4c	Concentration, lower states.	148
IV-5	Variables obtained from shock solution versus adjusted laboratory time (associated parameters are listed along fifth row of table IV-1)	
IV-5a	Temperatures.	150
IV-5b	Concentrations	151
IV-5c	Concentration, lower states and molecular.	152
IV-5d	Vibrational coupling factor	153
IV-6	Variables obtained from shock solutions versus adjusted laboratory time (associated parameters are listed along sixth row of table IV-1)	
IV-6a	Temperatures.	154
IV-6b	Concentrations	155
IV-6c	Concentration, lower states.	156
IV-6d	Vibrational coupling factor	157

LIST OF ILLUSTRATIONS (Continued)

Figure		Page
IV-7	Variables obtained from shock solutions versus adjusted laboratory time (associated parameters are listed along seventh row of table IV-1)	
IV-7a	Temperatures.	158
IV-7b	Concentrations	159
IV-7c	Concentration, lower states and molecular.	160
IV-7d	Vibrational coupling factor	161
IV-7e	Derivative, $\bar{Q}^{\bar{Y}A}$, and component terms, $\bar{Q}_i^{\bar{Y}A}$	162
IV-7f	Derivative, $\bar{Q}^{\bar{Y}a}$, and component terms, $\bar{Q}_i^{\bar{Y}a}$	163
IV-7g	Derivative, $\bar{Q}^{\bar{Y}B}$, and component terms, $\bar{Q}_i^{\bar{Y}B}$	164
IV-7h	Derivative, Q^{TA} , and component terms, Q_i^{TA}	165
IV-7i	Derivative, Q^{TB} , and component terms, Q_i^{TB}	166
IV-8	Induction time computed using two different methods and compared with experimental data of Wray	169
IV-9	Variables obtained from nozzle solution versus distance measured from the throat (associated parameters are the same as listed for figure IV-5)	
IV-9a	Temperatures.	175
IV-9b	Concentrations	176
IV-9c	Concentration, lower states and molecular.	177
IV-9d	Dimensionless static pressure.	179
IV-9e	Dimensionless static density.	180
IV-9f	Velocity.	181
IV-9g	Vibrational coupling factor	183
IV-9h	Derivative, $\bar{Q}^{\bar{Y}A}$, and component terms, $\bar{Q}_i^{\bar{Y}A}$	184
IV-9i	Derivative, $\bar{Q}^{\bar{Y}a}$, and component terms, $\bar{Q}_i^{\bar{Y}a}$	185
IV-9j	Derivative, $\bar{Q}^{\bar{Y}B}$, and component terms, $\bar{Q}_i^{\bar{Y}B}$	186
IV-9k	Derivative, Q^{TA} , and component terms, Q_i^{TA}	187
IV-9l	Derivative, Q^{TB} , and component terms, Q_i^{TB}	190

LIST OF ILLUSTRATIONS (Continued)

Figure		Page
IV-10	Anharmonicity effects from model equations compared with Landau-Teller theory, characteristic vibrational relaxation time.	195
A-1	Diagram showing relative placement of vibrational energy levels for model as compared to anharmonic-oscillator molecules	206
A-2	Comparison of vibrational partition function computed using different models	211
A-3	Dimensionless plot of the component factors required for the model vibrational energy function	215
A-4	Comparison of the vibrational energy function computed using different models	218
A-5	Comparison of the vibrational specific heat computed using different models	222
B-1	Plot showing relative deviation of the rate anharmonicity coefficients computed using different adiabaticity factors.	229
B-2	Approximation scheme for including anharmonic effects	232
B-3	Comparison of the vibrational energy level computed by different methods that yields a maximum "rate of vibrational quantum transfer".	237
B-4	Comparison of the "rate-of-quantum-transfer quantity," (χ_R)	
B-4a	$T = \Theta_{A_1}$	238
B-4b	$T = 2\Theta_{A_1}$	239
B-4c	$T = 5\Theta_{A_1}$	240
B-4d	$T = 10\Theta_{A_1}$	241
B-5	Comparison of the "rate-of-quantum-transfer" quantity, (χ_F)	
B-5a	$T = \Theta_{A_1}$	244
B-5b	$T = 2\Theta_{A_1}$	245
B-5c	$T = 5\Theta_{A_1}$	246
B-5d	$T = 10\Theta_{A_1}$	247

LIST OF ILLUSTRATIONS (Continued)

Figure		Page
B-6	Plots of the parameter $\chi(T)$ versus temperature	248
D-1	Comparison of relaxation behavior for case of uncoupled vibrational relaxation where a representative number of vibrational energy states are included	
D-1a	$T = 8,000$ °K	261
D-1b	$T = 12,000$ °K	262
D-1c	$T = 16,000$ °K	263
D-2	Comparison of relaxation behavior for uncoupled vibrational relaxation where only a portion of the vibrational energy states are included	
D-2a	$T = 8,000$ °K	264
D-2b	$T = 16,000$ °K	265
E-1	Parameters characterizing the numerical aspects of shock wave solutions versus adjusted shock passage time (associated model parameters are listed along first row of table IV-1)	
E-1a	Eigenvalues, λ	282
E-1b	$ \lambda_{\min} h $	283
E-1c	$ \lambda_{\max} h $	284
E-2	Parameters characterizing the numerical aspects of shock wave solutions versus adjusted shock passage time (associated model parameters are listed along the sixth row of table IV-1)	
E-2a	Eigenvalues, λ	285
E-2b	$ \lambda_{\min} h $	286
E-2c	$ \lambda_{\max} h $	287
E-3	Parameters characterizing the numerical aspects of nozzle solutions versus distance along nozzle (associated model parameters are those of figure IV-5)	
E-3a	Eigenvalues, λ	288
E-3b	$ \lambda_{\max} h $	289
E-3c	$ \lambda_{\min} h $	290



NOMENCLATURE

$A(x)$	streamtube cross-sectional area
a	integer representing the separation between the lower widely spaced vibrational energy levels having relatively long relaxation times and the upper narrowly spaced energy levels having shorter relaxation times
a_j	number of atoms in the j -th species ($a_j = 2$ when j signifies molecules; $j = 1$ for atoms) (eq. (A2d))
$a_{i,j}$	elements of the Jacobian matrix $\frac{\partial F_i}{\partial w_j}$ (eq. (E15))
B^*	coefficient matrix of the derivatives of the dependent variable vector (eq. (E8) or (F1))
b	integer representing the separation point between the vibrational energy levels having a temperature T_A and the energy levels having a temperature T_B
C_1	constant coefficient in the relation for the characteristic vibrational relaxation time (see eq. (III-11b))
C_2	constant in the characteristic vibrational relaxation time (see eq. (III-12))
$c_{p_j}(T)$	specific heat at constant pressure associated with j -th species (energy/mole-°K)
$c_{p_{i,j}}(T)$	specific heat at constant pressure associated with i -th energy mode and j -th species (energy/mole-°K)
$c_{v_{i,j}}(T)$	specific heat at constant volume associated with i -th energy mode and j -th species (energy/mole-°K)
E_v	energy associated with the v -th vibrational quantum level
E_{b-1}	energy associated with the level just below that level separating the vibrational levels having a temperature T_A and those having a temperature T_B

E_i	energy separating quantum levels of model molecule ($i = A_1, A_2, \text{ or } B$), see Appendix A
$E_{i,j}$	energy separating quantum levels i and j (eq. (B1d))
$e_{i,j}(T)$	internal energy associated with i -th mode and j -th species (energy/mole)
$e_j(T)$	internal energy associated with j -th species (energy/mole)
e	total specific energy (energy/mass)
F_i	element of vector of derivatives (Appendix E and F)
$f(\omega\tau)$	adiabaticity factor (eq. (B4))
$f(n,m)$	steric factor associated with collisions involving particles n and m (eq. (C4))
$G(T,\nu;x_0)$	factor accounting for effects of anharmonicity on the transition rates (eq. (B1a))
$g_{l,j}$	degeneracy associated with l -th quantum level and j -th species (eq. (A1d))
$g_{\nu+l,\nu}$	g -function (eq. (II-9))
h	specific enthalpy (energy/mass)
\hbar	Planck's constant divided by 2π
$h_{i,j}$	partial enthalpy associated with i -th internal energy mode and j -th species (energy/mole)
h_j°	"heat of formation" associated with j -th species (energy/mole)
I	unit matrix
I_j	moment of inertia for j -th species (mass \times length ²)
k	Boltzmann constant
$k_{1,0}^{(1)}$	transition rate associated with the vibrational transitions from the first to the zeroth energy level (see eq. (B16))

$k_{1,0}^{(2)}$	special "equivalent" transition rate associated with the upper vibrational energy levels where $k_{1,0}^{(2)} = k_{1,0}^{(1)} \chi(T)$ (see Appendix B and in particular eqs. (B14) or (B23))
$k_F^{(1)}(T_A, T)$	forward transition rate associated with the vibration-translation interactions yielding vibrational states denoted B (see eqs. (II-35b) or (II-39b))(cm ³ /mole-sec)
$k_R^{(1)}(T_B, T)$	reverse transition rate associated with the vibration-translation interactions yielding vibrational states denoted A (see eqs. (II-35a) or (II-39a))(cm ³ /mole-sec)
$k_{F\text{eq.}}(T)$	"equilibrium" dissociation rate constant (eqs. (III-13) or (C10)) (cm ³ /mole-sec)
$k_{1,j}^{l,m}$	transition rate associated with the vibrational transitions $i \rightarrow j$ and $l \rightarrow m$ that follow as a result of a bimolecular collision (cm ³ /mole-sec)
$\mathcal{L}_i(T)$	truncation factor (i refers to specific grouping of energy levels) (see, e.g., eq. (A29)) (dimensionless)
$\mathcal{E}_i(T)$	truncation factor associated with vibrational specific heat (i has same meaning as in \mathcal{L}_i) (eq. (A46)) (dimensionless)
m_j	mass of j -th species (g)
m	$m = \sum n_i$ total particle concentration $p = mkT$
N	first unbound vibrational energy level (dissociation limit)
N_0	Avagadro's number
n	molecular density (molecules/unit vol.)
n_a	atom density
n_i	density of species i (particles/unit vol.)
p_i	probability that a dissociation occurs from i -th level (eq. (C1))
p	pressure

$Q_{ij}(T)$	partition function for the i -th internal energy mode, j -th species (eq. (A1))
$Q_j(T)$	$Q_j(T) = \prod_{i=1} Q_i(T)$ partition function of the j -th species, (eq. (A1))
$Q^j = \sum_l Q_l^j$	rate of production of quantity j per unit length along a streamline (eq. (IV-7))
$q_i^\infty(T)$	vibrational energy of harmonic oscillators having an infinite number of energy levels separated by a spacing that is identical to that of the grouping of energy levels denoted i (energy/mole), (see, e.g., eq. (A28))
$q_i(T)$	vibrational energy associated with the grouping of levels denoted i (energy/mole) (see, e.g., eq. (A30))
R_0	universal gas constant
R	gas constant per unit mass, $\sum_i (\gamma_i)_0 R_0$
S_{ij}	elements of scaling matrix (eq. (E23))
s_j	entropy associated with j -th species (energy/mole-°K) (eq. (A7))
s	specific entropy (energy/mass -°K)
s	arbitrary independent integration variable (eq. (E9))
T	gas temperature (or transitional or kinetic temperature), (°K)
T_i	$i = A$ or B , vibrational temperature of lower or upper states, respectively, (°K)
T_F	characteristic "vibrational temperature" at which energy is removed by dissociation (eq. (C7)), (°K)
T_U	measure of how rapidly dissociation drops off for the lower vibrational levels in the preferential dissociation model (eq. (C4)) (°K)
t	time

$V(T_B, T)$	vibrational coupling factor (eq. (II-93) and (C10))
V	volume of some arbitrary element
v	fluid velocity
w_i	element of the vector of variables (Appendix E and F)
x	distance measured along streamline
x_0	anharmonicity coefficient associated with the quadratic term of the vibrational energy (eq. (A10b))
y_0	anharmonicity coefficient associated with the cubic term of the vibrational energy (eq. (A10b))
$z(n, m)$	bimolecular collision rate associated with collision involving particles m and n (eq. (B3b))
Z	compressibility factor (see eq. (E3b) and discussion)
α_F, α_R	dimensionless constant (eqs. (B10a) and (B18a))
β	reducing factor, dimensionless constant (eq. (IV-8))
β_{ij}	difference of stoichiometric coefficients (eq. (A8d))
γ_i	concentration of species i in units of moles per unit total mass (eq. (II-108a))
Δ	anharmonicity parameter 2, $aE_{A_1} (1 - \delta) + (E_{A_2} - E_{A_1})$ (eq. (II-73a))
δ	anharmonicity parameter 1, $\delta = \chi^{-1}(T)$ (eq. (II-73b))
$\epsilon_i(\gamma_i, T)$	specific value of vibrational energy (energy/mass) of species i (eq. (II-108b))
Θ_{b-1}	characteristic temperature of the $b-1$ vibrational energy level (E_{b-1}/k)
Θ_i	characteristic temperature associated with energy of separation of model molecule ($i = A_1, A_2, \text{ or } B$), $\Theta_i = E_i/k$

$\Theta_{E_{l,\ell,j}}$	characteristic electronic excitation temperature ($^{\circ}\text{K}$) of the l -th electronic energy level and the j -th species, $\frac{E_{ch}}{k}$ (A1d)
$\Theta_{R,j}$	characteristic rotation temperature, $\frac{\sigma_j \hbar^2}{2I_j k}$ (eq. A1c)
$\kappa_B(T)$	partial equilibrium constant (eq. (C12))
$\kappa_i(T)$	equilibrium constant associated with j -th species (eq. (A8))
λ	eigenvalue (see Appendix E)
μ_{ij}	reduced mass of a pair of particles i and j
ν_{ij}, ν'_{ij}	stoichiometric coefficient of the i -th reaction and j -th species (unprimed are reactants and primed are products)
φ_0	dimensionless parameter (eq. (B8))
ρ	mass density
σ	scaling constant (eq. (E9))
τ	effective collision time (see discussion following eq. (B3F))
τ_i	vibrational relaxation time associated with i -th grouping of vibrational energy levels $\tau_i = \left\{ m \hat{k}_{1,0}^{(i)} \left[1 - \exp\left(-\frac{E_i}{kT}\right) \right] \right\}^{-1}$ (eq. (B25))
$\chi(T)$	parameter related to the slope of "rate of quantum transfer" (eqs. (B14c) and (B23) (dimensionless))
Ω	measure of the deviation from local thermodynamic equilibrium of the vibrational energy mode (eqs. (II-96, II-97))
ω_0	angular frequency associated with the spacing $E_{1,0}$ (see discussion following eq. (B3f))

Subscripts

A, A_1, A_2, B	specific groupings of vibrational energy states (see Appendix A)
D	dissociation

E_l	electronic excitation mode
R	rotational mode
T	translational mode
T-V	translation-vibration energy interchange
V	vibrational mode
V-V	vibration-vibration energy interchange
o	"low temperature" value
1	initial value

Superscripts and Special Symbols

t	transpose (vector or matrix), see Appendixes E and F
*	all energy modes except the vibrational mode (see Appendix E)
*	value of a dependent variable as determined in quasi-steady zone
'	relevant quantities (partition function, energy, specific heat, etc.) associated with a grouping of vibrational levels are evaluated relative to the separate lowest energy state and not the molecular ground energy state (see, e.g., Appendix A)
\wedge	units of per particle (this superscript is removed by multiplying by Avagadro's number)
[]	matrix or vector
— (bar)	average
— (bar)	natural logarithm (when placed over the concentration variables γ_i)

CHAPTER 1

INTRODUCTION

The purpose of this work is to develop a relatively simple mathematical model that is useful for studying the effects of vibration-dissociation coupling in fluid flows. The work may be viewed as a logical continuation of the sequence of papers by Hammerling, Teare, and Kivel (36), Treanor and Marrone (90, 91, 93), and Marrone and Treanor (58). In each of these cases an effort was made to devise a model containing the smallest possible number of parameters that would yield results in agreement with existing experimental data. Such a model would be of value for extrapolation of rate processes beyond the temperatures and densities accessible to laboratory evaluation. Of equal importance, the resulting formalism would lend itself readily to fluid-flow calculations. The model presented here is analogous in many respects to those introduced in the aforementioned papers, although more complex. The theory is applicable to polyatomic species (see, e.g., (41a)), but only diatomic species are considered here. The rotational mode is taken to be in equilibrium with the translational (kinetic-energy) mode and only the lowest molecular electronic states are considered. However, instead of the single vibrational temperature considered in the previous papers (36, 58, 90, 91, 93), two independent vibrational temperatures are used to allow for the perturbing effects of dissociation and recombination in the upper levels. Also, the reduced energy-level spacing of the upper levels is approximately accounted for as well as the anharmonic oscillator rates associated with these levels.

Historically, the subject of energy exchange between external degrees of freedom (translation) and "internal" degrees of freedom (rotation, vibration, dissociation, electronic excitation, ionization) has received considerable attention. In addition to the intrinsic interest the subject commands, it is significant in the general field of chemical kinetics and has an important bearing on many gas-dynamical and combustion problems. Recently an increasing interest in gas lasers has added impetus to the need for understanding the mechanisms of

molecular energy exchange (33, 42, 60). Theoretical treatment of the problem is impeded by the complexity arising from the large number of interacting particles. During a collision a molecule in a given energy state (specified translational, rotational, vibrational, and electronic coordinates) may undergo a transition to one of many possible final states. A satisfactory theoretical treatment must necessarily consider the likelihood and importance of all of these transitions (4, 5, 34, 56). Considerable research, both theoretical and experimental, has been carried out on this subject, involving many specialized studies on rate constants and collision or relaxation mechanisms. However, important as the prior research is, a comprehensive survey of all the significant papers that contribute to an understanding of the complete problem and that would be helpful in placing the present work in perspective will not be attempted. Instead the reader is referred to the books by Vincenti and Kruger (97), Clarke and McChesney (22) (an excellent source for a review of prior research), Stupochenko et al. (86), Bradley (10), and Zel'dovich and Raizer (100). Herzberg and Litovitz (41), Cottrell and McCoubrey (23), and Nikitin (64) are also excellent sources for an understanding of rates and relaxation mechanisms. Although a fully comprehensive survey will not be given, it is worthwhile to discuss briefly a few papers that are closely related and contribute to the underlying ideas of the specific approach adopted here.

Previously developed schemes for finding first-energy-moment "summed" relations of the population equations and thus obtaining the simple relaxation equation

$$\frac{dq^\infty(T_V)}{dt} = \frac{q^\infty(T) - q^\infty(T_V)}{\tau(T,p)} \quad (I-1)$$

are basic to the model to be introduced here. In this relation q^∞ is the average vibrational energy (per mole), a known function of the temperature T or T_V , and $\tau(T,p)$ is a characteristic relaxation time that depends on temperature and pressure. The equation describes vibrational relaxation in the absence of dissociation and is often referred to as the Landau-Teller or the Bethe-Teller relaxation model. Landau and Teller (49) were the first to observe that, providing

the vibrational transition rates vary linearly with vibrational quantum number, as do those for a harmonic oscillator (46, 49), a rate equation can be derived from the first-energy-moment relations that contains only the single characteristic relaxation time τ . Later Bethe and Teller (8) identified the summation quantities that appear in the equation as the thermodynamic quantity $q^{\infty*}$. The basic equations used were the population or "master" equations which express the rate of change of the population of each energy state. Imbedded in the Landau-Teller or Bethe-Teller approach are the following assumptions: (1) the vibrational transitions occur step-wise from one vibrational energy level to the next adjacent level ("ladder climbing"); (2) vibrational transition rates vary linearly with vibrational quantum number; (3) the energy levels are equally spaced; and (4) the molecular population over the various vibrational energy states is Boltzmann and thus describable in terms of a single parameter, the vibrational temperature T_V .

The Landau-Teller relaxation equation is a remarkably simple result considering the internal processes that it describes. The question arises as to how accurately the actual physical processes are represented. In studies by Rubin and Shuler (75, 76) and Montroll and Shuler (62), assumptions (1), (2) and (3) were imposed and for the case of oscillators subjected to an impulsive change in heat-bath temperature, a solution of the complete set of master equations was obtained. It was shown that, for molecules having a Boltzmann distribution initially, relaxation occurs through a continuous sequence of Boltzmann distributions. These results add validity to the Landau-Teller theory. Early experimental studies using shock-tubes (e.g., Camac (20), Cottrell and McCoubrey (23), Losev and Osipov (56) have also yielded results in excellent agreement with the simple theory. However, more exact theoretical studies including the effects of molecular anharmonicity (Bazley et al. (6), Osipov and Stupochenko (67), Bray (15, 16), and Nikitin (65)) suggest that at higher temperatures relaxation occurs with a

*Landau and Teller (49) applied the relaxation equation to the acoustic problem of sound dispersion in gases. Later Bethe and Teller (8) used the equation for studying vibrational relaxation behind shock waves.

smaller characteristic relaxation time. These studies tend to support the validity of the vibrational temperature concept (that is, a Boltzmann distribution of vibrational energy). More recent experimental studies of flow in nozzles also indicate a departure from the Landau-Teller relaxation model (1, 2, 43, 44, 45, 61, 78, 79, 80). Additional complication enters the problem when the molecular concentration can no longer be considered dilute (74). One must then include the effects of vibration-vibration (V-V) energy interchange (15, 16, 66, 74, 88, 92, 92a, 101), which also lead to departures from simple relaxation theory (15, 16).

On the basis of the foregoing studies it may be concluded that the Landau-Teller relaxation model (8, 49) accurately represents the processes occurring only when the upper vibrational states are not appreciably populated. When large populations of the upper states exist, modification of the theory is required to account for nonuniform energy-level spacing (4) and nonlinear vibrational transition rates (24, 37, 39, 65, 73). The major simplifying feature that the prior studies suggest might remain valid is the concept of a single vibrational temperature, that is, population according to a Boltzmann distribution (62, 81, 82, 83, 84).

When the effects of dissociation and recombination can no longer be neglected, additional complication is introduced. The simple Landau-Teller theory for vibrational relaxation no longer applies, since chemical effects by their very nature suggest a significant population of the upper states. These effects also have a perturbing influence on the population distribution, yielding other than Boltzmann distributions. If the characteristic time required to populate the upper energy states is comparable to or greater than the time required for dissociation, vibrational relaxation will also have an appreciable effect on the rates of dissociation (vibration-dissociation coupling) (Wray (99) and Rice (72a, 72b)). Finally, the possibility of coupling of both dissociation and vibrational excitation with rotational excitation should be considered (Bauer (3) and Bauer and Tsang (4)).

The foregoing complications, not accounted for by the Landau-Teller theory, are summarized in the following list:

- (1) Molecular anharmonicity
 - (a) nonuniformity of the vibrational energy-level spacing

- (b) nonlinear vibrational transition rates
- (c) multiple-level transitions
- (2) Non-Boltzmann population distributions
- (3) Vibration-rotation energy interchange
- (4) For nondilute molecular mixtures the effects of vibration-vibration energy interchange

and, in addition, the chemical effects that occur according to the following mechanisms:

- (5) Dissociation via vibrational excitation
- (6) Dissociation via rotational excitation
- (7) Recombination occurring preferentially into the upper vibrational and rotational levels.

Varied approaches have been adopted in theoretical studies of dissociation rates and of the transition probabilities that appear in the master equations. The variational theory of reaction rates utilizes the basic assumption that a reactive system can be described by the motion of a representative point in the phase space of the system (Keck (47)). The procedure requires the computation of "trajectories" of these points to determine the net rate at which the representative points pass through a particular surface in the phase space. By this method Snider (85)* obtained values of the effective dissociation and recombination rates for the quasi-steady zone behind a normal shock wave (for a description of this zone see Chapters III and IV), and showed that the ratio of these rates is the chemical equilibrium constant. In this work, Snider considered all effects in the above list except multiple-level transitions (1c). In an independent study, Treanor (94) obtained similar results. Montroll and Shuler (62a) considered the problem of dissociation as a one-dimensional random walk (through the vibrational energy levels) with an absorption barrier (dissociation). The rate of activation is related to the mean passage time of the "walker." In other studies (Keck and Carrier (48) and Brau et al. (12)), the investigators introduced

*The paper by Snider (85) also contains an excellent summary of prior research results, in particular, as applied to dissociation and recombination studies.

a diffusion analogy for the master equations (effects (1a, b), (2), (5) and (7) were accounted for). Vibrational excitation with eventual dissociation is thereby explained in terms of energy diffusion through the vibrational energy states. The conclusions arrived at by this method are similar to those of the studies described above. These investigations relate primarily to the processes associated with dissociation. Benson and Fueno (7) using a deactivation theory, obtained results applicable for the inverse process of recombination.

The above investigations have contributed to an understanding of the observed temperature dependence of experimentally determined rates, as well as indicating the types of population distributions to be expected. It is significant that deviations from a Boltzmann distribution are found primarily in the uppermost vibrational energy levels, where the influence of dissociation or recombination is greatest (see, e.g., 11, 12, 13, 48, 84, 94). These studies have been confined, for the most part, to the quasi-steady zone where the fractional molecular population in each vibrational energy state is constant and as a result solutions are relatively easy to obtain. In this situation integration of the complete set of rate equations is not required.

Few solutions are available for the more difficult problem of integration of the complete set of master equations. Difficulties encountered in this task are well known (18, 29, 77). The importance of such solutions, aside from providing a description of the entire relaxation process, is in obtaining values for the "incubation" or "induction" time behind a normal-shock wave (11, 12, 13, 58), which is the time required to populate the upper vibrational energy levels, observed experimentally as a delay prior to the onset of dissociation (99). To explain this phenomenon, a manifestation of coupling of vibration and dissociation, Marrone and Treanor (58) introduced a relatively simple set of relations that were an outgrowth of equations used by previous researchers (36). The resulting formalism may be considered an extension of the Landau-Teller model, since the basic structure of "vibrational relaxation" follows Landau-Teller theory and additional terms are included to account for the effects of dissociation and recombination.

Despite its simplicity the Marrone-Treanor model contains most of the essential elements of vibration-dissociation coupling and has been widely used (27, 31, 32, 35, 41a, 57, 87, 89, also see discussion in 86). Their model is based on the assumption that the vibrational degrees of freedom may be represented by a single vibrational temperature. Dissociation preferentially from the upper vibrational levels is presumed, the dissociation probability being weighted in such a manner that it decreases exponentially for the lower energy levels (see Appendix C). The weighting factor contains a parameter that can be varied. As previously mentioned, the term that describes vibrational relaxation in the equations is formally identical to that of the Landau-Teller or Bethe-Teller model but involves different variables. In one version a truncated harmonic oscillator was used as a basis for defining the temperature dependence of the quantity q^∞ (93). Alternatively, q^∞ was based on the actual vibrational energies obtained from spectra (58). The "effective rate of dissociation" that results from their model contains a "vibrational coupling factor" that depends on the vibrational as well as the translational temperature. This factor is responsible for a delay in dissociation behind a normal shock wave. Thus the solutions for such flows do exhibit an incubation time prior to the onset of appreciable dissociation. Treanor and Marrone (90) suggest that their model is not completely satisfactory in that a strong temperature dependence occurs for the pre-exponential factor in the effective dissociation rate and this is not observed experimentally. Also, allowance is not made for other complications given in the earlier listing. In particular, nonlinear transition probabilities, deviations from a Boltzmann distribution, and rotational effects were not considered, although it is possible that an implicit inclusion of these effects may occur depending on the choice of parameters.

In the present work the Marrone-Treanor model is generalized to include effects (1) and (2), that is, the effects of molecular anharmonicity and a non-Boltzmann distribution. This is done formally by starting with the master equations and using a procedure similar to that of Bethe and Teller (8). Rotational effects are not explicitly included. The formalism is sufficiently general,

however, that later inclusion of these effects may be possible when the associated rate parameters are better understood. The method follows, in principle, a suggestion by Carrington (21): "in systems of many levels, it may be useful to combine some levels into groups, and calculate average transition probabilities between groups. It may be that the difficulties of interpretation connected with the significance of the averages will be less than the difficulties caused by insufficient quantity or accuracy of the data in the system with the full number of levels." In the spirit of these remarks an effort has been made to hold to a minimum the number of parameters that are to be evaluated from experimental data.

In Chapter II the model equations are derived by means of an energy-moment procedure operating on the master equations. It is shown that by separating the complete set of vibrational energy levels into two sub-groups and assigning a separate vibrational temperature to each sub-group, the complete set of master equations is reduced to a set of only four equations. The "reduced" equations are a complete set and are still general in that they include the effects of multi-level vibrational transitions. However, as in previous investigations (7, 8, 12, 48, 49, 73, 75), the generalization is not continued throughout the paper because explicit representations for the various rate parameters are not available.

In the later sections of Chapter II it is shown that further simplification of the equations can be made. An additional independent separation of the vibrational energy levels is introduced, below which the energy-level spacings are large and the transition rates small relative to the corresponding quantities above the separation. The procedure for evaluating these quantities is discussed in Appendix B. Essentially, the procedure involves consideration of the "rate of quantum transfer" resulting from molecular collisions. This quantity is evaluated and approximated by linear segments. Such a procedure allows an extension of the Landau-Teller theory in a systematic manner to include the effects of anharmonicity. The thermodynamic quantities associated with the vibrational mode are evaluated in Appendix A and it is shown that, with the method used to approximate the effects of anharmonicity, accurate evaluations of the

thermodynamic quantities result (partition function, energy, and specific heat). In the final section of Chapter II the dissociation and recombination terms are introduced. These terms are treated in a manner similar to that of Marrone and Treanor in that preferential dissociation is presumed. Only vibrationally excited molecules that belong to the "upper group" of vibrational energy states are allowed to dissociate. The model equations that result are listed at the end of the chapter. These equations are not greatly different in their outward appearance from those used by Marrone and Treanor (58). The major difference, aside from the appearance of two vibrational temperatures and the inclusion of anharmonic effects, is in the vibrational relaxation term. It is shown that the proper inclusion of the effects of truncation results in a term that is the same as the Landau-Teller relaxation equation except for a truncation factor. This factor is important when the vibrational temperatures are large. An interesting feature of the model equations is that they reduce to the Landau-Teller equation when the vibrational temperatures are not large.

At this stage the model equations contain parameters that must be evaluated. In Chapter III tentative values of the parameters are assigned and solutions obtained for the quasi-steady zone behind a normal-shock wave. An iterative numerical procedure is developed for this purpose. A unique determination of all parameters does not result from this investigation but several general statements can be made. It is shown that when the level that separates the regions of different vibrational temperatures is placed about midway up the vibrational-energy well, a highly preferential dissociation is required to achieve the proper pre-exponential temperature dependence of the effective dissociation rate. Separations lying above the midpoint energy yield results in disagreement with experiment.

In Chapter IV numerical solutions of the model equations coupled with the equations of flow are presented. For flow behind a normal-shock wave, it is shown that the midpoint separation of vibrational energy states yields induction times that are about a factor of ten too large compared with experimental results. It is concluded from this investigation that readjustments of the tentatively

chosen point of separation as well as other parameters of the model are required for agreement. In later sections of Chapter IV the model equations are investigated as applied to nozzle flow. It is shown that the characteristic vibrational relaxation time that the theory gives for such flows is qualitatively consistent with recent experimental results in that it is smaller by a factor of about $1/4$ as compared with results from Landau-Teller theory. Such reductions in the characteristic vibrational relaxation time, however, are realized only when freezing occurs at high vibrational temperatures.

It should be emphasized that consideration of the complete set of master equations is complex and numerical solutions difficult to obtain (18, 77). A primary motive behind this investigation was the attainment of a smaller set of equations that retains the essential mechanisms of the complete set. The solutions demonstrate that the system obtained here can readily be solved numerically in conjunction with the flow equations. A numerical procedure developed by Lomax and Bailey (53) was found to be of great value for this purpose. Application of the method to the present problem is explained in Appendix E.

CHAPTER II

DERIVATION OF THE VIBRATION-DISSOCIATION MODEL EQUATIONS

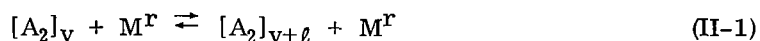
In this chapter the basic equations required for a study of the effects of vibration-dissociation coupling will be introduced. It will then be shown in a formal manner how this rather large number of basic equations may be reduced to obtain a set of only four "model" equations. The formalism requires separating the vibrational energy states into two groupings and then assigning a vibrational temperature to each group. The resulting system of equations still contains the effects of multiple transitions. In single-step transitions (vibrational "ladder climbing" model) it is also demonstrated how one may include the effects of anharmonicity by introducing additional separations in the vibrational energy states and still retain the relative simplicity of a Landau-Teller approach (8,49) as regards the form of the equations.

In the first sections of the chapter only vibrational transitions not leading to dissociation are considered. Later the effects of dissociation are added and at the end of the chapter the equations to be studied further in the subsequent chapters are listed.

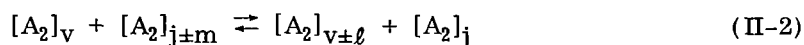
II-A. Introductory Comments

The mechanisms of vibrational energy interchange with translation (abbreviated T-V), of vibrational-vibrational energy exchange (V-V), and of dissociation (D) may be described by the following chemical equations:

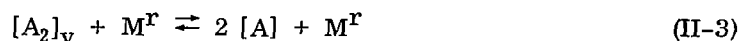
translation-vibration



vibration-vibration



dissociation



The symbol $[A_2]_v$ denotes a molecule (anharmonic oscillator) in the v th vibrational energy state; $[A]$ symbolizes the atoms obtained by dissociation of the molecules $[A_2]$; and M^r represents some species, specifically designated by the superscript r (r may denote atoms, molecules, or some chemically inert species, e.g., argon), that gains or loses kinetic energy and momentum during the reaction. Electronic states are excluded from the above description and it is assumed in the work that follows that any effect produced by electronically excited molecules may be assumed negligibly small. Such an assumption is perhaps not always valid, depending, of course, on the gas temperatures encountered. Taylor (87) and Brau (13) have shown that the electronic states have some effect on vibration and dissociation, particularly at high temperatures, but that the effect is not large.

To facilitate the description of the model a sketch showing the intermolecular potential of an arbitrary molecule is presented in figure II-1. The various levels, numbered on the right-hand side of the potential curve, are the vibrational energy states attainable by the molecule. The lowest level is the zeroth state and the $(N-1)$ th corresponds to the uppermost bound energy state. The N th level defines the dissociation threshold and the dissociation energy. A molecule having vibrational energy exceeding this limit will have dissociated becoming a pair of atoms. In the model to be introduced the assumption is made that the vibrational energy states can be separated into two groups, a lower and an upper, designated by the letters A and B, respectively, as shown on the sketch. The separation is indicated by the dashed line between the levels b and $b-1$. Once this separation is made, it is further assumed that the distribution of energy in each individual group is Boltzmann and hence expressible in terms of parameters that are characterized as the vibrational temperatures of the separate groups. Further, only the B-molecules will be allowed to dissociate. Additional assumptions are also included that are not severe so far as the construction of the model is concerned, but are introduced in order to retain a form of the resulting equations that contains the fewest parameters possible. These assumptions are as follows:

1. Dissociation occurs preferentially from the B states, that is, dissociation from the higher levels is exponentially weighted over those from

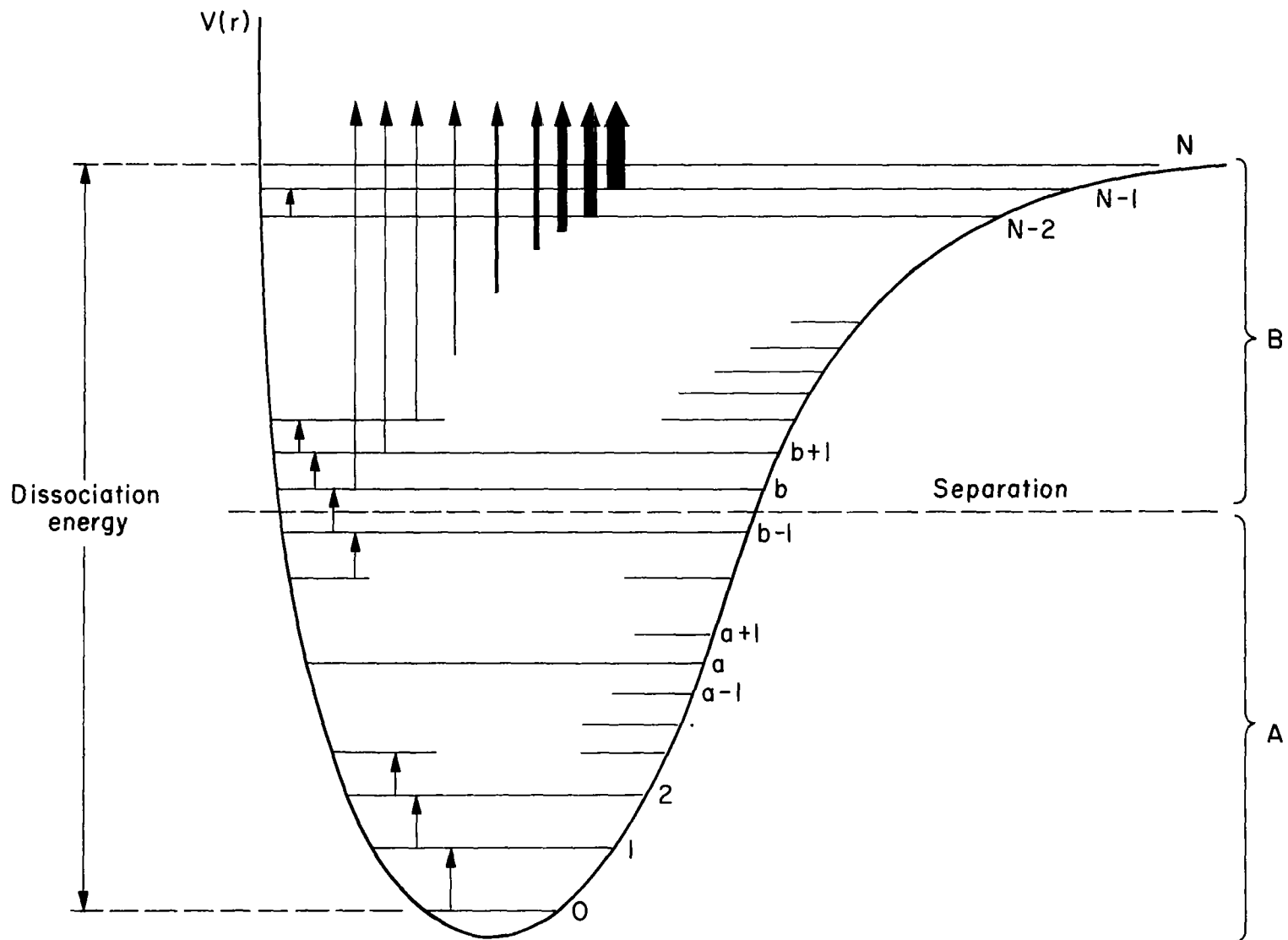


Figure II-1. Schematic representation of the intermolecular potential of an anharmonic oscillator molecule

the lower levels (Marrone and Treanor (58)). This is indicated by the arrows that are broadened as their length decreases.

2. The effect of anharmonicity is accounted for by introducing another separation parameter a . The energy levels are taken to be equally spaced above and below this level and the rates used are harmonic-oscillator rate relations that vary linearly in terms of the vibrational level number. The spacing for the levels above the separation, however, is much reduced and the associated rates much greater than the corresponding quantities below the separation (see Appendix A and B).

In applying the second assumption the effect of anharmonicity is actually accounted for by approximating the "rate of quantum transfer" (see Appendix B), which occurs as a result of vibration-translation energy interchange, with linear relations. In this thesis the approximation is carried out only for the case of "stepwise" transitions and with only two linear relations.

The significance of the separation b , the boundary between groups A and B, is exemplified further in figure II-2. If one were to plot an actual population distribution, represented by the ratio n_v/n , in terms of a parameter Θ_v , defined by the equation

$$n_v/n = \exp(-E_v/k\Theta_v) \quad (\text{II-4})$$

for some arbitrary point in the region behind a normal shock wave (Treanor (94), and Keck and Carrier (48)), one would obtain the continuous curve drawn in the figure. The ratio n_v/n represents the fractional population of molecules having energy associated with the v th vibrational energy state. The significance of the parameter Θ_v is that, in terms of this parameter, a Boltzmann distribution would be represented by a horizontal line. The continuous curve in figure II-2 illustrates the fact that the mechanism of dissociation perturbs the actual distribution from being Boltzmann (48, 84, 94). The model approximates the actual non-Boltzmann distribution by two Boltzmann distributions that are described by the upper and lower vibrational temperatures, T_A and T_B , respectively.

The separations a and b will allow for a generalization of Landau-Teller theory to include, respectively, the effects of anharmonicity and the effects of non-Boltzmann-like population distributions. The assignment of values to these

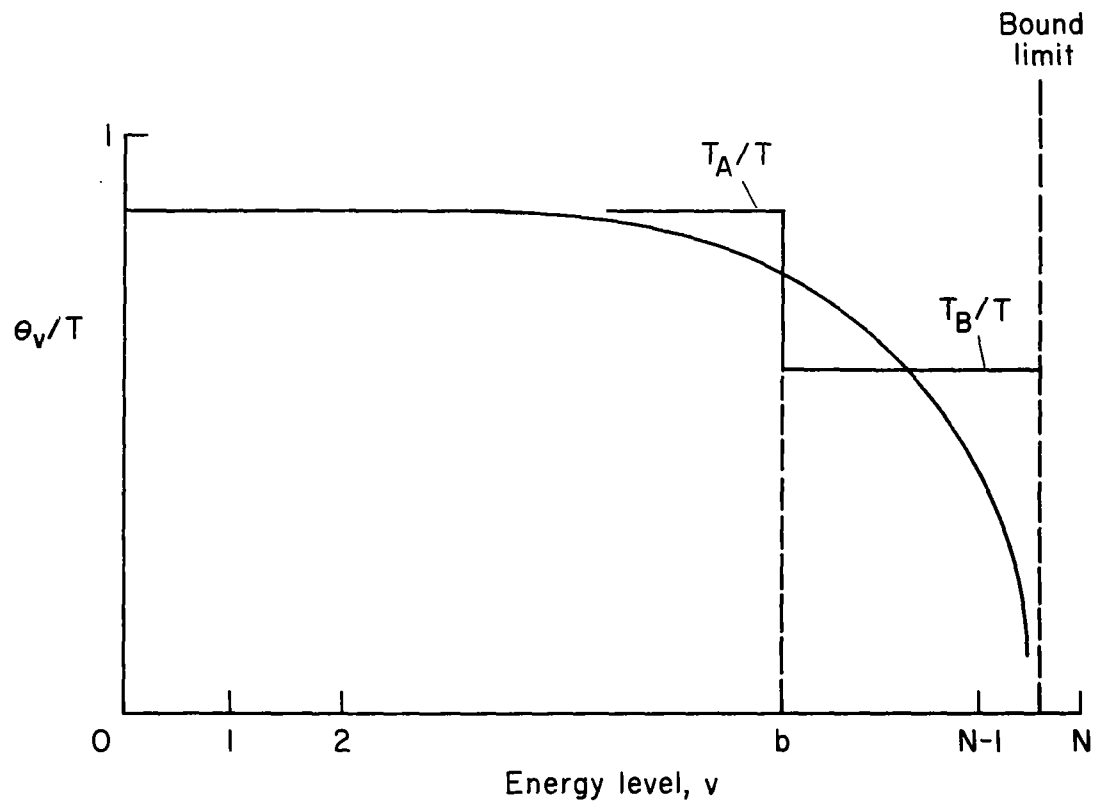


Figure II-2. Diagram of the molecular distribution of energy states at some point behind a normal-shock wave



quantities is the subject of the later chapters and it suffices to state now that the b-level separation will always have a value that exceeds or at least is equal to that of the a-level separation; that is, $0 < a \leq b < N$.

The equations for the model are obtained in a manner analogous to that used by Heims (38) in that energy-moment equations of the population distribution are derived. The procedure deviates from Heims' since the form of the population distribution among the vibrational energy states is assumed and hence not as many moment relations are required in order to obtain a complete set of equations. The zeroth-moment equations denote the number of molecules in the lower and upper energy groups (i.e., groups A and B), and the first-moment equations give the average vibrational energy per diatomic molecule for each group. Four nonlinear ordinary differential equations thus result to describe the model molecule.

The basic equations from which the model equations will be derived are described in what follows. The general equations that represent the net population gain or loss per unit time and volume for molecules in the v th vibrational energy state (commonly referred to as the "master equations") are given by the sum of the following partial contributions. The contributions follow according to the interaction processes described, respectively, by the chemical equations (II-1) through (II-3).

$$\left[\frac{dn_v}{dt} \right]_{T-V} = \sum_{r=1}^S m_r \left\{ \sum_{\ell=1}^{N-v-1} \hat{k}_{v+\ell, v}^r \left[n_{v+\ell} - n_v \exp\left(-\frac{E_{v+\ell} - E_v}{kT}\right) \right] - \sum_{\ell=1}^v \hat{k}_{v, v-\ell}^r \left[n_v - n_{v-\ell} \exp\left(-\frac{E_v - E_{v-\ell}}{kT}\right) \right] \right\} \quad (\text{II-5})$$

$$\left[\frac{dn_v}{dt} \right]_{V-V} = \sum_{j=0}^{N-1} \sum_{\ell=1}^{N-v-1} \sum_{m=1}^{N-j-1} \hat{k}_{v+\ell, v}^{j, j+m} \left[n_{v+\ell} n_j - n_v n_{j+m} \exp\left(-\frac{E_{v+\ell} - E_v}{kT} + \frac{E_{j+m} - E_j}{kT}\right) \right] - \sum_{j=0}^{N-1} \sum_{\ell=1}^{v \neq 0} \sum_{m=1}^{N-1-j} \hat{k}_{v, v-\ell}^{j, j+m} \left[n_v n_j - n_{v-\ell} n_{j+m} \exp\left(-\frac{E_v - E_{v-\ell}}{kT} + \frac{E_{j+m} - E_j}{kT}\right) \right] + (\text{equivalent terms with } m=-1, \dots, -j \neq 0) \quad (\text{II-6})$$

$$\left[\frac{dn_v}{dt} \right]_D = \sum_{r=1}^S \left[-\hat{k}_{v,N}^r n_v m_r + \hat{k}_{N,v}^r n_a^2 m_r \right] \quad (\text{II-7})$$

where

$$v = 0, 1, \dots, N - 1$$

and

- m net number density of collision partners ($m = \sum_{r=1}^S m_r$)
- m_r number density of collision partner of kind r
- n_a number of atoms per unit volume
- $\hat{k}_{i,j}^r$ probability per second per unit concentration of oscillators that a collision with species r will result in the vibrational transition from state i to state j
- $\hat{k}_{i,j}^{\ell,k}$ probability per second per unit concentration of oscillators that a collision of a molecule in the i th state with another molecule in the ℓ th state results in the transitions $i \rightarrow j, \ell \rightarrow k$, respectively
- $\hat{k}_{v,N}^r$ probability per second per unit concentration of oscillators that a collision of a molecule in the v th vibrational state with a species of kind r results in dissociation
- $\hat{k}_{N,v}^r$ probability per second per unit squared concentration of atoms that a pair of atoms as a result of a three-body collision with the third body being the species of the kind r results in a molecule in the v th state
- E_v vibrational energy of a molecule in the v th state ($= E_0 v(1 - x_0 v + y_0 v^2)$, see e.g., Herzberg (40))
- T translational or gas-kinetic temperature.

One notes that equations (II-5) and (II-6) involve vibrational transitions between bound states only. The terms in the summation over ℓ in equation (II-5), and over ℓ and m in equation (II-6) represent the contributions due to one-step transitions, two-step transitions, and so on. These equations are thus general in that they include all possible transitions between vibrational energy states. The solution of the set of equations given by

$$\frac{dn_v}{dt} = \left[\frac{dn_v}{dt} \right]_{T-V} + \left[\frac{dn_v}{dt} \right]_{V-V} + \left[\frac{dn_v}{dt} \right]_D \quad (\text{II-8})$$

$$v = 0, 1, \dots, N - 1$$

coupled with the fluid-dynamic equations and the atom-conservation equation, would constitute, in principle, a solution of the complete problem of vibration-dissociation coupling. As will be pointed out later, such solutions are difficult to obtain even numerically (18,77) and have questionable value since the required transition probabilities have uncertain values.

The most often practiced procedure in studies of such equations is to:

- (1) Assume that only single-step transitions are important (although dissociation may still involve a multistep transition), and thus only the first terms in the sums over ℓ in equation (II-5) are retained;
- (2) Consider only problems in which the molecular concentration is sufficiently small in a medium containing a high relative concentration of inert diluent that the nonlinear vibration-vibration exchange reactions (eq. (II-6)) may be neglected.

These restrictions are generally valid (Rich and Rehm, 74). In the analysis that follows, however, the first condition will not be applied immediately in order to increase the generality of the equations that are derived, but will be applied later for the system of equations that are solved. The second restriction will be adopted since only relatively dilute molecular systems are considered in this thesis on the grounds that the inclusion of equations (II-6) make the resulting equations too complex for this study.

In the derivations that follow, each term in equation (II-8), representing equations (II-5) and (II-7) (excluding the term subscripted V-V), will be investigated separately. On the basis of the declared assumptions these terms will be simplified and the equations that result, containing few parameters, will then be the equations for the model.

II-B. Development of the Equations

It will be very helpful for the analysis that follows to make the notation more compact by introducing a function $g_{v+l,v}^r$, defined as follows:

$$g_{v+l,v}^r = m_r \hat{k}_{v+l,v}^r \left[n_{v+l} - n_v \exp\left(-\frac{E_{v+l} - E_v}{kT}\right) \right] \quad (\text{II-9a})$$

$$= m_r \left[\hat{k}_{v+l,v}^r n_{v+l} - \hat{k}_{v,v+l}^r n_v \right] \quad (\text{II-9b})$$

This function denotes the net rate of change of the population density of the v th state as a result of transitions to and from the $(v + \ell)$ th state when these transitions occur from translation-vibration energy interchange involving a species of kind r . Further, to avoid a cumbersome notation that is not immediately relevant to the derivations, the effect of the superscript r will be ignored initially. The effect of r can be neglected here since: (1) the kind of collision partner causing the vibrational excitation affects the equations in a linear manner. The final equations may be readjusted to include r simply by superposition of the resulting equations (i.e., by reinserting the superscript and reintroducing the summation over r); (2) only dilute molecular mixtures are of interest in this study; the effects of considering other than the diluent species (e.g., argon) as the collision partner will be small.

The introduction of the g -function greatly simplifies the notation required for equations (II-5). Substituting appropriate values for the subscripts in the relation given for the g -function above, we obtain the following simple form:

$$\left[\frac{dn_v}{dt} \right]_{T-V} = \sum_{\ell=1}^{N-v-1} g_{v+\ell,v} - \sum_{\ell=1}^v g_{v,v-\ell} \quad (\text{II-10})$$

(II-B-1). T-V Energy Interchange, Multiple Transitions.

(II-B-1a). Zeroth Moment Equations

We now seek a relation that represents the net rate of change of the total number of molecules in the A-group of energy states. This is easily done by summing equation (II-10) for all the vibrational levels, v , such that $0 \leq v \leq b - 1$. The equation that results, called the zeroth energy-moment equation for A-states, is

$$\left[\frac{dn_A}{dt} \right]_{T-V} = \sum_{v=0}^{b-1} \sum_{\ell=1}^{N-v-1} g_{v+\ell,v} - \sum_{v=1}^{b-1} \sum_{\ell=1}^v g_{v,v-\ell} \quad (\text{II-11})$$

where

$$n_A = \sum_{v=0}^{b-1} n_v \quad (\text{II-12})$$

Certain elements in the second double summation on the right-hand side of equation (II-11) may be combined with terms in the first double sum. The procedure for combining these terms may be more easily followed after introduction of figure II-3. Each mesh point in this figure represents a pair of coordinates in a two-dimensional coordinate space in which one coordinate represents the vibrational quantum number and the other denotes the number of steps involved in a transition. It should be pointed out that transitions involving the points in the triangular region above the line $v = N - \ell - 1$ are not allowed in (T-V)-type reactions since the transitions associated with such points would involve dissociation. Such reactions are contained in equations (II-7). The mesh points in the crosshatched region correspond to transitions that result in a crossing of the separation boundary between the states $b-1$ and b , shown in figure II-1. The first term on the right-hand side of equation (II-11) is a double summation involving the g -function evaluated at each mesh point in the closed region ABCDA. The second sum includes values of g at each point in the region EFDE. We now rewrite equation (II-11) to obtain an expression having summations with identical arguments so that the g -functions can be related. This is done by noting that each element in the first sum is to the left of the boundary defined by the line $v = N - \ell - 1$ and each element in the second sum is above the line $v = \ell$. Equation (II-11) may then be written

$$\left[\frac{dn_A}{dt} \right]_{T-V} = \sum_{\ell=1}^{N-b} \sum_{v=0}^{b-1} g_{v+\ell, v} + \sum_{\ell=N-b+1}^{N-1} \sum_{v=0}^{N-\ell+1} g_{v+\ell, v} - \sum_{\ell=1}^{b-1} \sum_{v=\ell}^{b-1} g_{v, v-\ell} \quad (\text{II-13})$$

The subscripts and summing interval on the third term may be altered without affecting the sum to give

$$\text{third term} = \sum_{\ell=1}^{b-1} \sum_{v=0}^{b-\ell-1} g_{v+\ell, v} \quad (\text{II-14})$$

We now observe that the various double sums involve the same argument, and we may therefore combine the appropriate individual terms. This will be shown graphically. We recall that terms one and two are double sums involving $g_{v+\ell, v}$ evaluated at points in the region ABCDA. However, the third term involves the

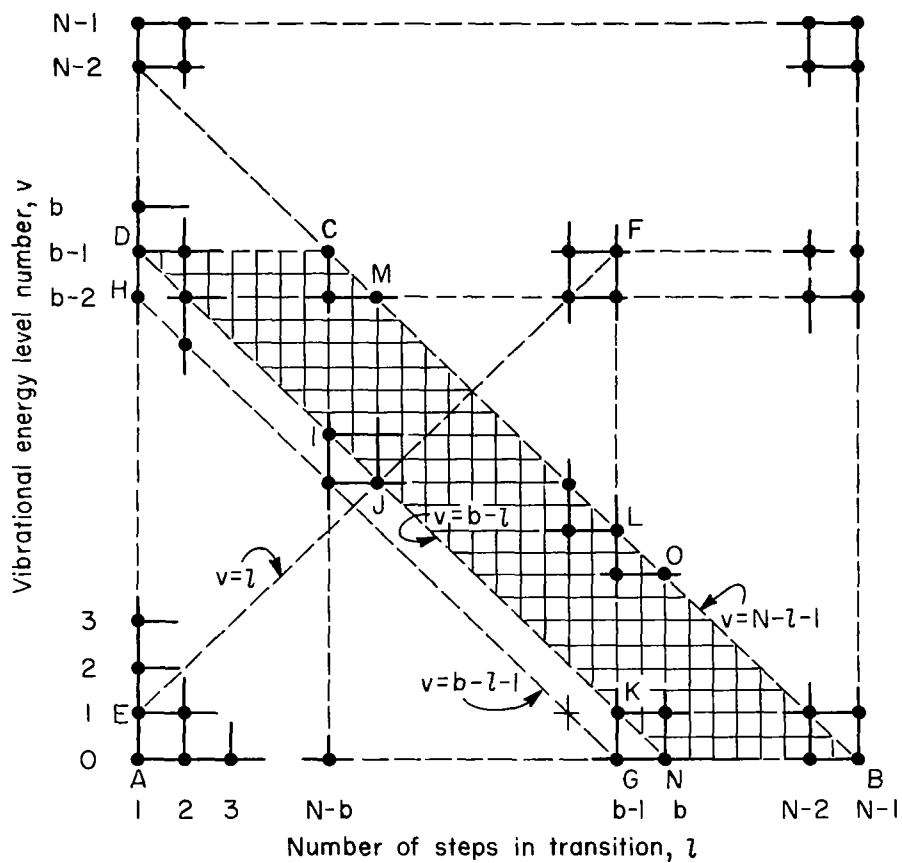


Figure II-3. Diagram showing mesh points in a two-dimensional coordinate space where one coordinate is the vibrational quantum number and the other coordinate is the number of steps involved during a vibrational transition

same g -function, but evaluated at each point in the region AGHA. We may subtract these common terms and the terms that remain are those values of $g_{v+l,v}$ for each point between the pairs of lines $v = b-l$ and $v = N-l-1$, but below $v = b-1$, that is, the points shown in the crosshatched region in figure II-3.

Equation (II-13) thus becomes

$$\begin{aligned} \left[\frac{dn_A}{dt} \right]_{T-V} &= \sum_{\ell=1}^{N-b} \sum_{v=b-\ell}^{b-1} g_{v+\ell,v} + \sum_{\ell=N-b+1}^b \sum_{v=b-\ell}^{N-\ell-1} g_{v+\ell,v} \\ &+ \sum_{\ell=b+1}^{N-1} \sum_{v=0}^{N-\ell-1} g_{v+\ell,v} \end{aligned} \quad (\text{II-15})$$

where the first term involves the mesh points in the region DICD, the second in JKLMJ, and the third in NBON. Equation (II-15) may also be more compactly written as

$$\begin{aligned} \left[\frac{dn_A}{dt} \right]_{T-V} &= \sum_{v=0}^{b-1} \sum_{\ell=b-v}^{N-v-1} g_{v+\ell,v} \\ &= \sum_{v=0}^{b-1} \sum_{\ell=b}^{N-1} g_{\ell,v} \end{aligned} \quad (\text{II-16})$$

The significance of equation (II-15) is seen if a few of the terms involved in the summations are displayed:

$$\begin{aligned} \left[\frac{dn_A}{dt} \right]_{T-V} &= \underbrace{g_{b,b-1}}_{1 \text{ step}} + \underbrace{(g_{b+1,b-1} + g_{b,b-2})}_{2 \text{ step}} \\ &+ \underbrace{(g_{b+2,b-1} + g_{b+1,b-2} + g_{b,b-3})}_{3 \text{ step}} + \dots \end{aligned} \quad (\text{II-17})$$

Each term represents the loss (or gain) in the total number of molecules in the A-group of levels as a result of the transitions, one-step, two-step, and so on, that cross the separation b . Although equations (II-15) and (II-16) are equivalent, the first expression, equation (II-15), involving the sum over ℓ , is more advantageous in practice since the terms are ordered in a monotonic sequence

of decreasing values, that is, as ℓ increases, each succeeding term is less than the preceding term (see, e.g., 24, 37, 39). The series converges so rapidly that in most cases only the first term is important.

The equivalent sum representing the net rate of change of the total number of molecules with energy in the B-group of states is also readily obtained. As noted previously, equations (II-10) (or (II-15)) exclude transitions that result in dissociation. It then follows that the T-V interactions conserve the number of molecules; that is,

$$\frac{d}{dt} \left[\sum_{v=0}^{N-1} n_v \right]_{T-V} = 0 \quad (\text{II-18})$$

This identity may also be proved by summing equation (II-10) for all v in the range $0 \leq v \leq N-1$. From this equation it follows that

$$\begin{aligned} \left[\frac{dn_B}{dt} \right]_{T-V} &= - \left[\frac{dn_A}{dt} \right]_{T-V} \\ &= - \sum_{\ell=1}^{N-b} \sum_{v=b-\ell}^{b-1} g_{v+\ell, v} - \sum_{\ell=N-b-1}^b \sum_{v=b-\ell}^{N-\ell-1} g_{v+\ell, v} \\ &\quad - \sum_{\ell=b+1}^{N-\ell} \sum_{v=0}^{N-\ell-1} g_{v+\ell, v} \end{aligned} \quad (\text{II-19})$$

or

$$\left[\frac{dn_B}{dt} \right]_{T-V} = - \sum_{v=0}^{b-1} \sum_{\ell=b}^{N-1} g_{\ell, v} \quad (\text{II-20})$$

where

$$n_B = \sum_{v=b}^{N-1} n_v \quad (\text{II-21})$$

(II-B-1b). First Energy-Moment Equations

The differential equations that yield the change in the net vibrational energy (first-moment equations) for both the lower and the upper vibrational energy states are also required. These are obtained by first multiplying each equation

of the set of equations (II-10) by the energy associated with the respective level, E_v ; the resulting equations are then summed over all the levels associated with the particular group.

Thus for the A-states we obtain

$$\frac{d}{dt} \left[\sum_{v=0}^{b-1} E_v n_v \right]_{T-V} = \sum_{v=0}^{b-1} \sum_{\ell=1}^{N-v-1} E_v g_{v+\ell, v} - \sum_{v=0}^{b-1} \sum_{\ell=1}^v E_v g_{v, v-\ell} \quad (\text{II-22})$$

The order of the summations is now interchanged and requires that one keep track of the regions involved within the summations. We introduce the expression equivalent to equation (II-14) but appropriate to the above equation, and there results

$$\begin{aligned} \frac{d}{dt} \left[\sum_{v=0}^{b-1} E_v n_v \right]_{T-V} &= \sum_{\ell=1}^{b-1} \sum_{v=0}^{b-\ell-1} E_v g_{v+\ell, v} + \sum_{\ell=1}^{N-b} \sum_{v=b-\ell}^{b-1} E_v g_{v+\ell, v} \\ &+ \sum_{\ell=N-b-1}^b \sum_{v=b-\ell}^{N-\ell-1} E_v g_{v+\ell, v} + \sum_{\ell=b+1}^{N-1} \sum_{v=0}^{N-\ell-1} E_v g_{v+\ell, v} \\ &- \sum_{\ell=1}^{b-1} \sum_{v=0}^{b-\ell-1} E_{v+\ell} g_{v+\ell, v} \end{aligned} \quad (\text{II-23})$$

The first and last terms can be combined and equation (II-23) becomes

$$\begin{aligned} \frac{d}{dt} \left[\sum_{v=0}^{b-1} E_v n_v \right]_{T-V} &= \sum_{\ell=1}^{b-1} \sum_{v=0}^{b-\ell-1} (E_v - E_{v+\ell}) g_{v+\ell, v} \\ &+ \sum_{\ell=1}^{N-b} \sum_{v=b-\ell}^{b-1} E_v g_{v+\ell, v} + \sum_{\ell=N-b+1}^b \sum_{v=b-\ell}^{N-\ell-1} E_v g_{v+\ell, v} \\ &+ \sum_{\ell=b+1}^{N-1} \sum_{v=0}^{N-\ell-1} E_v g_{v+\ell, v} \end{aligned} \quad (\text{II-24})$$

Interchanging the order of summation and combining the last two terms, we obtain the simpler-appearing equation

$$\begin{aligned} \frac{d}{dt} \left[\sum_{v=0}^{b-1} E_v n_v \right]_{T-V} &= \sum_{\ell=1}^{b-1} \sum_{v=0}^{b-\ell-1} (E_v - E_{v+\ell}) g_{v+\ell,v} \\ &+ \sum_{v=0}^{b-1} E_v \sum_{\ell=b}^{N-1} g_{\ell,v} \end{aligned} \quad (\text{II-24a})$$

The last term in this equation yields the gain (or loss) in vibrational energy as a result of transitions that shift the molecule from the A- to the B-group of energy states (this term is analogous to the terms in eq. (II-15) or (II-16)), while the first term represents vibrational-energy relaxation within the A-group of states (note the summation region). This point will be made clear in a later section.

The comparable equation that relates the rate of change of net vibrational energy per unit volume for the upper energy states can be obtained by first deriving the energy-relaxation equation for the complete molecule and then subtracting that portion, equation (II-24a), associated with the lower states. The equation for the complete molecule, obtained by multiplying equation (II-10) by E_v and summing over all molecular energy states $0 \leq v \leq N-1$, is

$$\frac{d}{dt} \left[\sum_{v=0}^{N-1} E_v n_v \right]_{T-V} = \sum_{v=0}^{N-1} \sum_{\ell=1}^{N-v-1} E_v g_{v+\ell,v} - \sum_{v=0}^{N-1} \sum_{\ell=1}^v E_v g_{v,v-\ell} \quad (\text{II-25})$$

Interchanging the order of summation and again altering the indices and summation scheme associated with the second term to obtain the same g-function as contained in the first term results in the equation

$$\frac{d}{dt} \left[\sum_{v=0}^{N-1} E_v n_v \right]_{T-V} = \sum_{\ell=1}^{N-1} \sum_{v=0}^{N-\ell-1} E_v g_{v+\ell,v} - \sum_{\ell=1}^{N-1} \sum_{v=0}^{N-\ell-1} E_{v+\ell} g_{v+\ell,v} \quad (\text{II-26})$$

The summation intervals are identical, that is, both terms involve the same mesh points; hence each term may be combined individually giving

$$\frac{d}{dt} \left[\sum_{v=0}^{N-1} E_v n_v \right]_{T-V} = \sum_{\ell=1}^{N-1} \sum_{v=0}^{N-\ell-1} (E_v - E_{v+\ell}) g_{v+\ell,v} \quad (\text{II-27})$$

Since dissociation is not contained in the translation-vibration energy-interchange equations (i.e., the (T-V)-subscripted equations), the above equation characterizes vibrational energy relaxation for the molecule (compare with the first term of eq. (II-24)). Subtracting equation (II-24) from the above relation yields the equation representing the rate of change of vibrational energy for the upper states as follows:

$$\begin{aligned}
\frac{d}{dt} \left[\sum_{v=b}^{N-1} E_v n_v \right]_{T-V} &= \frac{d}{dt} \left[\sum_{v=0}^{N-1} E_v n_v \right]_{T-V} - \frac{d}{dt} \left[\sum_{v=0}^{b-1} E_v n_v \right]_{T-V} \\
&= \sum_{\ell=0}^{N-1} \sum_{v=0}^{N-\ell-1} (E_v - E_{v+\ell}) g_{v+\ell,v} \\
&\quad - \sum_{\ell=1}^{b-1} \sum_{v=0}^{b-\ell-1} (E_v - E_{v+\ell,v}) g_{v+\ell,v} \\
&\quad - \sum_{\ell=1}^{N-b} \sum_{v=b-\ell}^{b-1} E_v g_{v+\ell,v} - \sum_{\ell=N-b+1}^b \sum_{v=b-\ell}^{N-\ell-1} E_v g_{v+\ell,v} \\
&\quad - \sum_{\ell=b+1}^{N-1} \sum_{v=0}^{N-\ell-1} E_v g_{v+\ell,v} \tag{II-28}
\end{aligned}$$

The first and second terms may be rearranged and we obtain

$$\begin{aligned}
\frac{d}{dt} \left[\sum_{v=b}^{N-1} E_v n_v \right]_{T-V} &= \sum_{\ell=1}^{b-1} \sum_{v=b-\ell}^{N-\ell-1} (E_v - E_{v+\ell}) g_{v+\ell,v} \\
&\quad + \sum_{\ell=b}^{N-1} \sum_{v=0}^{N-\ell-1} (E_v - E_{v+\ell}) g_{v+\ell,v} \\
&\quad - \sum_{\ell=1}^{N-b} \sum_{v=b-\ell}^{b-1} E_v g_{v+\ell,v} - \sum_{\ell=N-b+1}^b \sum_{v=b-\ell}^{N-\ell-1} E_v g_{v+\ell,v} \\
&\quad - \sum_{\ell=b+1}^{N-1} \sum_{v=0}^{N-\ell-1} E_v g_{v+\ell,v} \tag{II-29}
\end{aligned}$$

or, after combining terms,

$$\begin{aligned}
 \frac{d}{dt} \left[\sum_{v=b}^{N-1} E_v n_v \right]_{T-V} &= \sum_{\ell=1}^{b-1} \sum_{v=b-\ell}^{N-\ell-1} (E_v - E_{v+\ell}) g_{v+\ell,v} \\
 &+ \sum_{\ell=b}^{N-1} \sum_{v=0}^{N-\ell-1} (E_v - E_{v+\ell}) g_{v+\ell,v} \\
 &- \sum_{v=0}^{b-1} E_v \sum_{\ell=b}^{N-1} g_{\ell,v}
 \end{aligned} \tag{II-29a}$$

The first two terms, associated with the B-group vibrational relaxation, involve evaluating the function $(E_v - E_{v+\ell})g_{v+\ell,v}$ at the points between the lines $v = b-\ell$ and $v = N-\ell-1$ in figure II-3. The change in vibrational energy due to transitions that involve a crossing of the separation boundary between the A- and B-groups are given by the last three terms in equation (II-29) or the last term in equation (II-29a).

(II-B-1c). Vibrational Temperatures

The essential equations required to specify the vibrational-energy relaxation processes for a molecule still excluding the effect of dissociation, are given by equations (II-15), (II-19), (II-24), and (II-29) (or equivalently eqs. (II-16), (II-20), (II-24a), and (II-29a)). These equations are a complete set, provided the population distribution within each group of energy states is known. As pointed out earlier, we assume that this distribution can be reasonably represented by a Boltzmann distribution, that is, by

$$(n_{v+1})_i = (n_v)_i \exp \left[-\frac{(E_{v+1} - E_v)}{kT_i} \right] \tag{II-30}$$

where i denotes the group, either A or B, and T_i is the temperature appropriate to the group. The validity of such an assumption has been shown by Rubin, Montroll, and Shuler (62, 75, 76, 81, 82, 83, 84) for single-step transitions only for which the transition probabilities are those of harmonic oscillator

molecules. For such conditions we have $T_A = T_B$. Little is known about the effects associated with multiple transitions as a perturbing influence on the distribution. Bazley et al. (6), while solving a problem comparable to Montroll and Shuler's (62) but including the effects of anharmonicity and of some multiple transitions, has shown that the relaxation processes are comparable with those obtained for harmonic oscillators. Thus, existing theories appear to validate the use of the Boltzmann distribution except when dissociation becomes important (12, 48, 84, 94). The perturbing influence of dissociation is, of course, being considered in the present model by the separation of the energy levels into two groups with separate temperatures T_A and T_B .

Assuming a population distribution, in our case a Boltzmann distribution, allows one to reduce manyfold the number of dependent variables required for a description of the vibrational mode. Ultimately, the problem of determining the vibrational state of the molecular system will be reduced to one of obtaining values of the four variables n_A , n_B , T_A , and T_B , where n_A and n_B are defined by equations (II-12) and (II-21) and T_A and T_B are obtained on the basis of equation (II-30). The population density in any vibrational level can be expressed in terms of the total group population by the equations

$$n_{A_v} = \frac{n_A}{Q_A(T_A)} \exp\left(-\frac{E_{A_v}}{kT_A}\right) \quad (\text{II-31a})$$

$$n_{B_v} = \frac{n_B}{Q_B(T_B)} \exp\left(-\frac{E_{B_v}}{kT_B}\right) \quad (\text{II-31b})$$

$$= \frac{n_B}{Q'_B(T_B)} \exp\left[-\frac{E_{B_v} - E_b}{kT_B}\right] \quad (\text{II-31c})$$

where the energy of the vibrational level is subscripted to designate its group, that is,

$$E_{A_v} = E_v \quad 0 \leq v \leq b-1$$

$$E_{B_v} = E_v \quad b \leq v \leq N-1$$

The A and B subscripts may be dropped if no ambiguity results. The functions $Q_A(T)$ and $Q_B(T)$ (or $Q'_B(T)$) are the partition functions associated with the A- and B-molecules, that is, the A and B grouping of molecular states, and are defined by

$$Q_A(T) = \sum_{v=0}^{b-1} \exp\left(-\frac{E_v}{kT}\right) \quad (\text{II-32a})$$

$$Q_B(T) = \sum_{v=b}^{N-1} \exp\left(-\frac{E_v}{kT}\right) \quad (\text{II-32b})$$

$$= Q'_B(T) \exp\left(-\frac{E_b}{kT}\right) \quad (\text{II-32c})$$

The partition function Q'_B differs from Q_B by the reference energy.[†]

Simplification of the equations is now possible. Substitution of the g-function, equation (II-9), into equation (II-16) yields

$$\left[\frac{dn_A}{dt}\right]_{T-V} = m \sum_{v=0}^{b-1} \sum_{\ell=b}^{N-1} \hat{k}_{\ell,v} n_{\ell} - m \sum_{v=0}^{b-1} \sum_{\ell=n}^{N-1} \hat{k}_{\ell,v} n_v \exp\left(-\frac{E_{\ell} - E_v}{kT}\right) \quad (\text{II-33})$$

We observe that the left term involves only n_{ℓ} , where $b \leq \ell \leq N-1$, and the right-hand term only n_v , where $0 \leq v \leq b-1$, that is, the left-hand term contains only B-state population densities and the right-hand term only A-state densities. In view of equations (II-31), equation (II-33) may also be written

$$\left[\frac{dn_A}{dt}\right]_{T-V} = m \left[n_B \hat{k}_R^{(1)}(T_B, T) - n_A \hat{k}_F^{(1)}(T_A, T) \right] \quad (\text{II-34a})$$

[†]The energy levels in Q_A and Q_B are referenced with respect to the molecular ground state; in Q'_B they are referenced with respect to the lowest energy level of the B-group of energy states (see Appendix A for discussion).

and the rate equation for n_B , equation (II-20), is similarly given by

$$\left[\frac{dn_B}{dt} \right]_{T-V} = -m \left[n_B \hat{k}_R^{(i)}(T_B, T) - n_A \hat{k}_F^{(i)}(T_A, T) \right] \quad (\text{II-34b})$$

In both of these equations we have defined the following rate constants:

$$\hat{k}_R^{(i)}(T_B, T) = \frac{1}{Q'_B(T_B)} \sum_{v=0}^{b-1} \sum_{\ell=b}^{N-1} \hat{k}_{\ell, v}(T) \exp \left[-\frac{(E_{B\ell} - E_b)}{kT_B} \right] \quad (\text{II-35a})$$

$$\hat{k}_F^{(i)}(T_A, T) = \frac{1}{Q_A(T_A)} \sum_{v=0}^{b-1} \sum_{\ell=b}^{N-1} \hat{k}_{\ell, v}(T) \exp \left[-\frac{(E_{B\ell} - E_{Av})}{kT} - \frac{E_{Av}}{kT_A} \right] \quad (\text{II-35b})$$

Similar relations can be obtained for the energy rate equations. We first introduce the energy averages defined by the barred quantities given in the following identities:

$$\bar{E}_R(T_B, T) \hat{k}_R^{(i)}(T_B, T) = \frac{1}{Q'_B(T_B)} \sum_{v=0}^{b-1} E_v \sum_{\ell=b}^{N-1} \hat{k}_{\ell, v}(T) \exp \left[-\frac{(E_{B\ell} - E_b)}{kT_B} \right] \quad (\text{II-36a})$$

$$\bar{E}_F(T_A, T) \hat{k}_F^{(i)}(T_A, T) = \frac{1}{Q_A(T_A)} \sum_{v=0}^{b-1} E_v \sum_{\ell=b}^{N-1} \hat{k}_{\ell, v}(T) \exp \left[-\frac{(E_{B\ell} - E_{Av})}{kT} - \frac{E_{Av}}{kT_A} \right] \quad (\text{II-36b})$$

Substituting these relations and equations (II-12) and (II-21) into equations (II-24a) and (II-29a), we obtain the energy equations

$$\begin{aligned} \frac{d}{dt} \left[n_A \hat{q}_A(T_A) \right]_{T-V} &= \sum_{\ell=1}^{b-1} \sum_{v=0}^{b-\ell-1} (E_v - E_{v+\ell}) g_{v+\ell, v} \\ &+ m n_B \bar{E}_R(T_B, T) \hat{k}_R^{(i)}(T_B, T) - m n_A \bar{E}_F(T_A, T) \hat{k}_F^{(i)}(T_A, T) \end{aligned} \quad (\text{II-37a})$$

$$\begin{aligned}
\frac{d}{dt} \left[n_B \hat{q}_B (T_B) \right]_{T-V} &= \sum_{\ell=1}^{b-1} \sum_{v=b-\ell}^{N-\ell-1} (E_v - E_{v+\ell}) g_{v+\ell, v} \\
&+ \sum_{\ell=b}^{N-1} \sum_{v=0}^{N-\ell-1} (E_v - E_{v+\ell}) g_{v+\ell, v} \\
&- m n_B \bar{E}_R (T_B, T) \hat{k}_R^{(1)} (T_B, T) \\
&+ m n_A \bar{E}_F (T_A, T) \hat{k}_F^{(1)} (T_A, T)
\end{aligned} \tag{II-37b}$$

where

$$n_A \hat{q}_A (T_A) = \sum_{v=0}^{b-1} E_v n_v \tag{II-38a}$$

$$n_B \hat{q}_B (T_B) = \sum_{v=b}^{N-1} E_v n_v \tag{II-38b}$$

$$= n_B \left[\hat{q}'_B (T_B) + E_b \right] \tag{II-38c}$$

A brief discussion of these equations is worthwhile. The population equations (eqs. (II-34a) and (II-34b)) are precisely analogous to the master equations from which they are derived. Each equation contains only two terms, one representing the rate of loss and the other the rate of gain. The rate coefficients in these equations contain the net effect of all possible transitions whether they be one-step, two-step, etc., or any combination thereof. The rate coefficients also depend on the vibrational temperatures of the respective grouping of levels. These temperatures may, in principle, be obtained from equations (II-37). The functions \hat{q}_A and \hat{q}_B are known single-valued functions of their arguments (see, e.g., Appendix A) and once the value of these functions has been found, one may readily compute the temperatures T_A and T_B . It is difficult to discern the significance of the individual terms contained in equation (II-37) at this time. It will be shown in the next section that the first term containing the double summation, is proportional to the difference $\hat{q}_A (T) - \hat{q}_A (T_A)$ in equation (II-37a) and

$\hat{q}_B(T) - \hat{q}_B(T_B)$ in equation (II-37b). For this reason they will be called the vibrational-energy relaxation terms (they are analogous to the Landau-Teller expression (8, 49) that describes vibrational relaxation). However, one can derive such explicit relations only for single-step transitions and only if the transition rates are linearly related to the vibrational level v .

The present problem requiring solutions of equations (II-34) and (II-37), although less complicated than the original problem in which one seeks a solution of the complete set of master equations, still contains far too many parameters $\hat{k}_{v,v-1}$ for easy evaluation (i.e., if one is to compare solutions of the equations with experimental data as a means of evaluating these parameters). These equations are also too complex to be useful as a model for flow field calculations. It will now be shown that further simplification is possible after the introduction of additional approximating assumptions.

(II-B-2). T-V Energy Interchange, Stepwise Transitions

The formalism used and the equations obtained in the previous sections are general. The only limitation in the final form of the equations concerns the assumption of the population distributions. Although general expressions are much sought after, in practice such expressions often have only limited utility. For example, a solution of the problem outlined in the last paragraph of the previous section would probably have only limited value, since it would be difficult to relate the parameters $\hat{k}_{i,j}$ to experimental results. Rather than solve this problem, additional approximations will be introduced here that will result in a final set of vibrational-relaxation equations that are only slightly more complex than those obtained by Landau and Teller (see, e.g., eq. (I-1) in Chapter I).

The significant assumptions to be introduced in this section are as follows:

- (1) Vibrational relaxation occurs in a stepwise manner, that is, the effect of multiple transitions may be assumed negligible ($\hat{k}_{i,j} = 0$ for $|i - j| = \ell > 1$).
- (2) The effect of anharmonicity regarding both the thermodynamic functions and the transition rates, may be approximated by use of equal energy-level spacing and harmonic oscillator transition-rate relations above

and below some separation a , where large energy-level spacings and small transition rates are used for the lower levels and much smaller spacings and much larger rates are used for the upper levels.

It is worthwhile to remark briefly on these assumptions. The first is generally valid, except perhaps for the uppermost vibrational energy levels of a molecule (24, 37, 39, 67). For the uppermost levels, however, the probabilities for multiple transitions from any given level are still less than the probability for a single-quantum transition from that level (24, 37, 39). As a matter of interest, it will be shown in the next chapter that if the separation b is taken near the midpoint of the vibrational potential well, the observed pre-exponential temperature dependence is best accounted for by a dissociation model that has dissociation occurring primarily from the very uppermost level. A nonpreferential model for dissociation that presumes equal probability of dissociation from any of the B-group of vibrational energy levels does not yield results that agree with the experimentally observed pre-exponential temperature dependence. Hence, there is an apparent consistency between the use of assumption (1) and an equivalent assumption for the dissociation model that will be introduced in a later section.

Assumption (2) is discussed in Appendix B. It will only be remarked here that the approximation procedure can be further expanded. The approximation, as used, depends on the use of two linear functions for approximating the "rate of quantum transfer" that results from single-step transitions (see Appendix B). Including more linear functions and thus additional separation levels would, in principle, improve the model equations. It will be shown, however, that the additional complication may not be warranted as a result of the insufficient accuracy of the available experimental data (considerable "scatter" in the data). As more refined experimental measurements become available, additional refinement of the model equations may also be required. The formalism allows for such improvements.

As a matter of emphasis, it is worthwhile to point out again that the reason for introducing the a -level separation is quite different from that for the b -level

separation. The b-level was introduced to take account of the fact that the distribution of energy in the various vibrational states is not Boltzmann. The a-level allows an approximation for the molecular anharmonicity effects, both as regards the energy-level spacing and the transition probabilities. The assumptions given earlier will be introduced in turn in the analysis that follows.

We find on imposing (1) that the resulting equations are greatly simplified. Equations (II-35) and (II-37) become

$$\hat{k}_R^{(1)}(T_B, T) = \frac{\hat{k}_{b,b-1}(T)}{Q'_B(T_B)} \quad (\text{II-39a})$$

$$\hat{k}_F^{(1)}(T_A, T) = \frac{\hat{k}_{b-1,b}}{Q_A(T_A)} \exp\left(-\frac{E_{b-1}}{kT_A}\right) \quad (\text{II-39b})$$

$$\frac{d}{dt} \left[n_A \hat{q}_A(T_A) \right]_{T-V} = \sum_{v=0}^{b-2} (E_v - E_{v+1}) g_{v+1,v} + E_{b-1} \left[\frac{dn_A}{dt} \right]_{T-V} \quad (\text{II-40a})$$

$$\frac{d}{dt} \left[n_B \hat{q}_B(T_B) \right]_{T-V} = \sum_{v=b-1}^{N-2} (E_v - E_{v+1}) g_{v+1,v} - E_{b-1} \left[\frac{dn_A}{dt} \right]_{T-V} \quad (\text{II-40b})$$

In the latter two equations use has been made of the resulting simplification that occurs for the averages in equations (II-36), which are now given by $\bar{E}_F = \bar{E}_R = E_{b-1}$. Equations (II-34) are unchanged after the application of condition (1), except that the rate constants $\hat{k}_F^{(1)}$ and $\hat{k}_R^{(1)}$ are given by equations (II-39) rather than by equations (II-35).

As a result of imposing condition (1), the rate equations (II-34) may be expressed simply as the first term of equation (II-17), that is, by

$$\left[\frac{dn_A}{dt} \right]_{T-V} = g_{b,b-1} \quad (\text{II-41a})$$

$$= - \left[\frac{dn_B}{dt} \right]_{T-V} \quad (\text{II-41b})$$

With these relations it is a simple matter to remove the explicit dependence of equation (II-40b) on the rate of change of the total number of molecules in the A-states. This we do by shifting the B-state reference energy by substituting

the appropriate expression for \hat{q}_B in terms of \hat{q}'_B , equation (II-38c), and then combine terms after using equation (II-41a) for $(dn_A/dt)_{T-V}$ and equation (II-9) for the g-function. The alternate form for equation (II-40b) that results is

$$\frac{d}{dt} \left[n_B \hat{q}'_B(T_B) \right]_{T-V} = \sum_{v=b}^{N-2} (E_v - E_{v+1}) g_{v+1,v} \quad (\text{II-42})$$

The summation contains no A-state quantities. The reason for making such an alteration is that all terms in the series in this equation involve only B-state quantities and thus are to be evaluated at the vibrational temperature T_B . This simplifies bookkeeping in the derivations that follow.

Further simplification of equations (II-40a) and (II-42) now requires the introduction of assumption (2) given earlier. In addition, a procedure is required that is similar in many respects to that used by Bethe and Teller (8), described also by Vincenti and Kruger (97) and Clarke and McChesney (22), except that rather than consider a molecule that is a harmonic oscillator with an infinite number of energy levels we have one that is truncated and thus has only a finite number of levels. The procedure depends on the fact that, providing the energy levels are equally spaced, substitution of transition probabilities varying in a linear manner with the level number v , yields series expressions in the energy rate equations that are summable and may be identified with previously defined functions. The procedure depends on the following description for the level energies E_v (a diagram of these levels is given in fig. A-1):

$$E_v = E_{A_1} v \quad 0 \leq v \leq a - 1 \quad (\text{II-43a})$$

$$= E_a + E_{A_2} (v - a) \quad a \leq v \leq b - 1 \quad (\text{II-43b})$$

$$= E_b + E_{A_2} (v - b) \quad b \leq v \leq N - 1 \quad (\text{II-43c})$$

where

$$E_a = E_{A_1}(a - 1) + E_{A_2} \quad (\text{II-44a})^\dagger$$

$$E_b = E_a + (b - a) E_{A_2} \quad (\text{II-44b})^\dagger$$

In addition we require the transition probabilities (see Appendix B) given by

$$\hat{k}_{v,v-1} = v \hat{k}_{1,0}^{(1)} \quad 1 \leq v \leq a - 1 \quad (\text{II-45a})$$

$$= (v - a) \hat{k}_{1,0}^{(2)} + \hat{k}_{a,a-1}^{(2)} \quad a \leq v \leq N - 1 \quad (\text{II-45b})$$

$$\hat{k}_{v-1,v} = \exp\left(-\frac{E_{A_1}}{kT}\right) \hat{k}_{v,v-1} \quad 1 \leq v \leq a - 1 \quad (\text{II-46a})$$

$$= \exp\left(-\frac{E_{A_2}}{kT}\right) \hat{k}_{v,v-1} \quad a \leq v \leq N - 1 \quad (\text{II-46b})$$

$$\hat{k}_{a,a-1}^{(2)} = a \hat{k}_{1,0}^{(1)} \frac{E_{A_1}}{E_{A_2}} \quad (\text{II-47})$$

$$\hat{k}_{a-1,a}^{(2)} = \exp\left(-\frac{E_{A_2}}{kT}\right) \hat{k}_{a,a-1}^{(2)} \quad (\text{II-48})$$

The energy parameters E_a , E_b , and N and the energy-level spacings E_{A_1} and E_{A_2} are formulated and discussed in Appendix A. The rate parameters, $\hat{k}_{0,1}^{(1)}$ and $\hat{k}_{0,1}^{(2)}$ are discussed in detail in Appendix B. We will presume for the present that the above relations are valid representations of their actual equivalents and proceed to reduce equations (II-40a) and (II-42) to the simplest form consistent with the basic assumptions (1) and (2).

In what follows the key to successfully reducing the equations to a form that involves known functions and very few parameters depends on an efficacious grouping of terms. To this end, rather than work with equations that are extremely bulky and contain many terms that can overly complicate the

[†]The subject of the following chapters involves in part the assignment of appropriate values for these parameters. It suffices to state now that $0 < a \leq b < N$, that is, the b-level, has a value that is above or, in the least, is identical with the value of the a-level.

derivations, symbols will be assigned to certain individual terms. These terms will be separately investigated and simplified. One will find that in addition to greatly reducing the amount of algebra much insight is also acquired as to the expected form of a more general set of equations that would, in principle, even better approximate the actual relaxation processes. Such generality, however, involves the introduction of more parameters into a problem already plagued with too many difficult to evaluate parameters. Such generalization will not be explicitly exhibited here but the generalizing method will be made clear.

Concentrating for the present on equation (II-40a), we split the series contained in this equation into three parts. Two parts are series that contain vibrational relaxation terms that enclose the separation level "a," and the third is the separation term. We obtain

$$\begin{aligned} \frac{d}{dt} \left[n_A \hat{q}_A(T_A) \right]_{T-V} &= \overbrace{\sum_{v=0}^{a-2} (E_v - E_{v+1}) g_{v+1,v}}^{T_1} + \overbrace{\sum_{v=a}^{b-2} (E_v - E_{v+1}) g_{v+1,v}}^{T_2} \\ &\quad + (E_{a-1} - E_a) g_{a,a-1} + E_{b-1} \left[\frac{dn_A}{dt} \right]_{T-V} \end{aligned} \quad (\text{II-49})$$

The first term will be denoted as T_1 and the second as T_2 . There is little difference between equation (II-42), T_1 or T_2 , except for the summation limits. The difference is significant for T_1 only because there are no vibrational states below $v = 0$. The algebra required to reduce these relations to their simplest possible form is least for T_1 , and therefore attention will be focused first on this term. The complexity involved in reducing equations (II-42) and T_2 is nearly equivalent. However, it will be worthwhile to investigate equation (II-42) rather than T_2 , because more insight is gained as regards the generality of the method. The resulting equation immediately provides the proper expression for T_2 by simply reassigning different values for the summation indices b and N and by appropriately changing the subscripts. These parameters, of course, will be implicitly imbedded in the resulting equations. As a matter of emphasis it is fitting to point out again that the key to the successful application of the following procedure is in the recognition of sets of terms as

being previously defined functions. These functions are developed and discussed in detail in the last section of Appendix A. Being familiar with these functions is important, particularly those relating to the vibrational mode, that is, Q_{A_1} , Q_{A_2} , Q_B , \hat{q}_{A_1} , \hat{q}_{A_2} , \hat{q}_B , \mathcal{L}_{A_1} , \mathcal{L}_{A_2} , \mathcal{L}_B and their primed equivalents. These quantities will be reintroduced as required in the analysis that follows to facilitate the recognition of specific terms.

Concentrating now on T_1 , we substitute equation (II-9) giving the g-function, equation (II-31a) for the number density n_v , and, after the uppermost term in the series is adjusted, there results

$$T_1 = n_{A_1} m \left[\sum_{v=0}^{a-1} \frac{(E_{v-1} - E_v)}{Q_{A_1}(T_A)} \hat{k}_{v,v-1} \exp\left(-\frac{E_v}{kT_A}\right) - \sum_{v=0}^{a-1} \frac{(E_v - E_{v+1})}{Q_{A_1}(T_A)} \hat{k}_{v,v+1} \exp\left(-\frac{E_v}{kT_A}\right) + \frac{(E_{a-1} - E_a)}{Q_{A_1}(T_A)} \hat{k}_{a-1,a} \exp\left(-\frac{E_{a-1}}{kT_A}\right) \right] \quad (\text{II-50})$$

As already pointed out, the partition functions $Q_{A_1}(T_A)$ as well as the other thermodynamic quantities to be used are defined in Appendix A. The appropriate expressions for E_v and $\hat{k}_{i,j}$, equations (II-43a), (II-45a), and (II-45b), respectively, are now substituted into the above equation and $(\hat{k}_{1,0}^{(1)} - \hat{k}_{0,1}^{(1)})$ is removed as a factor. One then obtains

$$T_1 = -n_{A_1} \left\{ m(\hat{k}_{1,0}^{(1)} - \hat{k}_{0,1}^{(1)}) \left[\sum_{v=0}^{a-1} \frac{E_{A_1} v}{Q_{A_1}(T_A)} \exp\left(-\frac{E_{A_1} v}{kT_A}\right) - E_{A_1} \left(\frac{\hat{k}_{0,1}^{(1)}}{\hat{k}_{1,0}^{(1)}} \right) \frac{1}{1 - \left(\frac{\hat{k}_{0,1}^{(1)}}{\hat{k}_{1,0}^{(1)}} \right)} \sum_{v=0}^{a-1} \frac{\exp\left(-\frac{E_{A_1} v}{kT_A}\right)}{Q_{A_1}(T_A)} + E_{A_1} a \left(\frac{\hat{k}_{0,1}^{(1)}}{\hat{k}_{1,0}^{(1)}} \right) \frac{1}{1 - \left(\frac{\hat{k}_{0,1}^{(1)}}{\hat{k}_{1,0}^{(1)}} \right)} \frac{\exp\left[-\frac{(a-1)E_{A_1}}{kT_A}\right]}{Q_{A_1}(T_A)} \right] \right\} \quad (\text{II-51})$$

This expression is readily simplified. We observe in Appendix A that the first term in brackets is identified with the quantity

$$\hat{q}_{A_1}(T_A) = \sum_{v=0}^{a-1} \frac{E_{A_1} v}{Q_{A_1}(T_A)} \exp\left(-\frac{E_{A_1} v}{kT_A}\right) \quad (\text{II-52})$$

After substitution of the appropriate exponentials for the rate ratios, according to equation (II-46a), and it is noted again from Appendix A that

$$Q_{A_1}(T_A) = \sum_{v=0}^{a-1} \exp\left(-\frac{E_{A_1} v}{kT_A}\right) \quad (\text{II-53})$$

$$\hat{q}_{A_1}^{\infty}(T) = E_{A_1} \frac{\hat{k}_{0,1}^{(1)}}{\hat{k}_{1,0}^{(1)}} \frac{1}{1 - \left(\frac{\hat{k}_{0,1}^{(1)}}{\hat{k}_{1,0}^{(1)}}\right)} \quad (\text{II-54a})$$

$$= E_{A_1} \frac{\exp\left(-\frac{E_{A_1}}{kT}\right)}{1 - \exp\left(-\frac{E_{A_1}}{kT}\right)} \quad (\text{II-54b})$$

the second and third terms may then be readily identified. There results

$$T_1 = -n_{A_1} m \left(\hat{k}_{1,0}^{(1)} - \hat{k}_{0,1}^{(1)} \right) \left\{ \hat{q}_{A_1}(T_A) - \hat{q}_{A_1}^{\infty}(T) \left[1 - \frac{a \exp\left[-\frac{(a-1)E_{A_1}}{kT_A}\right]}{Q_{A_1}(T_A)} \right] \right\} \quad (\text{II-55})$$

the factor $m(\hat{k}_{1,0}^{(1)} - \hat{k}_{0,1}^{(1)})$, which may also be written $m\hat{k}_{1,0}^{(1)}[1 - \exp(-\frac{E_{A_1}}{kT})]$, is defined as the inverse of the vibrational relaxation time and is commonly given the symbol $1/\tau$ (see, e.g., 22,97). To differentiate this parameter from a similar parameter that will be introduced later, we adopt the notation

$$\tau_{A_1}(T,p) = \left\{ m \hat{k}_{1,0}^{(1)} \left[1 - \exp\left(-\frac{E_{A_1}}{kT}\right) \right] \right\}^{-1} \quad (\text{II-56})$$

Furthermore, referring again to Appendix A, we observe that the factor given in the brackets of equation (II-55) above is the truncation factor defined by

$$\mathcal{L}_{A_1}(T_A) = \left\{ 1 - \frac{a \exp \left[-\frac{(a-1) E_{A_1}}{kT_A} \right]}{Q_{A_1}(T_A)} \right\} \quad (\text{II-57})$$

The characteristics of this function are described in detail in Appendix A. Substituting these latter two quantities into equation (II-55) results in the following simple expression for the first term of equation (II-49):

$$T_1 = \frac{n_{A_1}}{\tau_{A_1}} \left[\hat{q}_{A_1}^{\infty}(T) \mathcal{L}_{A_1}(T_A) - \hat{q}_{A_1}(T_A) \right] \quad (\text{II-58a})$$

This expression is worthy of brief comment since it will turn out to be equivalent to the form used by previous workers studying vibrational relaxation in flow fields having relatively low temperature T . Noting equation (A30) in Appendix A, we rewrite equation (II-58a) as follows:

$$T_1 = \frac{n_{A_1}}{\tau_{A_1}} \left[\hat{q}_{A_1}^{\infty}(T) - \hat{q}_{A_1}^{\infty}(T_A) \right] \mathcal{L}_{A_1}(T_A) \quad (\text{II-58b})$$

The truncation factor is approximately unity provided $T_A < (a - 1) E_{A_1}/k$. With this approximation (equivalent to the requirement that the population in the upper levels be relatively small or that the effect of truncation be negligible), the equation is then identical in form to that of Bethe and Teller (see, e.g., (8) or Chapter I) and is the equation used by many researchers studying the effects of uncoupled vibrational relaxation (10, 22, 29, 30, 32, 97). We will note later that the other terms in equation (II-49) and also the term in equation (II-42) are negligible in this case. The above equation shows the correct use of relations for truncated harmonic oscillators. To illustrate the differences between this relation and relations used by other researchers (57, 58, 90, 91, 93) the equation can be cast in a different form. After the introduction of equation (A30), the above equation may also be written

$$T_1 = \frac{n_{A_1}}{\tau_{A_1}} \left[\hat{q}_{A_1}(T) \frac{\mathcal{L}_{A_1}(T_A)}{\mathcal{L}_{A_1}(T)} - \hat{q}_{A_1}(T_A) \right] \quad (\text{II-58c})$$

and this can be identified as the vibrational relaxation term used by the other researchers (see, e.g., Marrone and Treanor (58)), if the ratio $\mathcal{L}_{A_1}(T_A)/\mathcal{L}_{A_1}(T)$ is set equal to unity (for this comparison we consider a to be equal to N). The quantity \hat{q}_{A_1} is the truncated harmonic oscillator function that was used by the other researchers. This point will become clear as the other terms in equation (II-49) as well as the term in equation (II-42) are simplified. It should be evident, however, that the ratio $\mathcal{L}_{A_1}(T_A)/\mathcal{L}_{A_1}(T)$ is not unity in the case studied by Marrone and Treanor; furthermore, the use of more accurate quantities for the energy functions \hat{q}_A (e.g., see 57, 58) is of questionable value. Further discussion of this point will be deferred until later (see last page of section B-4 of this chapter).

Before proceeding with the simplification of equation (II-42) it will be helpful to abbreviate the notation by temporarily assigning the symbol T_3 to the summation for $\frac{d}{dt}[n_B \hat{q}'_B(T_B)]_{T-V}$, that is,

$$T_3 = \sum_{v=b}^{N-2} (E_v - E_{v+1}) g_{v,v+1} \quad (\text{II-59})$$

The procedure to reduce T_3 to the simplest functional form parallels that just employed to yield equations (II-58). We obtain

$$T_3 = m n_B \left[\sum_{v=b}^{N-1} \frac{(E_{v-1} - E_v)}{Q_B(T_B)} \hat{k}_{v,v-1} \exp\left(-\frac{E_v}{kT_B}\right) - \sum_{v=b}^{N-1} \frac{(E_v - E_{v+1})}{Q_B(T_B)} \hat{k}_{v,v+1} \exp\left(-\frac{E_v}{kT_B}\right) - \frac{(E_{b-1} - E_b)}{Q_B(T_B)} \hat{k}_{b,b-1} \exp\left(-\frac{E_b}{kT_B}\right) + \frac{(E_{N-1} - E_N)}{Q_B(T_B)} \hat{k}_{N-1,N} \exp\left(-\frac{E_{N-1}}{kT_B}\right) \right] \quad (\text{II-60})$$

as the expression analogous to equation (II-50). We note that the third term occurs here as a result of the non-zero lower summation limit. The fourth term is analogous to the third term in equation (II-58). The last two terms are required in order to obtain the appropriate summation limits for the set of energy states being investigated. Substitution of the appropriate form of the energies E_v and transition probabilities $\hat{k}_{i,j}$, given by equations (II-43c), (II-45b) and (II-46b), yields

$$\begin{aligned}
T_3 = & - n_B m \left\{ \sum_{v=b}^{N-1} \frac{E_{A_2} [(v-b) \hat{k}_{1,0}^{(2)} + (b-a) \hat{k}_{1,0}^{(2)} + \hat{k}_{a,a-1}^{(2)}]}{\exp\left(\frac{E_b}{kT_B}\right) Q_B(T_B)} \exp\left[-\frac{(v-b) E_{A_2}}{kT_B}\right] \right. \\
& - \sum_{v=b}^{N-1} \frac{E_{A_2} [(v-b) \hat{k}_{0,1}^{(2)} + (b-a+1) \hat{k}_{0,1}^{(2)} + \hat{k}_{a-1,a}]}{\exp\left(\frac{E_b}{kT_B}\right) Q_B(T_B)} \exp\left[-\frac{(v-b) E_{A_2}}{kT_B}\right] \\
& - \frac{E_{A_2} \hat{k}_{b,b-1}}{\exp\left(\frac{E_b}{kT_B}\right) Q_B(T_B)} + \frac{E_{A_2} [(N-b) \hat{k}_{0,1}^{(2)} + (b-a) \hat{k}_{0,1}^{(2)} + \hat{k}_{a-1,a}]}{\exp\left(\frac{E_b}{kT_B}\right) Q_B(T_B)} \\
& \left. \times \exp\left[-\frac{(N-b-1) E_{A_2}}{kT_B}\right] \right\} \quad (\text{II-61})
\end{aligned}$$

The denominator in each of the terms is $Q'_B(T_B)$. It is helpful now to list the additional thermodynamic quantities that will be required here. They are also given in Appendix A and are as follows:

$$Q'_B(T_B) = \sum_{v=b}^{N-1} \exp\left[-\frac{(v-b) E_{A_2}}{kT_B}\right] \quad (\text{II-62a})$$

$$= \exp\left(\frac{E_b}{kT_B}\right) Q_B(T_B) \quad (\text{II-62b})$$

$$\hat{q}_B^\infty(T) \equiv \hat{q}_{A_2}^\infty(T) \quad (\text{II-63a})$$

$$= \frac{E_{A_2} \exp\left(-\frac{E_{A_2}}{kT}\right)}{1 - \exp\left(-\frac{E_{A_2}}{kT}\right)} \quad (\text{II-63b})$$

$$= E_{A_2} \frac{\left(\frac{\hat{k}_{0,1}^{(2)}}{\hat{k}_{1,0}^{(2)}}\right)}{1 - \left(\frac{\hat{k}_{0,1}^{(2)}}{\hat{k}_{1,0}^{(2)}}\right)} \quad (\text{II-63c})$$

$$\mathcal{L}'_B(T_B) = 1 - \frac{(N-b)}{Q'_B(T_B)} \exp\left[-\frac{(N-b-1) E_{A_2}}{kT_B}\right] \quad (\text{II-64})$$

$$\hat{q}'_B(T_B) = \hat{q}^\infty_B(T_B) \mathcal{L}'_B(T_B) = \sum_{v=b}^{N-1} \frac{E_{A_2}(v-b)}{Q'_B(T_B)} \exp\left[-\frac{(v-b)E_{A_2}}{kT_B}\right] \quad (\text{II-65a,b})$$

We now combine the terms in equation (II-61) in such a manner that those containing the coefficients $\hat{k}_{0,1}^{(2)}$ and $\hat{k}_{1,0}^{(2)}$ are grouped together. The set of terms designated T_3 may now be written

$$\begin{aligned} T_3 = & -n_B \left\{ m(\hat{k}_{1,0}^{(2)} - \hat{k}_{0,1}^{(2)}) \left[\sum_{v=b}^{N-1} \frac{E_{A_2}(v-b)}{Q'_B(T_B)} \exp\left[-\frac{(v-b)E_{A_2}}{kT_B}\right] + E_{A_2}(b-a) \right. \right. \\ & - E_{A_2} \left(\frac{\hat{k}_{0,1}^{(2)}}{\hat{k}_{1,0}^{(2)}} \right) \frac{1}{1 - \left(\frac{\hat{k}_{0,1}^{(2)}}{\hat{k}_{1,0}^{(2)}} \right)} \left(1 - \frac{(N-b)}{Q'_B(T_B)} \exp\left[-\frac{(N-b-1)E_{A_2}}{kT_B}\right] \right) \right. \\ & \left. \left. - \frac{(b-a)}{Q'_B(T_B)} \exp\left[-\frac{(N-b-1)E_{A_2}}{kT_B}\right] \right] \right\} + m E_{A_2} (\hat{k}_{a,a-1}^{(2)} - \hat{k}_{a-1,a}^{(2)}) \\ & + E_{A_2} m \frac{\hat{k}_{a-1,a}^{(2)}}{Q'_B(T_B)} \exp\left[-\frac{(N-b-1)E_{A_2}}{kT_B}\right] - \frac{E_{A_2} m \hat{k}_{b,b-1}}{Q'_B(T_B)} \quad (\text{II-66}) \end{aligned}$$

To obtain this expression the partition-function representation $Q'_B(T_B)$ was substituted in place of its series as given by equation (II-62a). Certain of the terms above may be immediately identified. The first term is the quantity represented by equation (II-65b). The third and fourth terms together are the truncation factor $\mathcal{L}'_B(T_B)$, equation (II-64), and their coefficient is given by equation (II-63c). We thus obtain

$$\begin{aligned} T_3 = & -n_B \left\{ m(\hat{k}_{1,0}^{(2)} - \hat{k}_{0,1}^{(2)}) \left[\hat{q}'_B(T_B) + E_{A_2}(b-a) - \hat{q}^\infty_B(T) \mathcal{L}'_B(T_B) \right. \right. \\ & \left. \left. + \frac{\hat{q}^\infty_B(T)(b-a)}{Q'_B(T_B)} \exp\left[-\frac{(N-b-1)E_{A_2}}{kT_B}\right] \right] \right\} + m E_{A_2} (\hat{k}_{a,a-1}^{(2)} - \hat{k}_{a-1,a}^{(2)}) \\ & + E_{A_2} m \frac{\hat{k}_{a-1,a}^{(2)}}{Q'_B(T_B)} \exp\left[-\frac{(N-b-1)E_{A_2}}{kT_B}\right] - \frac{E_{A_2} m \hat{k}_{b,b-1}}{Q'_B(T_B)} \quad (\text{II-67}) \end{aligned}$$

The factor $m(\hat{k}_{1,0}^{(2)} - \hat{k}_{0,1}^{(2)})$, which may also be written $m\hat{k}_{1,0}^{(2)} \left[1 - \exp\left(-\frac{E_{A_2}}{kT}\right) \right]$, is similar to the factor that appears in equation (II-55). This factor has the same significance and will be similarly represented by

$$\tau_B(T,p) = \left\{ m\hat{k}_{1,0}^{(2)} \left[1 - \exp\left(-\frac{E_{A_2}}{kT}\right) \right] \right\}^{-1} \quad (\text{II-68})$$

which is the characteristic vibrational relaxation time associated with the upper states. With this newly defined quantity, the terms $mE_{A_2}(\hat{k}_{a,a-1}^{(2)} - \hat{k}_{a-1,a}^{(2)})$ may be written $\frac{E_{A_2}}{\tau_B} \frac{\hat{k}_{a,a-1}^{(2)}}{\hat{k}_{1,0}^{(2)}}$.

Further reduction of T_3 is not possible without first introducing a special identity, the significance of which will become apparent only when T_1 , T_2 , and T_3 are resubstituted into equations (II-49) and (II-42). This identity, which will presently be introduced, evolves from an investigation of the quantity $n_B E_{A_2} m \times \hat{k}_{b-1,b} \exp(E_{A_2}/kT_B) / Q'_B(T_B)$, which may be identified as the rate-of-energy transfer from the vibrational state $b-1$ to the state b when these states have Boltzmann populations with a vibrational temperature T_B . Substituting the appropriate values for the transition probability $\hat{k}_{b-1,b}$, as determined from equation (II-45b), into this quantity, we obtain the identity

$$\frac{n_B E_{A_2} m \hat{k}_{b-1,b}}{Q'_B(T_B)} \exp\left(\frac{E_{A_2}}{kT_B}\right) = \frac{n_B E_{A_2} [(b-a) \hat{k}_{0,1}^{(2)} + \hat{k}_{a-1,a}^{(2)}]}{Q'_B(T_B)} \exp\left(\frac{E_{A_2}}{kT_B}\right) \quad (\text{II-69a})$$

If we express $\hat{k}_{0,1}^{(2)}$ and $\hat{k}_{a-1,a}^{(2)}$ in terms of $\hat{k}_{1,0}^{(2)}$ and $\hat{k}_{a,a-1}^{(2)}$ by means of equations (II-46b) and (II-48), respectively, introduce the upper-state vibrational relaxation time given by equation (II-68), and transpose the left-hand term, the above identity becomes

$$\begin{aligned}
0 = & - \frac{n_B E_{A_2} m \hat{k}_{b-1,b}}{Q'_B(T_B)} \exp\left(\frac{E_{A_2}}{kT_B}\right) + \frac{n_B \hat{q}_B^\infty(T)}{\tau_B Q'_B(T_B)} \\
& \times \left[(b-a) + \frac{\hat{k}_{a,a-1}^{(2)}}{\hat{k}_{1,0}^{(2)}} \right] \exp\left(\frac{E_{A_2}}{kT_B}\right) \quad (\text{II-69b})
\end{aligned}$$

We may add this quantity to T_3 , as given by equation (II-67), without affecting the value of T_3 . We then observe that the terms containing exponentials may readily be identified with a previously defined thermodynamic quantity, as will be demonstrated by what follows. When the above identity, equation (II-69b), is introduced into equation (II-67), there results

$$\begin{aligned}
T_3 = & - n_B \left\{ \frac{1}{\tau_B} \left[\hat{q}'_B(T_B) - \hat{q}_B^\infty(T) \mathcal{L}'_B(T_B) \right] + \frac{E_{A_2}(b-a)}{\tau_B} \right. \\
& - \frac{(b-a)}{\tau_B} \frac{\hat{q}_B^\infty(T)}{Q'_B(T_B)} \left[1 - \exp\left[-\frac{(N-b)E_{A_2}}{kT_B}\right] \right] \exp\left(\frac{E_{A_2}}{kT_B}\right) + \frac{E_{A_2}}{\tau_B} \frac{\hat{k}_{a,a-1}^{(2)}}{\hat{k}_{1,0}^{(2)}} \\
& - \frac{1}{\tau_B} \frac{\hat{k}_{a,a-1}^{(2)}}{\hat{k}_{1,0}^{(2)}} \frac{\hat{q}_B^\infty(T)}{Q'_B(T_B)} \left[1 - \exp\left[-\frac{(N-b)E_{A_2}}{kT_B}\right] \right] \exp\left(\frac{E_{A_2}}{kT_B}\right) \\
& \left. + \frac{E_{A_2} m \hat{k}_{b-1,b}}{Q'_B(T_B)} \exp\left(\frac{E_{A_2}}{kT_B}\right) - \frac{E_{A_2} m \hat{k}_{b,b-1}}{Q'_B(T_B)} \right\} \quad (\text{II-70a})
\end{aligned}$$

With equations (II-62b) and (II-63b) we identify the coefficient $\left[1 - \exp\left[-\frac{(N-b)E_{A_2}}{kT_B}\right] \right] \exp\left(\frac{E_{A_2}}{kT_B}\right) / Q'_B(T_B)$ as $E_{A_2} / \hat{q}_B^\infty(T_B)$. Furthermore, if we express the quantity contained in the first bracket of the above equation in a form similar to that exhibited by equation (II-58b) by substitution of equation (II-65a), we can remove the quantity as a factor and obtain

$$\begin{aligned}
T_3 = & - \frac{n_B}{\tau_B} \left[\hat{q}_B^\infty(T_B) - \hat{q}_B^\infty(T) \right] \left[\mathcal{L}'_B(T_B) + \frac{E_{A_2}(b-a)}{\hat{q}_B^\infty(T_B)} + \frac{E_{A_2}}{\hat{q}_B^\infty(T_B)} \left(\frac{\hat{k}_{a,a-1}^{(2)}}{\hat{k}_{1,0}^{(2)}} \right) \right] \\
& - \frac{n_B E_{A_2} m \hat{k}_{b-1,b}}{Q'_B(T_B)} \exp\left(\frac{E_{A_2}}{kT_B}\right) + \frac{n_B E_{A_2} m \hat{k}_{b,b-1}}{Q'_B(T_B)} \quad (\text{II-70b})
\end{aligned}$$

This equation has nearly the desired form and would be satisfactory except that it would be desirable if the second factor of the first term could be related to a truncation factor, say $\mathcal{L}_B(T_B)$, in order that the entire first term be similar to that obtained for T_1 , equation (II-58). Such a representation is possible if we note, using equation (II-44a), that $E_{A_2}(b-a) = E_b - E_a$ and introduce the following equation (A41) from Appendix A:

$$\mathcal{L}_B(T_B) = \mathcal{L}'_B(T_B) + \frac{E_b}{\hat{q}_B^\infty(T)} \quad (\text{II-71})$$

The first two terms in the second factor may be identified immediately; if we then multiply both the numerator and denominator of the terms that remain by $\mathcal{L}_B(T_B)$ (this is a valid operation since $\mathcal{L}_B(T_B)$ is never zero) and introduce equation (II-65a) to represent the denominator, we obtain the following desired form:

$$\begin{aligned} T_3 = & -\frac{n_B}{\tau_B} [\hat{q}_B^\infty(T_B) - \hat{q}_B^\infty(T)] \mathcal{L}_B(T_B) \left[1 - \frac{\hat{\Delta}(T)}{\hat{q}_B(T_B)} \right] \\ & - \frac{n_B E_{A_2} m \hat{k}_{b-1,b}}{Q'_B(T_B)} \exp\left(\frac{E_{A_2}}{kT_B}\right) + \frac{n_B E_{A_2} m \hat{k}_{b,b-1}}{Q'_B(T_B)} \end{aligned} \quad (\text{II-72})$$

The parameter $\hat{\Delta}(T)$, which has been introduced here, will be one of the essential parameters in the model equations and is defined by

$$\begin{aligned} \hat{\Delta} &= E_a - E_{A_1} a \delta \\ &= E_a \left[1 - \frac{\delta}{1 - \left(1 - \frac{E_{A_2}}{E_{A_1}}\right)/a} \right] \\ &\approx E_a (1 - \delta) \end{aligned} \quad (\text{II-73a})$$

where

$$\delta = \frac{E_{A_2}}{E_{A_1}} \frac{\hat{k}_{a,a-1}^{(2)}}{a \hat{k}_{1,0}^{(2)}}$$

or

$$\delta = \frac{\hat{k}_{1,0}^{(1)}}{\hat{k}_{1,0}^{(2)}} \quad (\text{II-73b})$$

and

$$\chi(T) = \frac{\hat{k}_{1,0}^{(2)}}{\hat{k}_{1,0}^{(1)}} = \delta^{-1} \quad (\text{II-73c})$$

The second representations for both $\hat{\Delta}$ and δ as given above follow directly after equations (II-44a) and (II-47) are introduced. The quantity $\chi(T)$ may be either χ_R , equation (B14), or χ_F , equation (B23). The parameters $\hat{\Delta}(T)$ and $\delta(T)$ will be called anharmonicity parameters (1) and (2), respectively; the values of these parameters are discussed in Appendix B. It is worthwhile to point out, however, that when $E_{A_1} = E_{A_2}$ and $\delta = 1$,[†] the anharmonicity parameter (1), $\hat{\Delta}(T)$, is zero. Furthermore, both parameters are temperature dependent, but the dependence of (1) on temperature is only through (2). It will turn out that when the effect of anharmonicity can be ignored, δ is unity and $\hat{\Delta}$ is zero, and when the effects of anharmonicity are large $0 \leq \delta \leq 1$ and $\hat{\Delta}(T) \approx E_a$.

It is helpful now to recall the definition of T_3 , as given by equation (II-59), and rewrite equation (II-72) as follows:

$$\begin{aligned} \sum_{v=b}^{N-2} (E_v - E_{v+1}) g_{v,v+1} &= \frac{n_B}{\tau_B} \left[\hat{q}_B^\infty(T) \mathcal{L}_B(T_B) - \hat{q}_B(T_B) \right] \left[1 - \frac{\hat{\Delta}(T)}{\hat{q}_B(T_B)} \right] \\ &\quad - \frac{n_B E_{A_2} m}{Q'_B(T_B)} \hat{k}_{b-1,b} \exp\left(\frac{E_{A_2}}{kT_B}\right) \\ &\quad + \frac{n_B E_{A_2} m}{Q'_B(T_B)} \hat{k}_{b,b-1} \end{aligned} \quad (\text{II-74a})$$

The last two terms in this equation are not readily reduced to a more simple representation involving known functions. One notes, however, that when the upper-state temperature T_B is equal to the translational or fluid temperature

[†] It will be shown in Appendix B that $\delta = 1$ implies $E_{A_2} = E_{A_1}$ and vice versa.

T, their sum is zero. As a result of vibrational nonequilibrium these terms are related to the net transfer of energy across the lowest state in the respective group of energy levels under consideration (in this case the group designated B). Comparable terms do not exist for a similar energy transfer across some uppermost state. In fact, the upper summation limit is implicitly embedded only in the truncation factor $\mathcal{L}_B(T_B)$ (recall that $\hat{q}_B(T_B) = \hat{q}_B^\infty(T_B) \mathcal{L}_B(T_B)$ and that $\hat{q}_B^\infty(T_B)$ is independent of any summation limits). These points are best exemplified by equation (II-74a) rewritten in such a manner that the dependence of the various quantities on the parameters are exhibited. This dependence has not been included in the notation heretofore in order to avoid excessive complication of the derivations and of the notation; in order to know the parameter dependence, one must refer to Appendix A. Rewriting equation (II-74a), using the appropriate functional representations, we obtain

$$\begin{aligned}
 & \left[\sum_{v=b}^{N-2} (E_v - E_{v+1}) g_{v,v+1} \right]_{T-V} = \\
 & \frac{n_B}{\tau(T; E_{A_2}, \hat{k}_{1,0}^{(2)})} \left[\hat{q}_B^\infty(T; E_{A_2}) - \hat{q}_B^\infty(T_B; E_{A_2}) \right] \mathcal{L}_B[T_B; (N-b), E_{A_2}] \\
 & \times \left\{ 1 - \frac{\hat{\Delta}\left(T; \frac{E_{A_2}}{E_{A_1}}, \frac{\hat{k}_{1,0}^{(2)}}{k_{1,0}^{(1)}}\right)}{\hat{q}_B^\infty(T_B; E_{A_2}) \mathcal{L}_B[T_B; (N-b), E_{A_2}]} \right\} - \frac{n_B E_{A_2} m \hat{k}_{b-1,b}}{Q'_B[T_B; (N-b), E_{A_2}]} \\
 & \times \exp\left(\frac{E_{A_2}}{kT_B}\right) + \frac{n_B E_{A_2} m \hat{k}_{b,b-1}}{Q'_B[T_B; (N-b), E_{A_2}]} \tag{II-74b}
 \end{aligned}$$

We note that changes in $(N - b)$, the difference of lower and upper sum parameters, affects the truncation factor \mathcal{L}_B , and the last two terms are affected also by changes in b . It should be emphasized that $\hat{\Delta}(T)$ is independent of either summation limit. If we desire to approximate the effects of anharmonicity better by introducing a new level separation, say a_1 , above which the energy

levels have a different energy spacing, and also have different linear transition probability functions, we will note that all the functions, including $\hat{\Delta}$, will be different, but only to the extent of their dependence on the parameters. The general functional character of equation (II-74) will be unchanged. No further remarks will be made concerning possible generalization of the method.

From these remarks the correct expression to use for T_2 (see eq. (II-49)) should now be evident. It is written as follows:

$$\begin{aligned}
 T_2 &\equiv \sum_{v=a}^{b-2} (E_v - E_{v+1}) g_{v+1,v} \\
 &= \frac{n_{A_2}}{\tau_B} \left[\hat{q}_B^\infty(T) - \hat{q}_B^\infty(T_A) \right] \mathcal{L}_{A_2}(T_A) \left[1 - \frac{\hat{\Delta}(T)}{\hat{q}_B^\infty(T_A) \mathcal{L}_{A_2}(T_A)} \right] \\
 &\quad - \frac{n_{A_2} E_{A_2} m}{Q'_{A_2}(T_A)} \hat{k}_{a-1,a} \exp\left(\frac{E_{A_2}}{kT_A}\right) + \frac{n_{A_2} E_{A_2} m}{Q'_{A_2}(T_A)} \hat{k}_{a,a-1} \quad (\text{II-75})
 \end{aligned}$$

We recall that the vibrational temperature of these states is T_A , since the states lie below b . Furthermore, in order to retain consistency in the notation we define $\hat{q}_{A_2}^\infty(T_A) \equiv \hat{q}_B^\infty(T_A)$ and write

$$\begin{aligned}
 \hat{q}_{A_2}(T) &= \hat{q}_B^\infty(T) \mathcal{L}_{A_2}(T) \\
 &= \hat{q}_{A_2}^\infty(T) \mathcal{L}_{A_2}(T) \quad (\text{II-76})
 \end{aligned}$$

All the required relations are now available such that the rate equations for the relaxation of vibrational energy, equations (II-40a) and (II-42), may be appropriately found. Substitution of equations (II-58a) and (II-75) into equation (II-49) yields for equation (II-40a)

$$\begin{aligned}
\frac{d}{dt} [n_A \hat{q}_A(T_A)]_{T-V} &= \frac{n_{A_1}}{\tau_{A_1}} [\hat{q}_{A_1}^\infty(T) \mathcal{L}_{A_1}(T_A) - \hat{q}_{A_1}(T_A)] \\
&+ \frac{n_{A_2}}{\tau_B} [\hat{q}_{A_2}^\infty(T) \mathcal{L}_{A_2}(T_A) - \hat{q}_{A_2}(T_A)] \times \left[1 - \frac{\hat{\Delta}(T)}{\hat{q}_{A_2}^\infty(T_A)} \right] \\
&+ (E_{a-1} - E_a) g_{a,a-1} - \frac{n_{A_2} E_{A_2} m}{Q'_{A_2}(T_A)} \hat{k}_{a-1,a} \exp\left(\frac{E_{A_2}}{kT_A}\right) \\
&+ \frac{n_{A_2} E_{A_2} m \hat{k}_{a,a-1}}{Q'_{A_2}(T_A)} + E_{b-1} \left[\frac{dn_A}{dt} \right]_{T-V} \quad (\text{II-77})
\end{aligned}$$

Investigating the separation term $(E_{a-1} - E_a) g_{a,a-1}$, we obtain the following expression after substitution of the g-function (eq. (II-9)), and the number-density ratios (see, e.g., eq. (A17) in Appendix A):

$$(E_{a-1} - E_a) g_{a,a-1} = m (E_{a-1} - E_a) \left[\frac{\hat{k}_{a,a-1} n_{A_2}}{Q'_{A_2}(T_A)} - \frac{\hat{k}_{a-1,a} n_{A_1}}{Q_{A_1}(T_A)} \exp\left(-\frac{E_{a-1}}{kT_A}\right) \right] \quad (\text{II-78})$$

Since the vibrational temperature of the states A_1 is the same as that of the states A_2 , namely T_A , we may relate n_{A_1} and n_{A_2} as follows:

$$n_{a-1} = \frac{n_{A_1}}{Q_{A_1}(T_A)} \exp\left(-\frac{E_{a-1}}{kT_A}\right) = \frac{n_{A_2}}{Q'_{A_2}(T_A)} \exp\left(-\frac{E_{a-1} - E_a}{kT_A}\right) \quad (\text{II-79})$$

There is a degree of arbitrariness as to whether the reduced spacing E_{A_2} first occurs between the levels $a-1$ and a or between levels a and $a+1$ without affecting the evaluation of the series while the closed-form expressions are being derived for the partition functions (see Appendix A). However, the choice taken (eq. (II-43)) is such that $E_{A_2} = E_a - E_{a-1}$. It follows that the separation term may be written

$$(E_{a-1} - E_a) g_{a,a-1} = -\frac{n_{A_2} E_{A_2} m}{Q'_{A_2}(T_A)} \hat{k}_{a,a-1} + \frac{n_{A_2} E_{A_2} m}{Q'_{A_2}(T_A)} \hat{k}_{a-1,a} \exp\left(\frac{E_{A_2}}{kT_A}\right) \quad (\text{II-80})$$

Furthermore, one observes that this term is just the negative of the two adjacent terms in equation (II-77). The lower-state energy rate equation thus becomes

$$\begin{aligned} \frac{d}{dt} [n_A \hat{q}_A(T_A)]_{T-V} &= \frac{n_{A_1}}{\tau_{A_1}} [\hat{q}_{A_1}^\infty(T) \mathcal{L}_{A_1}(T_A) - \hat{q}_{A_1}(T_A)] \\ &+ \frac{n_{A_2}}{\tau_B} [\hat{q}_{A_2}^\infty(T) \mathcal{L}_{A_2}(T_A) - \hat{q}_{A_2}(T_A)] \left[1 - \frac{\hat{\Delta}(T)}{\hat{q}_{A_2}(T_A)} \right] \\ &+ E_{b-1} \left[\frac{dn_A}{dt} \right]_{T-V} \end{aligned} \quad (\text{II-81})$$

The reasons for introducing the term leading to the identity given by equation (II-69b) should now be partially evident. It leads to a relatively simple representation for T_3 and, furthermore, to the cancellation of the separation term in equation (II-49) (the term in the series involving A-state levels that separates the A_1 - and A_2 -groupings of energy levels). It will be shown next that the expression introduced will also lead to a term in the upper-state vibrational-energy relaxation equation that is rate limiting in its effect on dissociation.

Before making this identification we substitute the summation represented by T_3 , equation (II-72), into equation (II-42) to obtain the upper-state energy relaxation equation

$$\begin{aligned} \frac{d}{dt} [n_B \hat{q}'_B(T_B)]_{T-V} &= \frac{n_B}{\tau_B} [\hat{q}_B^\infty(T) \mathcal{L}_B(T_B) - \hat{q}_B(T_B)] \left[1 - \frac{\hat{\Delta}(T)}{\hat{q}_B(T_B)} \right] \\ &- \frac{n_B E_{A_2} m}{Q'_B(T_B)} \hat{k}_{b-1,b} \exp\left(\frac{E_{A_2}}{kT_B}\right) + \frac{n_B E_{A_2} m}{Q'_B(T_B)} \hat{k}_{b,b-1} \end{aligned} \quad (\text{II-82a})$$

The significance of the last two terms in this equation becomes apparent if we substitute the appropriate expression relating the quantities $\hat{q}'_B(T_B)$ and $\hat{q}_B(T_B)$, using equation (II-38c), and introduce equations (II-41) into the resulting equation:

$$\begin{aligned}
\frac{d}{dt} [n_B \hat{q}_B(T_B)]_{T-V} &= \frac{n_B}{\tau_B} [\hat{q}_B^\infty(T) \mathcal{L}_B(T_B) - \hat{q}_B(T_B)] \left[1 - \frac{\hat{\Delta}(T)}{\hat{q}_B(T_B)} \right] \\
&+ (E_{b-1} - E_b) g_{b,b-1} - E_{b-1} \left[\frac{dn_A}{dt} \right]_{T-V} \\
&- \frac{n_B E_{A_2} m}{Q'_B(T_B)} \hat{k}_{b-1,b} \exp\left(\frac{E_{A_2}}{kT_B}\right) + \frac{n_B E_{A_2} m}{Q'_B(T_B)} \hat{k}_{b,b-1}
\end{aligned} \tag{II-82b}$$

In this case, the quantity in the above equation involving the g-function is given by

$$- E_{A_2} m \left[\frac{\hat{k}_{b,b-1} n_B}{Q'_B(T_B)} - \frac{n_A \hat{k}_{b-1,b}}{Q_A(T_A)} \exp\left(\frac{E_{b-1}}{kT_A}\right) \right]$$

These terms do not lead to a complete cancellation of their equivalents in the above rate equation in the manner that the analogous terms lead to cancellations in equations (II-77), but lead to the expression displayed as the last term in the equation that follows:

$$\begin{aligned}
\frac{d}{dt} [n_B \hat{q}_B(T_B)]_{T-V} &= \frac{n_B}{\tau_B} [\hat{q}_B^\infty(T) \mathcal{L}_B(T_B) - \hat{q}_B(T_B)] \left[1 - \frac{\hat{\Delta}(T)}{\hat{q}_B(T_B)} \right] \\
&- E_{b-1} \left[\frac{dn_A}{dt} \right]_{T-V} + E_{A_2} n_A m \hat{k}_F^{(1)}(T_A, T) \\
&\times \left\{ 1 - \frac{n_B}{n_A} \frac{Q_A(T_A)}{Q_B(T_B)} \exp\left[-E_{b-1} \left(\frac{1}{T_B} - \frac{1}{T_A}\right)\right] \right\} \tag{II-82c}
\end{aligned}$$

where we have introduced the rate constant $\hat{k}_F^{(1)}(T_A, T)$, defined by equation (II-39b), to simplify the notation. The dependent variables n_A and n_B are not necessarily related in terms of a ratio of partition functions in the manner that we found for n_{A_1} and n_{A_2} . Their values depend on the complete solution of the model equations. Only when the upper and lower temperatures, T_A and T_B , are equal will the ratio of upper and lower population densities be

related to a ratio of partition functions. The last term in the above equation will then be zero. It will be shown in Chapter IV, when the parameter b is appropriately evaluated, that the last term has the effect of limiting the rate of dissociation; for this reason the level b will be denoted the "rate-limiting" level. At this time the term represents the net rate of transfer of energy across a level b that separates those levels with populations with a temperature T_A from those levels with a temperature T_B .

The equations considered thus far are applicable only for translation-vibration energy interchange in a gas containing a relatively dilute mixture of molecules, that is, for vibrational nonequilibrium processes that may be properly described by the first chemical equation, equation (II-1). The equations that finally result (eqs. (II-34a,b), (II-81), (II-82c), and eqs. (II-39)) are sufficient to describe the internal properties of a gas, provided the effects of dissociation are negligible (and also the effects of resonance vibration-vibration energy interchange, which will not be considered in this paper). When there is appreciable dissociation and/or recombination, additional complication will ensue. In the next section these complications will be taken into account.

(II-B-3). Dissociation

This section deals with obtaining the set of rate equations that are valid for describing the translation-vibration energy interchange involving dissociation. Four rate equations, subscripted D , will result from the analysis, and will be combined with the equations found in the previous sections to yield the relations needed for the study of vibration-dissociation coupling.

The procedure for obtaining the model equations for the dissociation process is similar to that already used. In the previous sections the effect of vibration-translation energy interchange, resulting in vibrational relaxation, was investigated by obtaining zeroth and first moment equations of the population distribution using equations (II-5) as the basic equations. These moment relations were then simplified by the introduction of various assumptions yielding the final equations (II-34), (II-39), (II-81), and (II-82c), which contain a

relatively small number of parameters. The procedure involved a method of accounting for molecular anharmonicity effects both in the energy level spacing and in the transition probabilities.

This section will be based on equation (II-7). The procedure for simplifying this equation will be similar to that used in the previous sections in that the zeroth and first moment equations of the population distribution will again be obtained. The procedure will deviate to the extent that the preferential dissociation model of Marrone and Treanor (58) will be introduced to obtain simple relations describing the dissociation. Anharmonicity effects will be accounted for by using the energy-level spacings introduced in the previous sections. The preferential dissociation model of Marrone and Treanor is described in detail in Appendix C. Suffice it to say here that the Marrone and Treanor model provides a method whereby one may reasonably approximate the level transition probabilities $\hat{k}_{v,N}^r$ and $\hat{k}_{N,v}^r$. Their scheme is simple and its employment introduces few additional unknowns into the problem. The essence of the model is that the probability of dissociation is exponentially weighted in such a manner that dissociation from the uppermost levels is most likely. In the derivations that follow the Marrone-Treanor model will be slightly modified. In particular, it will be assumed that dissociation and recombination involving molecules in the A-group of energy states are so improbable that they may be neglected.

The zeroth moment expression of the population distribution for the interactions involving dissociation is obtained by summing equation (II-7) over the subscript v , including only those states in the sum appropriate to the group of energy states under consideration. The result for the A-states is

$$\left[\frac{dn_A}{dt} \right]_D = \sum_{v=0}^{b-1} \left[\frac{dn_v}{dt} \right]_D = \sum_{v=0}^{b-1} \sum_{r=1}^s \left[-\hat{k}_{v,N}^r n_r m_r + \hat{k}_{N,v}^r n_a^2 m_r \right] \quad (\text{II-83})$$

As already mentioned, however, dissociation and recombination of molecules in these states is assumed to be extremely improbable. Therefore

$$\hat{k}_{v,N}^r = \hat{k}_{N,v}^r \approx 0 \quad v \leq b - 1 \quad (\text{II-84})$$

and we have

$$\left[\frac{dn_A}{dt} \right]_D = 0 \quad (\text{II-85})$$

Similarly, the first moment relation of the A-state population distribution, obtained by multiplying equation (II-7) by E_V and then summing, is also zero; that is,

$$\frac{d[n_A \hat{q}_A(T_B)]_D}{dt} = 0 \quad (\text{II-86})$$

The direct effect of dissociation will then only be felt by the upper group of molecular energy states.

Before proceeding with the derivations it will be helpful to remove from the equations the effect of the dependence on r , that is, on the kind of species involved in the collision. This may be done by either temporarily ignoring the effect, as was done earlier, or by removing it by an appropriate averaging procedure. We do the latter by writing

$$\left[\frac{dn_V}{dt} \right]_D = -n_V m \bar{k}_{V,N} + n_A^2 m \bar{k}_{N,V} \quad (\text{II-87})$$

where the rates $\bar{k}_{V,N}$ and $\bar{k}_{N,V}$ are defined by the averages

$$\bar{k}_{V,N} = \sum_{r=1}^S \frac{m_r}{m} \hat{k}_{V,N}^r \quad (\text{II-88a})$$

$$\bar{k}_{N,V} = \sum_{r=1}^S \frac{m_r}{m} \hat{k}_{N,V}^r \quad (\text{II-88b})$$

As previously remarked, only dilute molecular mixtures are being considered; that is, we assume that the mixture contains relatively small concentrations of molecules and of atoms obtained by molecular dissociation, plus some inert species that is the major constituent (e.g., argon). If the population fractions m_r/m are sufficiently small for the molecules and reacting atoms compared with that for the inert species, equation (II-87) may be accurately represented

if the quantities \hat{k} are those of the inert species only. To simplify notation we will henceforth ignore the bar on \hat{k} .

Using the equations given above we now write the zeroth and first moment expressions for the B-group of molecular energy states as follows:

$$\left[\frac{dn_B}{dt} \right]_D = - \sum_{v=b}^{N-1} \hat{k}_{v,N} n_v m + \sum_{v=b}^{N-1} \hat{k}_{N,v} n_a^2 m \quad (\text{II-89})$$

$$\frac{d [n_B \hat{q}_B(T_B)]_D}{dt} = - \sum_{v=b}^{N-1} \hat{k}_{v,N} E_v n_v m + \sum_{v=b}^{N-1} \hat{k}_{N,v} E_v n_a^2 m \quad (\text{II-90})$$

where n_B and $\hat{q}_B(T_B)$ are the quantities defined previously by equations (II-21) and (II-38b). The transition rates $\hat{k}_{v,N}$ and $\hat{k}_{N,v}$ peculiar to the preferential-dissociation model, are derived in Appendix C (see eq. (C14)). The expressions given in the appendix may be substituted into the above equations. In addition, if one notes the identities $\sum_{v=0}^{N-1} p_v = 1$, $\sum_{v=b}^{N-1} E_v p_v = \hat{q}_B(T_F)$, and

$\sum_{v=b}^{N-1} E_v p_{veq.} = \hat{q}_B(-T_U)$, we obtain the following equations:

$$\left[\frac{dn_B}{dt} \right]_D = - \hat{k}_{F\text{eq.}}(T) V(T_B, T) n_B m + \frac{\hat{k}_{F\text{eq.}}(T)}{\kappa_B(T)} n_a^2 m \quad (\text{II-91})$$

$$\left[\frac{dn_B \hat{q}_B(T_B)}{dt} \right]_D = - \hat{q}_B(T_F) n_B m \hat{k}_{F\text{eq.}}(T) V(T_B, T) + \hat{q}_B(-T_U) \frac{\hat{k}_{F\text{eq.}}(T) n_a^2 m}{\kappa_B(T)} \quad (\text{II-92})$$

where the quantity $\hat{k}_{F\text{eq.}}(T)$ is the equilibrium dissociation rate (i.e., the rate applicable when the vibrational mode is assumed to be in equilibrium). This quantity is discussed further in Chapter III. The function $\kappa_B(T)$ is the partial equilibrium constant (see Appendix C, eq. (C13)); the quantities p_v are normalized probabilities that are also discussed in Appendix C; and the factor $V(T_B, T)$, called the vibrational coupling factor after Marrone and Treanor (58), is a known

function containing ratios of upper-state vibrational partition functions as follows (see Appendix C for discussion):

$$V(T_B, T) = \frac{Q_B(T) Q_B(T_F)}{Q_B(T_B) Q_B(-T_U)} \quad (\text{II-93})$$

The variable T_F is the characteristic temperature at which energy is removed by dissociation (distinct from the dissociation temperature, Θ_D ; see Appendix A) and is defined as follows (from eq. (C7))

$$\frac{1}{T_F} = \frac{1}{T_B} - \frac{1}{T} - \frac{1}{T_U} \quad (\text{II-94})$$

The negative quantity T_U (a constant) in the above relations may be considered as the characteristic "vibrational temperature" (pointed out by Marrone and Treanor (58)) at which energy is returned to the vibrational mode after recombination. The value of T_U also describes how rapidly the dissociation probability drops off for the lower vibrational energy levels. The assigned value of T_U is discussed in the next chapter.

(II-B-4). Combined Effect of Vibrational Excitation and Dissociation

The model equations obtained in the earlier sections, equations (II-34), (II-81), and (II-82c), may now be generalized to be valid when the effects of dissociation and recombination are important. The generalization for the number densities requires the superposing of equations (II-34), (II-85), and (II-91) (see, e.g., eq. (II-8) and the discussion following that equation). The result is

$$\frac{dn_A}{dt} = m \left[n_B \hat{k}_R^{(1)}(T_B, T) - n_A \hat{k}_F^{(1)}(T_A, T) \right] \quad (\text{II-95a})$$

$$\frac{dn_B}{dt} = -\frac{dn_A}{dt} - \hat{k}_{F \text{ eq.}}(T) V(T_B, T) n_B m + \frac{\hat{k}_{F \text{ eq.}}(T) n_a^2 m}{\kappa_B(T)} \quad (\text{II-95b})$$

The energy rate equations are obtained by superposing equations (II-81), (II-82c), and (II-86), (II-92), respectively. We obtain

$$\begin{aligned}
\frac{d [n_A \hat{q}_A(T_A)]}{dt} &= \frac{n_A}{Q_A(T_A)} \left\{ \frac{Q_{A_1}(T_A)}{\tau_{A_1}} [\hat{q}_{A_1}^\infty(T) \mathcal{L}_{A_1}(T_A) - \hat{q}_{A_1}(T_A)] \right. \\
&\quad \left. + \frac{Q_{A_2}(T_A)}{\tau_{A_2}} [\hat{q}_{A_2}^\infty(T) \mathcal{L}_{A_2}(T_A) - \hat{q}_{A_2}(T_A)] \left[1 - \frac{\hat{\Delta}(T)}{\hat{q}_{A_2}(T_A)} \right] \right\} \\
&\quad + E_{b-1} \frac{dn_A}{dt} \tag{II-95c}
\end{aligned}$$

$$\begin{aligned}
\frac{d [n_B \hat{q}_B(T_B)]}{dt} &= \frac{n_B}{\tau_B} [\hat{q}_B^\infty(T) \mathcal{L}_B(T_B) - \hat{q}_B(T_B)] \left[1 - \frac{\hat{\Delta}(T)}{\hat{q}_B(T_B)} \right] - E_{b-1} \frac{dn_A}{dt} \\
&\quad + E_{A_2} n_A m \hat{k}_F^{(1)}(T_A, T) \left\{ 1 - \frac{n_B}{n_A} \frac{Q_A(T_A)}{Q_B(T_B)} \exp \left[-E_{b-1} \right. \right. \\
&\quad \left. \left. \times \left(\frac{1}{T_B} - \frac{1}{T_A} \right) \right] \right\} \\
&\quad - \hat{q}_B(T_F) n_B m \hat{k}_{Feq.}(T) V(T_B, T) \\
&\quad + \frac{\hat{q}_B(-T_U) n_a^2 m \hat{k}_{Feq.}(T)}{\kappa_B(T)} \tag{II-95d}
\end{aligned}$$

In equation (II-95c) the densities n_{A_1} and n_{A_2} have been expressed in terms of the dependent variable n_A and appropriate ratios of partition functions (see, e.g., eq. (A19) in Appendix A).

The above equations are cumbersome in their present form, and a more concise formulation is desirable. With this in mind the following notation will be adopted.

$$\hat{\Omega}_{A_1}^\infty(T, T_A) = \hat{q}_{A_1}^\infty(T) - \hat{q}_{A_1}^\infty(T_A) \tag{II-96a}$$

$$\hat{\Omega}_{A_2}^\infty(T, T_A) = \hat{q}_{A_2}^\infty(T) - \hat{q}_{A_2}^\infty(T_A) \tag{II-96b}$$

$$\hat{\Omega}_B^\infty(T, T_B) = \hat{q}_B^\infty(T) - \hat{q}_B^\infty(T_B) \tag{II-96c}$$

$$\hat{\Omega}_{A_1}(T, T_A) = \hat{\Omega}_{A_1}^{\infty}(T, T_A) \mathcal{L}_{A_1}(T_A) \quad (\text{II-97a})$$

$$\hat{\Omega}_{A_2}(T, T_A) = \hat{\Omega}_{A_2}^{\infty}(T, T_A) \mathcal{L}_{A_2}(T_A) \quad (\text{II-97b})$$

$$\hat{\Omega}_B(T, T_B) = \hat{\Omega}_B^{\infty}(T, T_B) \mathcal{L}_B(T_B) \quad (\text{II-97c})$$

There is some redundancy in the above notation, equations (II-96), since $\hat{q}_{A_2}^{\infty} = \hat{q}_B^{\infty}$ and hence $\hat{\Omega}_{A_2}^{\infty} = \hat{\Omega}_B^{\infty}$ when $T_A = T_B$. However, this redundancy is removed in equations (II-97). The quantities $\hat{\Omega}_{A_2}$ and $\hat{\Omega}_B$ are not necessarily equal even when the temperatures T_A and T_B are equal. The quantities Ω defined above may be considered as measures of the departure of the respective grouping of vibrational energy levels from local thermodynamic equilibrium. When the argument temperatures are equal, these quantities are zero, and as the differences of the argument temperatures increase in a uniform manner the quantities themselves also increase in a uniform manner. In addition to the foregoing we also write

$$\left[\frac{dn}{dt} \right]_F = \hat{k}_{F \text{eq.}}(T) V(T_B, T) n_B m \quad (\text{II-98a})$$

$$\left[\frac{dn}{dt} \right]_R = \hat{k}_{F \text{eq.}}(T) \frac{n_a^2 m}{\kappa_B(T)} \quad (\text{II-98b})$$

This notation has been used previously by Marrone and Treanor (58,93). The first expression denotes the rate at which molecules dissociate and the second is the rate at which molecules are formed as a result of recombination. That these expressions apply appropriately to the molecules and not just to the upper grouping of energy states is evident if we sum equations (II-95a) and (II-95b) and note that $n = n_A + n_B$ is the total molecular density including all vibrational states.

We now rewrite equations (II-95) using the notation of equations (II-96), (II-97), and (II-98). There results

$$\frac{dn_A}{dt} = m \left[n_B \hat{k}_R^{(1)}(T_B, T) - n_A \hat{k}_F^{(1)}(T_A, T) \right] \quad (\text{II-99a})$$

$$\frac{dn_B}{dt} = -\frac{dn_A}{dt} - \left[\frac{dn}{dt} \right]_F + \left[\frac{dn}{dt} \right]_R \quad (\text{II-99b})$$

$$\begin{aligned} \frac{d[n_A \hat{q}_A(T_A)]}{dt} &= \frac{n_A}{Q_A(T_A)} \left\{ \frac{Q_{A_1}(T_A)}{\tau_{A_1}} \hat{\Omega}_{A_1}(T, T_A) + \frac{Q_{A_2}(T_A)}{\tau_{A_2}} \hat{\Omega}_{A_2}(T, T_A) \right. \\ &\quad \left. \times \left[1 - \frac{\hat{\Delta}(T)}{\hat{q}_{A_2}(T_A)} \right] \right\} + E_{b-1} \frac{dn_A}{dt} \end{aligned} \quad (\text{II-99c})$$

$$\begin{aligned} \frac{d[n_B \hat{q}_B(T_B)]}{dt} &= \frac{n_B}{\tau_B} \hat{\Omega}_B(T, T_B) \left[1 - \frac{\hat{\Delta}(T)}{\hat{q}_B(T_B)} \right] - E_{b-1} \frac{dn_A}{dt} - \hat{q}_B(T_F) \left[\frac{dn}{dt} \right]_F \\ &\quad + \hat{q}_B(-T_U) \left[\frac{dn}{dt} \right]_R + E_{A_2} n_A m \hat{k}_F^{(1)}(T_A, T) \\ &\quad \times \left\{ 1 - \frac{n_B}{n_A} \frac{Q_A(T_A)}{Q_B(T_B)} \exp \left[-\Theta_{b-1} \left(\frac{1}{T_B} - \frac{1}{T_A} \right) \right] \right\} \end{aligned} \quad (\text{II-99d})$$

The above equations together with the atom conservation equation

$$n + \frac{n_a}{2} = n_A + n_B + \frac{n_a}{2} = \text{constant} \quad (\text{II-99e})$$

constitute the complete set of equations required to determine the internal properties (vibrational mode) of the gas and thereby the effects of vibration-dissociation coupling. Since these equations are a complete set it is perhaps fitting to summarize the physical significance of the various terms and then compare these equations with those used by the other researchers.

The individual terms in the first two equations are easily identified. The terms in equation (II-99a) represent the gain and loss of the A-state molecules due to the transitions yielding B-states. The first term in equation (II-99b) represents the converse processes, that is, the net effects on the B-states due to the transitions that yield A-states. The second and third terms represent the loss and gain of B-state molecules as a result, respectively, of molecular dissociation and recombination.

The energy equations (II-99c) are slightly more complex than the population equations just described. The terms within the braces of the A-state vibrational-energy equation (II-99c) represent the relaxation of vibrational energy for the subgroups A_1 and A_2 of the A-states where each sub-group has different associated characteristic relaxation times. The first term in the braces is for the subgroup of states denoted A_1 that has an associated characteristic relaxation time τ_{A_1} and the second term is for the subgroup denoted A_2 that has a relaxation time τ_{A_2} . It is worthwhile to remark that although $\tau_{A_2} < \tau_{A_1}$, this effect is counteracted by the partition-function fractions Q_{A_1}/Q_A and Q_{A_2}/Q_A . As a result, the lower state vibrational relaxation depends most strongly on the first term, in particular, when the temperature T_A is not large (e.g., see Chapter IV). The third term in equation (II-99c) represents the rate of gain (or loss) of vibrational energy from the A-states due to transitions from B to A states (or the reverse). The first term in equation (II-99d) describes the vibrational-energy relaxation occurring in the B-states. The second term is the converse of the similar term in equation (II-99c), while the third and fourth terms represent the loss and gain of the vibrational energy of the B-states due to dissociation and recombination. The last term represents an additional gain (or loss) of net vibrational energy due to the interaction with the translational mode. Such an effect arises when molecules make transitions from a system at one temperature T_A to a system at a different temperature T_B . This term is zero when the two temperatures are equal. It is difficult to ascribe a direct physical significance to this term, because of the manner in which it was introduced. It will be shown in Chapter IV that a similar term yields a rate-limiting effect on the rate equations. In this respect the term may produce the effect analogous to the "bottle-neck" discussed by Bray (14) and by Pritchard (71).

It is worthwhile to compare these equations (II-99) with those used by Marrone and Treanor (58) in their study of vibration-dissociation coupling. In the Marrone-Treanor model the assumption was made that the distribution of energy in the vibrational energy states can be described by a single vibrational

temperature T_V . Here we have introduced an additional temperature into the description. Furthermore, in the Marrone-Treanor model the effects of anharmonicity were accounted for only to the extent that more accurate quantities for the thermodynamic energy function were used (it will be shown that this is not essential). It was not possible with their formulation to account for effective decreases in characteristic vibrational relaxation time for the upper levels that occur as a result of molecular anharmonicity.

Although the model presented here contains additional detail as regards the description of the vibrational degrees of freedom, it also includes additional complication. There may be problems where the additional complication is not warranted and the Marrone-Treanor model will be of value. With this in mind it is worthwhile to investigate the functional form of the rate equations derived in this paper as the complexity is reduced by further assumptions.

We first assume (58,93) that a single temperature is appropriate for a description of the vibrational mode, that is, $T_V = T_A = T_B$. We observe that the last term in equation (II-99d) then vanishes. The subscripts A and B are no longer significant and we, therefore, can combine equations (II-99a) and (II-99b) to obtain

$$\left[\frac{dn}{dt} \right] = - \left[\frac{dn}{dt} \right]_F + \left[\frac{dn}{dt} \right]_R \quad (\text{II-100})$$

Likewise we combine equations (II-99c) and (II-99d) to obtain

$$\begin{aligned} \frac{d}{dt} [n\hat{q}(T_V)] &= \frac{n_A}{\tau_{A_1}} \frac{Q_{A_1}(T_V)}{Q_A(T_V)} \hat{\omega}_{A_1}(T, T_V) + \frac{n_A}{\tau_B} \frac{Q_{A_2}(T_V)}{Q_A(T_V)} \hat{\omega}_{A_2}(T, T_V) \\ &\times \left[1 - \frac{\hat{\Delta}(T)}{\hat{q}_{A_2}(T_V)} \right] + \frac{n_B}{\tau_B} \hat{\omega}_B(T, T_B) \left[1 - \frac{\hat{\Delta}(T)}{\hat{q}_B(T_V)} \right] \\ &- \hat{q}_B(T_F) \left[\frac{dn}{dt} \right]_F + \hat{q}_B(-T_U) \left[\frac{dn}{dt} \right]_R \end{aligned} \quad (\text{II-101})$$

where we have used

$$n\hat{q}(T_V) = n_A \hat{q}_A(T_V) + n_B \hat{q}_B(T_V) \quad (\text{II-102})$$

A more useful formulation of the above equation is obtained by first relating the densities n_A and n_B in terms of the net molecular density n and appropriate ratios of partition functions. There results

$$\begin{aligned} \frac{dn\hat{q}(T_V)}{dt} &= \frac{n}{Q_V(T_V)} \left\{ \frac{Q_{A_1}(T_V)}{\tau_{A_1}} \hat{\omega}_{A_1}(T, T_V) + \frac{Q_{A_2}(T_V)}{\tau_B} \hat{\omega}_{A_2}(T, T_V) \left[1 - \frac{\hat{\Delta}(T)}{\hat{q}_{A_2}(T_V)} \right] \right. \\ &\quad \left. + \frac{Q_B(T_V)}{\tau_B} \hat{\omega}_B(T, T_B) \left[1 - \frac{\hat{\Delta}(T)}{\hat{q}_B(T_V)} \right] \right\} - \hat{q}_B(T_V) \left[\frac{dn}{dt} \right]_F \\ &\quad + \hat{q}_B(-T_U) \left[\frac{dn}{dt} \right]_R \end{aligned} \quad (\text{II-103a})$$

We then combine the second pair of terms in braces to obtain the desired formulation

$$\begin{aligned} \frac{dn\hat{q}(T_V)}{dt} &= \frac{n}{Q_V(T_V)} \left\{ \frac{Q_{A_1}(T_V)}{\tau_{A_1}} \hat{\omega}_{A_1}(T, T_V) + \frac{Q_{A_2-B}(T_V)}{\tau_B} \hat{\omega}_{A_2-B}(T, T_V) \right. \\ &\quad \left. \times \left[1 - \frac{\hat{\Delta}(T)}{\hat{q}_{A_2-B}(T_V)} \right] \right\} - \hat{q}_B(T_V) \left[\frac{dn}{dt} \right]_F + \hat{q}_B(-T_U) \left[\frac{dn}{dt} \right]_R \end{aligned} \quad (\text{II-103b})$$

where the following relations have been introduced, consistent with the previously defined similar quantities:

$$Q_{A_2-B}(T_V) = Q_{A_2}(T_V) + Q_B(T_V) \quad (\text{II-104a})$$

$$Q_{A_2-B}(T_V) \mathcal{L}_{A_2-B}(T_V) = Q_{A_2}(T_V) \mathcal{L}_{A_2}(T_V) + Q_B(T_V) \mathcal{L}_B(T_V) \quad (\text{II-104b})$$

$$\hat{q}_{A_2-B}(T_V) = \hat{q}_{A_2}(T_V) \mathcal{L}_{A_2-B}(T_V) \quad (\text{II-104c})$$

The subscript A_2-B is used to denote the union of the vibrational states contained in the groups A_2 and B .

Equations (II-100) and (II-103b) are analogous to those used by Marrone and Treanor (58). We observe, however, that to account for the effect of anharmonicity it is not sufficient merely to use more accurate values for the vibrational energy function \hat{q} in the same manner as Marrone and Treanor, but an additional term must be introduced. This term is the second term given in the braces of equation (II-103b). If we are able to neglect the effects of anharmonicity (that is, if $\hat{\Delta}(T)/\hat{q}_{A_2-B}(T_V) \approx 0$ and $E_{A_1}/E_{A_2} \approx 1$) the terms in braces may be combined (see, e.g., eq. (A19) in Appendix A). Equation (II-103b) may then be written as follows:

$$\frac{dn\hat{q}(T_V)}{dt} = \frac{n}{\tau_{A_1}} \hat{\Omega}(T, T_V) - \hat{q}_B(T_F) \left[\frac{dn}{dt} \right]_F + \hat{q}_B(-T_U) \left[\frac{dn}{dt} \right]_R \quad (\text{II-105})$$

where

$$\hat{\Omega}(T, T_V) = [\hat{q}^\infty(T) - \hat{q}^\infty(T_V)] \mathcal{L}(T_V) \quad (\text{II-106a})$$

$$= \hat{q}(T) \frac{\mathcal{L}(T_V)}{\mathcal{L}(T)} - \hat{q}(T_V) \quad (\text{II-106b})$$

The exclusion of subscripts on the relevant quantities denotes that the vibrational states are all considered together as a group. The representation given above, with the exception of the dissociation and recombination terms, is similar to the form of equation (II-58c), which prompted the previous remarks (given after eq. (II-58c)). In this equation the effects of anharmonicity are assumed negligible (or ineffectual), and it is only the existence of the truncation factor ratio $\mathcal{L}(T_V)/\mathcal{L}(T)$ that causes the equation to differ from that used by Marrone and Treanor (58). The differences in the equations are not important provided that the temperatures T and T_V are both much less than the characteristic dissociation temperature $\Theta_D = E_{n-1}/k$. The truncation-factor ratio is then of order unity. For this case, however, there is negligible dissociation and the problem is not of great interest. At the higher temperatures, say $T = 16,500^\circ$ and $T_V = 300^\circ$ K, the factor $\mathcal{L}(T_V)/\mathcal{L}(T)$ for the example case of molecular oxygen is about 3, and hence the differences become important and

the Marrone-Treanor formulation questionable. This is discussed further in Appendix D.

II-C. The Rate Equations Applicable to Fluid-Flow Problems

In the previous sections the model rate equations have been derived that are applicable for studies of vibration-dissociation coupling. In these equations the time derivatives have been introduced without any discussion regarding their significance. To apply such equations to problems involving a moving fluid requires that some consideration be given to these derivatives. Formally, the equations that have been derived apply to a constant-mass, constant-volume system such as provided by a closed rigid container. To be applicable to a moving fluid this constraint must be removed. The procedure for doing this is described clearly by Vincenti and Kruger (p. 248 (97)). Briefly, we let σ represent any one of the variables (per unit volume) n_A , n_B , $(n_A \hat{q}_A)$, or $(n_B \hat{q}_B)$. The equations applicable to fluid flows, if we neglect diffusion effects, are given by

$$\frac{D\Sigma}{Dt} = \frac{1}{\rho} \frac{d\sigma}{dt} \quad (\text{II-107})$$

where Σ is the intensive (per unit mass) counterpart of the variable σ ($\sigma = \rho\Sigma$), and $\frac{D}{Dt}$ is the substantial or material derivative $\left(\frac{D}{Dt} = \frac{\partial}{\partial t} + \vec{v} \cdot \nabla\right)$. The variable \vec{v} is the mass velocity of the fluid. Since the equations for the derivative $d\sigma/dt$ have been derived for a closed fixed-volume system, the density ρ may be taken inside or outside this derivative as we wish.

The equations derived previously, equations (II-99), are readily modified to a form that is applicable for flow field calculations by simply changing the dependent variables to the Σ quantities. The equations will be listed below in terms of the appropriate variables, and this list will serve as a summary of the results heretofore obtained. The intensive variables γ_i and ϵ_i corresponding to the Σ quantities are defined by

$$\gamma_m = \frac{n_m}{\rho N_0} \quad (\text{II-108a})$$

$m = A, B, \text{ or } a$

$$\epsilon_i = \gamma_i q_i = \gamma_i N_o \hat{q}_i$$

$$i = A, A_1, A_2, \text{ or } B \quad (\text{II-108b})$$

where N_o is Avogadro's number. The rate parameters in the equations are defined according to the relations

$$k_{\text{Feq.}}^r(T) = N_o \hat{k}_{\text{Feq.}}^r(T) \quad (\text{II-109a})$$

$$k_{\text{R}}^{r,(i)}(T_B, T) = N_o \hat{k}_{\text{R}}^{r,(i)}(T_B, T) \quad (\text{II-109b})$$

$$k_{\text{F}}^{r,(i)}(T_A, T) = N_o \hat{k}_{\text{F}}^{r,(i)}(T_A, T) \quad (\text{II-109c})$$

With these quantities the rate equations become[†]

$$\frac{D\gamma_A}{Dt} = \rho \gamma_m \left[\gamma_B \sum_r \frac{\gamma_r}{\gamma_m} k_{\text{R}}^{r,(i)}(T_B, T) - \gamma_A \sum_r \frac{\gamma_r}{\gamma_m} k_{\text{F}}^{r,(i)}(T_B, T) \right] \quad (\text{II-110a})$$

$$\frac{D\gamma_B}{Dt} = -\frac{D\gamma_A}{Dt} - \left(\frac{D\gamma}{Dt} \right)_F + \left(\frac{D\gamma}{Dt} \right)_R \quad (\text{II-110b})$$

$$\begin{aligned} \frac{D\epsilon_A}{Dt} = & \frac{\gamma_A}{Q_A(T_A)} \sum_r \frac{1}{\tau_{A_1}^r} \left\{ Q_{A_1}(T_A) \Omega_{A_1}(T, T_A) + Q_{A_2}(T_A) \left(\frac{\tau_{A_1}^r}{\tau_B^r} \right) \Omega_{A_2}(T, T_A) \right. \\ & \left. \times \left[1 - \frac{\Delta^r(T)}{q_{A_2}(T_A)} \right] \right\} + R_o \Theta_{b-1} \frac{D\gamma_A}{dt} \end{aligned} \quad (\text{II-110c})$$

[†]In equations (II-110) the effects of the type of collision partner have been re-introduced into the equations. This requires introducing the superscripts and sums for r . These equations are the model equations for the reactions (II-1) and (II-3) when the effects of vibration-vibration energy interchange (II-2) may be considered negligible.

$$\begin{aligned}
\frac{D\epsilon_B}{Dt} &= \gamma_B \Omega_B(T, T_B) \sum_{\mathbf{r}} \frac{1}{\tau_{B\mathbf{r}}} \left[1 - \frac{\Delta^{\mathbf{r}}(T)}{q_B(T_B)} \right] - R_0 \Theta_{b-1} \frac{D\gamma_A}{Dt} \\
&\quad - q_B(T_F) \left(\frac{D\gamma}{Dt} \right)_F + q_B(-T_U) \left(\frac{D\gamma}{Dt} \right)_R + R_0 \Theta_{A_2} \rho \gamma_A \gamma_m \sum_{\mathbf{r}} \frac{\gamma_{\mathbf{r}}}{\gamma_m} \\
&\quad k_{F_1}^{\mathbf{r},(1)}(T_A, T) \left\{ 1 - \frac{\gamma_B}{\gamma_A} \frac{Q_A(T_A)}{Q_B(T_B)} \exp \left[-\Theta_{b-1} \left(\frac{1}{T_B} - \frac{1}{T_A} \right) \right] \right\} \quad (\text{II-110d})
\end{aligned}$$

$$\frac{D\gamma_a}{Dt} = -2 \left\{ - \left(\frac{D\gamma}{Dt} \right)_F + \left(\frac{D\gamma}{Dt} \right)_R \right\} \quad (\text{II-110e})$$

The last equation is obtained by differentiating the atom-conservation equation (II-99e). The molecular rate terms subscripted F and R are defined by

$$\left(\frac{D\gamma}{Dt} \right)_F = \rho V(T_B, T) \gamma_B \gamma_m \sum_{\mathbf{r}} \frac{\gamma_{\mathbf{r}}}{\gamma_m} k_{F\text{eq.}}^{\mathbf{r}}(T) \quad (\text{II-111a})$$

$$\left(\frac{D\gamma}{Dt} \right)_R = \frac{\rho^2 \gamma_a^2 \gamma_m}{\kappa_B(T)} \sum_{\mathbf{r}} \frac{\gamma_{\mathbf{r}}}{\gamma_m} k_{F\text{eq.}}^{\mathbf{r}}(T) \quad (\text{II-111b})$$

The constants Θ_{b-1} and Θ_{A_2} are characteristic temperatures defined, respectively, by $\Theta_{b-1} = E_{b-1}/k$ and $\Theta_{A_2} = E_{A_2}/k$. The quantity $R_0 = kN_0$ is the universal gas constant. The symbols containing a caret (^) differ from the like quantities without the caret by the factor N_0 , Avogadro's number.

An alternate form of these equations that turns out to be more useful for numerical work (see, e.g., Appendix F) is obtained by re-expressing them in terms of the dependent variables $\bar{\gamma}_A, \bar{\gamma}_B, T_A, T_B$, and $\bar{\gamma}_a$. The bar here denotes that these quantities are natural logarithms of their unbarred equivalents, that is,

$$\bar{\gamma}_A = \ln \gamma_A \quad (\text{II-112a})$$

$$\bar{\gamma}_B = \ln \gamma_B \quad (\text{II-112b})$$

$$\bar{\gamma}_a = \ln \gamma_a \quad (\text{II-112c})$$

The rate equations expressed in terms of these quantities are

$$\frac{D\bar{\gamma}_A}{Dt} = \rho \gamma_m \left[\exp(\bar{\gamma}_B - \bar{\gamma}_A) \sum_r \frac{\gamma_r}{\gamma_m} k_R^{r,(1)}(T_B, T) - \sum_r \frac{\gamma_r}{\gamma_m} k_F^{r,(1)}(T_A, T) \right] \quad (\text{II-113a})$$

$$\frac{D\bar{\gamma}_B}{Dt} = - \exp(\bar{\gamma}_A - \bar{\gamma}_B) \frac{D\bar{\gamma}_A}{Dt} - \exp(-\bar{\gamma}_B) \left[\left(\frac{D\gamma}{Dt} \right)_F - \left(\frac{D\gamma}{Dt} \right)_R \right] \quad (\text{II-113b})$$

$$\begin{aligned} \frac{DT_A}{Dt} = & \frac{1}{C_{vA}(T_A)} \left[\sum_r \frac{1}{\tau_{A_1}^r} Q_A(T_A) \left\{ Q_{A_1}(T_A) \Omega_{A_1}(T, T_A) \right. \right. \\ & + Q_A(T_A) \left(\frac{\tau_{A_1}^r}{\tau_B^r} \right) \Omega_A(T, T_A) \left[1 - \frac{\Delta^r(T)}{q_{A_2}(T_A)} \right] \left. \left. \right\} \right. \\ & \left. + [R_o \Theta_{b-1} - q_A(T_A)] \frac{D\bar{\gamma}_A}{Dt} \right] \quad (\text{II-113c}) \end{aligned}$$

$$\begin{aligned} \frac{DT_B}{Dt} = & \frac{1}{C_{vB}(T_B)} \left[\sum_r \frac{1}{\tau_B^r} \Omega_B(T, T_B) \left[1 - \frac{\Delta^r(T)}{q_B(T_B)} \right] \right. \\ & + q'_B(T_B) \exp(\bar{\gamma}_A - \bar{\gamma}_B) \frac{D\bar{\gamma}_A}{Dt} - \exp(-\gamma_B) \left\{ [q'_B(T_F) - q'_B(T_B)] \left(\frac{D\gamma}{Dt} \right)_F \right. \\ & - [q'_B(-T_U) - q'_B(T_B)] \left(\frac{D\gamma}{Dt} \right)_R \left. \right\} + R_o \Theta_{A_2} \rho \gamma_m \left\{ 1 - \exp \left[-\Theta_{A_2} \left(\frac{1}{T} - \frac{1}{T_B} \right) \right] \right\} \\ & \left. \times \sum_r \frac{\gamma_r}{\gamma_m} k_R^{r,(1)}(T_B, T) \right] \quad (\text{II-113d})^\dagger \end{aligned}$$

$$\frac{D\bar{\gamma}_a}{Dt} = - 2 \exp(-\bar{\gamma}_a) \left[- \left(\frac{D\gamma}{Dt} \right)_F + \left(\frac{D\gamma}{Dt} \right)_R \right] \quad (\text{II-113e})$$

[†]This equation may be obtained from equation (II-82b) or by appropriate arithmetic combination of equations (II-110).

where the specific heats $C_{v_A}(T_A)$ and $C_{v_B}(T_B)$, defined by the derivatives $dq_A(T_A)/dT_A$ and $dq_B(T_B)/dT_B$, respectively, are discussed in Appendix A.

The following table lists the quantities contained either explicitly or implicitly in the rate equations (II-110) or (II-113); alongside are the equation numbers of the formulas that may be used to evaluate the indicated quantities.

Table II-1

Table of Formula Numbers of Quantities Contained in the Rate Equations

Quantity	Description	Equation No. (Quantity)	Equation No. (Quantity Primed)
$\hat{k}_R^{(1)}(T_B, T)$	Reverse transition rate, lower levels	(II-39a)	-
$\hat{k}_F^{(1)}(T_A, T)$	Forward transition rate, lower levels	(II-39b)	-
$\hat{k}_{Feq.}(T)$	Forward dissociation rate, upper levels	(III-13)	-
$\kappa_B(T)$	Partial equilibrium constant	(C13)	-
$\kappa(T)$	Equilibrium constant	(A8)	-
Q_{A_1}	Partial vibrational partition function	(A14a)	
Q_{A_2}		(A14b)	(A15)
Q_A		(A14a)+(A14b)	-
Q_B		(A14c)	(A16)
Q_V		(A18)	-
$\hat{\Omega}_{A_1}^\infty$	Measure of departure from equilibrium of nontruncated harmonic oscillator	(II-96a)	-

Table II-1 (Continued)

Quantity	Description	Equation No. (Quantity)	Equation No. (Quantity Primed)
$\hat{\Omega}_{A_2}^\infty$		(II-96b)	-
$\hat{\Omega}_B^\infty$		(II-96c)	-
$\hat{\Omega}_{A_1}$	Measure of departure from equilibrium of truncated harmonic oscillator	(II-97a)	-
$\hat{\Omega}_{A_2}$		(II-97b)	-
$\hat{\Omega}_B$		(II-97c)	-
$\hat{q}_{A_1}^\infty$	Average vibrational energy of nontruncated harmonic oscillator	(A28)	-
$\hat{q}_{A_2}^\infty$		(A33)	-
\hat{q}_B^∞		(A34)	-
\hat{q}_{A_1}	Vibrational energy of truncated harmonic oscillator	(A30)	-
\hat{q}_{A_2}		(A23), (A37)	(A35)
\hat{q}_A		(A41b)	-
\hat{q}_B		(A24), (A38)	(A36)
q_V		(A41a)	-
\mathcal{L}_{A_1}	Truncation factor	(A29)	-
\mathcal{L}_{A_2}		(A39)	(A31)
\mathcal{L}_B		(A40)	(A32)

Table II-1 (Continued)

Quantity	Description	Equation No. (Quantity)	Equation No. (Quantity Primed)
C_{vA_1}	Vibrational specific heat	(A44a)	-
C_{vA_2}		(A44b)	-
C_{vA}		(A47a)	-
C_{vB}		(A44c)	-
C_{vV}		(A47b)	-
$V(T_B, T)$	Coupling factor	(II-93), (C-10)	-
T_F	Characteristic temperature	(II-94), (C7)	-
$\Delta(T)$	Anharmonicity parameter 1	(II-73a), (B26)	-
$\delta(T)$	Anharmonicity parameter 2	(II-73b)	-
$\chi_R(T)$	Slope function	(B28a)	-
$\chi_F(T)$	Slope function	(B28b)	-
τ_{A_1}	Vibrational relaxation time lower states	(B25a) or (III-11a)	-
τ_B	Vibrational relaxation time upper states	(B25b)	-
(τ_{A_1}/τ_B)	Ratio	(B25c)	-

The rate equations (II-110) or (II-113) are still sufficiently general to be applicable to flow fields that are spatially multidimensional and unsteady. Such generality, however, will not be considered in the chapters that follow where only steady one-dimensional flows are investigated. A more convenient notation for the rate equations is given by

$$Q^\Sigma = \frac{1}{v} \left(\frac{D\Sigma}{Dt} \right) \quad (\text{II-114a})$$

$$= \frac{d\Sigma}{dx} \quad (\text{II-114b})$$

where Σ denotes either $\gamma_A, \gamma_B, \gamma_a, \epsilon_A, \epsilon_B, T_A$, or T_B . The Q^Σ quantities represent the differential change of the associated quantities along streamlines and are obtained directly by dividing the right hand side of either equations (II-110) or (II-113) by the mass velocity v .

The rate equations also contain a number of basic parameters that are for the most part dependent on the molecular species chosen to be investigated, in particular, the quantities $k_{1,0}^{(1)}, k_{1,0}^{(2)}, \Delta(T), E_{A_1}, E_{A_2}, N, a, b, k_{\text{F eq.}}(T)$, and T_U . Once appropriate values are assigned to these quantities, one can investigate the effects of vibration-dissociation coupling on fluid flows. The next chapters will be directed primarily toward a study of these quantities.

CHAPTER III

SPECIAL SOLUTIONS OF THE MODEL EQUATIONS

A set of rate equations applicable for studies of vibration-dissociation coupling was derived in the previous chapter. There remains, however, the problem of assigning values for the embedded parameters. As an additional complication, many of the parameters are not constants, but are functions of temperature. Unfortunately, there is no simple procedure available for this problem. One must specify values for all of the quantities before a solution can be obtained, and only after one has compared the solutions with observed (experimental) data can the parameters be confidently evaluated. It turns out that the values of the parameters have to be tentatively assigned and the results studied. These values are altered and the effect of the change is then investigated. In this manner one may hope to obtain a final set that effects good agreement when the solutions are compared with experimental data. The problem is further complicated by the fact that the complete solutions of the rate equations are relatively costly both from the point of view of expense and of computer time, since the solutions require an integration of the model equations and in addition the equations of flow. These equations are nonlinear and require electronic machine integration. Fortunately, there are a set of special solutions that do not require numerical integration and, therefore, are relatively easy to obtain. In particular, in the quasi-steady region behind a normal shock wave, to be described later, certain combinations of the rate equations may be set equal to zero (it will be shown that in this region the quantities T_A , T_B , and γ_B/γ_A are constant) and the resulting equations solved. An investigation of these solutions yields considerable insight into the effects that occur as a result of varying the values of embedded parameters and thus are of great value. This chapter concerns an investigation of the effect of changes of the embedded parameters on the quasi-steady solutions.

III-A. Introductory Comments

It is well known (see, e.g., 11, 12, 13, 48, 85, 90, 94) that the region behind a normal shock wave, subject to vibration-dissociation coupling, can be separated into three rather distinct zones, one of which will be discussed in this chapter. The justification for this separation will be made clear (Chapter IV) when the complete numerical solutions are exhibited showing the full relaxation to equilibrium behind a normal shock wave. For the present, the zones will merely be described with an eye to lending purpose to the solutions to be obtained. In the order of their occurrence behind the shock wave the zones are: (1) the transient zone, immediately behind the shock, in which vibrational relaxation occurs and where chemical effects are negligible; (2) the quasi-steady zone where both the changes in the fractional molecular population, n_v/n , of the vibrational energy states, and the effect of atom recombination may be considered negligible, and where dissociation is observed; and (3) the final relaxation zone in which the nonequilibrium vibrational and chemical effects diminish rapidly until the gas reaches equilibrium.

The transient zone (1) and the final relaxation zone (3) persist for relatively short periods of time, so that experimental study of these regions is difficult. Furthermore, an analytical study of these zones requires an integration of the complete set of master equations (or of the equivalent set of equations introduced in this paper), and such investigation is not simple. As a result the rate constants and molecular kinetics are least understood in these regions. The quasi-steady zone, however, persists for a relatively long period and has been the subject of considerable experimental study (19, 22, 56, 86, 99). An analytical investigation of the master equations for the flow region characterized as quasi-steady requires solving the system of equations obtained by setting the derivatives $d(n_v/n)/dt$ equal to zero. This, compared with the integration of the complete set of rate equations, is a much simpler problem and thus also a subject of considerable study (see, e.g., 13, 48, 73, 85, 94).

For these reasons comparisons between theory and experiment are most easily made in the quasi-steady zone, the temperature dependence of the

dissociation rate being that function used as a basis for comparison. Treanor and Marrone assessed the validity of their nonpreferential (90, 91) and preferential (58) vibration-dissociation models by making experimental comparisons of the pre-exponential temperature dependence of the effective dissociation rate constant. Similar studies were also conducted by Keck and Carrier (48) and by Snider (85). Before pursuing the subject further it is worthwhile to digress briefly to obtain somewhat of an understanding of the temperature dependent qualities of the dissociation rate constant.

An intuitive feeling for the significance of the temperature dependence of the dissociation rate can be obtained from "Collision Theory" (see, e.g., Vincenti and Kruger (97), p. 221), in which an expression is obtained for the dissociation rate. Basically, it is assumed that only those collisions are effective in promoting dissociation for which the net energy of collision (i.e., the relative line-of-center energy plus a contribution of internal energy (vibrational and/or rotational)) is greater than the molecular binding energy. This is a quasi-equilibrium theory in that the vibrational mode is assumed to be equilibrated along with the rotational and translational modes. It is shown that the temperature dependence of the dissociation rate constant is given by $T^{3/2-s} \exp(-\epsilon_0/kT)$ where the constant ϵ_0 is the dissociation (or activation) energy and the quantity s is one-half the number of square terms that contribute effectively to the energy of collision (see, e.g., (97), p. 227). The pre-exponential temperature dependence is given by the factor $T^{3/2-s}$. For example, if only the relative translational motion is effective in the dissociation process, then two quadratic terms are important (i.e., the two coordinates required to specify the line of centers) and $s = 1$. The dissociation rate is then proportional to $T^{1/2} \exp(-\epsilon_0/kT)$; the pre-exponential factor is, of course, $T^{1/2}$. If additional internal energy modes must be considered then $s > 1$. It may occur that only a fraction of the energy of some modes contribute to dissociation in which case fractional values of s may be observed. It should be emphasized that Collision Theory is a quasi-equilibrium theory and hence of value only in that it provides some insight to

the effect of the internal modes on the temperature dependence of the dissociation rate constant. If, as an upper bound, we presume that the translational, rotational, and vibrational modes are all effective during an atom-molecule collision, we might expect on the basis of this theory a rate constant with a temperature dependence of $T^{-3/2} \exp(-\epsilon_0/kT)$ (see, e.g., (97), pp. 223 and 227).

In the case of argon-oxygen collisions Camac and Vaughn (19) obtained experimentally a dissociation rate constant with a pre-exponential factor of $T^{-1 \pm .2}$ over the temperature range $3,400^\circ \leq T \leq 7,500^\circ \text{ K}$ (in this case $s = 5/2 \pm .2$). Wray (99), in an independent experiment over a wider temperature range, $5,000^\circ \leq T \leq 18,000^\circ \text{ K}$, suggested a dissociation rate without any pre-exponential temperature dependence (inferring $s = 3/2$). It will be shown later that there is considerable scatter in the experimental data and the problem of accurately determining a pre-exponential temperature dependence is difficult. It will be shown, however, that a $T^{-1/2}$ factor is not unreasonable for either Camac and Vaughn's or Wray's data.

The non-preferential dissociation model of Treanor and Marrone (90) is consistent with a T^{-1} factor (91), but fails to predict a satisfactory induction time (58), that is, delay time before the onset of molecular dissociation (this will be discussed further in Chapter IV). The preferential dissociation model of Marrone and Treanor (58), although providing qualitatively correct transient characteristics, yields a T^{-2} pre-exponential variation (58, 90). The exponent is too large on the basis of collision theory or experiment. It was partly the inadequacy of either of the two models to describe quantitatively both the transient and quasi-steady behavior that this thesis study was suggested by Doctor Charles E. Treanor of the Cornell Aeronautical Laboratory.

III-B. Quasi-Steady State in a Dissociation Experiment

In the work that follows the effects associated with the model will be investigated in a manner similar to that of Treanor and Marrone (58, 90, 91, 94) and of other researchers (13, 48, 73, 85). First the conditions that characterize the quasi-steady zone will be pointed out, and from these conditions

the required equations will become evident. Since only systems that contain a dilute mixture of molecules are being considered, the translational temperature may be assumed constant behind the shock. A brief explanation will be included on the procedure used to solve the system of equations for the quasi-steady zone. A discussion will then be given of the values of the parameters that will be used, and finally the numerical solutions will be presented and discussed.

In the introductory comments it was pointed out that the quasi-steady zone is that region of the flow field where the ratio $(n_v/n)^*$ (the asterisk denotes values in the quasi-steady zone) is not a function of the independent variables of the problem (time or distance measured from the shock). Furthermore the effects of molecular recombination may be neglected, that is,

$\left(\frac{d\gamma}{dx}\right)_F \gg \left(\frac{d\gamma}{dx}\right)_R$. The first constraint yields the relations

$$\left(\frac{\gamma_A}{\gamma}\right)^* = \text{constant} \quad (\text{III-1a})$$

$$\left(\frac{\gamma_B}{\gamma}\right)^* = \text{constant} \quad (\text{III-1b})$$

$$\begin{aligned} \left(\frac{\gamma_A}{\gamma}\right)^* \left[q_A (T_A^*) + \left(\frac{\gamma_B}{\gamma_A}\right)^* q_B (T_B^*) \right] &= \sum_{v=0}^{N-1} \left(\frac{n_v}{n}\right)^* (N_0 E_v) \\ &= \text{constant} \end{aligned} \quad (\text{III-1c})$$

where

$$\gamma = \gamma_A + \gamma_B \quad (\text{III-1d})$$

These relations are satisfied by the conditions[†]

$$T_A^* = \text{constant} \quad (\text{III-2a})$$

$$T_B^* = \text{constant} \quad (\text{III-2b})$$

[†]In the next chapter it also will be shown that equations (III-2) are indeed valid conditions for the quasi-steady zone.

$$\left(\frac{\gamma_B}{\gamma_A}\right)^* = \text{constant} \quad (\text{III-2c})$$

The equations required for the investigation of the quasi-steady zone are readily obtained by substituting equations (III-2a) and (III-2b) into equations (II-113c) and (II-113d), respectively, and substituting equations (III-2c) into the equation obtained after subtracting (II-113a) from (II-113b). Neglecting the atom recombination terms, we thus obtain the following set of transcendental equations to be solved for T_A^* , T_B^* , and $(\gamma_B/\gamma_A)^*$:

$$\begin{aligned} Q_{A_1}(T_A^*) \Omega_{A_1}(T, T_A^*) + Q_{A_2}(T_A^*) \frac{\tau_{A_1}}{\tau_B} \Omega_{A_2}(T, T_A^*) \left[1 - \frac{\Delta(T)}{q_{A_2}(T_A^*)} \right] \\ + Q_A(T_A^*) [R_0 \Theta_{b-1} - q_A(T_A^*)] \tau_{A_1} (v_Q \bar{\gamma}_A)^* = 0 \end{aligned} \quad (\text{III-3a})$$

$$\begin{aligned} \left(\frac{\tau_{A_1}}{\tau_B}\right) \Omega_B(T, T_B^*) \left[1 - \frac{\Delta(T)}{q_B(T_B^*)} \right] + q'_B(T_B^*) \exp(\bar{\gamma}_A - \bar{\gamma}_B)^* \tau_{A_1} (v_Q \bar{\gamma}_A)^* \\ - [q'_B(T_F^*) - q'_B(T_B^*)] V(T_B^*, T) (\tau_{A_1} \rho \gamma_m k_{\text{Feq.}}(T)) \\ + R_0 \Theta_{A_2} \left[\tau_{A_1} \rho \gamma_m k_R^{(i)}(T_B^*, T) \right] \times \left\{ 1 - \exp \left[-\Theta_{A_2} \left(\frac{1}{T} - \frac{1}{T_B^*} \right) \right] \right\} = 0 \end{aligned} \quad (\text{III-3b})$$

$$[1 + \exp(\bar{\gamma}_A - \bar{\gamma}_B)^*] (v_Q \bar{\gamma}_A)^* + V(T_B^*, T) \rho \gamma_m k_{\text{Feq.}}(T) = 0 \quad (\text{III-3c})$$

where

$$(v_Q \bar{\gamma}_A)^* = \rho \gamma_m \left[\exp(\bar{\gamma}_B - \bar{\gamma}_A)^* k_R^{(i)}(T_B^*, T) - k_F^{(i)}(T_A^*, T) \right] \quad (\text{III-3d})$$

$$\frac{1}{T_F^*} = \frac{1}{T_B^*} - \frac{1}{T} - \frac{1}{T_U} \quad (\text{III-3e})$$

The above equations are sufficiently complex that it is worthwhile to alter their form before considering a procedure for their solution. To simplify notation we first introduce the definitions

$$\bar{\gamma}_R^* \equiv \bar{\gamma}_B^* - \bar{\gamma}_A^* = \ell n \left(\frac{\gamma_B^*}{\gamma_A^*} \right) \quad (\text{III-4a})$$

$$\tau_D \equiv \left(\rho \gamma_m k_{\text{Feq.}} \right)^{-1} \quad (\text{III-4b})$$

$$\tau_b \equiv \left(\rho \gamma_m k_{b,b-1} \right)^{-1} \quad (\text{III-4c})$$

and the ratio of the rates given by equations (II-39)

$$\begin{aligned} \frac{k_F^{(1)}(T_A^*, T)}{k_R^{(1)}(T_B^*, T)} &= \frac{k_{b-1,b}}{k_{b,b-1}} \frac{Q'_B(T_B^*)}{Q_A(T_A^*)} \exp \left(- \frac{\Theta_{b-1}}{T_A^*} \right) \\ &= \frac{Q'_B(T_B^*)}{Q_A(T_A^*)} \exp \left[\Theta_{A_2} \left(\frac{1}{T_A^*} - \frac{1}{T} \right) - \frac{\Theta_b}{T_A^*} \right] \end{aligned} \quad (\text{III-5})$$

This last equation results after the substitution $k_{b-1,b}/k_{b,b-1} = \exp \left(- \frac{\Theta_{A_2}}{T} \right)$.

With the above quantities we rewrite the equations as follows:

$$\begin{aligned} Q_{A_1}(T_A^*) \Omega_{A_1}(T, T_A^*) + Q'_{A_2}(T_A^*) \left[\frac{\tau_{A_1}}{\tau_B} \exp \left(- \frac{\Theta_a}{T_A^*} \right) \right] \Omega_{A_2}(T, T_A^*) \left[1 - \frac{\Delta(T)}{q_{A_2}(T_A^*)} \right] \\ + Q_A(T_A^*) \left[R_o \Theta_{b-1} - q_A(T_A^*) \right] \left[\tau_{A_1} \left(v Q^{\bar{\gamma}_A^*} \right)^* \right] = 0 \end{aligned} \quad (\text{III-6a})$$

$$\begin{aligned}
& \left(\frac{\tau_{A_1}}{\tau_B} \right) \Omega_B(T, T_B^*) \left[1 - \frac{\Delta(T)}{q_B(T_B^*)} \right] + q_B'(T_B^*) \exp(-\bar{\gamma}_R^*) \left[\tau_{A_1} \left(vQ^{\bar{\gamma}_A} \right)^* \right] \\
& - \left[q_B'(T_F^*) - q_B'(T_B^*) \right] V(T_B^*, T) \left(\frac{\tau_{A_1}}{\tau_D} \right) \\
& + \frac{R_o \Theta_{A_2}}{Q_B'(T_B^*)} \left(\frac{\tau_{A_1}}{\tau_b} \right) \left\{ 1 - \exp \left[-\Theta_{A_2} \left(\frac{1}{T} - \frac{1}{T_B^*} \right) \right] \right\} = 0 \quad \text{(III-6b)}
\end{aligned}$$

$$\left[1 + \exp(-\bar{\gamma}_R^*) \right] \left(vQ^{\bar{\gamma}_A} \right)^* + \frac{V(T_B^*, T)}{\tau_D} = 0 \quad \text{(III-6c)}$$

where

$$\left(vQ^{\bar{\gamma}_A} \right)^* = \frac{\exp(\bar{\gamma}_R^*)}{\tau_{A_1} Q_B'(T_B^*)} \left(\frac{\tau_{A_1}}{\tau_b} \right) \left\{ 1 - \frac{k_F^{(i)}(T_A^*, T)}{k_R^{(i)}(T_B^*, T)} \exp(-\bar{\gamma}_R^*) \right\} \quad \text{(III-6d)}$$

$$= \frac{\exp(\bar{\gamma}_R^*)}{\tau_{A_1} Q_B'(T_B^*)} \left(\frac{\tau_{A_1}}{\tau_b} \right) \left\{ 1 - \frac{Q_B'(T_B^*)}{Q_A(T_A^*)} \exp \left[\Theta_{A_2} \left(\frac{1}{T_A^*} - \frac{1}{T} \right) - \frac{\Theta_b}{T_A^*} - \bar{\gamma}_R^* \right] \right\} \quad \text{(III-6e)}$$

This system of equations, although still appearing quite complicated, can readily be solved numerically by the following procedure: First obtain an explicit representation for $\bar{\gamma}_R^*$ as a function of the temperature T and the unknown quantities T_A^* and T_B^* . Such a function is found by solving the quadratic equation in $\bar{\gamma}_R^*$ that results from the substitution of equation (III-6d) into equation (III-6c). The result is

$$\bar{\gamma}_R^* = \ln \left(\frac{2AC}{B + \sqrt{B^2 + 4AC}} \right) \quad \text{(III-7a)}$$

where the identities

$$AC = k_F^{(i)}(T_A^*, T) / k_R^{(i)}(T_B^*, T) \quad \text{(III-7b)}$$

$$B = 1 + \frac{\tau_b}{\tau_{A_1}} \frac{\tau_{A_1}}{\tau_D} Q_B'(T_B^*) V(T_B^*, T) - AC \quad \text{(III-7c)}$$

are introduced to simplify notation. To obtain the above formulation, the root of the quadratic equation containing the negative radical was discarded since $\gamma_R^* > 0$. The remaining root with the positive radical, of the form $(-B + \sqrt{B^2 + 4AC})/2$, was modified to obtain the equivalent form given by the equation above so as to avoid the numerical difficulties that occur due to subtraction of the quantities B and $\sqrt{B^2 + 4AC}$ when their values are very nearly equal.

Having an explicit representation for $\bar{\gamma}_R^*$ simplifies the problem of solving equation (III-6), since the problem may now be considered as one of solving a pair of coupled transcendental equations for the two unknowns T_A^* and T_B^* . Equation (III-6a), indicated symbolically by

$$f_1 [T, T_A^*, T_B^*, \bar{\gamma}_R (T, T_A^*, T_B^*)] = 0 \quad \text{(III-8a)}$$

is one of the equations and equation (III-6b), written

$$f_2 [T, T_A^*, T_B^*, \bar{\gamma}_R (T, T_A^*, T_B^*)] = 0 \quad \text{(III-8b)}$$

is the other. The second equation, when solved numerically on the assumption that values of T and T_A^* are given, may also be written

$$T_B^* = T_B (T_A^*, T) \quad \text{(III-9a)}$$

When substituted into equation (III-6a) this yields the equation

$$f_1 \{ T, T_A^*, T_B (T_A^*, T), \bar{\gamma}_R [T, T_A^*, T_B^* (T_A^*, T)] \} = 0 \quad \text{(III-9b)}$$

This equation may then be solved numerically for T_A^* once T is specified. Although this outlined procedure contains embedded iteration loops that are very inefficient from the computational time standpoint, it was found satisfactory since only a limited number of cases were run. About 8 seconds were

required with an IBM 7090/7094 DCS computer system to obtain a solution for one value of the temperature T . Both equations (III-9b) and (III-9a) were solved by means of a nested pair of iterations, which were based on the conventional Newton-Raphson method. It should also be pointed out that the order in which the equations are solved (as implied above) is important since the procedure of solving equation (III-8a), assuming values for T and T_B^* , may not yield a solution unless the iteration procedure is started with relatively accurate bounds and initial guesses for T_A^* and T_B^* .

It is worthwhile to discuss equations (III-6) briefly. One observes that these equations are independent of density, and thus their solutions will also be independent of density. The equations depend parametrically on the functions $\Delta(T)$, τ_{A_1}/τ_b , τ_{A_1}/τ_B , and τ_{A_1}/τ_D . Since τ is inversely proportional to pressure, the latter three ratios are independent of pressure and are functions only of the temperature T . Also embedded in equations (III-6) are the separation constants a and b and the constant parameter T_U . As a result of the procedure used to evaluate the transition probabilities (see Appendix B), the temperature-dependent quantities listed above, except τ_D , can be related to $\chi(T)$ (see Appendix B) as follows:

$$\tau_{A_1}/\tau_b = \frac{(b-a)\chi(T) - a\frac{E_{A_1}}{E_{A_2}}}{1 - \exp\left(-\frac{\Theta_{A_1}}{T}\right)} \quad (\text{III-10a})$$

$$\tau_{A_1}/\tau_B = \frac{1 - \exp\left(-\frac{\Theta_{A_2}}{T}\right)}{1 - \exp\left(-\frac{\Theta_{A_1}}{T}\right)} \chi(T) \quad (\text{III-10b})$$

and equation (II-73) relates the dependence of $\Delta(T)$ on $\chi(T)$. Also given in Appendix B are two suggested equations for evaluating $\chi(T)$, that is, $\chi_R(T)$ and $\chi_F(T)$. Solutions that depend on each function were obtained in order to assess the sensitivity of the resulting solutions to this parameter.

Solutions will also be exhibited for the hypothetical case $\chi(T) = 1$ that would occur if the transition probabilities were strictly those for a harmonic oscillator.

The characteristic vibrational relaxation time τ_{A_1} associated with the lower vibrational states (for discussion see Appendix B) is taken to be that quantity measured experimentally by Camac (20); that is,

$$\begin{aligned} (\tau_{A_1})^{-1} &\equiv (\tau_v)_{\text{Camac}}^{-1} \\ &= \rho \gamma_m C_1 T^{1/6} \left[1 - \exp\left(-\frac{2228}{T}\right) \right] \exp\left[-\left(\frac{C_2}{T}\right)^{1/3}\right] \end{aligned} \quad (\text{III-11a})$$

where

$$\begin{aligned} C_1 &= N_0 \hat{C}_1 \\ &= 7.22 \times 10^{16} \text{cc/mole-sec-}({}^\circ\text{K})^{1/6} \end{aligned} \quad (\text{III-11b})$$

$$\hat{C}_1 = 1.20 \times 10^{-7} \text{cc/particle-sec-}({}^\circ\text{K})^{1/6} \quad (\text{III-11c})$$

$$C_2 = 1.04 \times 10^7 \pm 30\% \text{ }^\circ\text{K} \quad (\text{III-11d})$$

To assess the sensitivity of the solutions to τ_{A_1} , two values of C_2 are used:

$$C_2^1 = 1.04 \times 10^7 \text{ }^\circ\text{K} \quad (\text{III-12a})$$

$$C_2^2 = 1.40 \times 10^7 \text{ }^\circ\text{K} \quad (\text{III-12b})$$

Here C_2^1 is the value suggested by Camac, and C_2^2 is slightly larger than the value associated with the upper error bound of 30 percent reported by Camac (see eq. (II-11d)).

The equilibrium dissociation rate k_{Feq} , contained in the characteristic dissociation time τ_D (see eq. (III-4b)) is evaluated in two ways for the results that will be shown. First, it is simply presumed that we have a $T^{1/2}$ pre-exponential factor (recall discussion of Collision Theory given earlier in this chapter). It then turns out that the vibrational coupling factor V^* obtained from the quasi-steady solution effectively adds an additional temperature dependence.

Second, the equilibrium dissociation rate $k_{\text{Feq.}}$ is considered in the same manner as in Marrone and Treanor (58), where it is assumed that the coupling factor contains the entire pre-exponential temperature behavior. For the first case we have

$$\left[k_{\text{Feq.}}(T) \right]_{\text{WR}} = 1.42 \times 10^{13} \sqrt{T} \exp\left(-\Theta_{\text{D}}/T\right) \quad (\text{III-13a})$$

and for the second case

$$\left[k_{\text{Feq.}}(T) \right]_{\text{MT}} = 9.00 \times 10^{14} \exp\left(-\Theta_{\text{D}}/T\right) \quad (\text{III-13b})$$

In both of the above equations the constant coefficients were evaluated so as to agree with Camac and Vaughn's experimentally determined rates at $T = 4,000^\circ \text{K}$, as was done by Marrone and Treanor (58).

The parameters a and b are chosen somewhat arbitrarily. The value of a (discussed in Appendix B) is such that the deviation of the approximate "rate-of-quantum-transfer" relation is not greater than about a factor of 2 (when compared with similar relations obtained from Morse oscillator quantities) at the vibrational energy level corresponding to the energy E_a . A value of $a = 9$ approximately satisfies this criterion. The choice of the value for b will ultimately depend on how accurately the solutions can be made to agree with experimental data. The choices $b = 16, 24,$ and 30 result in the fractional energies $E_b/E_{\text{D}} = 0.544, 0.786,$ and $0.968,$ respectively. The latter choice yields unsatisfactory pre-exponential behavior for the effective dissociation rate, as will be shown, and is only briefly considered. It is to be emphasized that these values of b are arbitrary, but appear reasonable on the basis of the results given in references 48, 84, 94.

A series of plots are given in figures III-1 through III-12 showing the solutions obtained from equations (III-6). Separate curves are given in each plot, each associated with a different value for the separation constant b , for each of the quantities $T_{\text{A}}^*/T, T_{\text{B}}^*/T, V^*,$ and $k_{\text{Feff.}}(T)/\exp\left(-\frac{\Theta_{\text{D}}}{T}\right)k_{\text{Feff.}}(4,000).$

For the reader's convenience Table III-1 lists the values and identifies the particular temperature-dependent quantities used for the solutions. For example, for figure III-1 the parameters have the values $T_U = \infty$ (actually, $T_U = 10^{23}$), $\chi = \chi_R$, $k_{\text{Feq.}} = 9 \times 10^{14} \exp\left(-\frac{\Theta_D}{kT}\right)$, $C_2 = 1.4 \times 10^7$, and $a = 9$. Associated with these values, figure III-1a shows six curves, of which three give T_A^*/T for $b = 16, 24$, and 30 , while the other three similarly give T_B^*/T . Figure III-1b contains three curves for the coupling factor V^* , with each curve again for a different value of the separation constant b . Figure III-1c shows the pre-exponential temperature dependence of the dissociation rate constant. The circles and squares are experimentally measured values, the circles from Wray's data (99) and the squares from Camac and Vaughn's data (19). The solid-line curve, labeled C & V, is the dissociation rate computed from the formula given by Camac and Vaughn (19) (representing a least squares fit of his data), but appropriately normalized. Since Wray (99) gave a formula without any pre-exponential temperature dependence, the horizontal line associated with 10^0 would be appropriate for his formula. The dotted-line curves are guides from which one may estimate the functional behavior of the various curves regarding temperature dependence. The lower dotted line represents a T^{-2} pre-exponential temperature dependence, and the upper dotted curve corresponds to $T^{-1/2}$. The two solid lines labeled $b = 16$ and $b = 24$ represent the pre-exponential temperature dependence as obtained from the present quasi-steady solutions.

An important point evident from figure III-1c is that the experimental values have less than the T^{-2} dependence obtained by Marrone and Treanor (58). Although Camac and Vaughn fit their data with a function that varies as T^{-1} , it would appear from Wray's higher temperature data that a variation of $T^{-1/2}$ would be more reasonable. It is to be emphasized that a different normalization would cause a shift of the dotted $T^{-1/2}$ curve and that a different placement of this curve can be made. Because of the scatter in the experimental data the most appropriate factor is still uncertain. The published data, however, do not show the same degree of scatter because the exponential

Table III-1

Parameters associated with the quasi-steady solutions,
figures III-1 through III-12.

Figure no.	T_U	χ	$k_{\text{Feq.}}$	C_2	b	a
III-1	∞	R	MT	(2)	16, 24, 30	9
III-2	∞	R	WR	(2)	16, 24, 30	9
III-3	$\Theta_D/3$	F	MT	(2)	16, 24, 30	9
III-4	$\Theta_D/3$	F	WR	(2)	16, 24, 30	9
III-5	$\Theta_D/10$	F	MT	(2)	16, 24, 30	9
III-6	$\Theta_D/10$	F	WR	(2)	16, 24, 30	9
III-7	$\Theta_D/10$	F	MT	(1)	16, 24, 30	9
III-8	$\Theta_D/20$	F	MT	(1)	16, 24, 30	9
III-9	$\Theta_D/50$	F	MT	(1)	16, 24, 30	9
III-10	$\Theta_D/100$	F	MT	(1)	16, 24, 30	9
III-11	—	F	MT	(1), (2)	16, 24	9
III-12	$\Theta_D/10$	$\chi(T) = 1$	MT	(1)	16, 24, 30	9

χ : R see eq. (B14c)

F see eq. (B23b)

$k_{\text{Feq.}}$: WR see eq. (III-13a)

MT see eq. (III-13b)

C_2 : 1 see eq. (III-12a)

2 see eq. (III-12b)

factor $\exp(-\Theta_D/kT)$, which actually dominates the measurements, is included.

The pre-exponential factor compared with the exponential factor represents a relatively small variation.

The problem of determining the appropriate values for the parameters embedded in the equations is difficult because of the relative uncertainty of the experimental data, the limited amount of such data, and the rather large number of parameters to be evaluated. The essential features exhibited by the solutions are

1. The relative values of T_A^*/T and T_B^*/T ,
2. The temperature dependence of V^* ,
3. A comparison of the pre-exponential temperature dependence of the effective dissociation rate constant.

It will turn out that these features together with certain facts obtained by other investigators will be sufficient for estimating appropriate values of the embedded parameters.

It is known that one effect of dissociation is to perturb the population in the upper states to values less than those appropriate for a Boltzmann population distribution (48, 84, 94). We would therefore expect that $T_B^*/T < T_A^*/T$, especially at the higher temperatures. Furthermore, we seek values for the parameters that will yield a pre-exponential temperature dependence that varies roughly as $T^{-1/2}$. Searching through the figures we note that the combination of parameters associated with figures III-1 may be discarded since, in this case, $T_B^*/T > T_A^*/T$ (see fig. III-1a) and, in addition, the pre-exponential temperature factor varies too weakly with temperature (see fig. III-1c). For the case in figure III-2 $k_{\text{Feq.}}(T)_{\text{MT}}$ is replaced by $k_{\text{Feq.}}(T)_{\text{WR}}$ and the results show that the perturbing effect of dissociation is now accounted for (see fig. III-2a). The pre-exponential temperature dependence, however, does not agree with the experimental result (see fig. III-2c). One observes that the $T^{1/2}$ factor contained in $k_{\text{Feq.}}(T)_{\text{WR}}$ produces effectively a positive pre-exponential temperature exponent rather than a negative exponent as is implied by the experimental data. Reducing T_U (see, e.g., figs. III-2, III-4, III-6) reduces the positive exponent, but not to such an extent as to effect satisfactory agreement with the experimental data. However, we also observe that reducing T_U reduces T_B^*/T relative to T_A^*/T and increases the pre-exponential variation with temperature (cf. figs. III-1 through III-6).

As explained earlier, the parameter T_U is a measure of how rapidly the dissociation probability drops off for the lower vibrational levels (see Appendix C for discussion). The larger values of T_U correspond to a relatively equal probability of dissociation from all the B-state levels and the smaller values to a relatively greater probability of dissociation from the uppermost levels. The quasi-steady solutions seemingly imply that a large pre-exponential temperature dependence requires small values of T_U . This is consistent with Treanor and Marrone's result (91, 93) in that $T_U = \infty$

(nonpreferential dissociation model) resulted in a T^{-1} pre-exponential temperature dependence while $T_U = \Theta_D/6$ (58) (preferential dissociation model) resulted in roughly a T^{-2} temperature dependence. Aside from including the vibrational temperatures T_A and T_B and the effect of anharmonicity, the model differs from Marrone and Treanor's preferential dissociation model (58) in that here only the vibrationally excited molecules, characterized as being in the B-states, are allowed to dissociate. The effect of decreasing b would result (although such calculations are not shown) in a pre-exponential temperature factor as large as theirs.

The discussion thus far has centered on figures III-1 through III-6, which show the solutions associated with the value of C_2 given by equation (III-12b) (see also table III-1), that is, which correspond to a relatively large characteristic vibrational relaxation time τ_{A_1} . Decreasing this parameter by use of the expression for C_2 suggested by Camac and Vaughn (i.e., using eq. (III-12a)) increases the values of T_B^*/T relative to T_A^*/T and also decreases the pre-exponential temperature factor. It thus has an effect opposite to that desired on the basis of the experimental data. This may be countered by further reduction in the value of T_U and the appropriate effects are illustrated in figures III-8, III-9, and III-10. However, comparing figures III-9 and III-10, we observe that there appears to be a small value of T_U below which smaller values have little effect on the pre-exponential temperature dependence. That this is true is illustrated in figures III-11, wherein the coupling factor V^* is plotted as a function of T_U for $T = 10,000^\circ$ and $20,000^\circ$ K, and for $b = 16$ and 24 . Comparing figures III-11a with III-11b we observe that a change in the value of C_2 of only about 36 percent (a factor of between 2 and 3 in the characteristic vibrational relaxation time τ_{A_1} over the range of temperatures of interest) has a rather large effect on the coupling factor or the pre-exponential temperature dependence. These figures also show that any incremental change in T_U , when this parameter is greater than 10^5 or less than 2×10^3 , has little effect on the coupling factor V^* (also see discussion in Appendix C). In the former limiting case we have nonpreferential dissociation from any B-state level and

in the latter case highly preferential dissociation — in essence, dissociation only from the very uppermost level. We note further that the latter limiting case yields the smallest values for the vibrational coupling factor V^* for any given temperature T and hence the greatest pre-exponential temperature dependence.

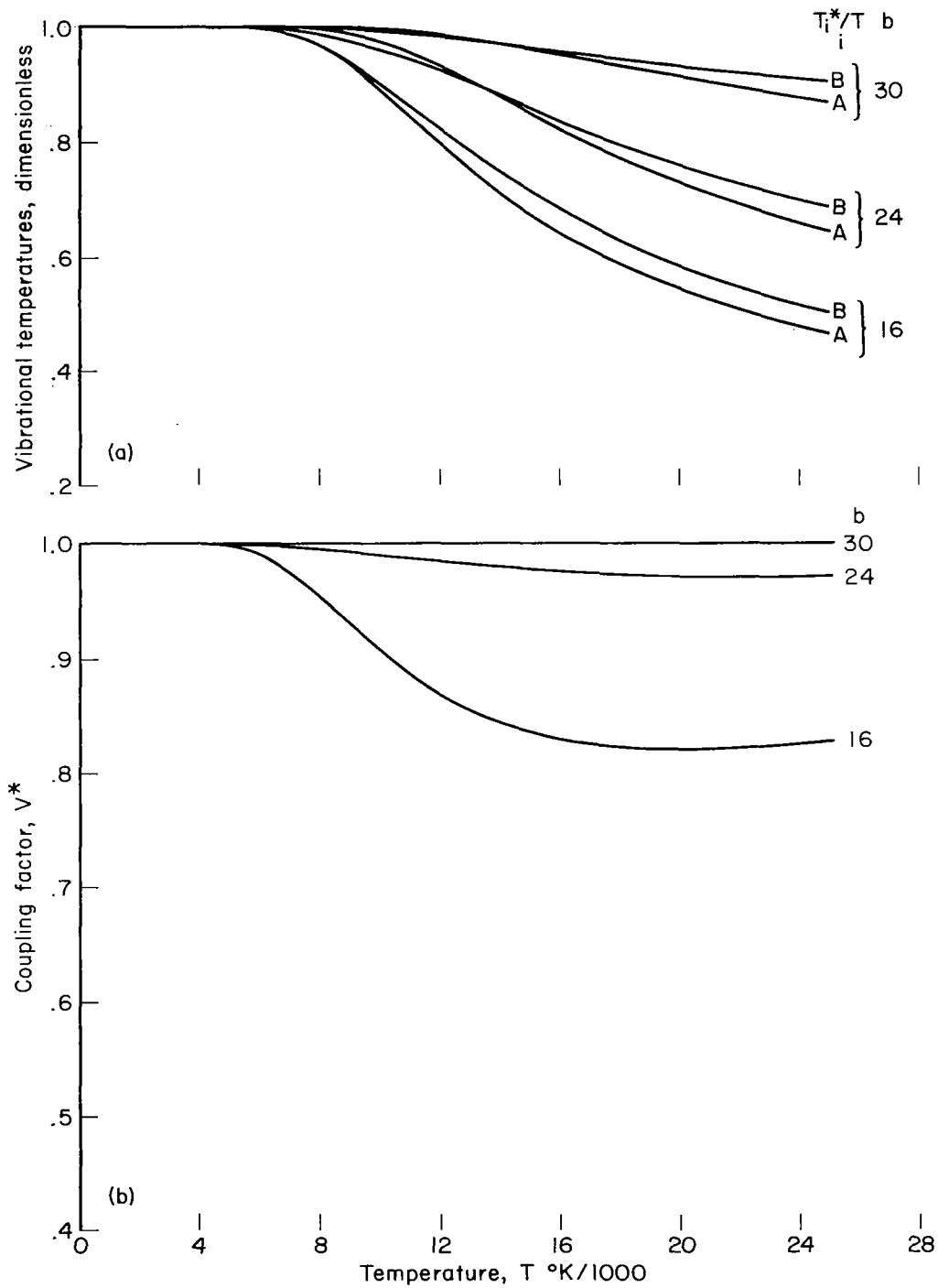
It then follows that the largest pre-exponential temperature variation obtainable with the assigned values of b is that shown in either figure III-9 or III-10. A greater pre-exponential temperature dependence will require smaller values of b . The results shown, however, are within the experimental data scatter; hence, 16 is the largest value of b that will yield favorable agreement with experiment.

No comparisons are shown from which one can estimate the effect of using the two specified values for $\chi(T)$ (see eqs. (B28a) and (B28b)). It turns out that the solutions are little affected by whether $\chi_F(T)$ or $\chi_R(T)$ is used for $\chi(T)$. The greatest effect is a difference in the values of T_A^*/T and T_B^*/T , amounting to about 2 percent, and occurs at the lower temperatures where the differences between the values of χ_F and χ_R are greatest (see Appendix B). At the higher temperatures the differences were observed to be less than 1/2 percent. One additional effect of χ is worth pointing out. The reader will observe that T_B^*/T crosses T_A^*/T for a few of the solutions (see, e.g., fig. III-7a). This crossover occurs because the approximations introduced for $\chi_R(T)$ or $\chi_F(T)$ in Appendix B are inaccurate at the lower temperatures, and hence it is probable that T_B^* is also in error at those temperatures. It is to be expected that an additional segment (that is, an additional separation comparable to the a-level separation) would eliminate the crossover and improve the value computed for T_B^* . It will be shown in the next chapter that such an additional segment may be advisable for other reasons also. On the other hand, the effect of such improvements is not expected to be large since the relative molecular population of the states that are affected is small (see discussion in Appendix B and also the discussion of the component derivative terms in the next chapter). This is further attested by the fact that the use of either χ_R or χ_F has only a small effect on the solutions. This is not to say that the effects of

anharmonicity may be ignored. One observes by comparing figures III-7 and III-12 that differences do occur depending on whether one includes or ignores the effect of anharmonicity on the transition rate, although the differences for the case of a normal-shock wave may be sufficiently small to be unobservable experimentally. It will be shown in the next chapter that for nozzle flow, the effects of including anharmonicity may be large and should not be ignored.

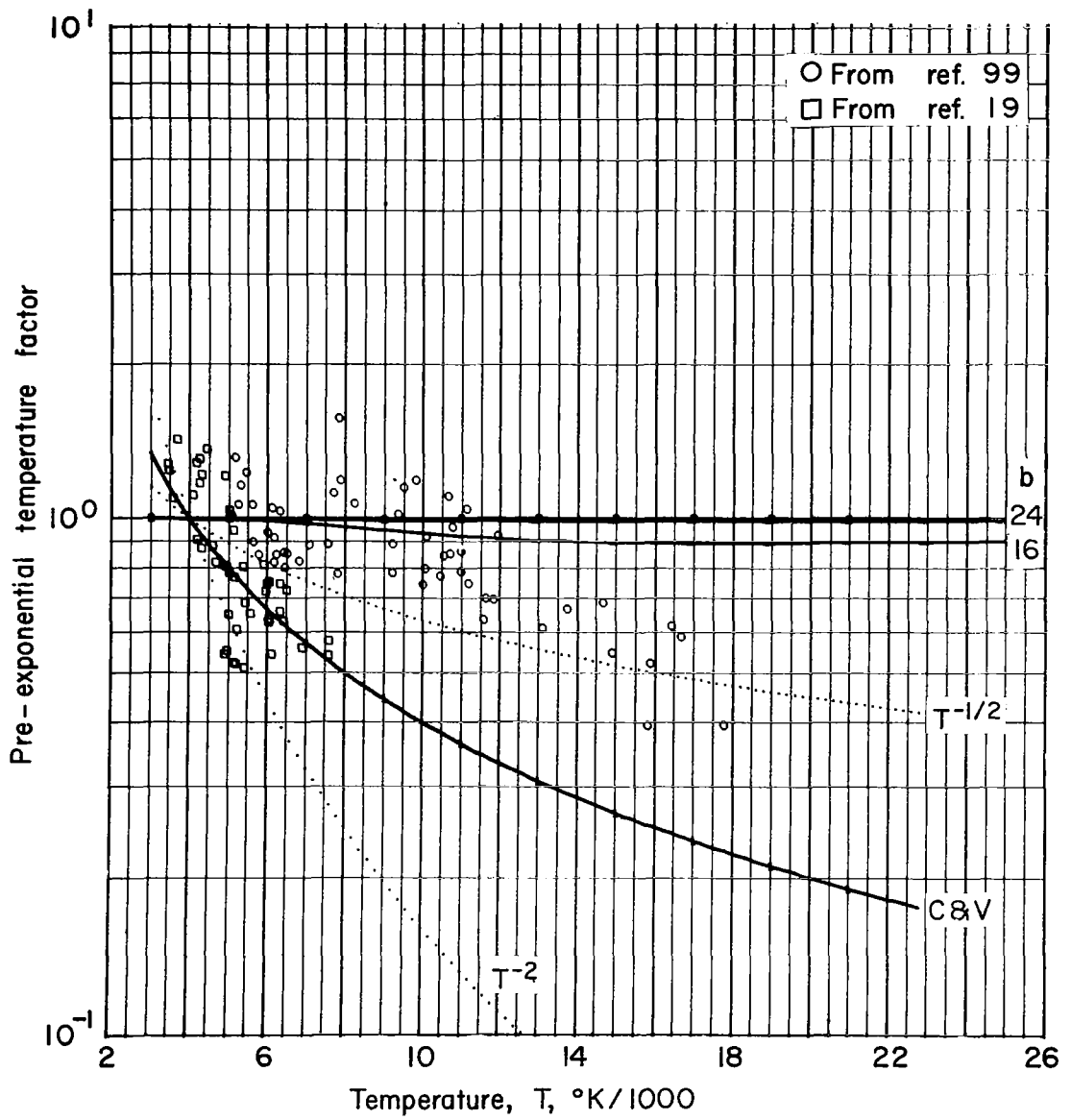
The investigation in this chapter has provided insight on the effect of the parameters and the effect of incremental changes in the values of the parameters on the quasi-steady solution. It should be apparent that the values of b corresponding to energies E_b that are greatly above the midpoint of the vibrational-energy potential well do not provide a sufficiently large pre-exponential temperature variation as compared to that found experimentally. For each b below the midpoint value, the parameter T_U can be adjusted to provide the proper pre-exponential temperature variation. Consequently, a unique choice of values for the embedded parameters cannot be found simply on the basis of the comparisons with the quasi-steady solutions. Additional comparisons must be made and this, in part, is the purpose of the investigations discussed in the next chapter.

Solutions will be obtained that show the details of the relaxation to equilibrium behind a normal shock wave. The effect of changes in C_2 , b , and T_U on the relaxation behavior will be investigated further, particularly, the effect of these variables on the induction time. Finally, an example will be given for nozzle flow together with a discussion of the distinguishing features associated with such flow.



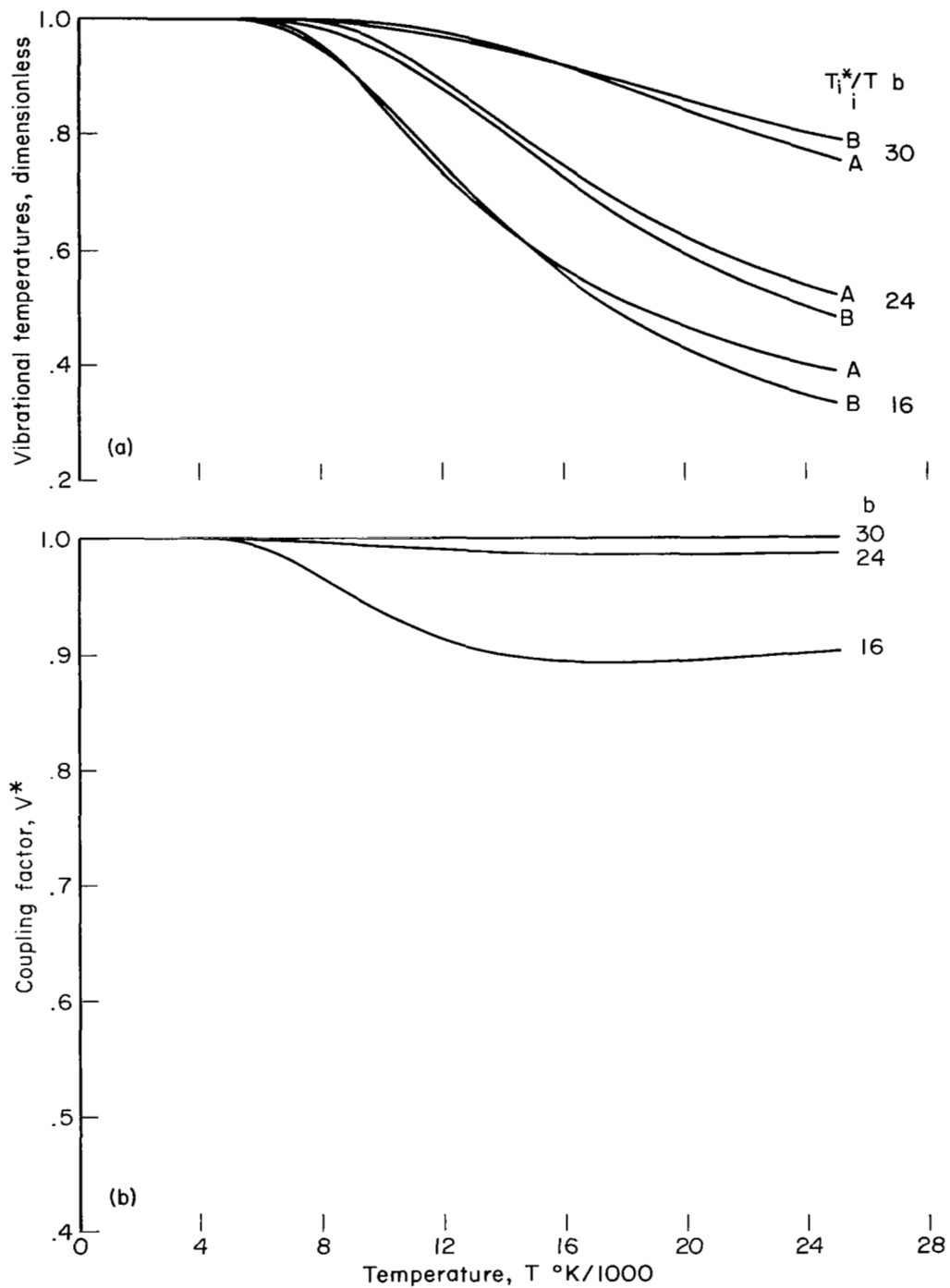
(a) Dimensionless vibrational temperatures
 (b) Vibrational coupling factor

Figure III-1. Variables obtained from quasi-steady solution versus temperature (associated parameters are listed along first row table III-1)



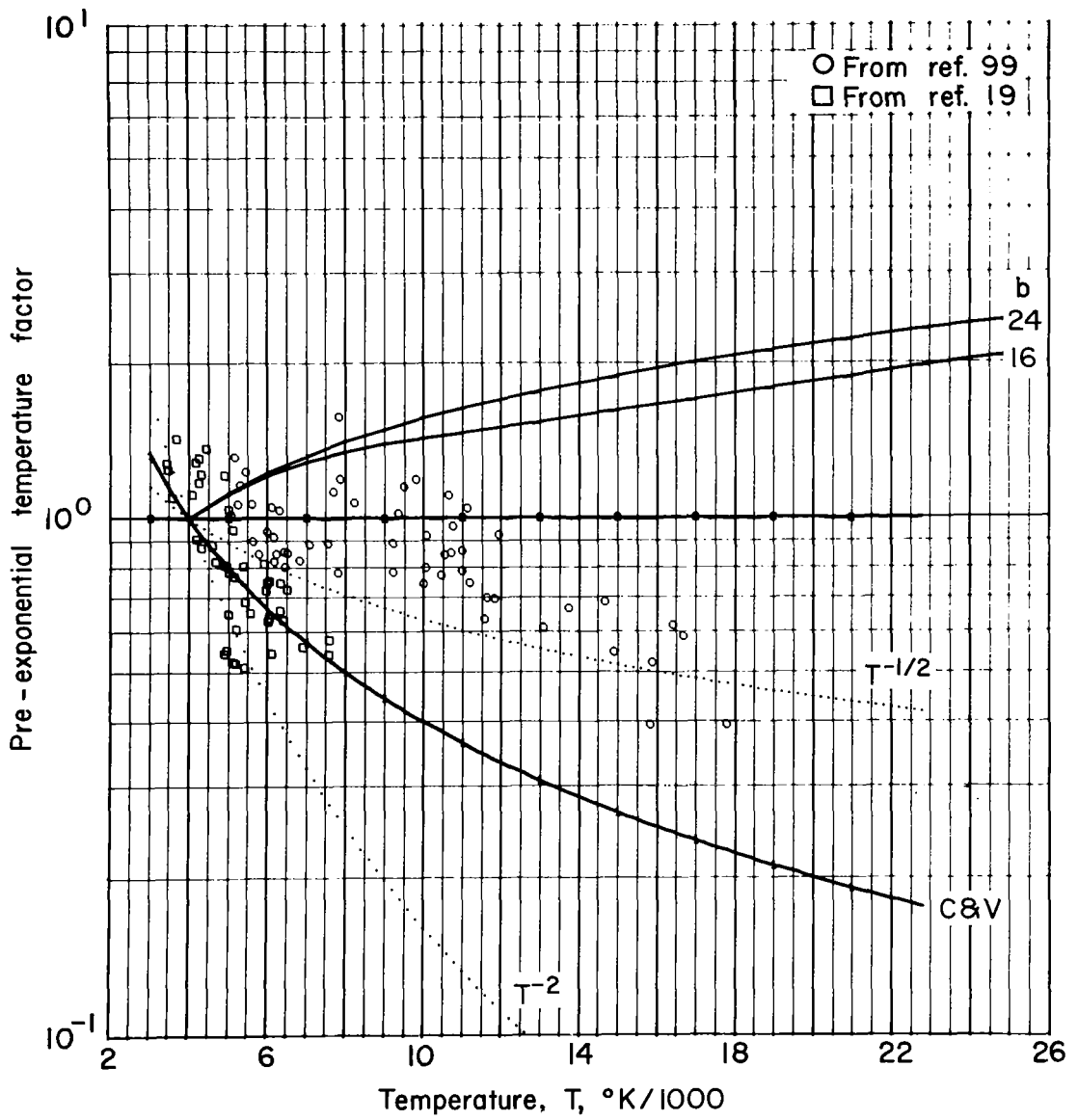
(c) Pre-exponential factor

Figure III-1 Continued

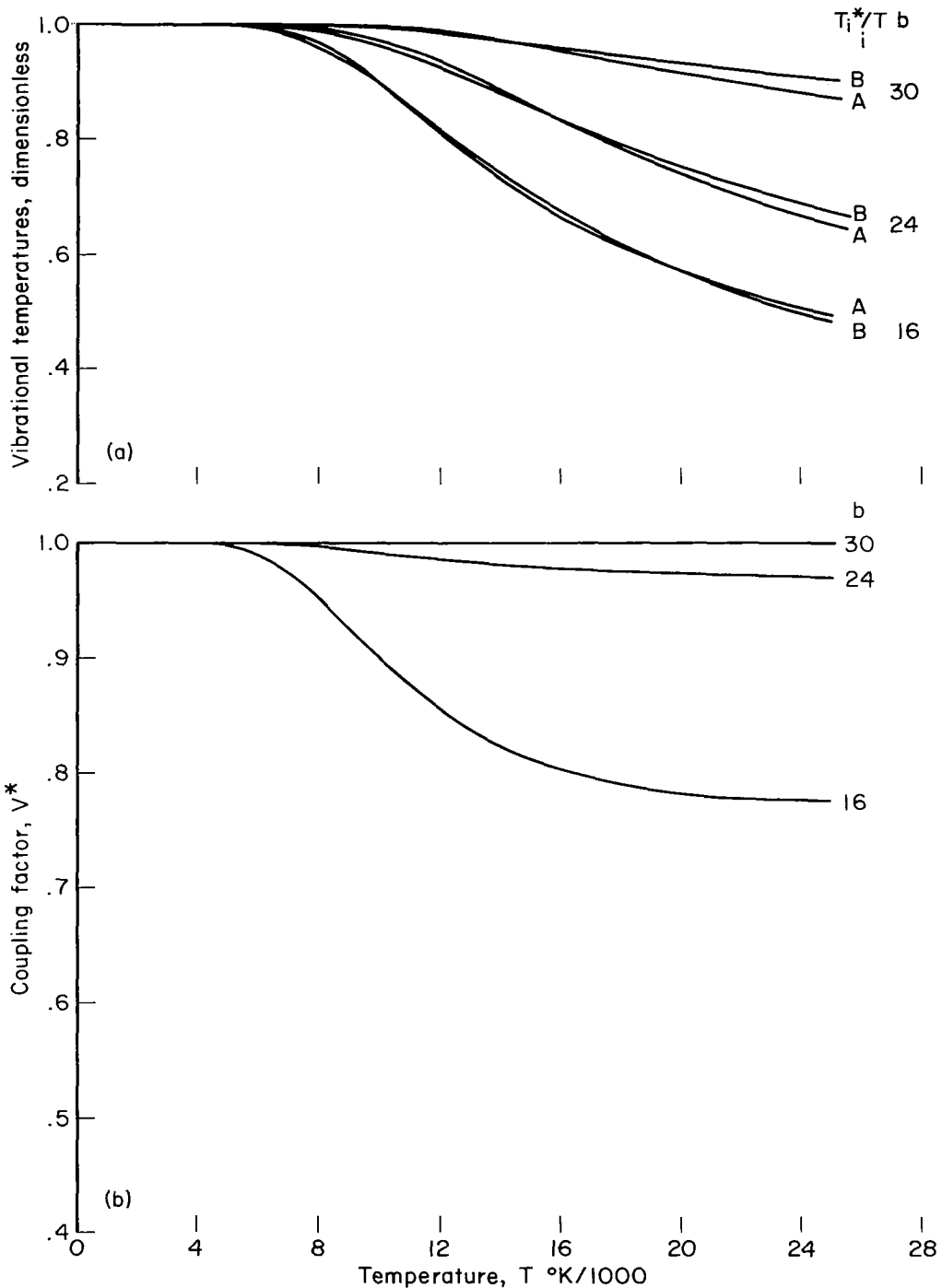


- (a) Dimensionless vibrational temperatures
- (b) Vibrational coupling factor

Figure III-2. Variables obtained from quasi-steady solution versus temperature (associated parameters are listed along second row of table III-1)

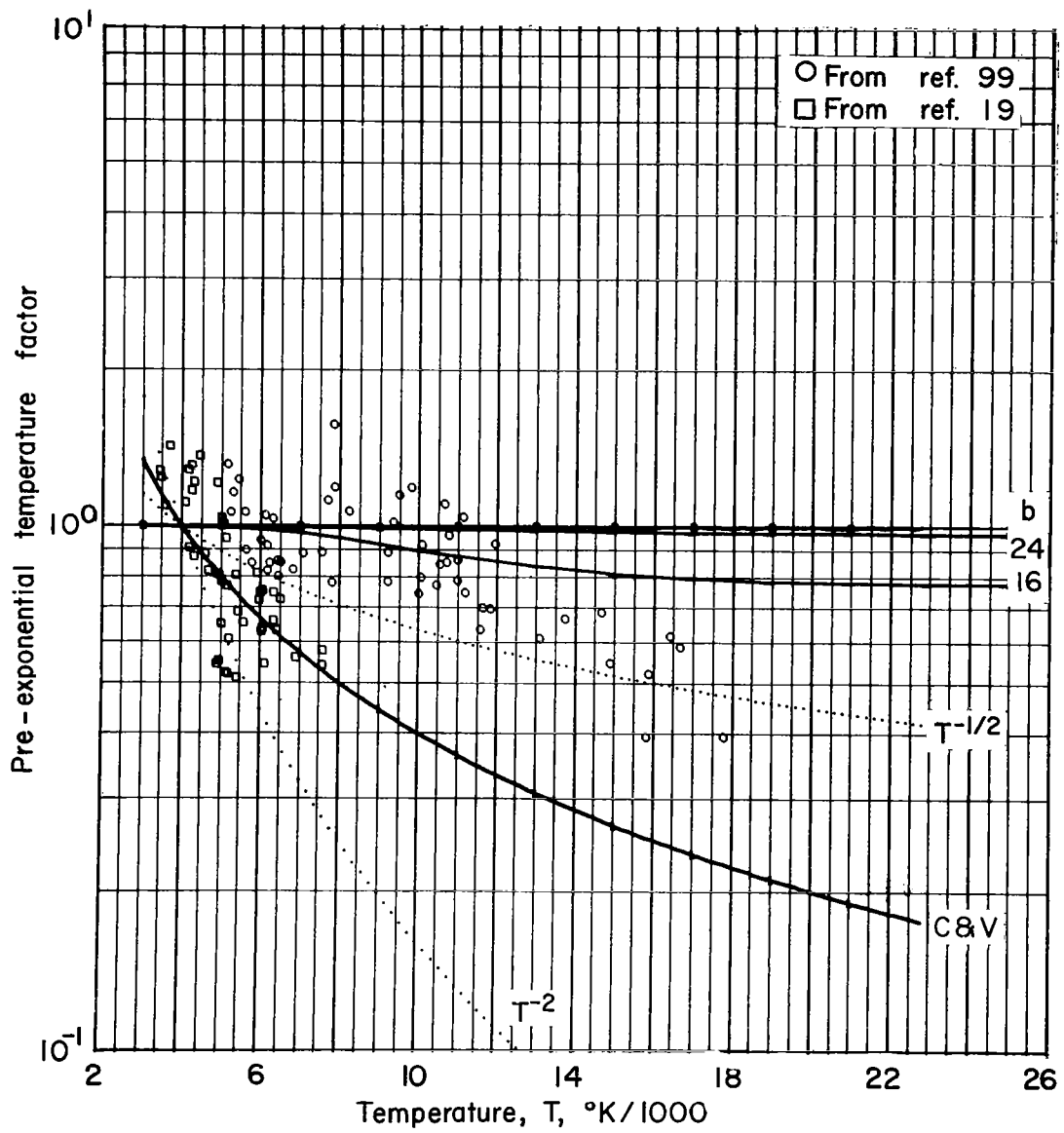


(c) Pre-exponential factor
 Figure III-2 Continued

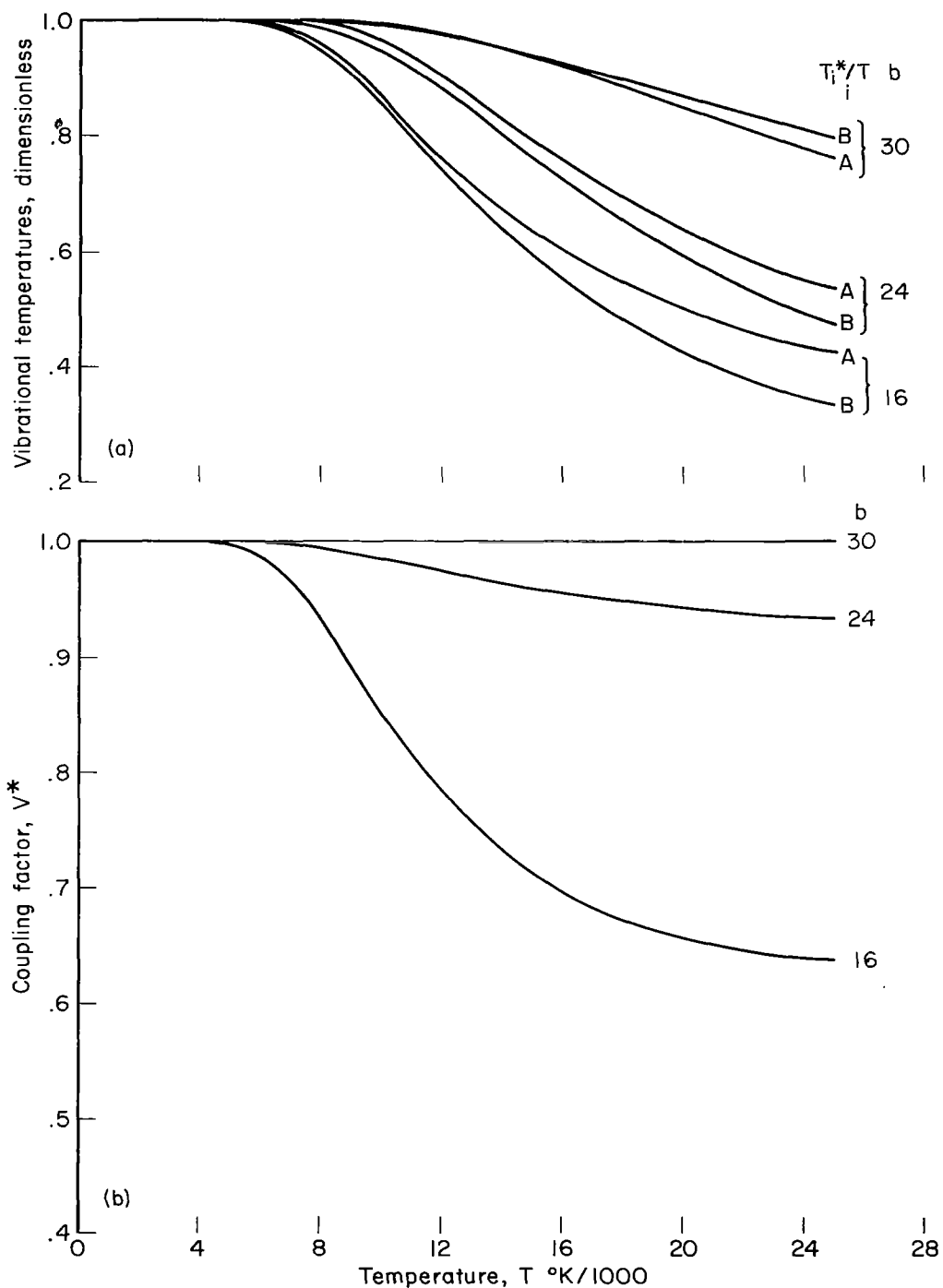


(a) Dimensionless vibrational temperatures
 (b) Vibrational coupling factor

Figure III-3. Variables obtained from quasi-steady solution versus temperature (associated parameters are listed along third row of table III-1)

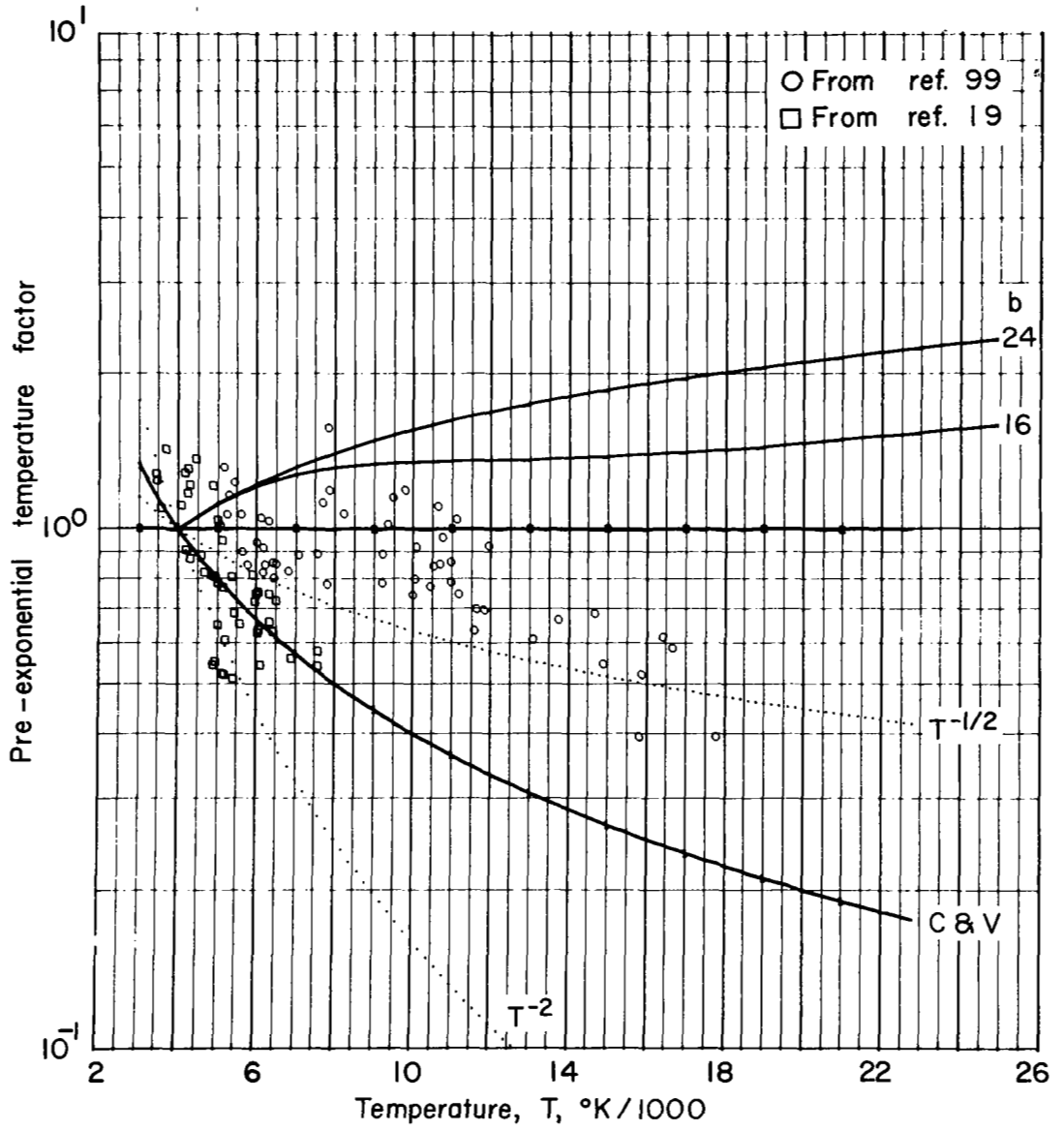


(c) Pre-exponential factor
 Figure III-3 Continued

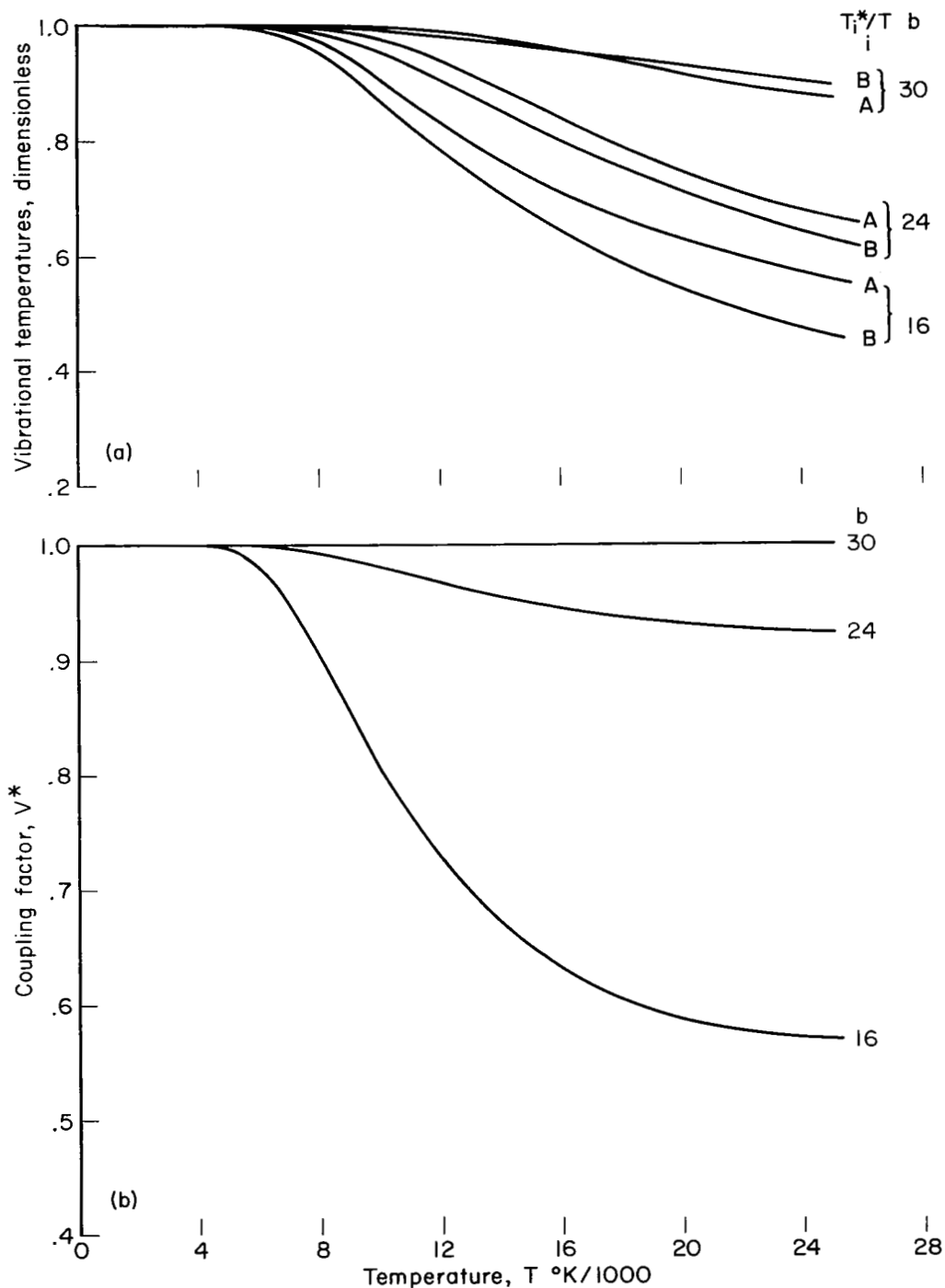


(a) Dimensionless vibrational temperatures
 (b) Vibrational coupling factor

Figure III-4. Variables obtained from quasi-steady solution versus temperature (associated parameters are listed along fourth row of table III-1)

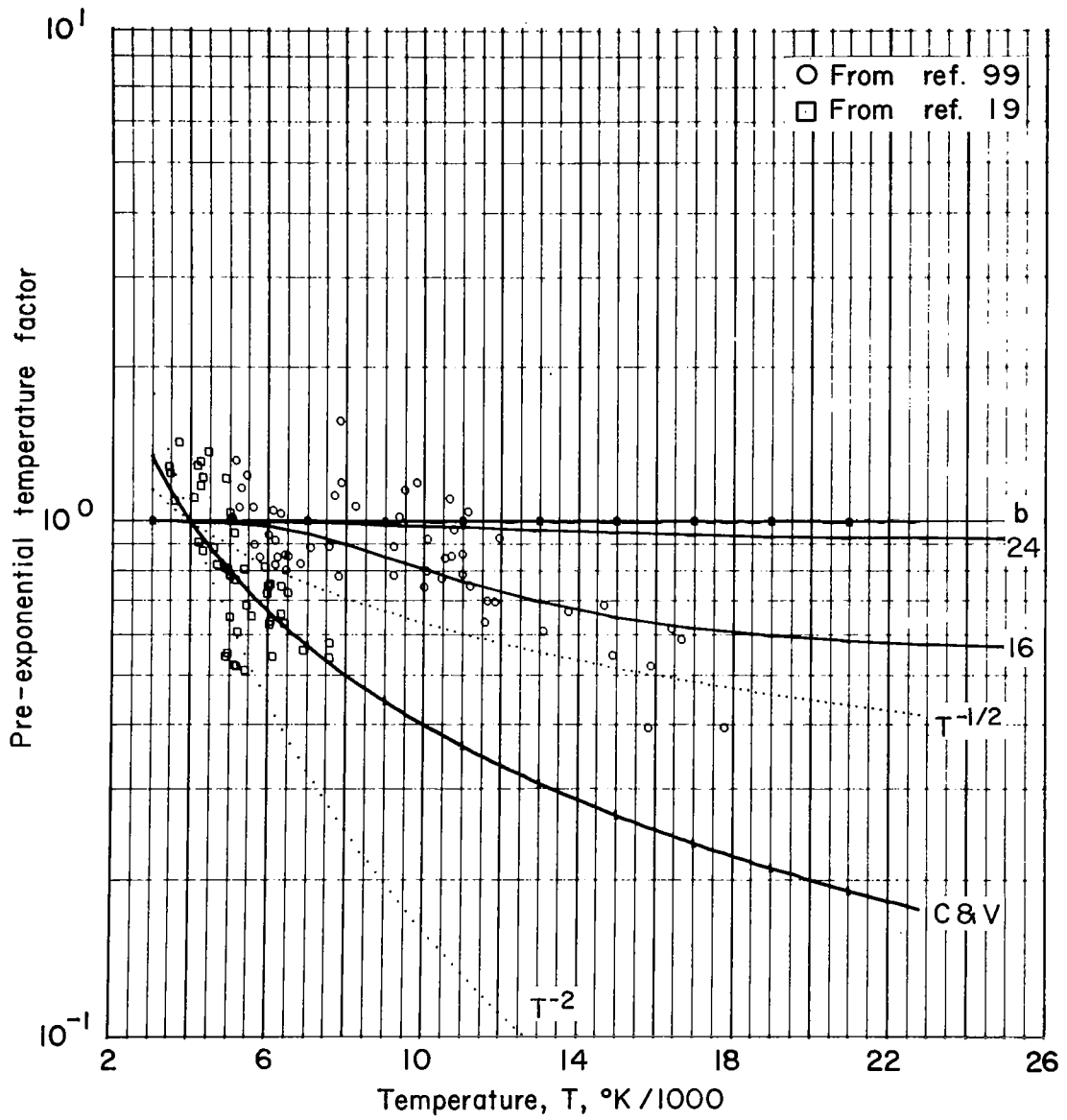


(c) Pre-exponential factor
 Figure III-4 Continued

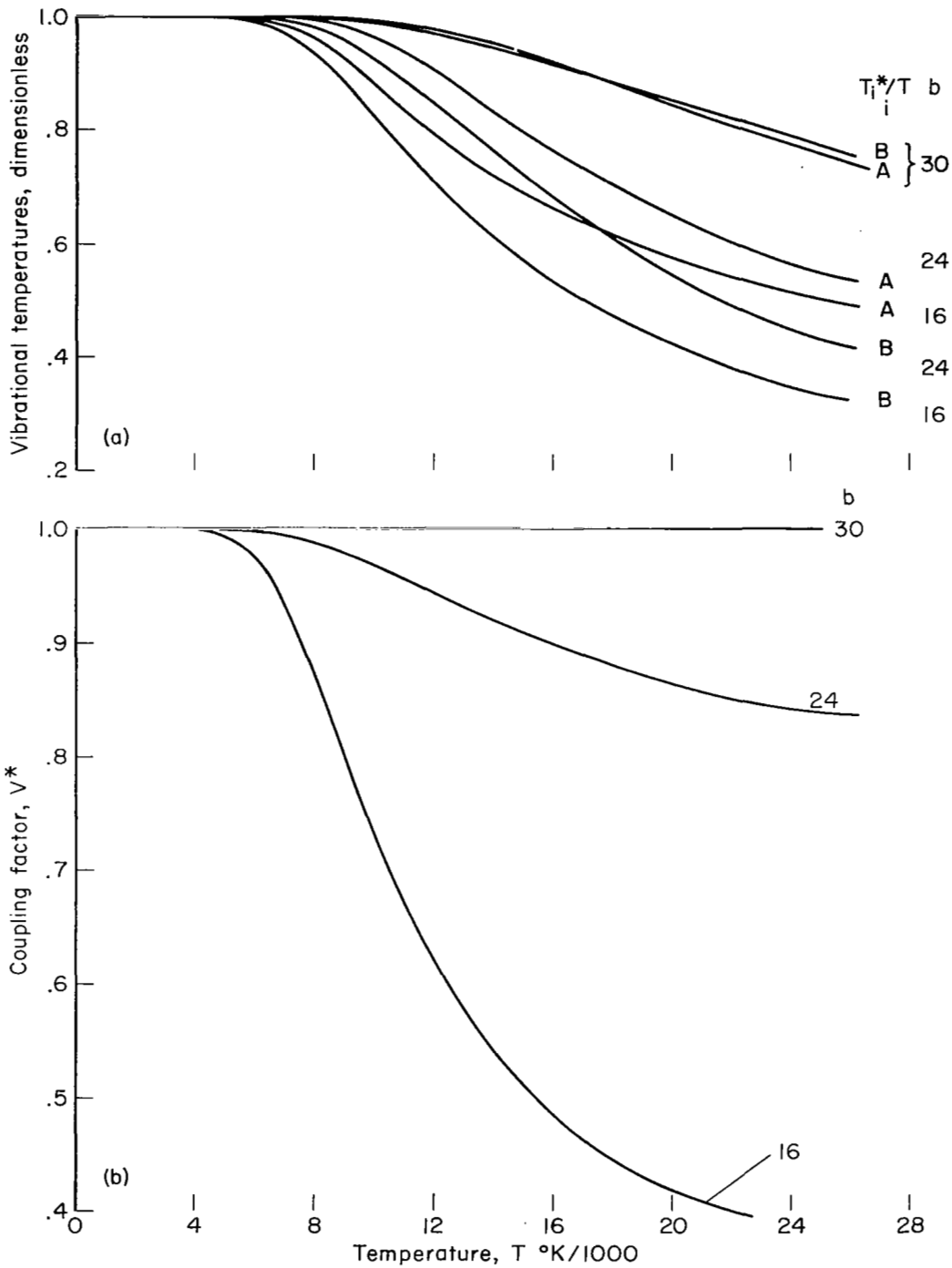


(a) Dimensionless vibrational temperatures
 (b) Vibrational coupling factor

Figure III-5. Variables obtained from quasi-steady solution versus temperature (associated parameters are listed along fifth row of table III-1)

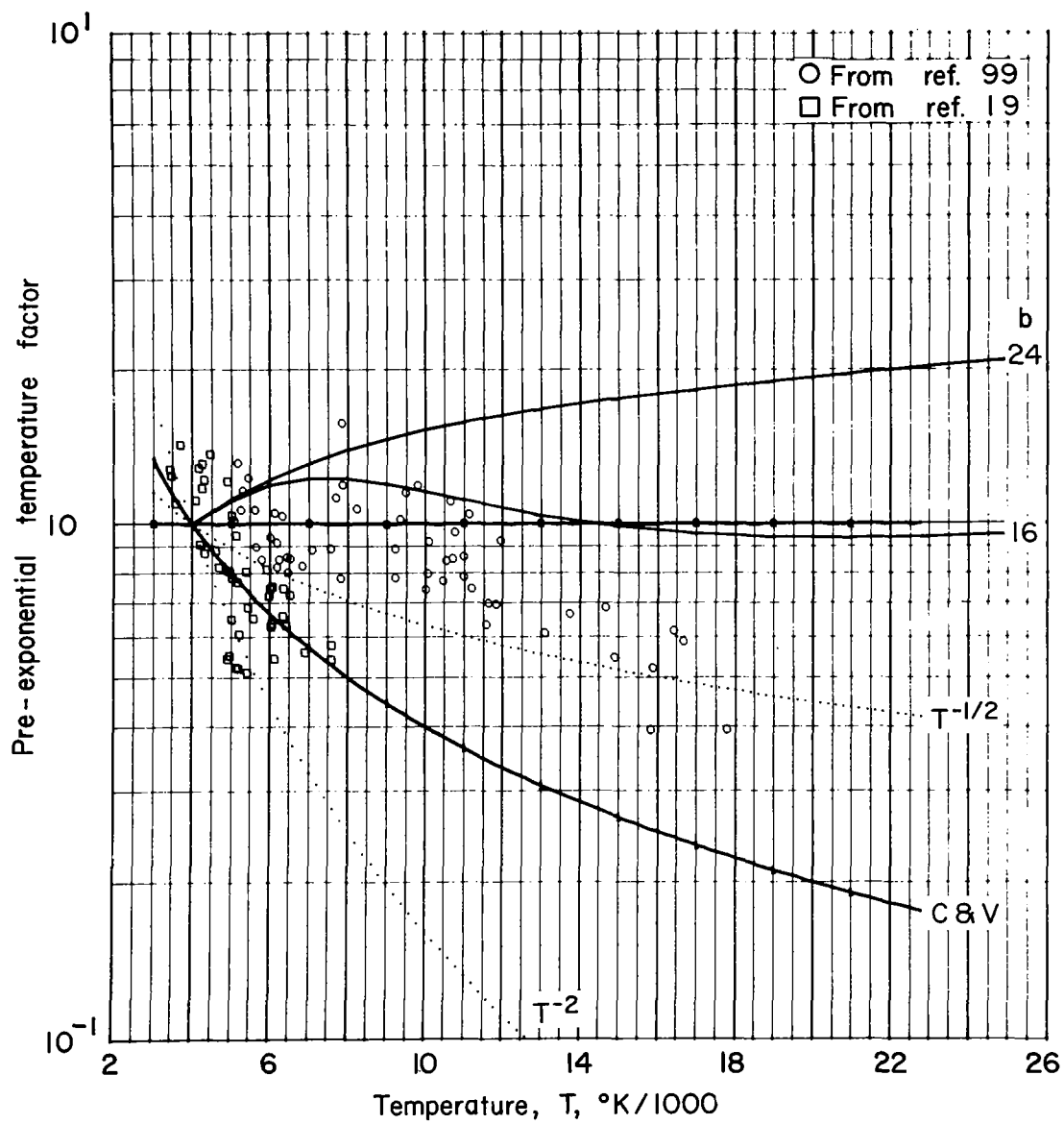


(c) Pre-exponential factor
 Figure III-5 Continued



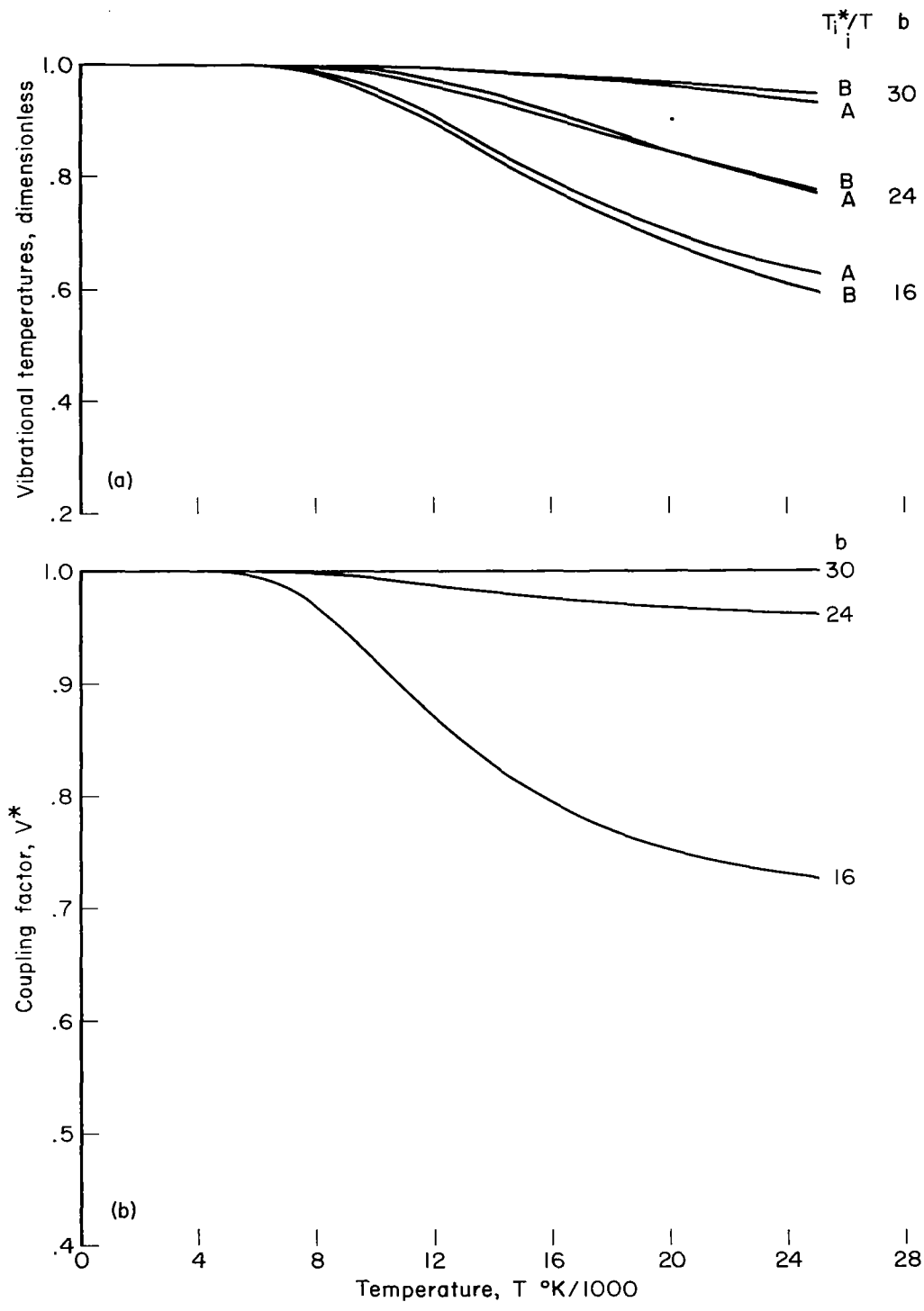
(a) Dimensionless vibrational temperatures
 (b) Vibrational coupling factor

Figure III-6. Variables obtained from quasi-steady solution versus temperature (associated parameters are listed along sixth row of table III-1)



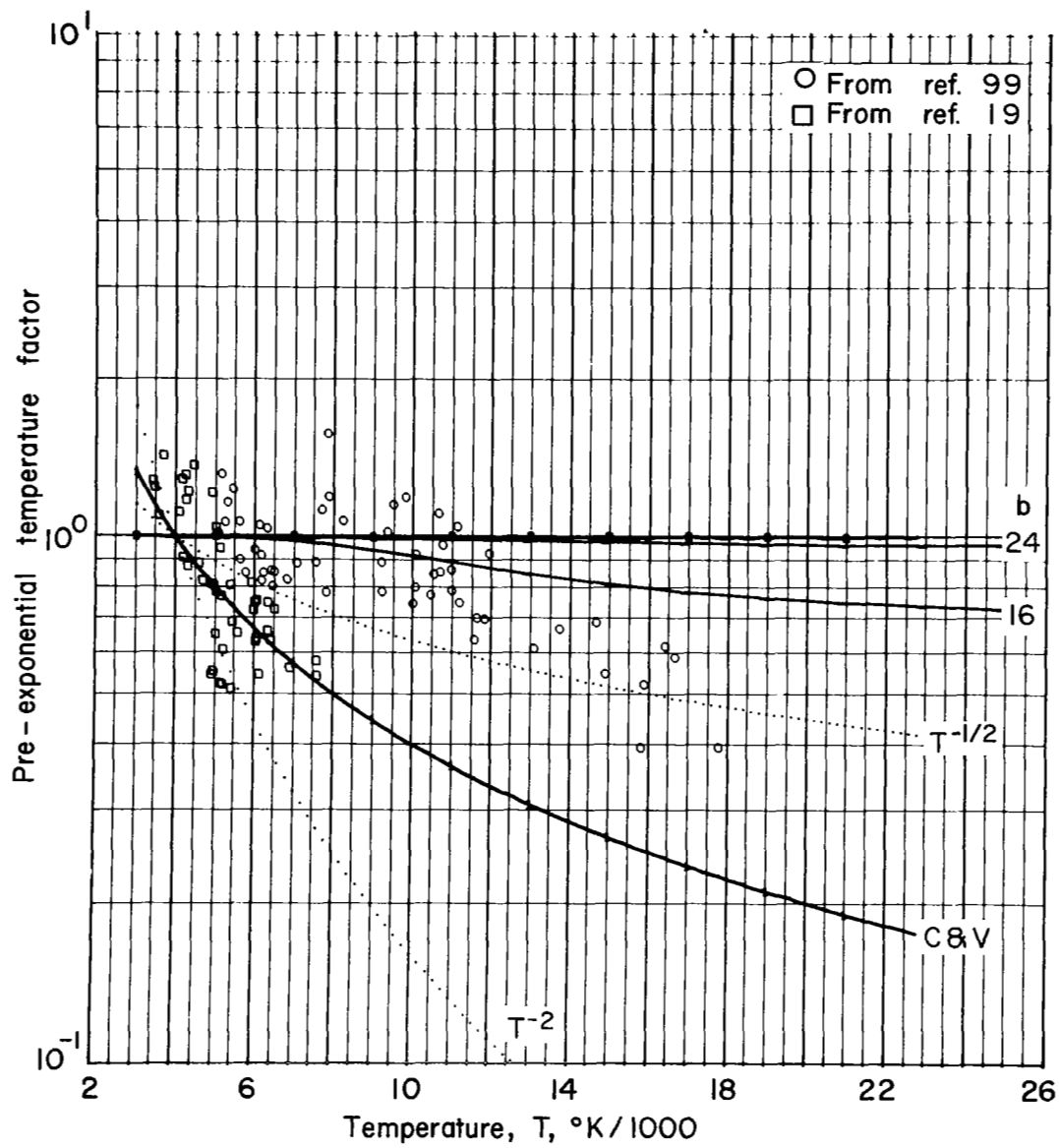
(c) Pre-exponential factor

Figure III-6 Continued



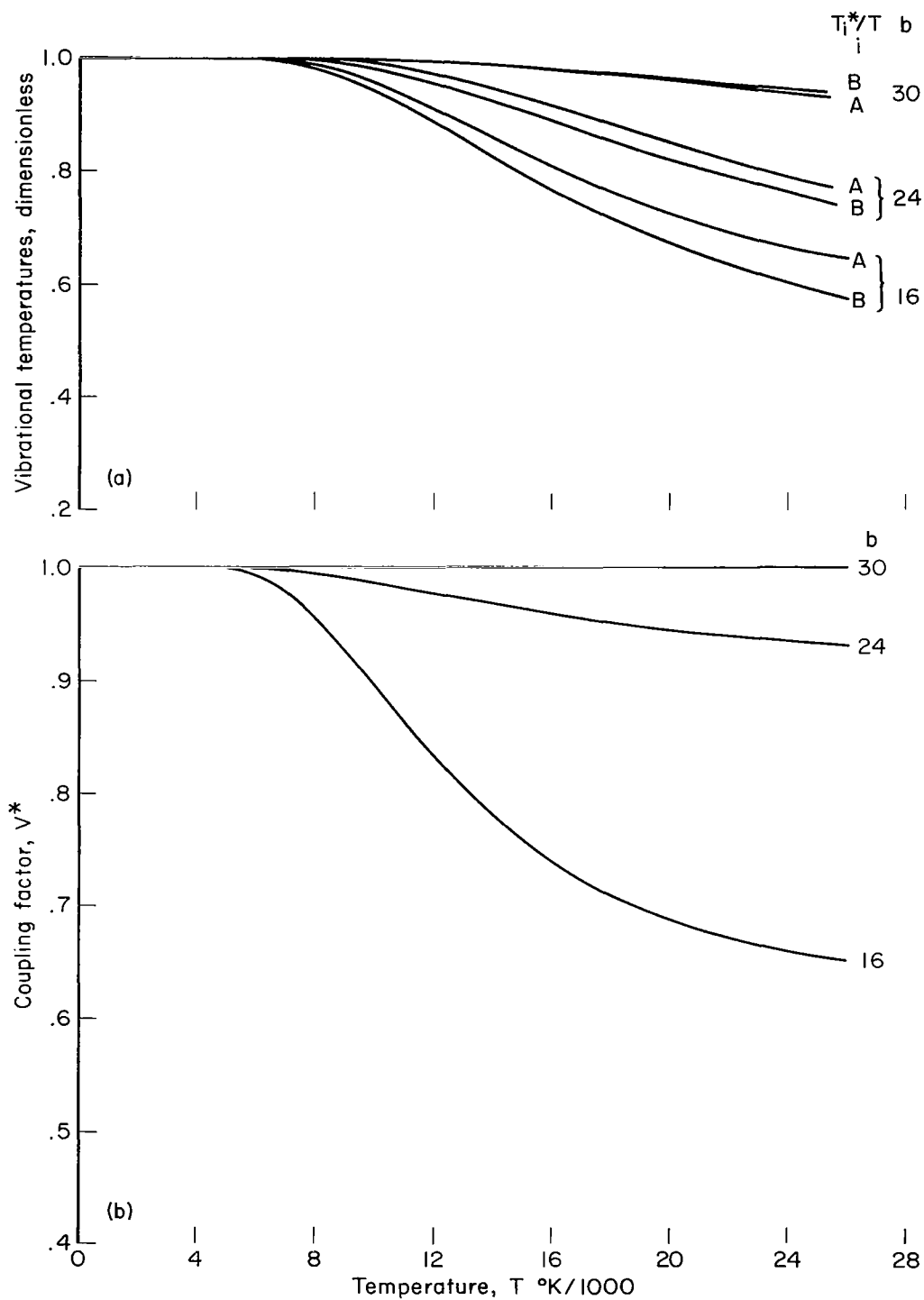
(a) Dimensionless vibrational temperatures
 (b) Vibrational coupling factor

Figure III-7. Variables obtained from quasi-steady solution versus temperature (associated parameters are listed along seventh row of table III-1)



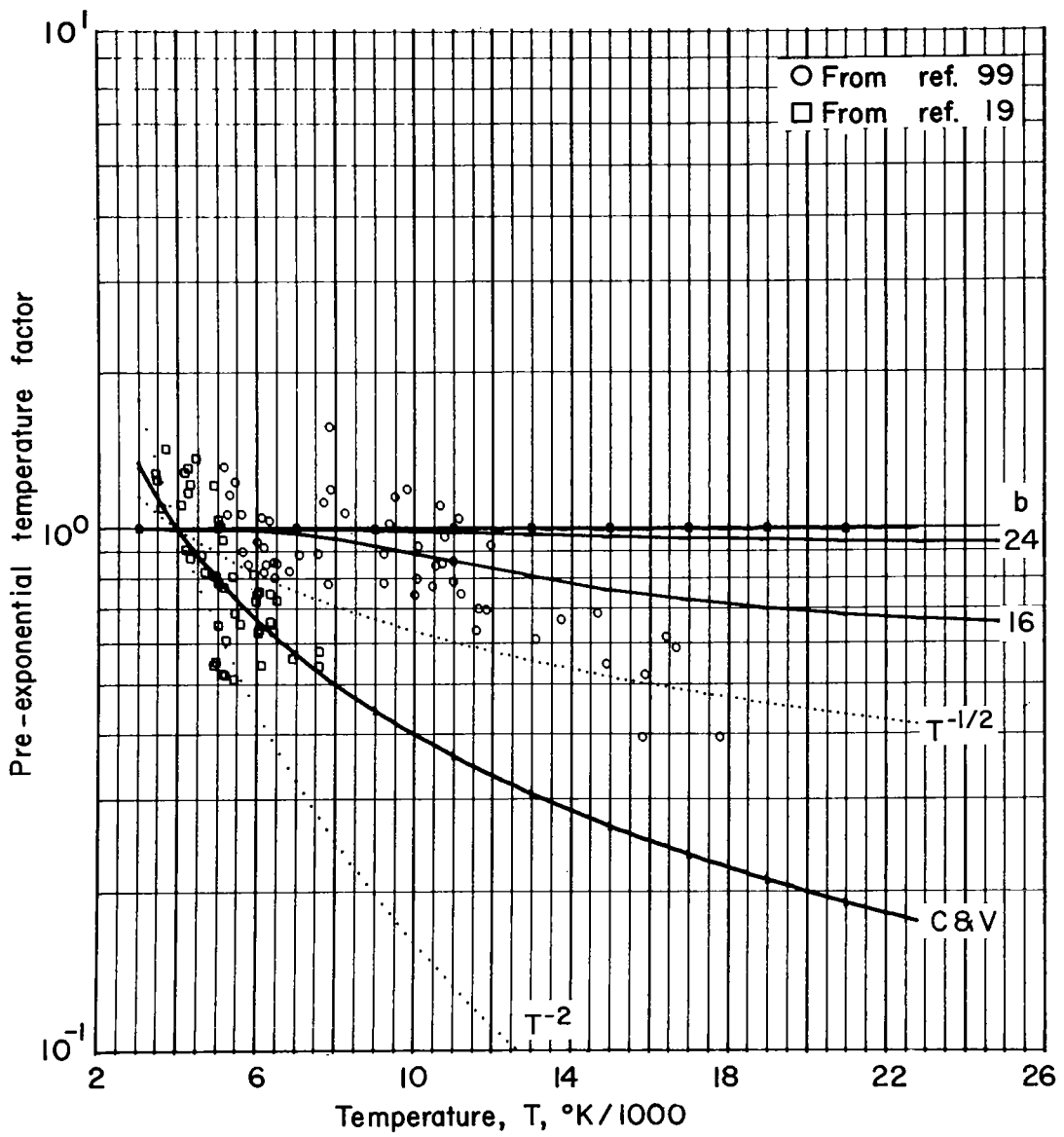
(c) Pre-exponential factor

Figure III-7 Continued

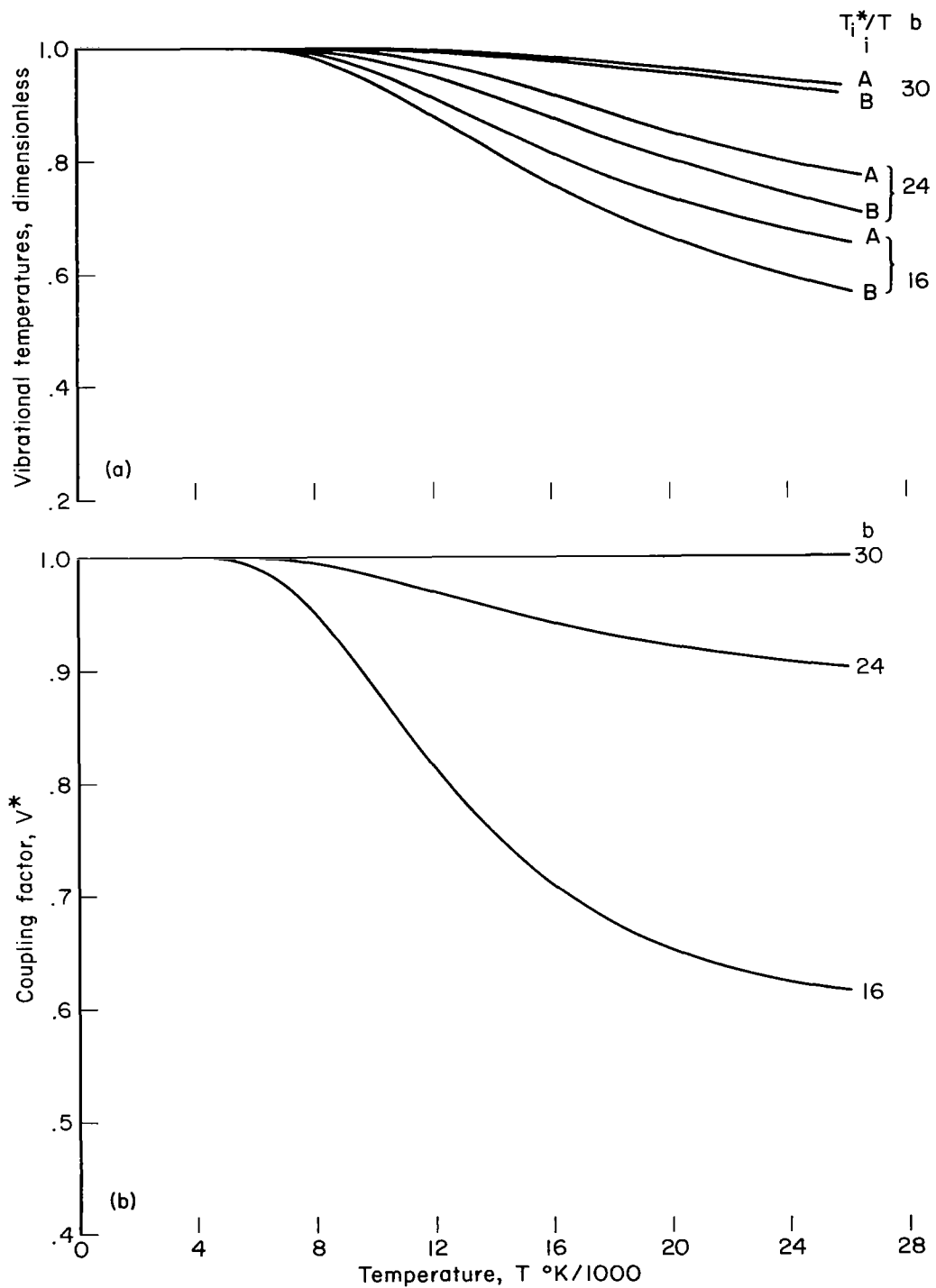


(a) Dimensionless vibrational temperatures
 (b) Vibrational coupling factor

Figure III-8. Variables obtained from quasi-steady solution versus temperature (associated parameters are listed along eighth row of table III-1)

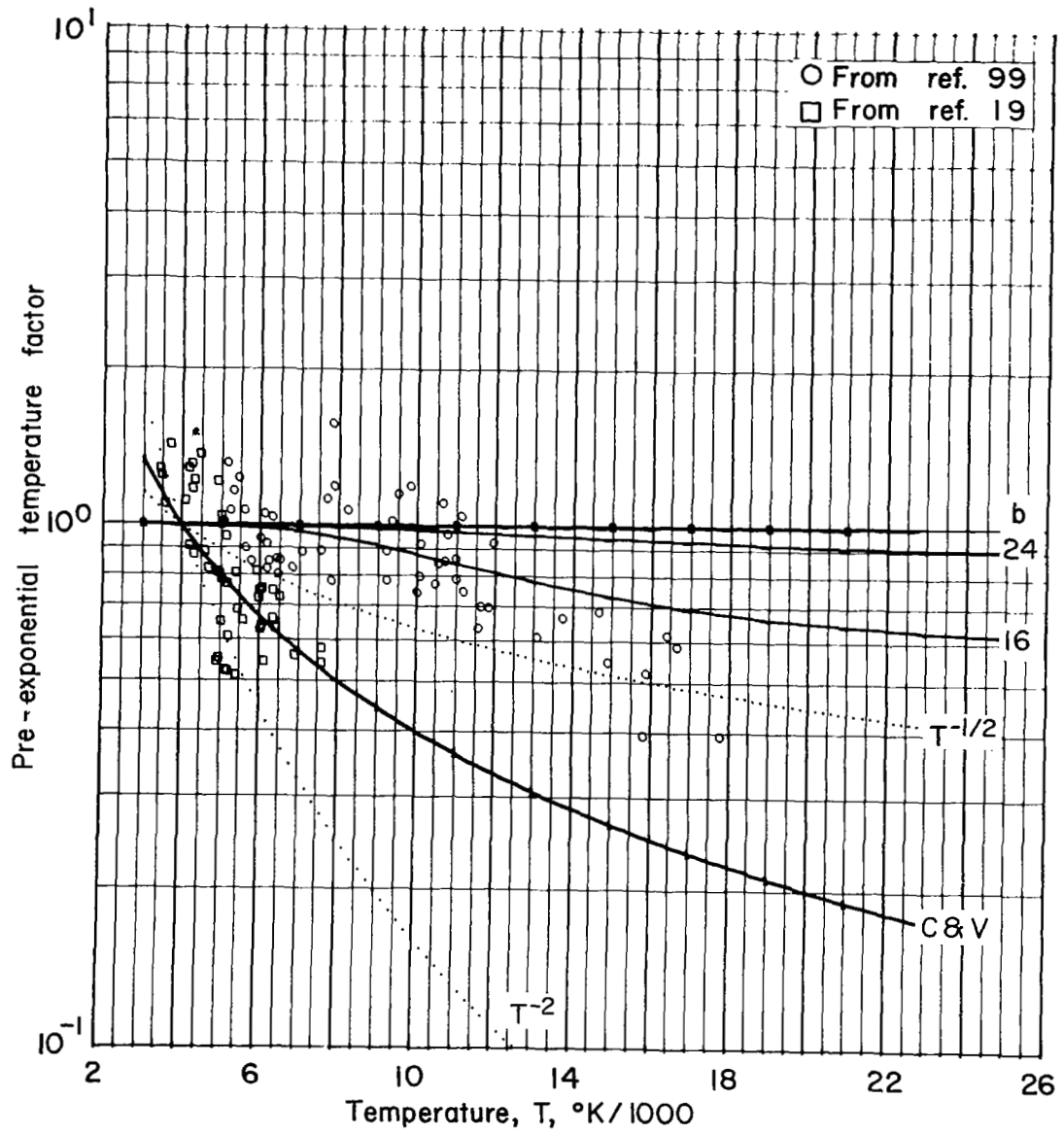


(c) Pre-exponential factor
 Figure III-8 Continued

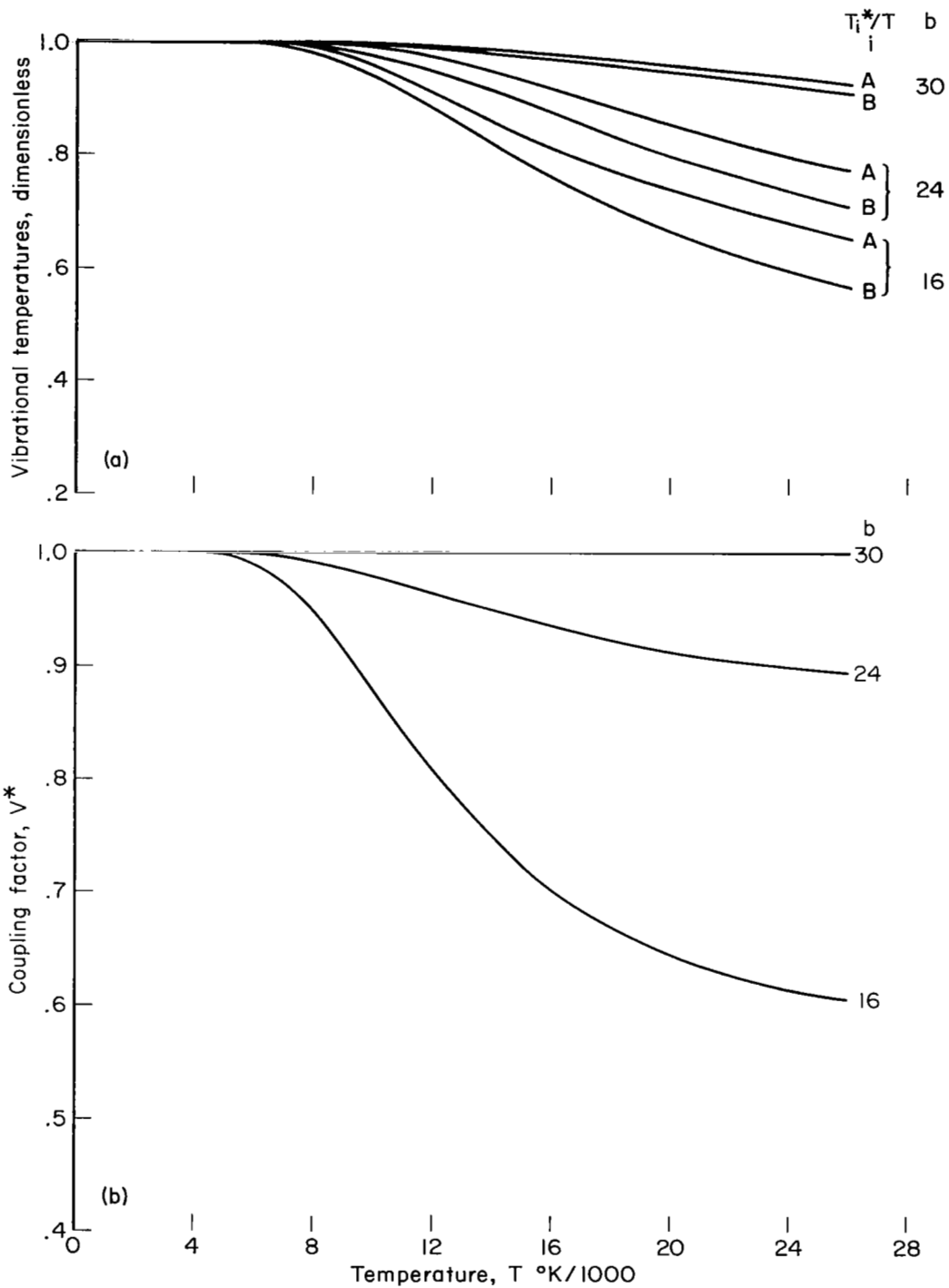


(a) Dimensionless vibrational temperatures
 (b) Vibrational coupling factor

Figure III-9. Variables obtained from quasi-steady solution versus temperature (associated parameters are listed along ninth row of table III-1)

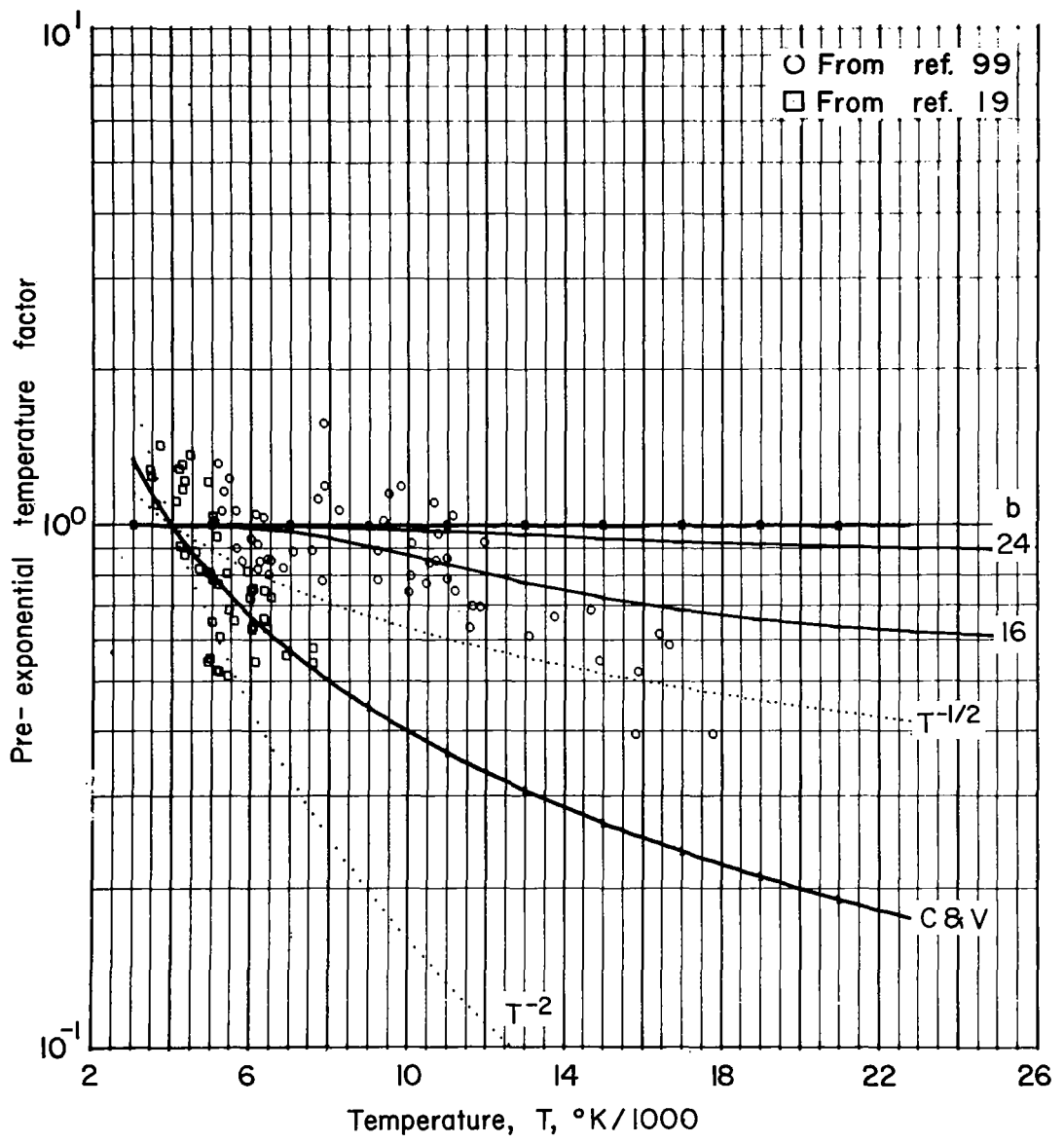


(c) Pre-exponential factor
 Figure III-9 Continued

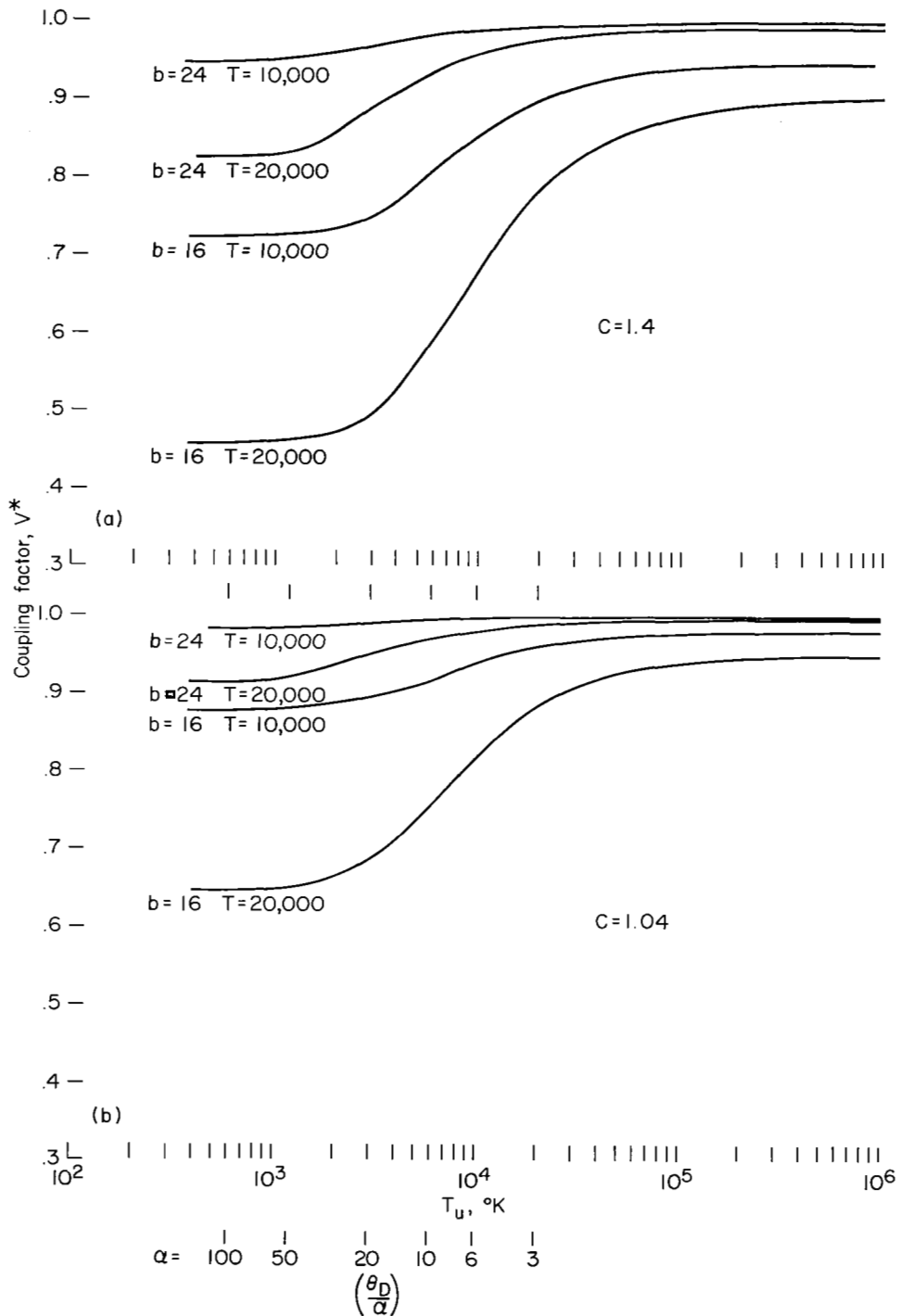


(a) Dimensionless vibrational temperatures
 (b) Vibrational coupling factor

Figure III-10. Variables obtained from quasi-steady solution versus temperature (associated parameters are listed along tenth row of table III-1)

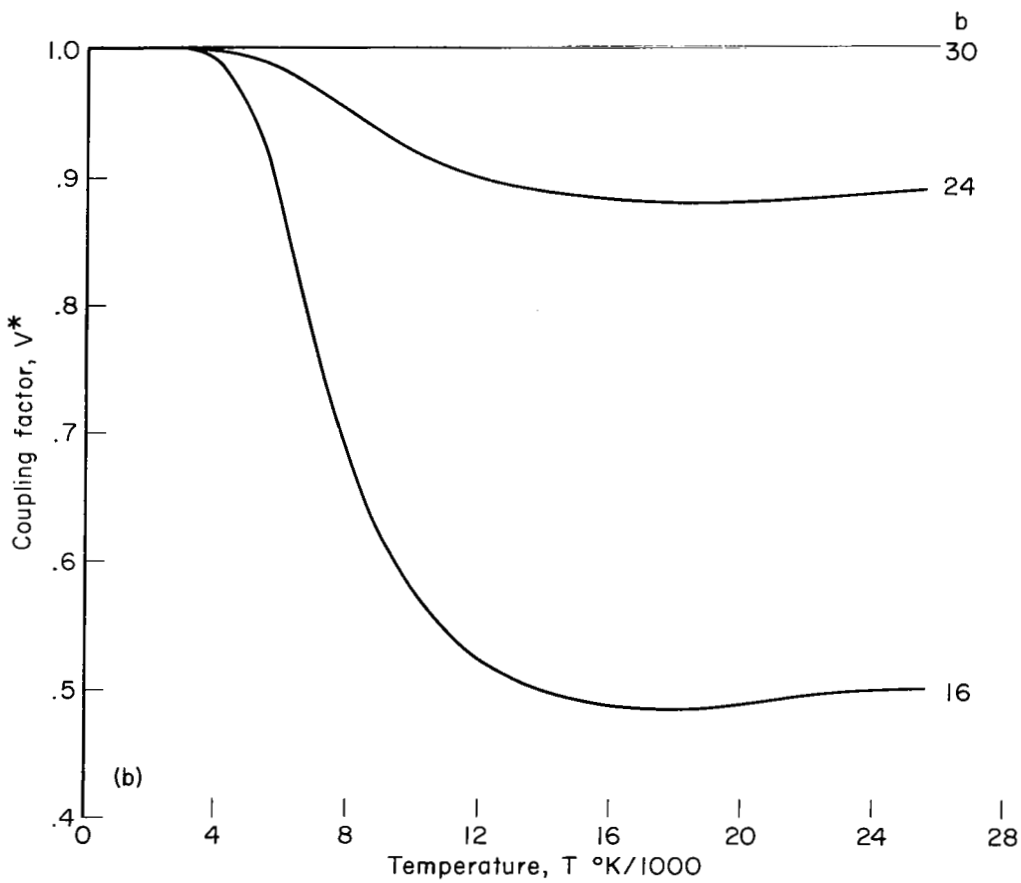
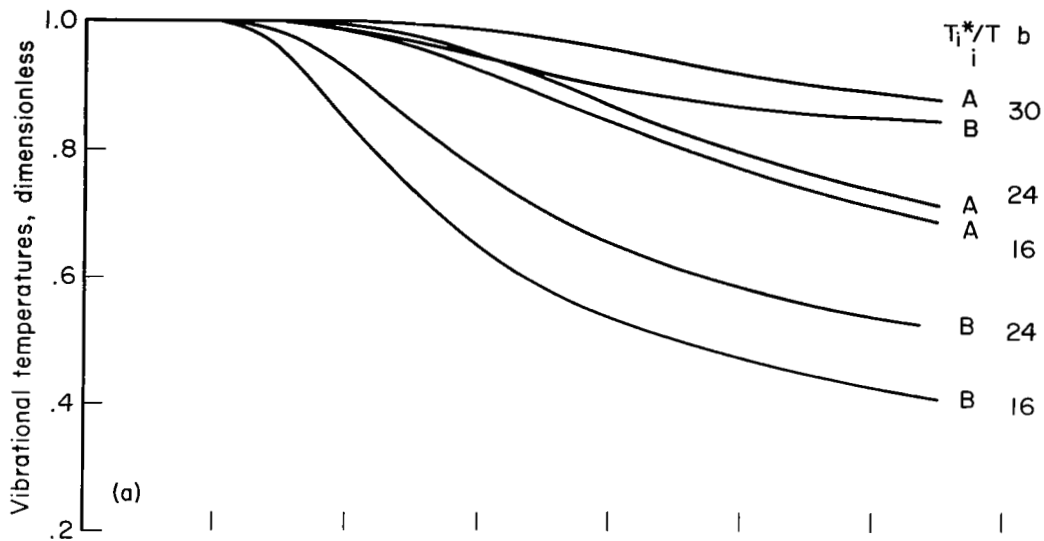


(c) Pre-exponential factor
 Figure III-10 Continued



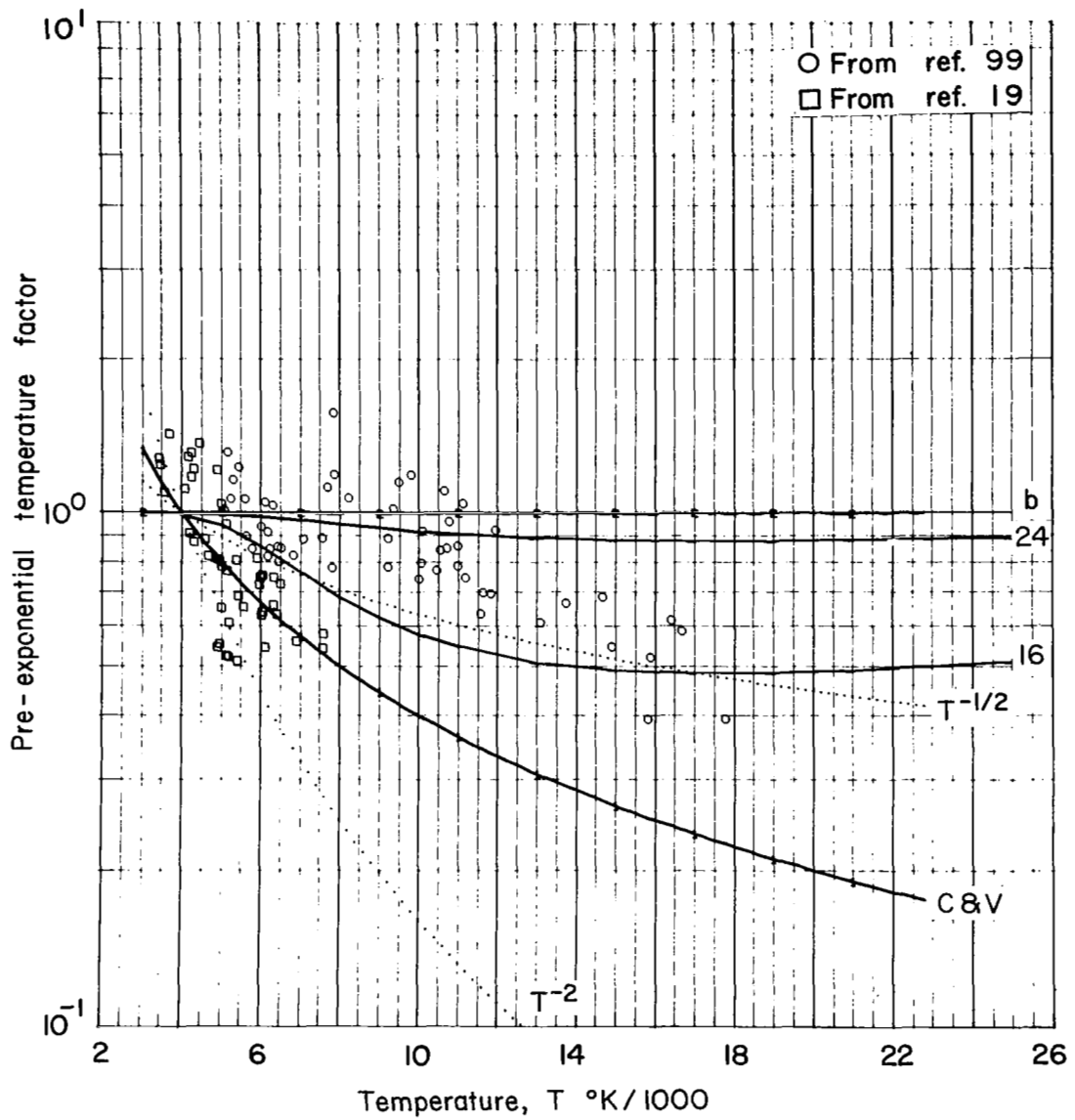
- (a) Relatively rapid vibrational relaxation time
- (b) "Correct" characteristic vibrational relaxation time

Figure III-11. Vibrational coupling factor obtained from quasi-steady solution versus temperature T_u (associated parameters are listed along eleventh row of table III-1)



(a) Dimensionless vibrational temperatures
 (b) Vibrational coupling factor

Figure III-12. Variables obtained from quasi-steady solution versus temperature (associated parameters are listed along twelfth row of table III-1)



(c) Pre-exponential factor
 Figure III-12 Continued

CHAPTER IV

COMPLETE SOLUTIONS OF THE MODEL EQUATIONS

IV-A. Introductory Comments

The preceding chapter was based on a study of the effects produced by changing the values of various parameters contained within the model equations. The investigation was greatly facilitated by the availability of easily obtained special solutions. Just as important, these special solutions had a particular significance in that they represent the conditions relevant to a comparison with many of the experimental rate observations. The solutions are particular to the quasi-steady zone behind a normal shock wave. The purpose of the investigation was primarily directed toward an assignment of values for the parameters. It is not possible, however, to evaluate the parameters in the model equations with certainty purely on the basis of comparisons with the quasi-steady solutions. As was observed, one may obtain equivalent results using different combinations of values for the parameters. In addition, because of the scatter in the experimental data, there is a broad range of values that one may assign to any one of the parameters and still effect satisfactory results. Additional comparisons are therefore advisable, and this is one purpose of the discussion in this chapter. In particular, we take advantage of the fact that measurements have been made on the delay time (incubation or induction time) that occurs before the onset of dissociation (99). These experimental measurements provide another and completely different basis for comparison. In addition, several measurements have been made of the characteristic vibrational relaxation times associated with expanding (nozzle) flows (98). However, because there is a considerable variation of the reported values of this quantity (44, 45, 61, 78, 79, 80, 98) (in some cases the values differ by several orders of magnitude), quantitative comparisons will not be made. It will be shown that the model yields qualitative agreement with these studies and, for the more recent references (98), the agreement appears quite good.



The essential difference between this and the preceding chapter is that here the discussion will involve the simultaneous solution of the model rate and fluid-flow equations. A rather complicated numerical integration procedure was required to obtain these solutions and the development of this procedure was a major task. A discussion of the numerical aspects of the problem is given in Appendix E, and the explicit form of the equations that are solved is given in Appendix F.

After the final comparisons are made, a single set of values can be defined for the embedded parameters that effect reasonable agreement of the model with available experimental data. The model, in this respect, is complete.

As a result of the formalism reported in Chapter II and used to derive the equations, the various terms constituting the rate equations have physical significance, and their investigation therefore is worthwhile. Such an investigation yields insight as to why differences should be expected when comparing, for example, characteristic vibrational relaxation times obtained from normal-shock wave and nozzle data.

In the section that follows, the discussion will first concern the shock structure that results from the complete solution of the model equations. Initially no emphasis will be made on the effects that result from any particular choice of parameter values. Qualitative features of the shock structure appear to be due to the structure of the equations regardless of specific values of the parameters. The relationships of the various terms to these features will first be discussed to promote an understanding of the vibration-dissociation coupling process. After the discussion on the shock structure, attention will be given to the differences caused by changing the values for the parameters. The effects of the parameters on the induction time will also be considered. Later sections provide a description of the events occurring in nozzle flow. An explanation is also given of the significant differences observed between shock-wave relaxation processes and the relaxation processes associated with expanding flows.

IV-B. Normal-Shock Wave Solutions

The results of this section are obtained by setting the derivatives dA/dx in equations (F16) equal to zero and then integrating the resulting equations according to the numerical integration procedure described in Appendix E. (The explicit method is used for about the first 125 computational points, and the implicit method is used thereafter.) The conditions downstream of the shock, which provide the initial values for the integration procedure, are obtained by an iteration procedure similar to that given by Vincenti and Kruger (p. 179 in 97). Here the nonequilibrium variables γ_A , γ_B , γ_a , T_A , and T_B are assumed to be frozen across the viscous shock. The gas mixture used for these solutions was 4 percent molecular oxygen and 96 percent argon. The effects of considering molecules other than argon as a colliding partner may therefore be taken as negligible (that is, the fractions γ_{O_2}/γ_m and γ_O/γ_m in eqs. (II-113) may be considered small and only the species argon considered for the summation index r).

A sampling of the results is given in figures IV-1 through IV-7. For the reader's convenience, table IV-1 lists the values for the temperature-dependent parameters in the cases plotted. The cases illustrate the effects occurring for several values of the parameters and for shock waves having values for the downstream temperature T_2 (kinetic temperature directly behind the shock wave) of 6,677° and 16,570° K. One sample case is plotted for the lower temperature purely to illustrate the differences that occur for weaker shocks. The abscissa scale for these figures corresponds to the time after passage of the shock (laboratory time) appropriately adjusted[†] so as to remove the dependence

[†]The abscissa scale is computed according to the formula

$$(t_{lab})_{adjusted} = t_{lab} \times (n_2/1.28 \times 10^{17}) \quad (IV-1)$$

where $n_2 = p_2/kT_2$, k is Boltzmann's constant, and the subscript 2 denotes values immediately downstream of the shock wave (see, e.g., p. 56 in 10 for discussion of t_{lab}). This adjustment is sufficiently accurate since the density behind the shock is nearly constant.

Table IV-1

Parameters Associated With Complete Solutions, Figures IV-1 Through IV-7

Figure no.	T_2	T_u	χ	k_{Feq}	C_2	b	a	Quasi-steady Fig. no.
IV-1	16,570	$\Theta_D/10$	F	MT	(1)	16	9	III-7
IV-2	16,570	$\Theta_D/10$	F	MT	(2)	16	9	III-5
IV-3	16,570	$\Theta_D/10$	F	MT	(1)	24	9	III-7
IV-4	16,570	$\Theta_D/10$	F	MT	(2)	24	9	III-5
IV-5	16,570	$\Theta_D/50$	F	MT	(1)	16	9	III-9
IV-6	6,677	$\Theta_D/10$	F	MT	(1)	16	9	III-7
IV-7	16,570	$\Theta_D/10$	$\chi = 1$	MT	(1)	16	9	III-12

χ : F see eq. (B23b)
 k_{Feq} : MT see eq. (III-13b)
 C_2 : (1) see eq. (III-12a)
(2) see eq. (III-12b)

of this scale on density. In this manner one can compare the effects occurring for different shock-wave solutions regardless of the density behind the shock. This procedure parallels that used by Wray (99) and in effect relates the effect of relaxation to a common density behind the shock of 1.28×10^{17} particles/cc.

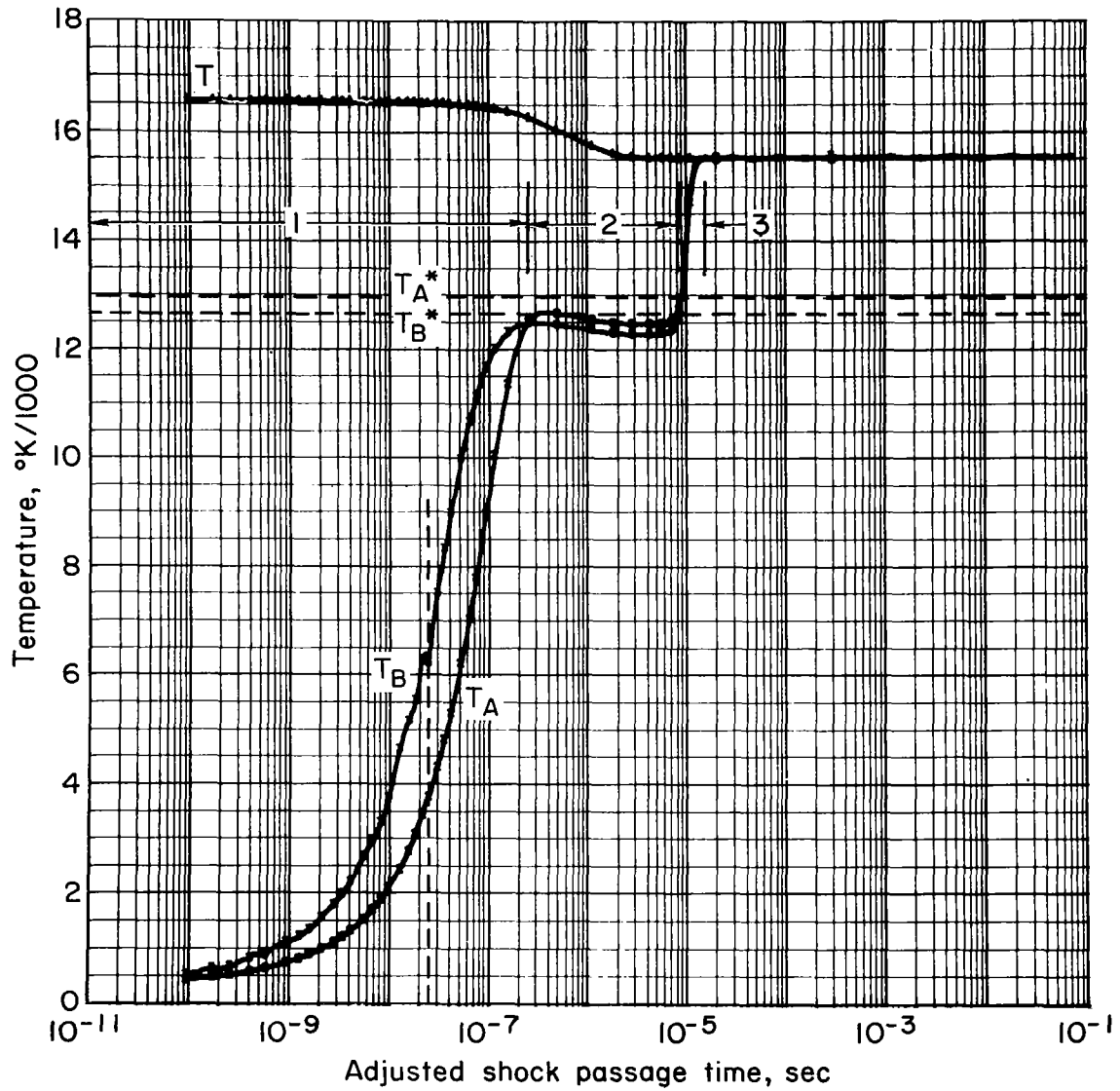
Before beginning the discussion of the solutions, a few comments of a general nature should be made concerning these figures. First, the reader is cautioned to observe that the time scales may be different for the different plots. The figures were generated automatically with a General Dynamics S-C 4020 Electronic Plotter (for a description of the system used, see 50). The scaling parameters were also obtained automatically and since the integrations were not always terminated at the same relative reference time, some plots encompass longer times after passage of the shock wave than others (e.g., compare figs. IV-1 and IV-2). The figures show the complete shock profiles; for the longer times, once equilibrium is reached, no further effects are observed and the values of the dependent variables remain constant. The plots show an

erratic behavior in the first transient zone that in some cases is of greater magnitude than for others (e.g., compare figs. IV-1 and IV-6). This behavior depends purely on the numerical integration procedure and represents the effects of numerical instability. It has no effect on the final values of the integrated variables. One has full control of the amplitude of the instability, and the effects are shown only to lend additional weight to the discussion on the numerical integration procedure given in Appendix E. For the present discussion one may ignore the instability phenomenon, since they do not affect the final results and since they are of no consequence to a physical description of the results. The correct values of the variables are made evident by a smooth curve fitted through the lower locus of computed points.

Given in each figure are plots of the variables T , T_A , T_B , γ_A , γ_B , γ_a , and the ratio γ_B/γ_A (this latter quantity becomes constant in the quasi-steady zone). In figures IV-1, 3, 5, 6 the vibrational coupling factors are also plotted and in figures IV-1 and IV-7 are shown, in addition, the derivatives and their component terms.

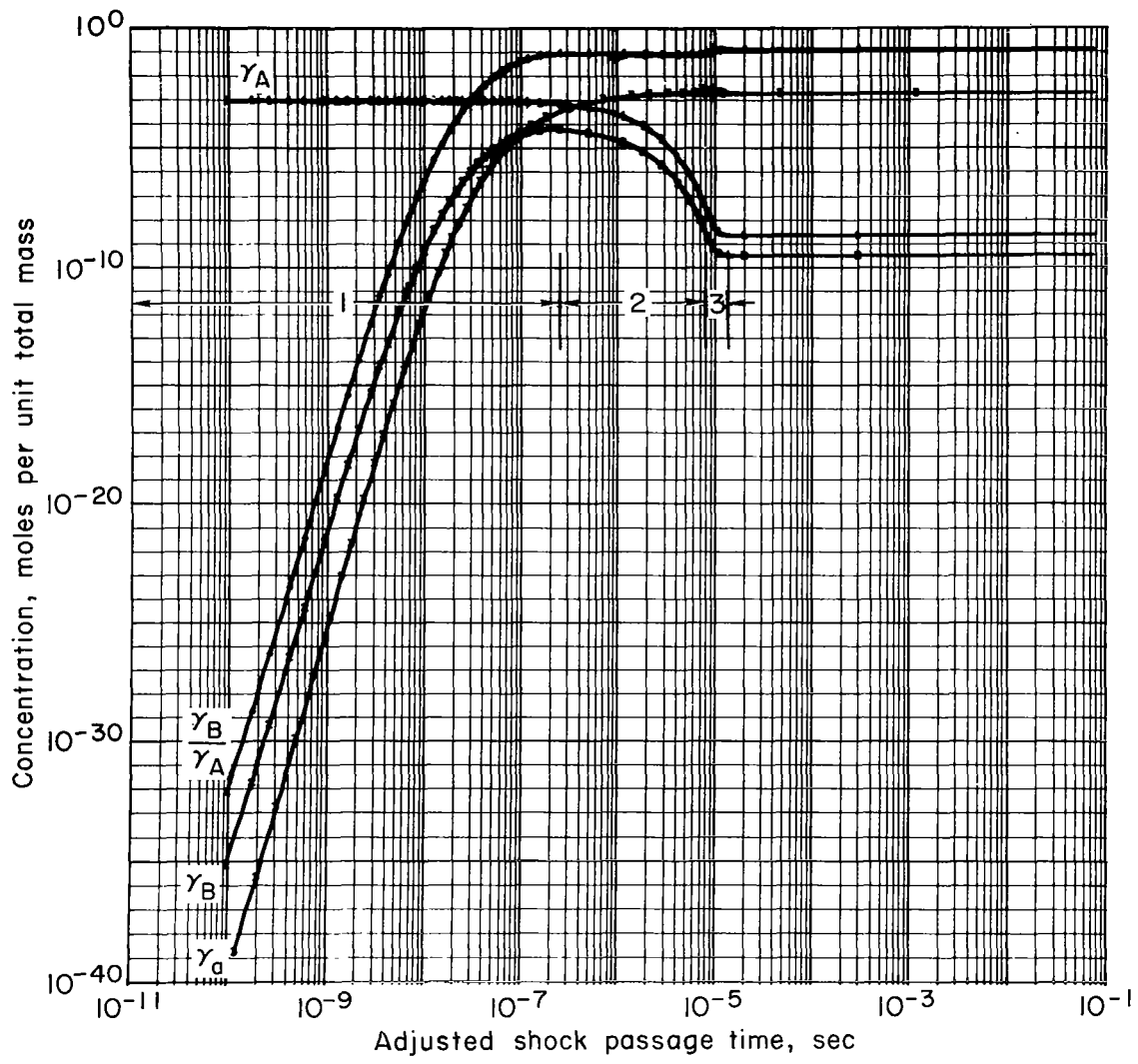
(IV-B-1). Shock-Wave Structure

We first consider in detail the shock structure resulting from a solution of the model equations, ignoring any consideration of effects peculiar to a particular choice for the embedded parameters. Figures IV-1, for example, give a complete picture of the relaxation processes (these processes are associated with a single set of parameters having the values listed along the first row in Table IV-1). The three characteristic zones mentioned previously are labeled in this figure by the numerals 1, 2, and 3 corresponding, respectively, to the transient, the quasi-steady, and the final relaxation zones. In the first region the vibrational temperatures, T_A and T_B , and the upper-state and atom concentrations, γ_B and γ_a , rapidly increase in value, attaining their quasi-steady values in about a quarter of a microsecond; that is, in the transient region, the upper vibrational states are rapidly populated, thermally "heated" and, at the same time, partially dissociated as evidenced by the increasing atom concentration (recall that only the B molecules are allowed to dissociate). In the



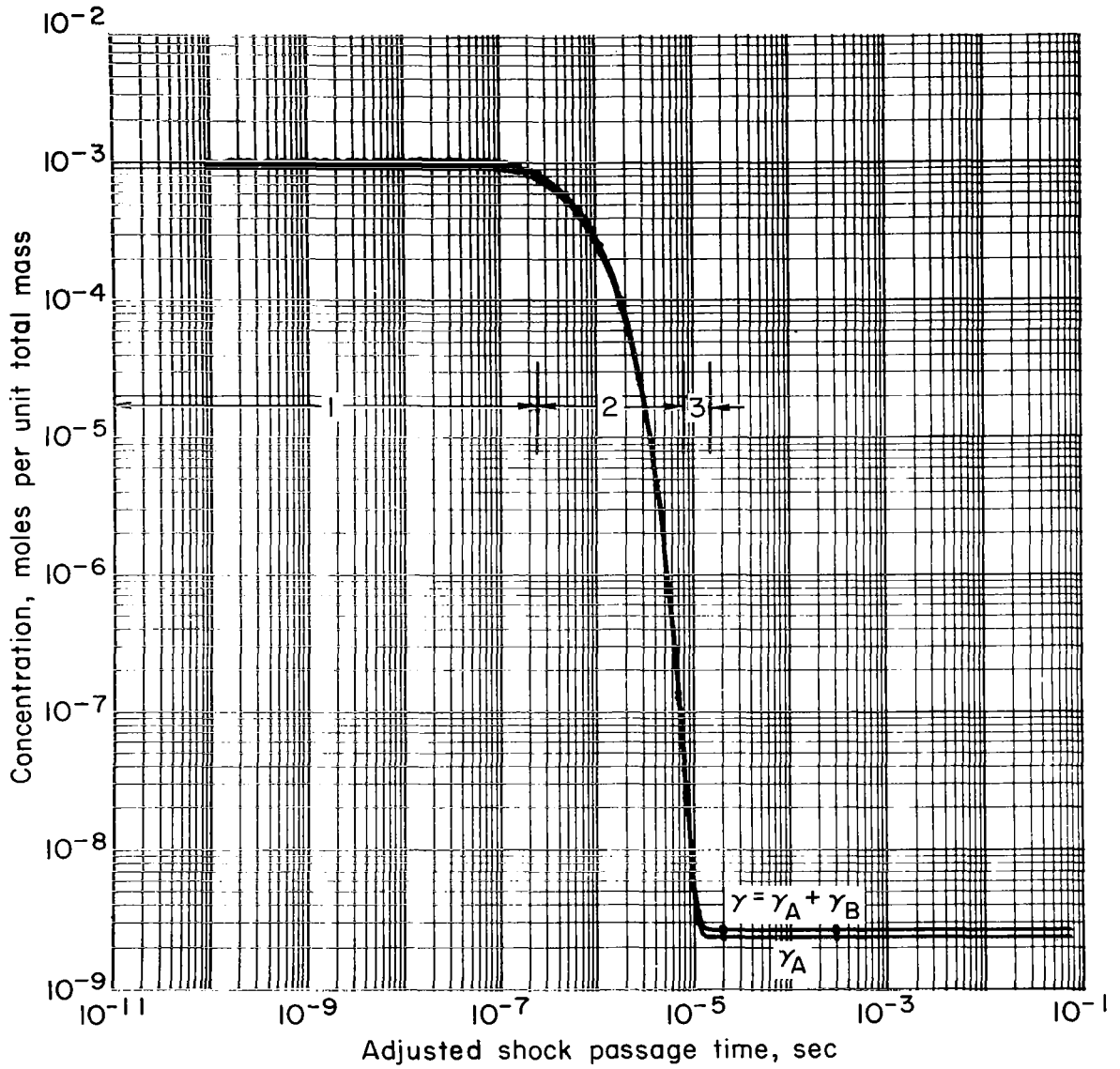
(a) Temperatures

Figure IV-1. Variables obtained from shock solution versus adjusted laboratory time (associated parameters are listed along first row of table IV-1)



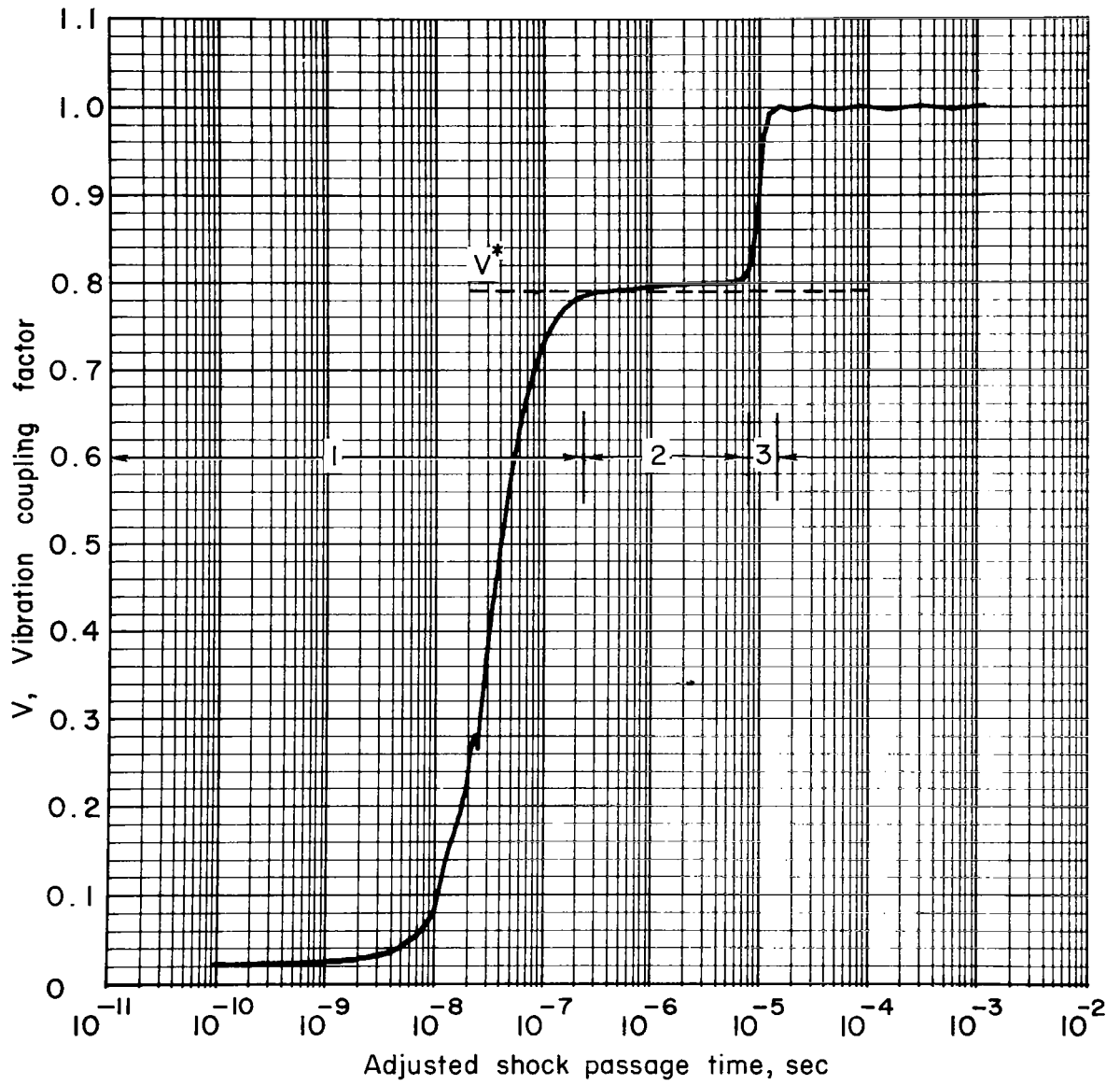
(b) Concentrations

Figure IV-1 Continued



(c) Concentration, Lower States and Molecular

Figure IV-1 Continued



(d) Vibrational coupling factor

Figure IV-1 Continued

transient zone, the lower-state molecular concentration remains relatively constant, and the vibrational coupling factor rapidly increases from its initially small value.

The quasi-steady zone is indicated in these figures, and the values obtained from the quasi-steady solutions of the preceding chapter are given.[†] These values are labeled by the variables superscripted with an asterisk. The quantity V^* compares accurately with the quasi-steady value obtained here, as can be seen in figure IV-1d. There is a slight discrepancy of about 2 percent, however, between the results for both T_A^* and T_B^* as computed in the previous chapter and as found here. This difference is attributed to the fact that the temperature T is not exactly constant as was assumed in the previous chapter, but changes about 10 percent as a result of the effects of dissociation (note that the temperature T varies only in the quasi-steady zone). The dissociation energy has a relatively large effect on the kinetic temperature even though the molecular concentration is small (initially 4 percent of the total mixture). The density and velocity, however, are not so greatly affected by dissociation. These quantities are nearly constant and are therefore not plotted. (They varied about 4 percent as a result of dissociation.) One notes that in the quasi-steady zone the ratio γ_B/γ_A and the temperatures T_A and T_B are nearly constant. The basic quasi-steady assumptions are thus in fact valid in these cases. It is also interesting that, although the concentrations γ_A and γ_B are varying, their ratio is indeed constant.

An additional feature characterizing the quasi-steady zone is that in this zone the effects of dissociation become appreciable, as is evidenced by the rapid decrease in the molecular concentration and by the effect on T . The entire molecular concentration is approximately contained in the states denoted "A" as a result of the relatively large difference in the concentration

[†]The temperatures T_2 and the applicable quasi-steady solutions are listed in Table IV-1. With this information the respective quasi-steady values for the variables are readily obtained from the figures of the preceding chapter.

variables γ_A and γ_B . This is exemplified further in figure IV-1c, where the lower-state concentration γ_A is plotted along with the total molecular concentration $\gamma = \gamma_A + \gamma_B$. It is also worthwhile to point out that the temperature T_B initially increases in the transient region at a more rapid rate than T_A , but near the end of this region T_A overtakes T_B . In the quasi-steady region the effect of dissociation is to cause T_B to be lower than T_A .

As regards the passage time of the latter two zones, for the case exemplified by figure IV-1 the quasi-steady zone persists about 8 μsec or about 30 times longer than the transient region. The final relaxation region persists about 7 μsec , during which time final relaxation to equilibrium occurs. From these results one can appreciate why many of the experimental observations are conducted during the rather long-time passage of zone 2. Although the final relaxation zone also requires a relatively long passage time, experimental measurements in this region are often hampered by other effects such as, for example, the arrival of a driver gas (shock-tube studies, see, e.g., 10, 70, 86).

We have so far been discussing the structure of a shock wave according to the behavior of the basic dependent variables. This discussion was based on a single "complete" solution. In figures IV-1e through IV-1i are plotted the complete derivatives and their separate terms associated with this solution. To facilitate a description of these figures the following notation is introduced for the terms that appear in equations (II-113):

$$Q_1^{\bar{\gamma}_A} = - \frac{\rho \gamma_m k_F^{(1)}(T_A, T)}{v} \quad (\text{IV-2a})$$

$$Q_2^{\bar{\gamma}_A} = \frac{\rho \gamma_m}{v} \frac{\gamma_B}{\gamma_A} k_R^{(1)}(T_B, T) \quad (\text{IV-2b})$$

$$Q_1^{\bar{\gamma}_a} = 2 \rho \gamma_m \frac{\gamma_B}{\gamma_a} V(T_B, T) k_{\text{Feq}}(T)/v \quad (\text{IV-3a})$$

$$Q_2^{\bar{\gamma}_a} = -2 \rho^2 \gamma_m \gamma_a \frac{k_{\text{Feq}}(T)}{\kappa_B(T)}/v \quad (\text{IV-3b})$$

$$Q_1^{\bar{\gamma}_B} = -Q_1^{\bar{\gamma}_A} \frac{\gamma_A}{\gamma_B} \quad (\text{IV-4a})$$

$$Q_2^{\bar{\gamma}_B} = -Q_2^{\bar{\gamma}_A} \frac{\gamma_A}{\gamma_B} \quad (\text{IV-4b})$$

$$Q_3^{\bar{\gamma}_B} = -\frac{1}{2} Q_1^{\bar{\gamma}_a} \frac{\gamma_a}{\gamma_B} \quad (\text{IV-4c})$$

$$Q_4^{\bar{\gamma}_B} = -\frac{1}{2} Q_2^{\bar{\gamma}_a} \frac{\gamma_a}{\gamma_B} \quad (\text{IV-4d})$$

$$Q_1^{T_A} = \frac{Q_{A_1}(T_A)}{Q_A(T_A)} \frac{\Omega_{A_1}(T, T_A)}{C_{vA}(T_A) \tau_{A_1}^v} \quad (\text{IV-5a})$$

$$Q_2^{T_A} = \frac{Q_{A_2}(T_A)}{Q_A(T_A)} \frac{\tau_{A_1}}{\tau_B} \frac{\Omega_{A_2}(T, T_A)}{C_{vA}(T_A) \tau_{A_1}^v} \left[1 - \frac{\Delta(T)}{q_{A_2}(T_A)} \right] \quad (\text{IV-5b})$$

$$Q_3^{T_A} = [R_0 \Theta_{b-1} - q_A(T_A)] Q^{\bar{\gamma}_A} \quad (\text{IV-5c})$$

$$Q_1^{T_B} = \frac{\tau_{A_1}}{\tau_B} \frac{\Omega_B(T, T_B)}{C_{vB}(T_B) \tau_{A_1}^v} \left[1 - \frac{\Delta(T)}{q_B(T_B)} \right] \quad (\text{IV-6a})$$

$$Q_2^{T_B} = \beta \frac{R_0 \Theta_{A_2} \gamma_m}{C_{vB}(T_B)^v} k_R^{(1)}(T_B, T) \left\{ 1 - \exp \left[-\Theta_{A_2} \left(\frac{1}{T} - \frac{1}{T_B} \right) \right] \right\} \quad (\text{IV-6b})$$

$$Q_3^{T_B} = \frac{q'_B(T_B)}{C_{vB}(T_B)} \frac{\gamma_A}{\gamma_B} Q^{\bar{\gamma}_A} \quad (\text{IV-6c})$$

$$Q_4^{T_B} = \left[\frac{q'_B(T_F) - q'_B(T_B)}{C_{vB}(T_B)} \right] Q_3^{\bar{\gamma}_B} \quad (\text{IV-6d})$$

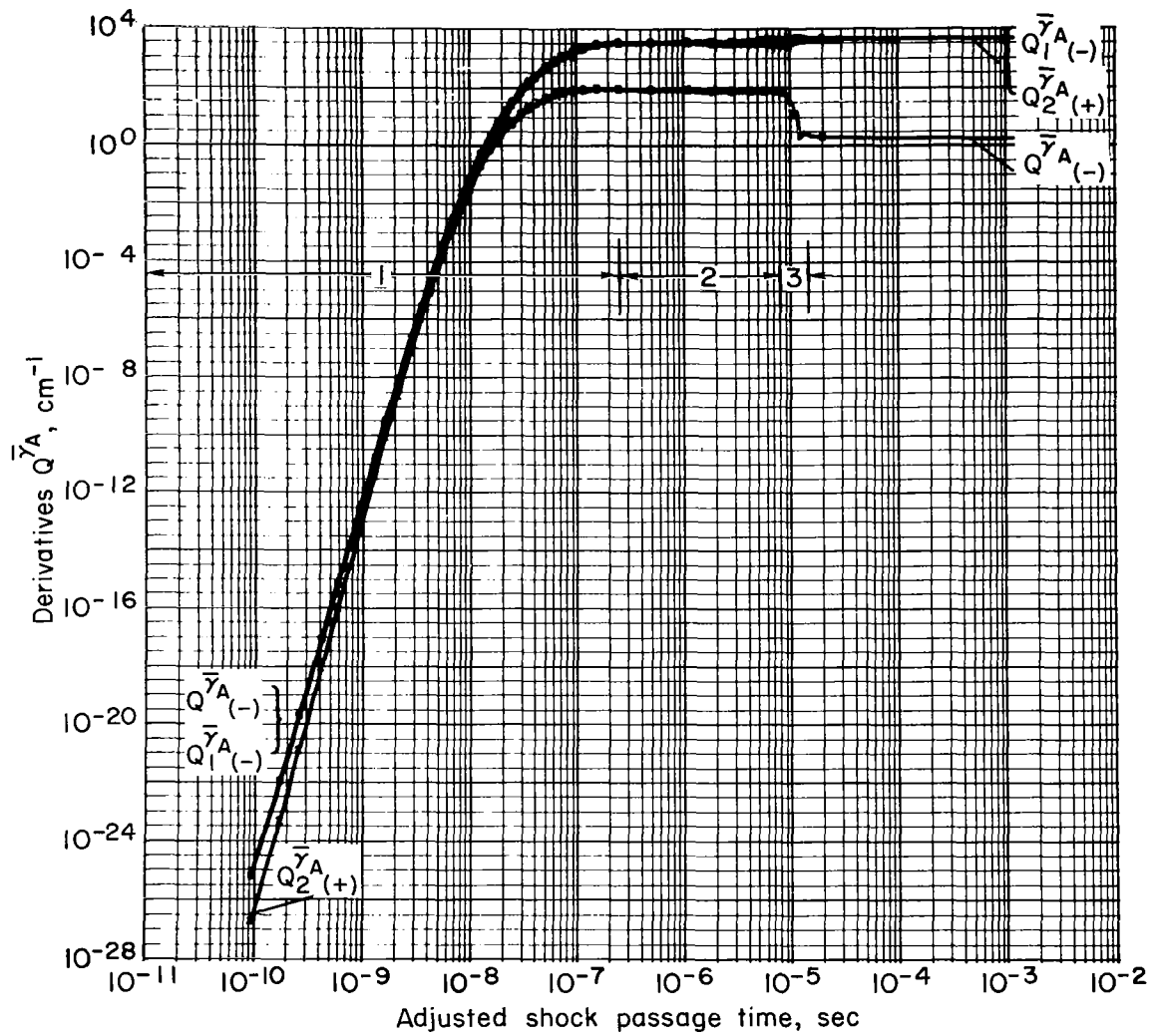
$$Q_5^{T_B} = \left[\frac{q'_B(T_U) - q'_B(T_B)}{C_{vB}(T_B)} \right] Q_4^{\bar{\gamma}_B} \quad (\text{IV-6e})$$

and

$$Q^i = \sum_j Q_j^i \quad i = \bar{\gamma}_A, \bar{\gamma}_B, T_A, T_B, \text{ and } \bar{\gamma}_a \quad (\text{IV-7})$$

This notation is consistent with that used by Lomax and Bailey (53) where, for example, $Q^{\bar{\gamma}_A}$ denotes the production of lower-state molecules, ($\bar{\gamma}_A = \ell n\gamma_A$), per unit distance along a stream line and has c.g.s. units of cm^{-1} . The reader should not confuse the superscripted Q-quantities with the earlier Q-quantities without superscripts, the notation used for the partition functions (cf., e.g., eqs. (IV-5)). The Q-quantities with superscripts only represent the sum of the Q-quantities having like superscripts and integer subscripts (note eq. (IV-7)). Except for the factor $1/v$ and also the factor β in equation (IV-6b), the reader can identify the above quantities as being the individual terms in equations (II-113) of Chapter II. The symbols not defined here have the same meaning as in Chapter II. The reason for introducing the factor β will be explained shortly.

In figure IV-1e are plotted the separate terms of the derivative for $\bar{\gamma}_A$ as well as the derivative itself. The values for these terms were obtained at the same time that the variables shown in figures IV-1a through IV-1d were found. The sign associated with the separate terms, as well as their sum, is indicated parenthetically after the labeling symbol (the logarithm of the absolute values are plotted, hence the sign must be indicated separately). The three zones are also labeled here for reference. In the transient region we see that the derivative and the component terms have very small values (resulting in no effect on γ_A) and that the loss term (negative term) $Q_1^{\bar{\gamma}_A}$ is dominant. This relative behavior continues throughout the transient zone. Near the end of this region we observe that, although the gain term (positive term) overtakes the loss term in value, their difference $Q^{\bar{\gamma}_A}$, or algebraic sum, approaches a maximum value that remains relatively constant throughout the quasi-steady region. At the end of this region, or at the beginning of the final relaxation zone, the gain term approaches even closer the value of the loss term, as is exemplified by the decrease in the value of the derivative $Q^{\bar{\gamma}_A}$. Finally, at



(e) Derivative, $\overline{Q}^{\overline{y}_A}$, and component terms, $\overline{Q}_i^{\overline{y}_A}$

Figure IV-1 Continued

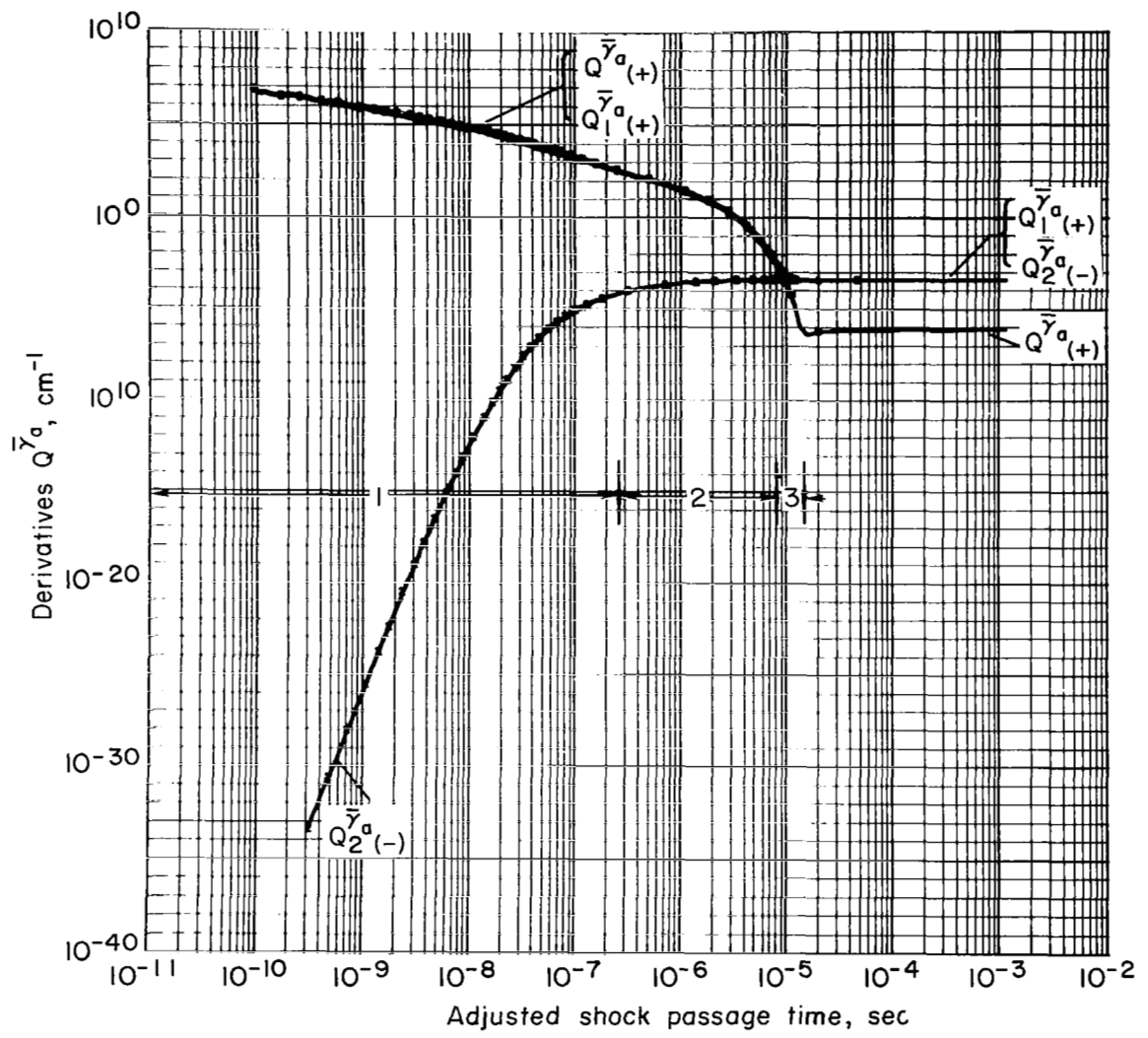
equilibrium the derivative is constant, but with a value sufficiently small so as to have only a negligible effect on the concentration variable γ_A .[†]

The derivative $Q^{\bar{\gamma}A}$ thus behaves in the manner expected. Since the derivative contains only single gain and loss terms such behavior could have been inferred from an examination of the behavior of the variable γ_A (fig. IV-1c). Likewise an equivalent statement may be made about the behavior of γ_a (see figs. IV-1b and IV-1f), where the processes are different only to the extent that the signs of the dominant terms are different. There is, however, an additional complexity associated with the derivatives $Q^{\bar{\gamma}B}$, Q^{TA} , and Q^{TB} that requires comment.

The separate terms of $Q^{\bar{\gamma}B}$ are plotted in figure IV-1g. The term $Q_4^{\bar{\gamma}B}$, associated with the recombination effects, is at first negligibly small (initially nearly 40 orders of magnitude smaller than the next larger term) and remains so throughout both the transient and quasi-steady zones. (This same effect can be noted for all the terms $Q_2^{\bar{\gamma}a}$, $Q_4^{\bar{\gamma}B}$, and Q_5^TB that represent the effects of atom recombination.) The dominant term in the transient region is the gain term $Q_1^{\bar{\gamma}B}$ that represents the gain in γ_B due to losses from γ_A .[‡]

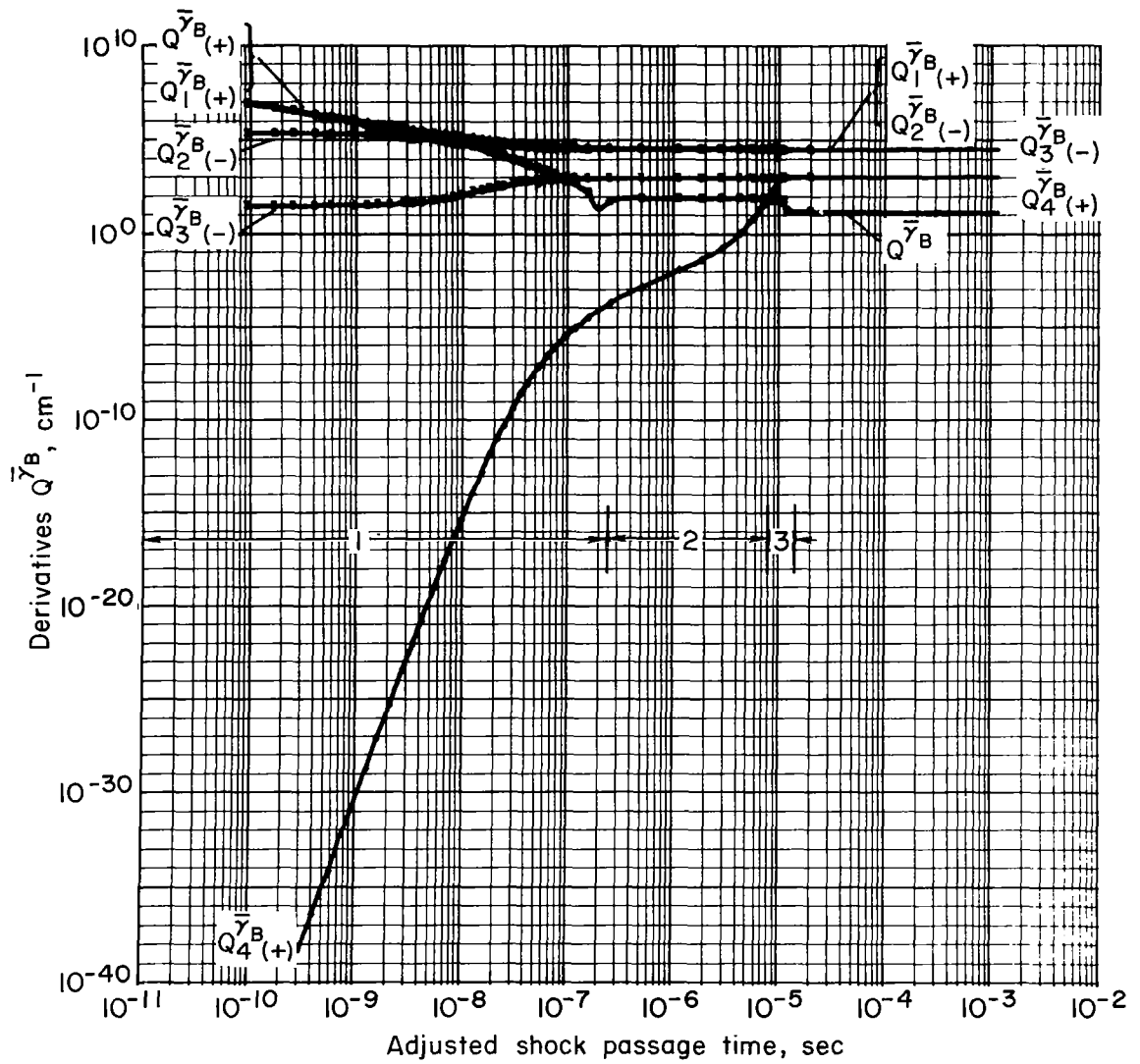
[†]The derivative $Q^{\bar{\gamma}A}$ (as well as the other derivatives) should become zero when the final relaxation to equilibrium has occurred. The fact that the derivative has a non-zero small value, that is, small relative to the values of its separate terms (four orders of magnitude less), indicates that the numerical integration is not exactly precise. In Appendix E it is pointed out that these solutions are only accurate to about 0.01 percent. This is further exemplified here by the fact that at equilibrium the difference between the separate terms is of this order.

[‡]It is interesting to observe that $Q_1^{\bar{\gamma}B}$ is proportional to $Q_1^{\bar{\gamma}A}$ (see eq. (IV-4a)) and that in the transient zone each term is the dominant term of the derivative in which it appears. The term $Q_1^{\bar{\gamma}B}$, however, causes a rapid variation in the variable γ_B while the term $Q_1^{\bar{\gamma}A}$ has no effect on γ_A until T_A is sufficiently large.



(f) Derivative, $Q^{\bar{y}a}$, and component terms, $Q_i^{\bar{y}a}$

Figure IV-1 Continued



(g) Derivative, $\bar{Q}^{\bar{\gamma}_B}$, and component terms, $Q_i^{\bar{\gamma}_B}$

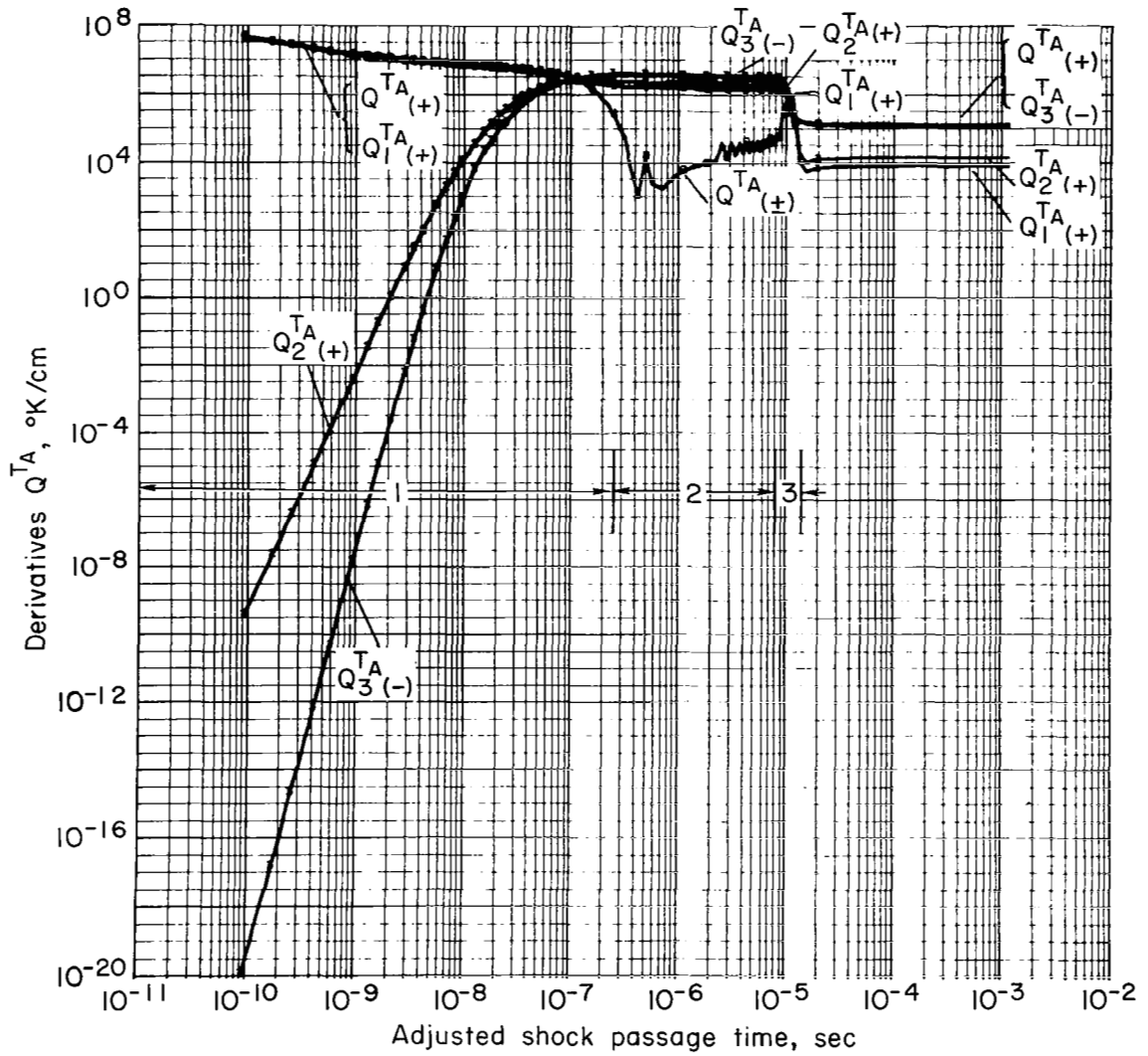
Figure IV-1 Continued

The depletion terms, in the rate equation for the upper-state population, are $Q_2 \bar{\gamma}_B$ and $Q_3 \bar{\gamma}_B$. The latter term, associated with molecular dissociation, has only a very small effect on the derivative $Q \bar{\gamma}_B$ ($Q_3 \bar{\gamma}_B \sim 10^{-5} Q \bar{\gamma}_B$), and continues to have only a small effect until the gain and loss due to the transitions $\gamma_B \rightleftharpoons \gamma_A$ are nearly balanced. This occurs near the end of the transient region. In the quasi-steady region the relative values of $Q_1 \bar{\gamma}_B$, $Q_2 \bar{\gamma}_B$, and $Q_3 \bar{\gamma}_B$ remain nearly constant and all have an equally important net effect on the derivative $Q \bar{\gamma}_B$. Note also that the derivative $Q \bar{\gamma}_B$ is smaller than any of its component terms (except the recombination term, $Q_4 \bar{\gamma}_B$, of course). The behavior in the quasi-steady region remains unchanged until the effects of atom recombination become important, after which the final relaxation takes place. In the final relaxation zone the derivative $Q \bar{\gamma}_B$ has a slightly lower value resulting in negligible changes in the value of $\bar{\gamma}_B$. This variable may thus be considered to have attained its final equilibrium value.

There are a few essential features that will be pointed out for emphasis. We note in particular (1) that the effects of atom recombination are negligible in both the transient and quasi-steady zone; and (2) that in the quasi-steady region the transitions causing molecular excitation are balanced by the effects of dissociation. These points are not original to this work, but have been discussed by previous researchers (see, e.g., 85, 94). Because of the relative simplicity of the present model, however, the effects are more readily exemplified here.

The rate equations discussed thus far are those relevant to the changes of the population variables γ_A , γ_B , and γ_a . Additional insight may be gained from a detailed examination of the energy relaxation processes from which, for example, the influence of anharmonicity effects may be explained.

In figure IV-1h are plotted the derivative $Q^T A$ and the associated component terms $Q_i^T A$. In this case the dominant term is the gain term $Q_1^T A$ that represents vibrational energy relaxation for the lowest energy states, denoted A_1 . The only loss term is $Q_3^T A$, which has only a negligible effect



(h) Derivative, Q^{TA} , and component terms, Q_i^{TA}

Figure IV-1 Continued

on the derivative Q^{TA} in the transient region. This term represents, in essence, the energy losses due to the transitions $\gamma_A \rightleftharpoons \gamma_B$. Perhaps the most interesting observation that can be made is that the effects of the vibrational relaxation processes Q_2^{TA} associated with the states denoted A_2 are also negligible in the transient region. This apparently means that in the transient region behind a normal-shock wave the effects of anharmonicity, although potentially large, because the characteristic relaxation time τ_{A_2} may be small, are not in fact important. A close examination of the term Q_2^{TA} suggests the reasons for this assertion. First we note that the factor $[1 - \Delta(T)/q_{A_2}(T_A)]$ is small since the ratio $\Delta(T)/q_{A_2}(T_A)$ is initially of order unity. The factor increases monotonically as this ratio decreases (T is constant and as T_A increases, $q_{A_2}(T_A)$ also increases), reaching a maximum value as $q_{A_2}(T_A)$ reaches its maximum. Even when the effects of anharmonicity can be considered negligibly small, however, (that is, when $\Delta(T) \sim 0$ and the factor $[1 - \Delta(T)/q_{A_2}(T_A)]$ is unity; see, e.g., discussion after eq. (II-73) of Chapter II), we have in addition the Boltzmann population factor $Q_{A_2}(T_A)/Q_A(T_A)$. This factor is also small and has the effect of lessening the influence of the characteristic relaxation time τ_{A_2} , hence, the effect of Q_2^{TA} on the derivative Q^{TA} . The noteworthy conclusion from this discussion is that the term Q_1^{TA} , which is analogous to the Landau-Teller expression (see discussion after eq. (II-58a) in Chapter II), governs the vibrational relaxation in the transient region for the A-states.

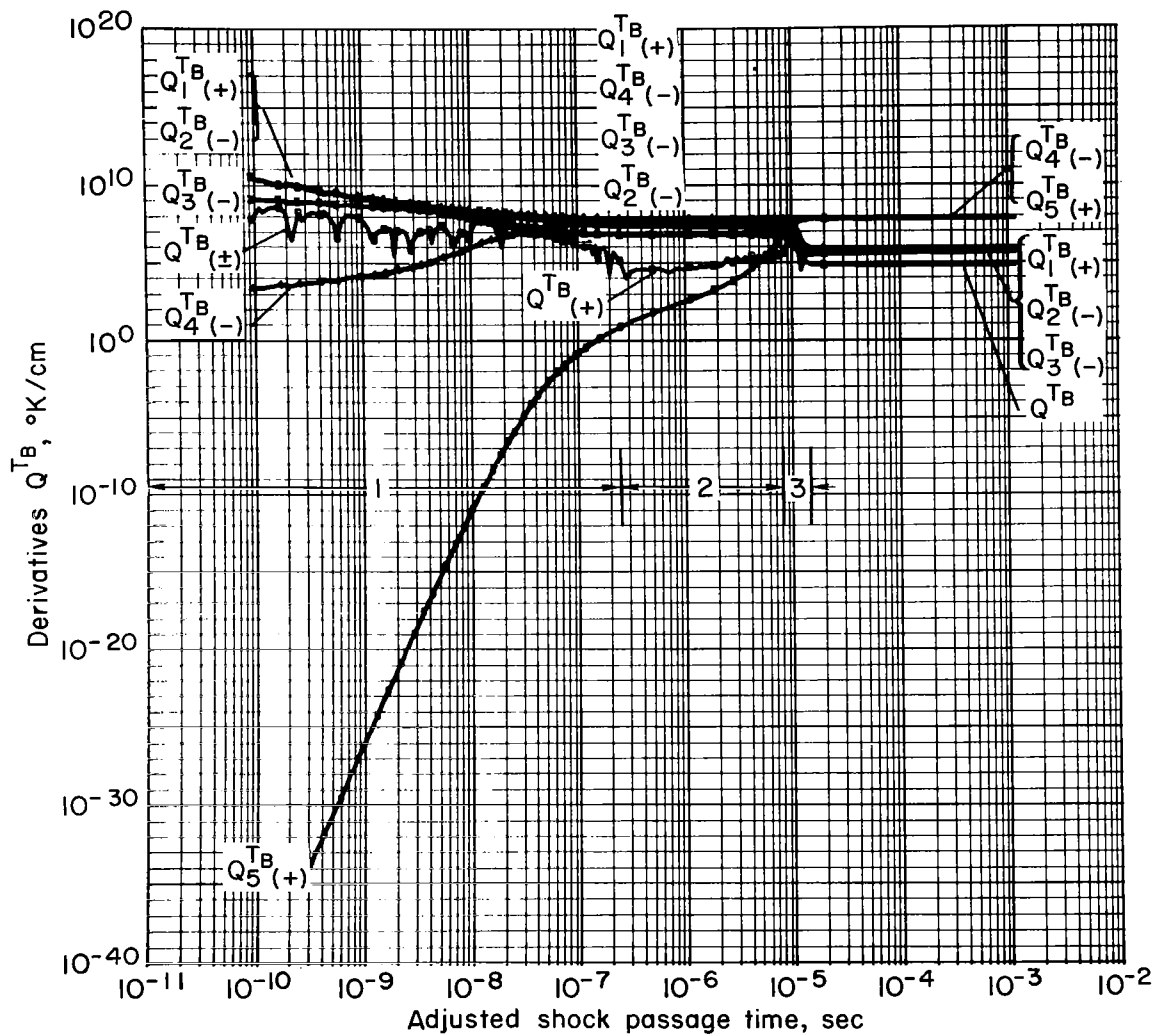
The foregoing behavior of the component terms continues throughout the transient zone. In the quasi-steady zone, where T_A becomes constant (see fig. IV-1a), the value of Q^{TA} decreases abruptly and all the terms become important. (Note also that in the quasi-steady zone the sign of Q^{TA} alternates between positive and negative values, as indicated by the oscillatory behavior of this quantity.) Actually, even in the quasi-steady region where Q_2^{TA} is slightly greater than Q_1^{TA} , it turns out that the effects of anharmonicity are also not appreciable (compare, e.g., solutions of the previous chapter, figs. III-7 and III-12).

An explanation of the interplay of the various terms that constitute the rate equation for Q^{TB} (fig. IV-1i) is considerably more complex since more terms are involved and the processes are more complicated. One observes that there are only two gain terms, Q_1^{TB} and Q_5^{TB} . The latter term, however, has a negligible effect on Q^{TB} in the transient and quasi-steady regions behind a normal shock. Thus, only one gain term has any effect on the upper-state energy relaxation processes, and it turns out that this term when combined appropriately with all the other terms yields (when $\beta = 1$) values for the derivative Q^{TB} that are slightly negative. This condition causes the system of equations that are solved for the region behind a normal shock wave to be inherently unstable. For this reason the factor β was included, and was so adjusted that the sum of all the separate terms yield a value of Q^{TB} that is very slightly positive. In particular, β was arbitrarily adjusted so as to satisfy the condition

$$|Q_1^{TB}| / (|Q_2^{TB}| + |Q_3^{TB}| + |Q_4^{TB}| + |Q_5^{TB}|) - 1 = 1 \times 10^{-5} \quad (\text{IV-8})$$

This condition introduces a problem to the extent that we are, in essence, arbitrarily defining the starting values for the derivative Q^{TB} . In practice, however, this problem was not serious for the following reasons: (1) the factor β was always of order unity (never smaller than 0.96 in value for the cases investigated), and imposing an uncertainty of this magnitude is certainly not great as compared with other uncertainties (e.g., the value of $k_R^{(1)}(T_B, T)$ contained in Q_2^{TB}). (2) The effect of this correction factor is quickly lost as the other terms become important. The introduction of the factor β was only required for the normal-shock problem. In obtaining the expanding flow, that is, the nozzle solutions that are to be discussed later, the factor was always set equal to unity.

The addition of the factor β therefore has the effect of making the system of equations that are solved stable. It may be seen, however, that the rate equation Q^{TB} still shows an unstable behavior (its value oscillates several orders of magnitude in value and, in addition, there are changes in its sign).



(i) Derivative, Q^{TB} , and component terms, Q_i^{TB}

Figure IV-1 Continued

Also, in contrast to the preceding derivative Q^{TA} , the beginning of the quasi-steady zone is not marked by any distinctive change in the value of Q^{TB} . We recall that in the preceding case the quasi-steady zone was indicated by a rather abrupt decrease in the value of Q^{TA} . (Note also that the derivative for T_A is smooth throughout the entire flow except for a relatively small variation in the quasi-steady region.)

The interpretation of the oscillatory behavior of Q^{TB} is complex. It requires an understanding of the numerical integration procedure (see Appendix E), in particular, as regards the capability of the procedure to resolve the effects of "parasitic eigenvalues" (see also 53 and 53a). In addition, an understanding of the concept of "local equilibrium state" (see, e.g., p. 236 of 97) is also helpful. It turns out that the oscillatory behavior of the complete derivative is largely a characteristic of implicit methods and occurs when the effects of large-magnitude negative eigenvalues (parasitic eigenvalues) are important. Such behavior is more often exhibited in the case of nozzle flow (see, e.g., 29, 53a) that is discussed in a later section.

To interpret this effect we reformulate Q^{TB} in the following manner (see p. 236 of 97):

$$\frac{dT_B}{dx} \equiv Q^{TB} = \frac{X_0(T, \rho, T_A, T_B, \gamma_A, \gamma_B, \gamma_a)}{v\tau(T, \rho, T_A, T_B, \gamma_A, \gamma_B, \gamma_a)} \quad (IV-9)$$

where τ is some relaxation time that characterizes the relaxation of Q^{TB} , and X_0 is some function that is zero when τ is zero. (The condition $\tau = 0$ is a formal characterization of local equilibrium.) In the formal case of local equilibrium Q^{TB} is equal to $0/0$ and therefore is indeterminate. In such cases T_B is customarily found by solving X_0 for T_B (see p. 237 in 97). For the case at hand such a procedure complicates the numerical computation and is not necessary since τ is always non-zero, although of small relative value (i.e., $v\tau$ corresponds to a relaxation distance that is small compared to other distances in the shock). One important aspect of the numerical integration

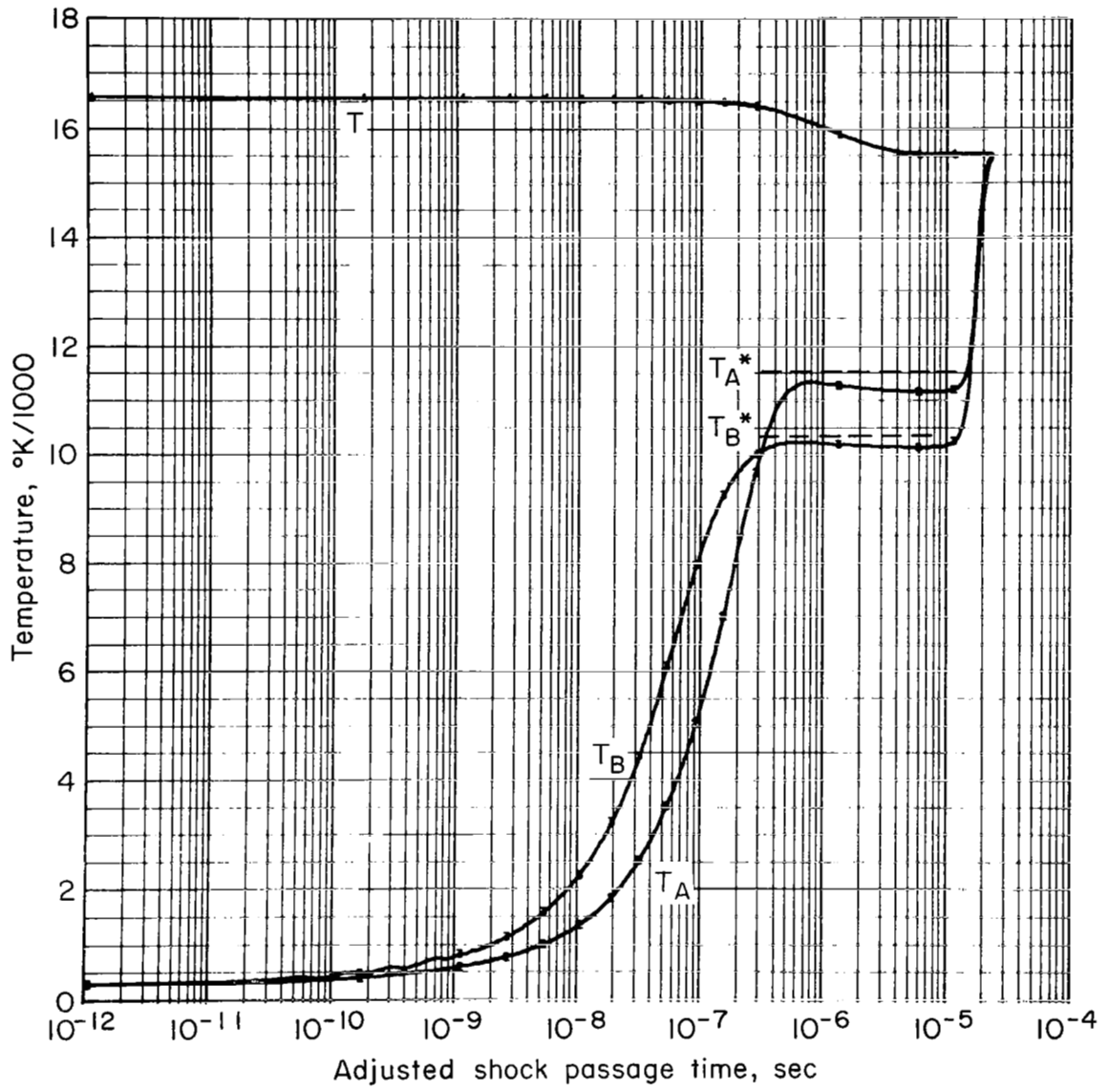
procedure is that it can be used in such cases. The oscillatory behavior of the derivative shown in figure IV-1i has a negligible effect on the solution and the resulting solution corresponds to that which would be obtained by setting X_0 equal to zero. An essential feature of these solutions is that the variables are smooth (see, e.g., fig. IV-1a) although their derivatives show an oscillatory behavior.

The state of local equilibrium for the temperature T_B prevails throughout the entire region behind the normal shock, irrespective of the relaxation zone (this relative behavior was noted for all of the cases studied). The dissociation terms assume an increasing importance in the quasi-steady zone and, finally, as the effect of recombination becomes significant, we have final and complete equilibrium.

It is of interest to observe the effect of Q_2^{TB} in these solutions. In Chapter II this term was designated as "rate limiting" and it may be seen from figure IV-1i that its effect is one of limiting the rate of "heating" of the upper vibrational energy levels. The term has the opposite sign from Q_1^{TB} and serves to cancel the effect of that term. In the quasi-steady zone it also has the effect of lessening the influence of the dissociation term. Because of the intercoupling of all the terms and their complexity, it is not yet clear whether Q_2^{TB} is rate-limiting in the sense used by Pritchard or Bray (14, 71).

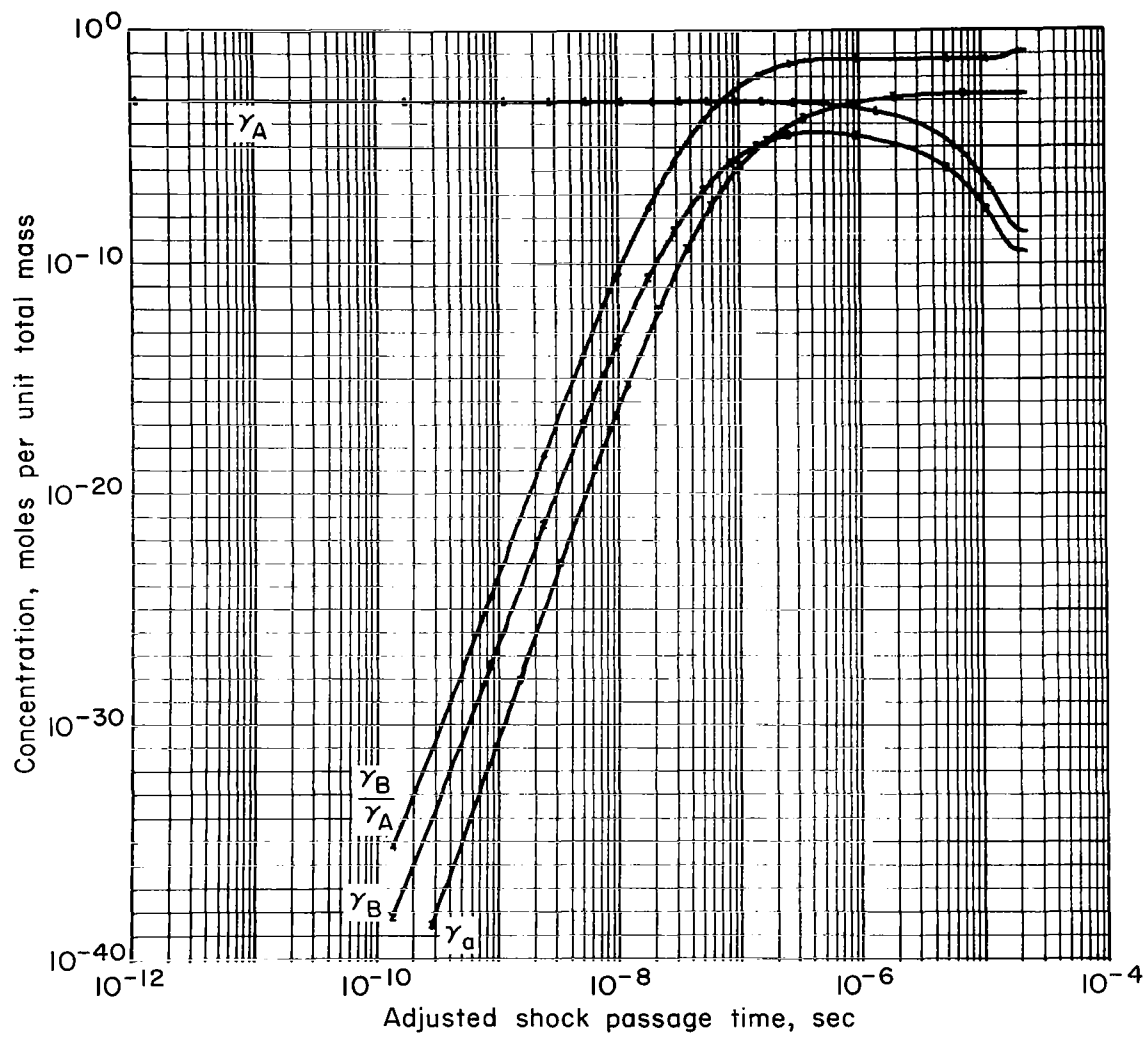
The discussion until now has centered on a description of the shock-wave structure without concern for the differences that occur as a result of using different values for the embedded parameters. In figures IV-2 through IV-7 the plotted solutions illustrate the results for other values of these parameters. The values used for these solutions are listed in Table IV-1. It is to be recalled that the abscissa scale represents the time after arrival of the shock wave normalized in such a manner that the effect of differing densities on the relaxation processes is removed.

We observe first, comparing figures IV-1 and IV-2, that the relative effects that occur as a result of increasing the value of the constant C_2 (the constant



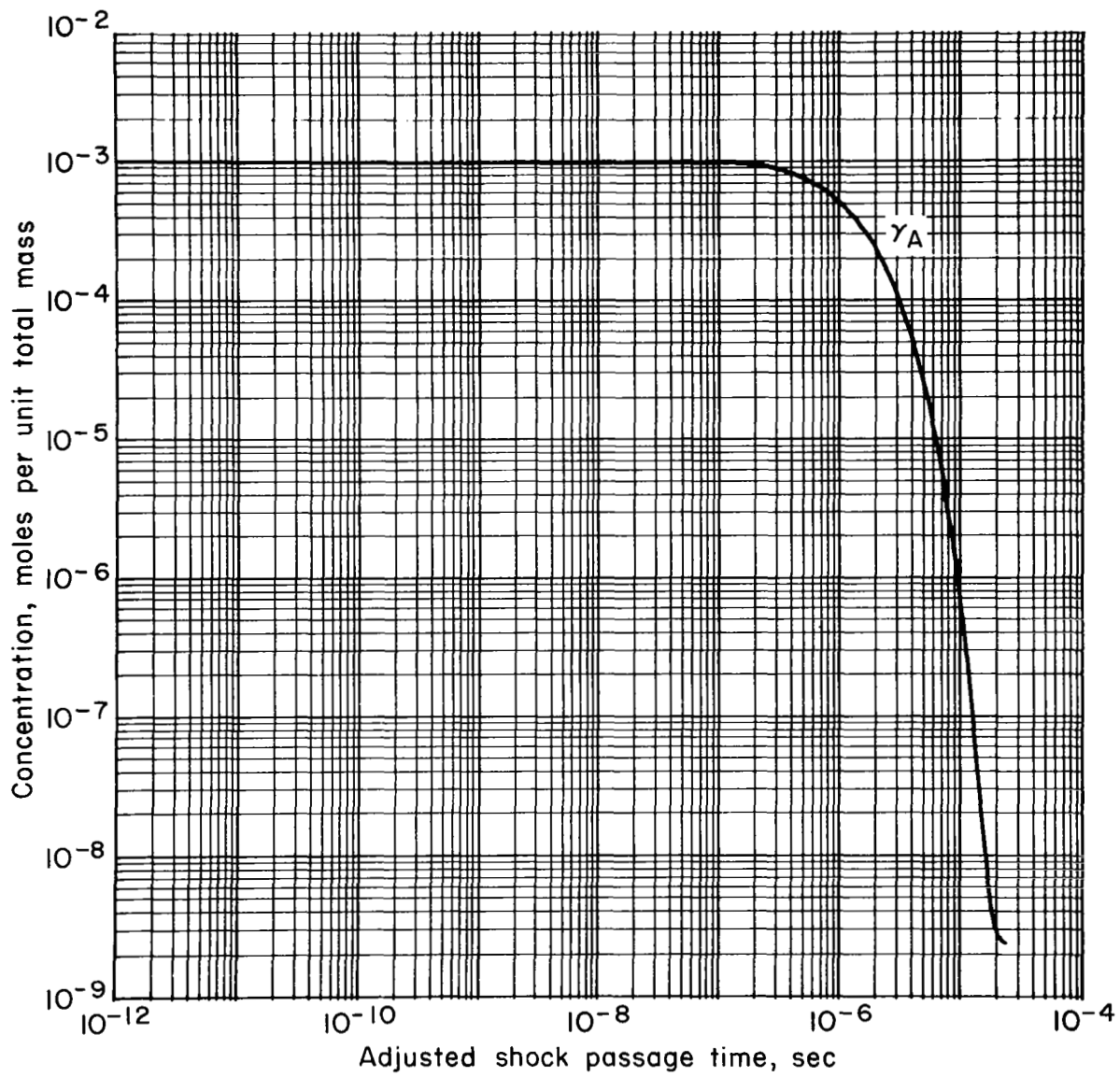
(a) Temperatures

Figure IV-2. Variables obtained from shock solution versus adjusted laboratory time (associated parameters are listed along second row of table IV-1)



(b) Concentrations

Figure IV-2 Continued

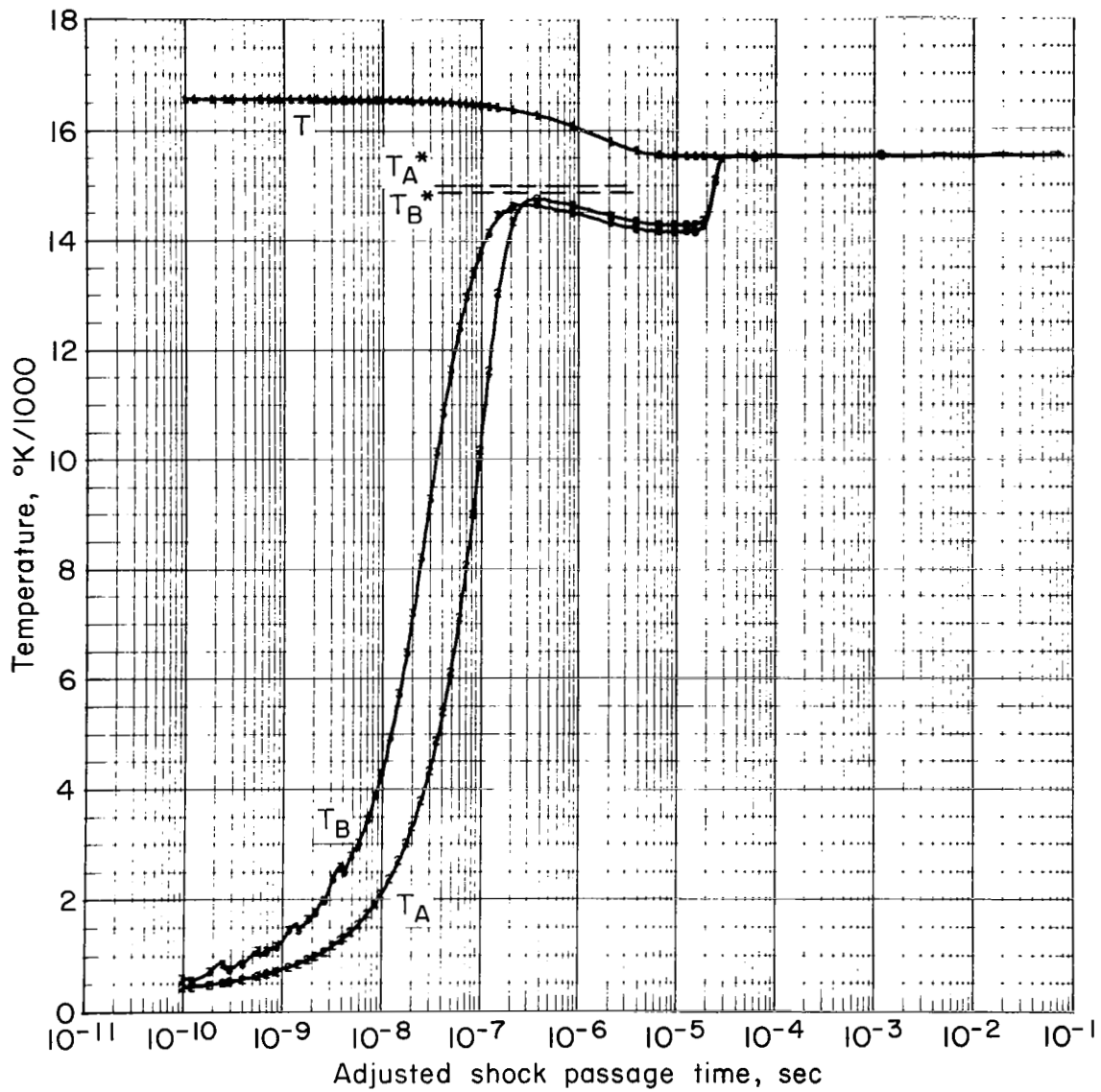


(c) Concentration, Lower States

Figure IV-2 Continued

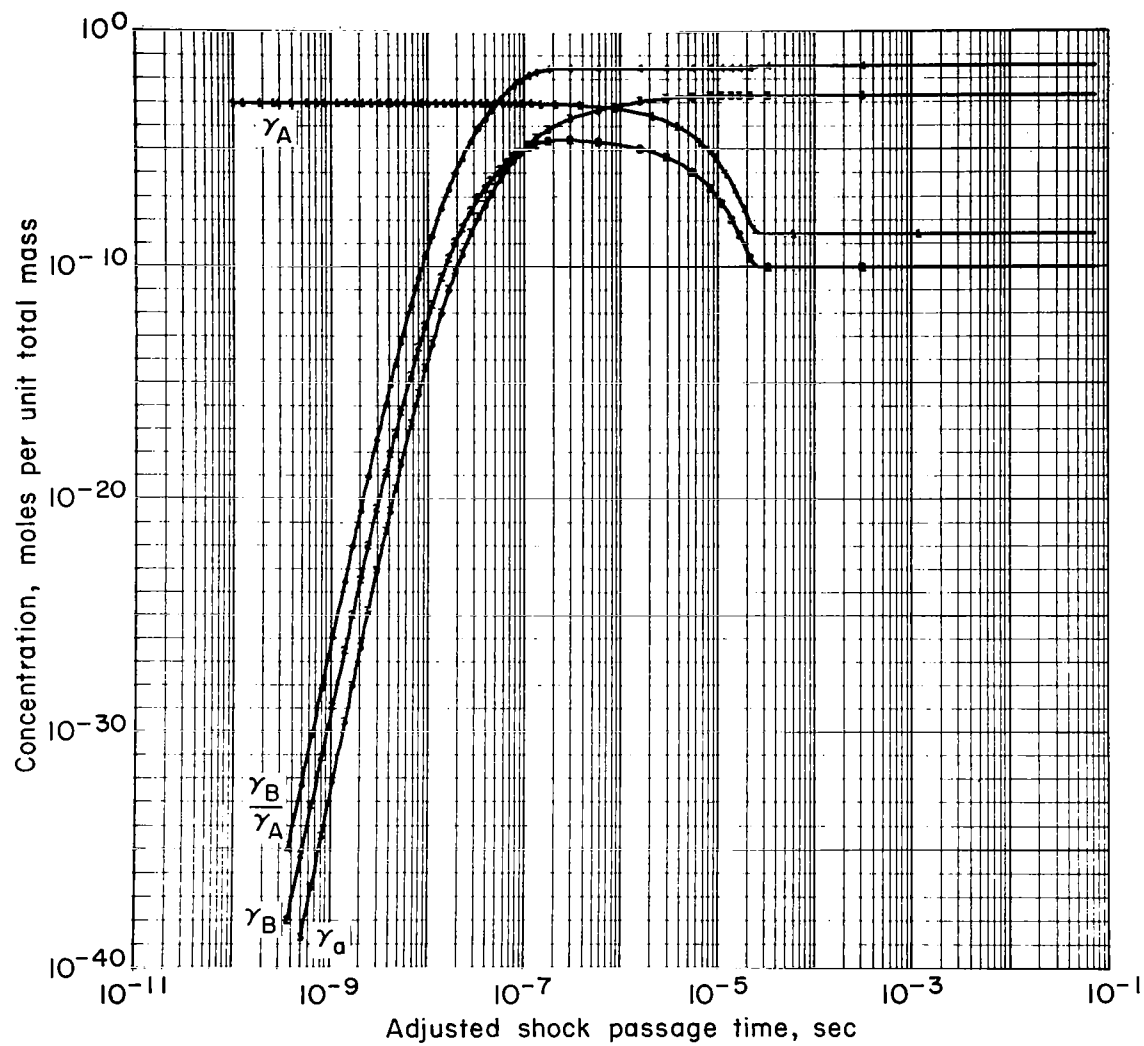
in τ_{A_1} ; note eq. (III-12)) by about 40 percent are important to T_A and T_B and of less importance to the concentrations. We recall also from Chapter III that the effect of changing C_2 in the manner indicated was effectively to increase the characteristic vibrational relaxation time (actually, by a factor of about 2 for a temperature T_2 of 16,500° K). This effect is observed here as roughly a factor of 2 increase in the passage time of the transient zone. Also, T_A and T_B are different from the values found for the previous solutions in the quasi-steady zone. The effect on the transient time is illustrated even more explicitly in figure IV-8, which will be discussed later. The increased transient passage time occurs because τ_{A_1} , in effect, defines the time scale for energy transfer to the upper levels; hence, increasing τ_{A_1} increases the transient-zone time. The rather large effect on the quasi-steady values for the temperatures T_A^* and T_B^* was already discussed in the previous chapter. The reader will also observe that there is also an effect on the time when final relaxation to equilibrium occurs, but the effect is not large (less than a factor of 2). No attempt will be made to find the correct values of T_A^* and T_B^* other than to show what happens when different values for the parameters are used. However, the importance of having experimental measurements of the relative amounts of energy contained in the vibrationally excited energy states is dramatically apparent here (in particular, regarding fluid flows). Such measurements would be sensitive indicators for the problem of inferring more accurate values of the transition rates (or vibrational relaxation times). The author is not aware that any such measurements have been made.

In figures IV-3 and IV-4 are plotted similar solutions that result after the value of the constant b is increased. One recalls that this constant denotes the separation between the vibrational energy levels having different temperatures T_A and T_B . The previous pair of solutions, figures IV-1 and IV-2, was for $b = 16$ ($\Theta_b/\Theta_D = 0.544$) and the present pair is for $b = 24$ ($\Theta_b/\Theta_D = 0.786$). A comparison of figures IV-1 with figures IV-3 or figures IV-2 with IV-4 will show that increasing b reduces the difference $T_B - T_A$, as was noted in the previous chapter, and has an opposite effect to that observed from

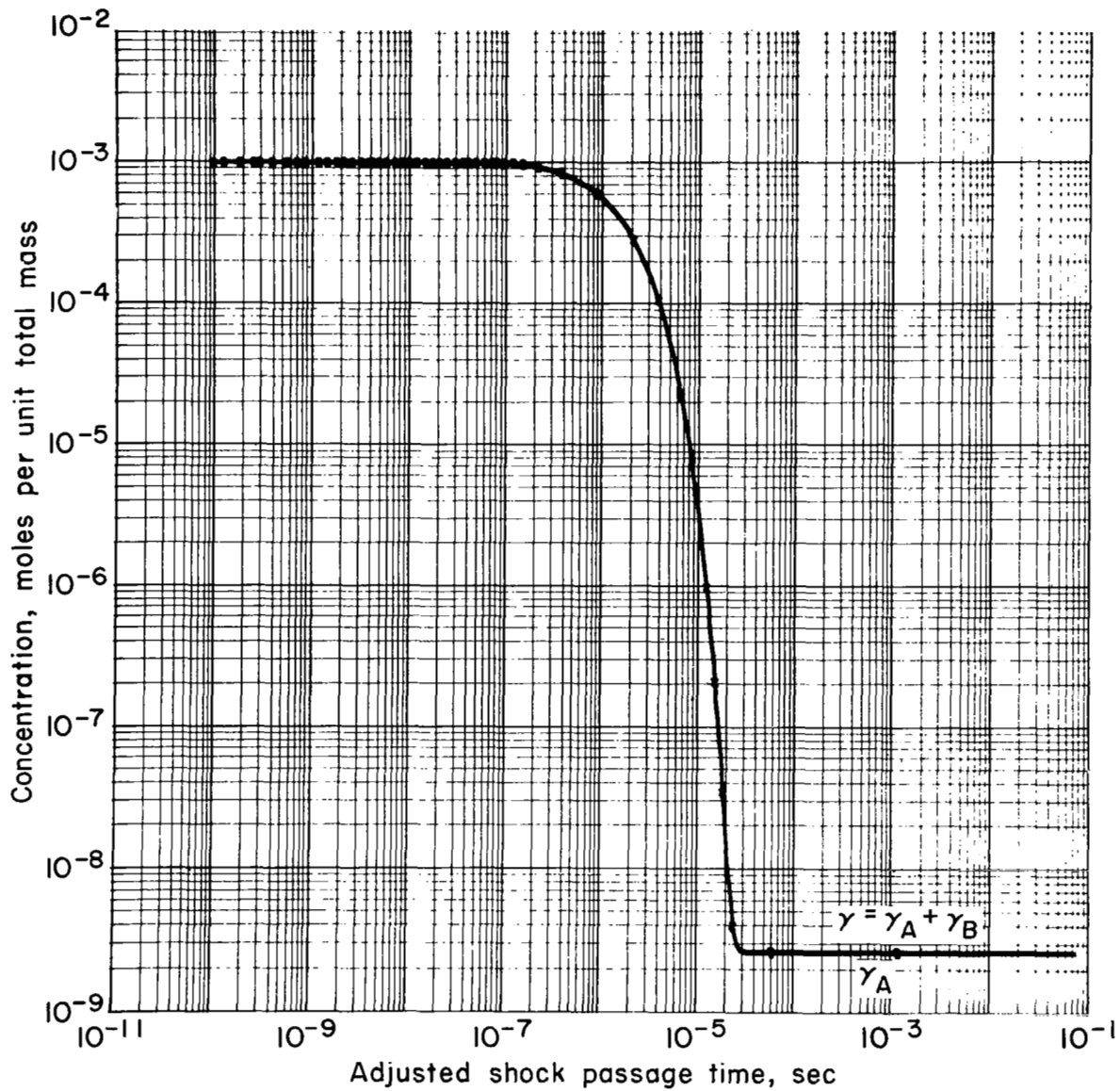


(a) Temperatures

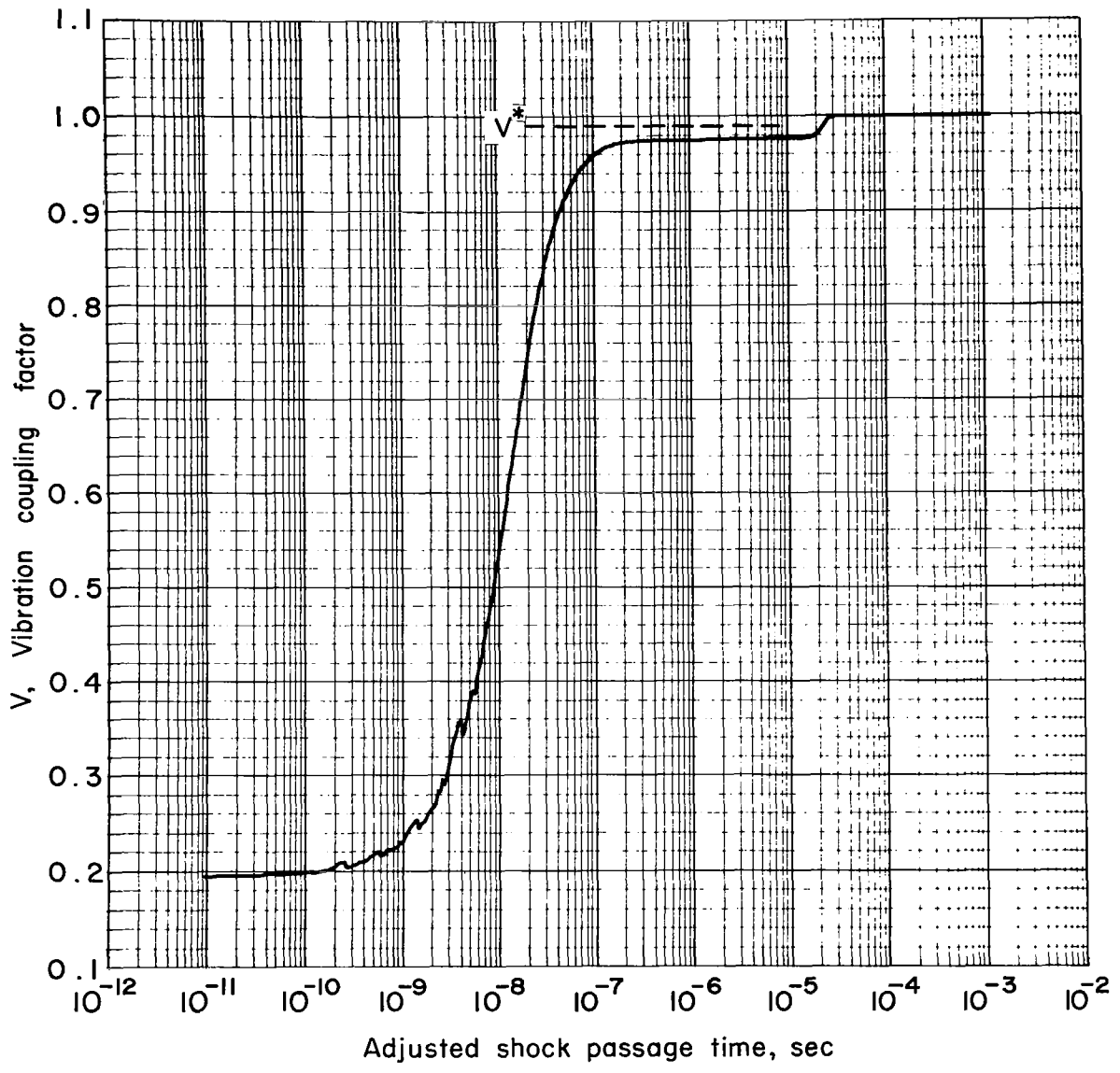
Figure IV-3. Variables obtained from shock solution versus adjusted laboratory time (associated parameters are listed along third row of table IV-1)



(b) Concentrations
 Figure IV-3 Continued

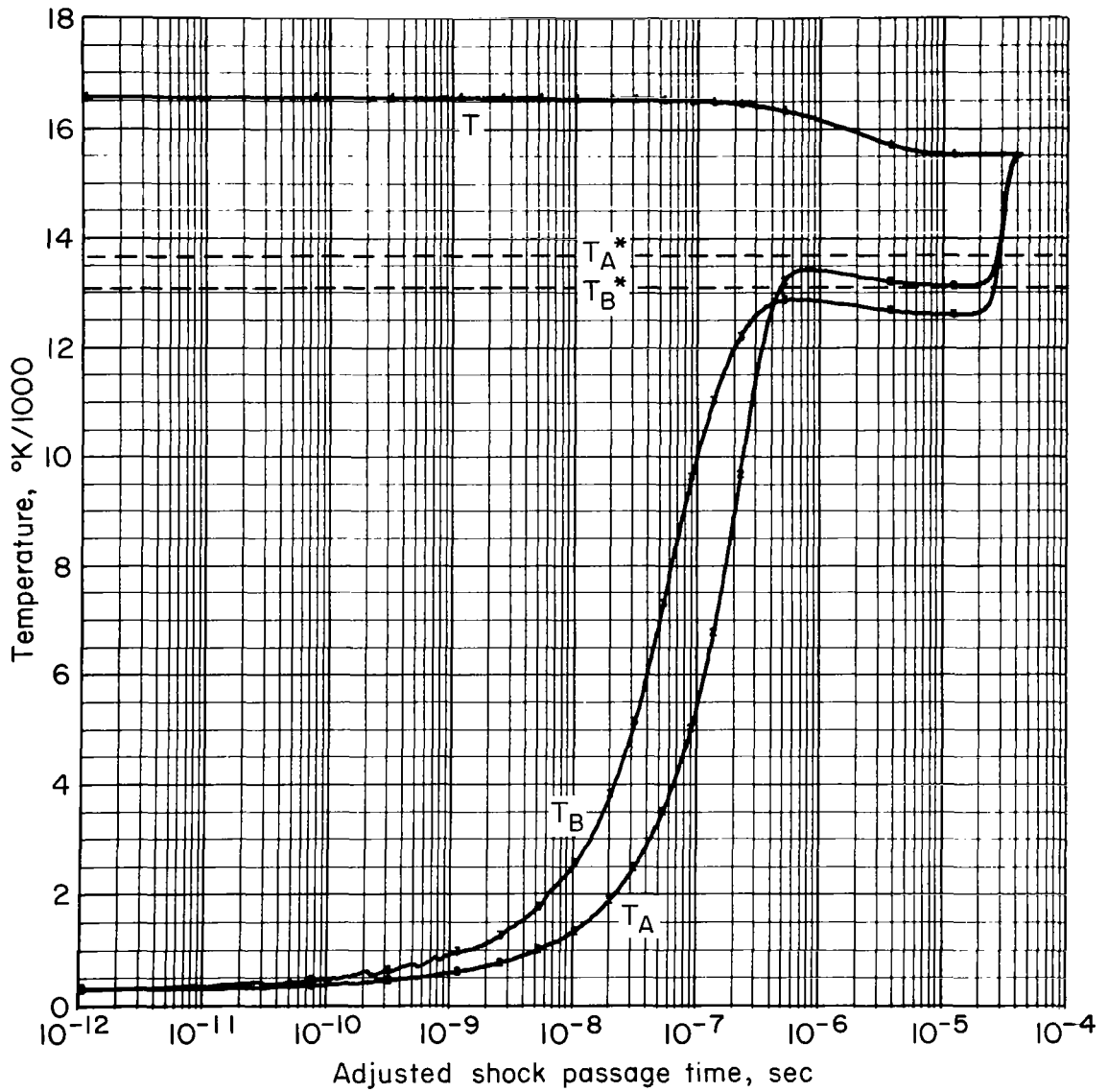


(c) Concentration, Lower States and Molecular
Figure IV-3 Continued



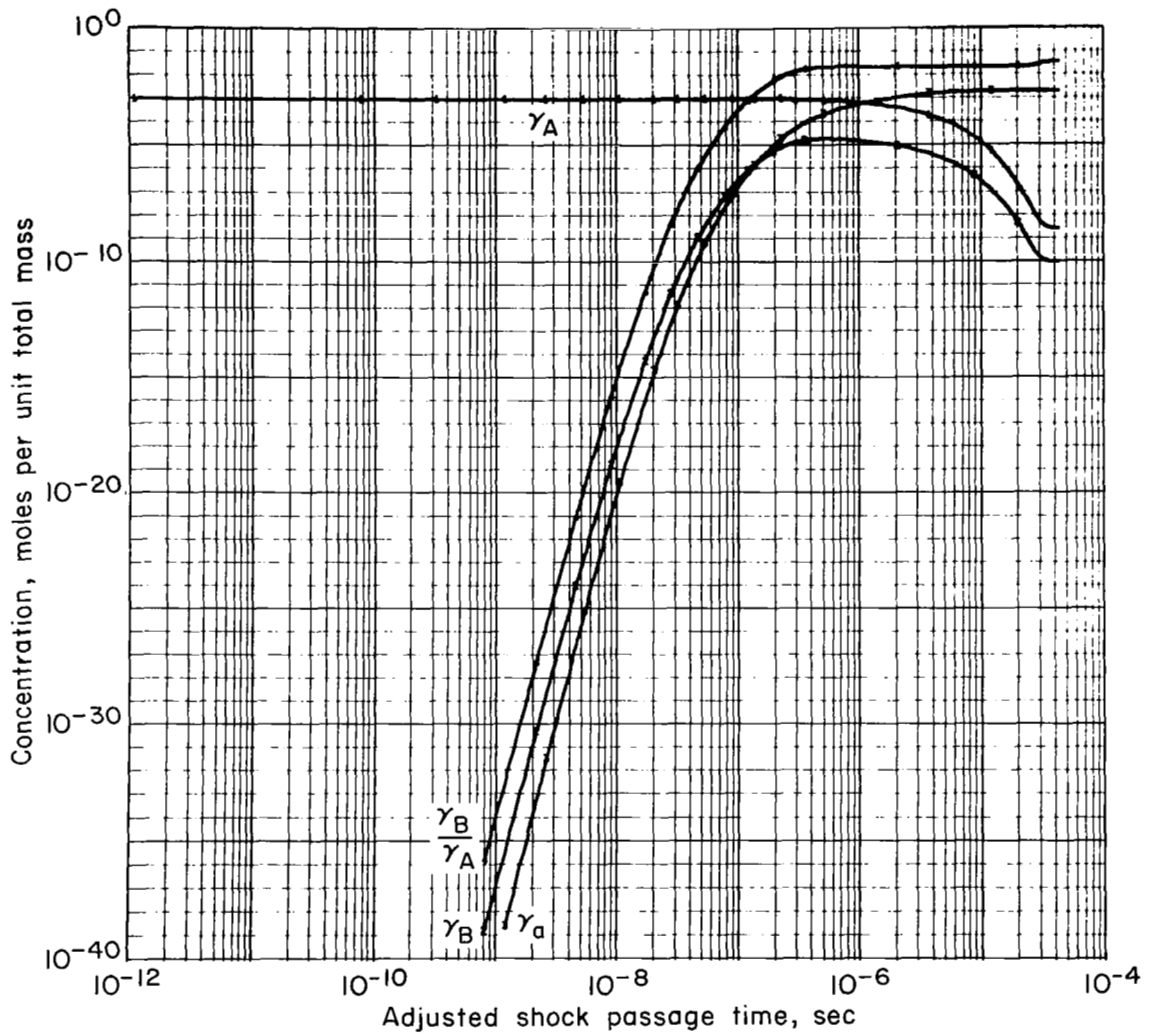
(d) Vibrational coupling factor

Figure IV-3 Continued

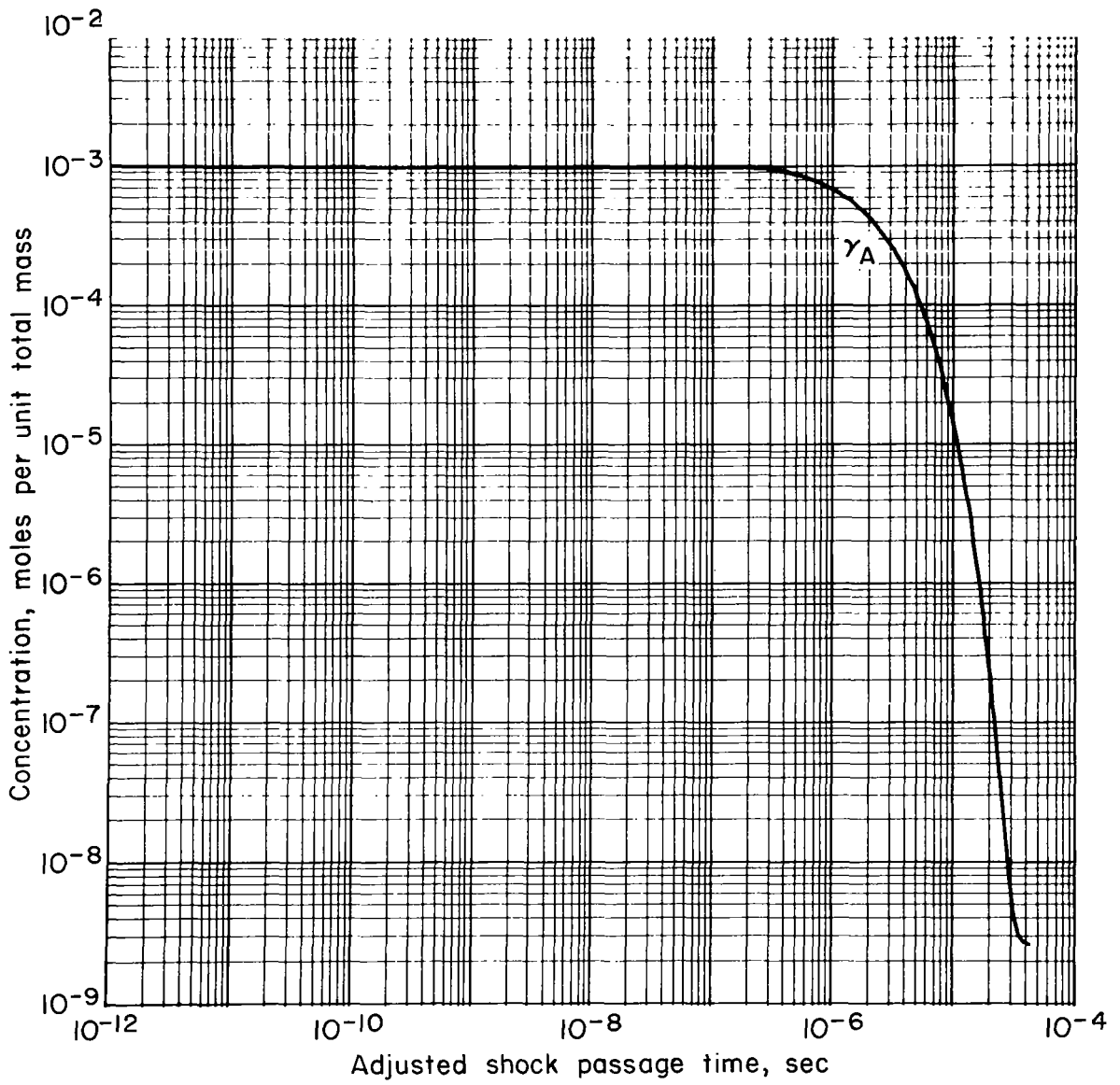


(a) Temperatures

Figure IV-4. Variables obtained from shock solution versus adjusted laboratory time (associated parameters are listed along fourth row of table IV-1)



(b) Concentrations
 Figure IV-4 Continued



(c) Concentration, Lower States

Figure IV-4 Continued

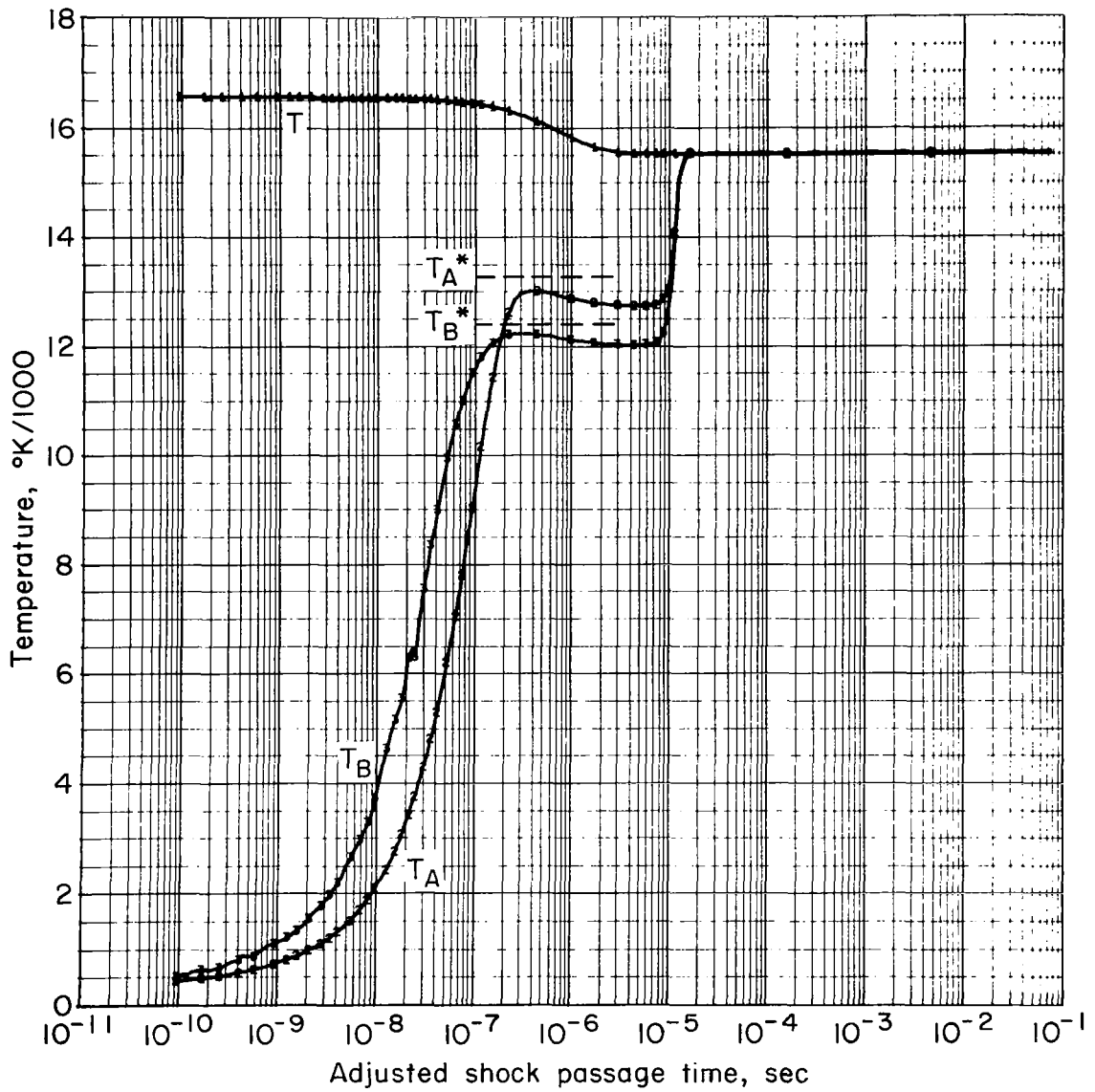
increasing C_2 (and hence τ_{A_1}). On the other hand, increasing b produces the same effect as increasing C_2 on the passage time of the various zones, as well as on the time required to reach equilibrium. In particular, these times become longer.

A comparison of figures IV-1 and IV-5 shows the result of decreasing the value of T_U from $\Theta_D/10$ to $\Theta_D/50$. In the latter case the embedded parameters were considered best from the standpoint of the quasi-steady solutions. It is to be recalled that the effect of reducing T_U to $\Theta_D/50$ is in the direction of making dissociation "highly preferential" so that only the most highly vibrationally excited molecules dissociate. One notes that although the differences between figures IV-1 and IV-5 are difficult to discern, this change does increase the time required for relaxation to equilibrium (also see fig. IV-8).

The effects occurring for weaker shock waves are illustrated in figure IV-6. Here the parameters have values identical to those used for the solution illustrated in figure IV-1 except that the temperature T_2 is lower. We note that in this case a relatively long time is required for the passage of the transient zone, and in the quasi-steady zone the temperatures T , T_A , and T_B are all equal. Once the transient zone has passed the entire vibrational population may thus be considered Boltzmann at the temperature T . Also, the internal processes relax in a sufficiently rapid manner that as soon as dissociation begins (note fig. IV-6c) the perturbing effect of dissociation has no effect on the vibrational population distribution.

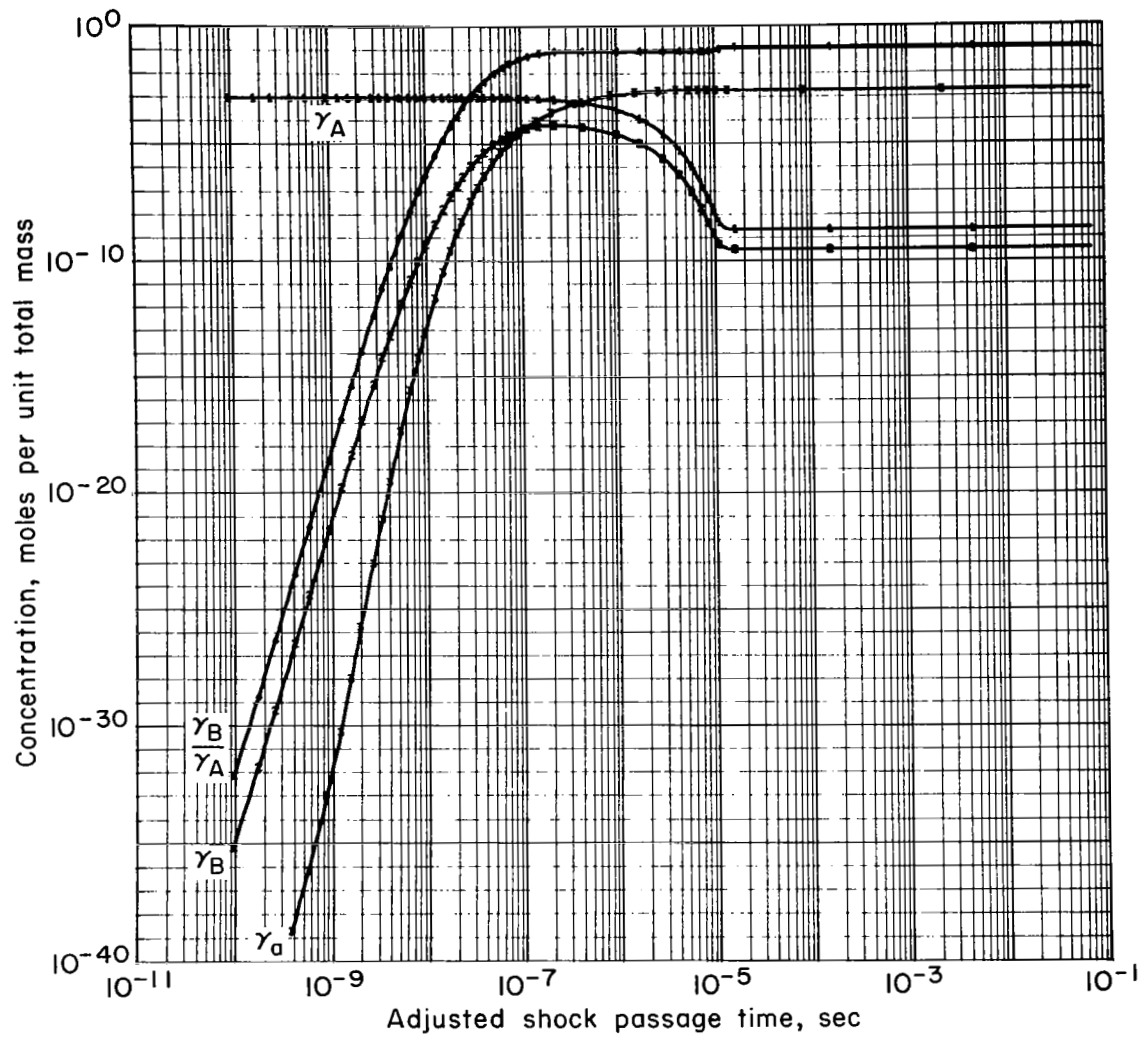
One particular feature to be noted from the figures IV-1 through IV-6 is the comparison of the quasi-steady values of the variables T_A , T_B , and V with the values obtained from the previous chapter. The reasonable agreement that is observed in all cases lends support to the basic quasi-steady assumptions that were introduced in the previous chapter in order that those solutions could be obtained.

A comparison of figures IV-1 and IV-7 shows the relative effects that result when $\chi = \chi_F$ and $\chi = 1$, respectively. This parameter accounts for

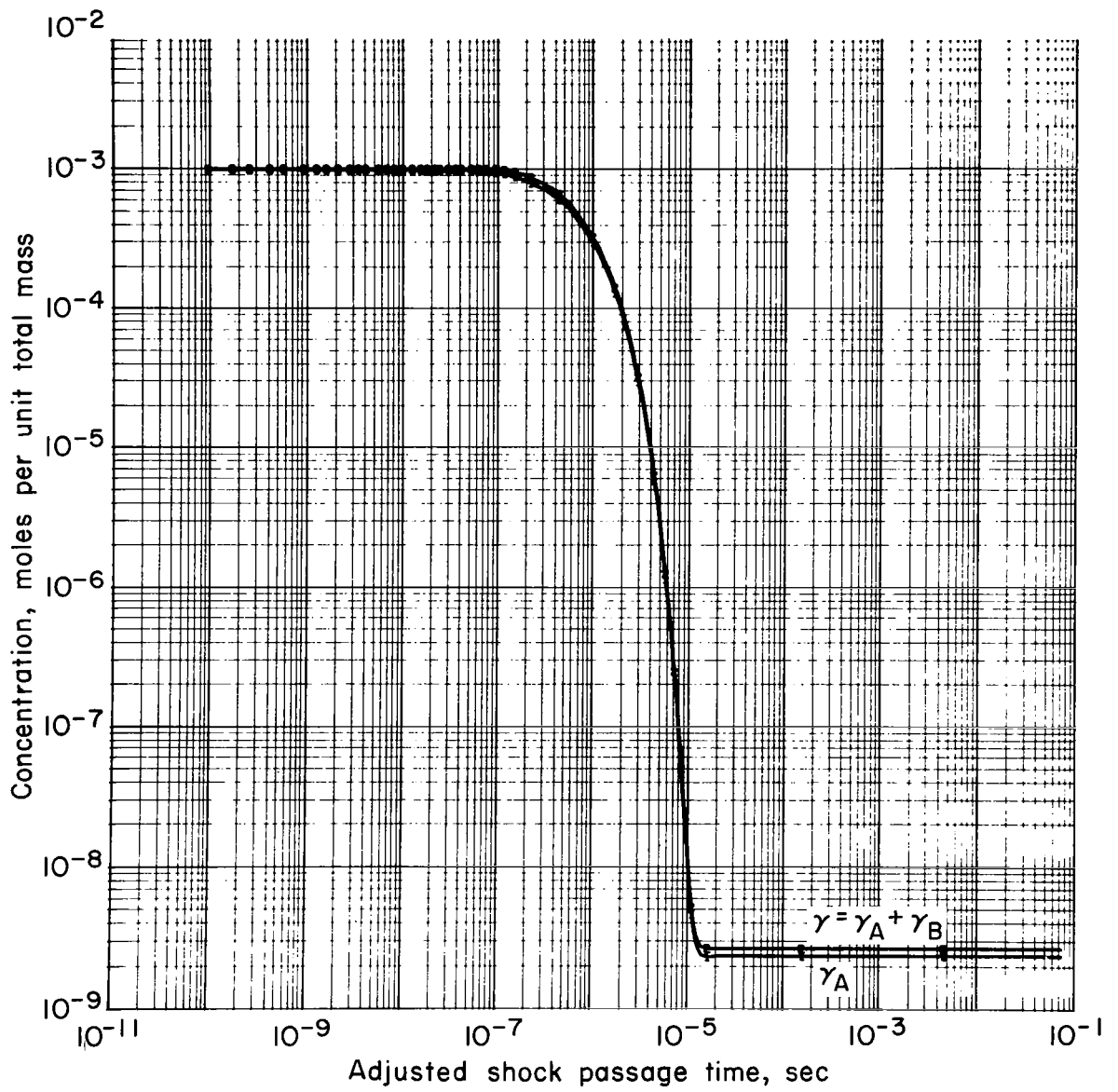


(a) Temperatures

Figure IV-5. Variables obtained from shock solution versus adjusted laboratory time (associated parameters are listed along fifth row of table IV-1)

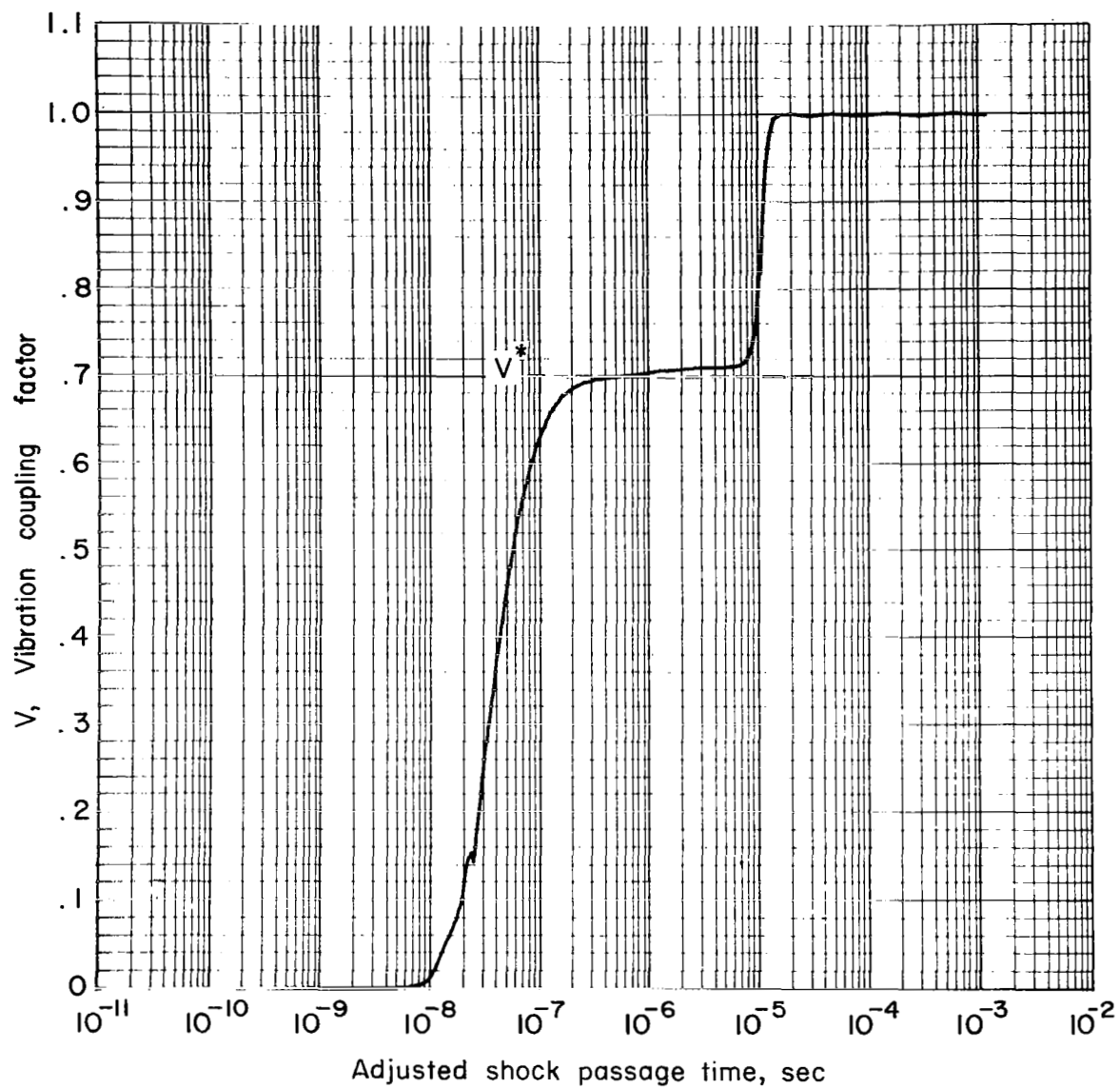


(b) Concentrations
 Figure IV-5 Continued



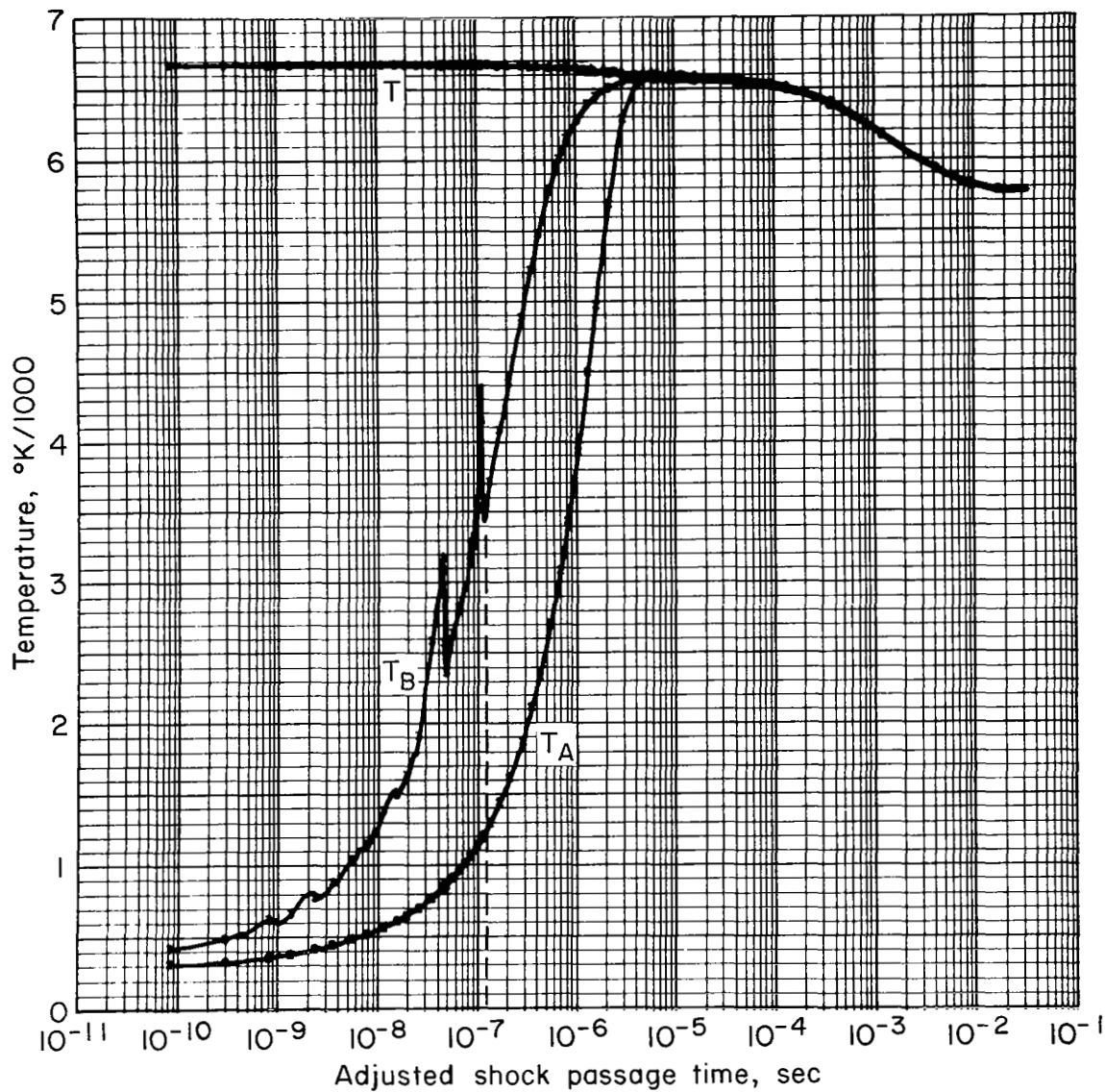
(c) Concentration, Lower States and Molecular

Figure IV-5 Continued



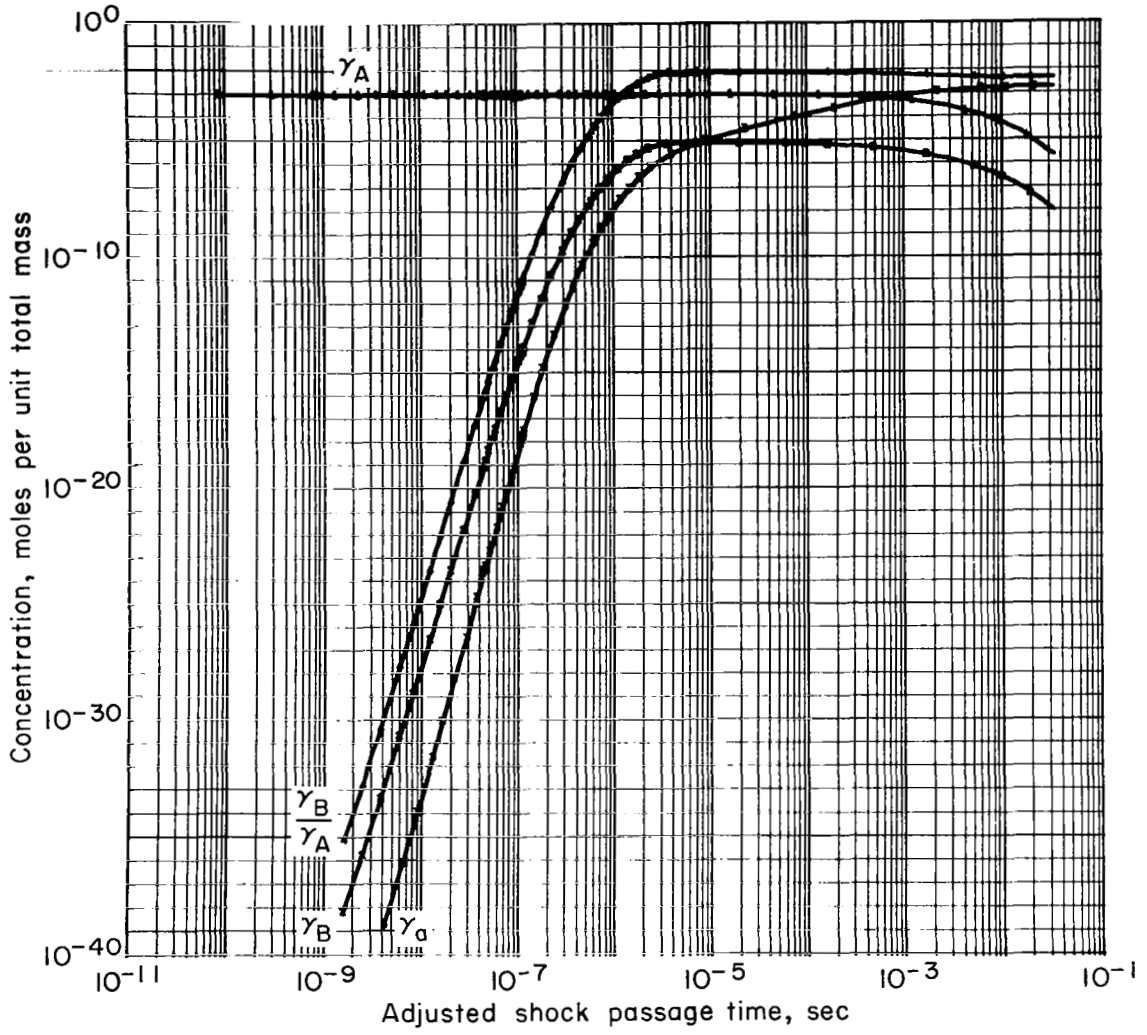
(d) Vibrational coupling factor

Figure IV-5 Continued

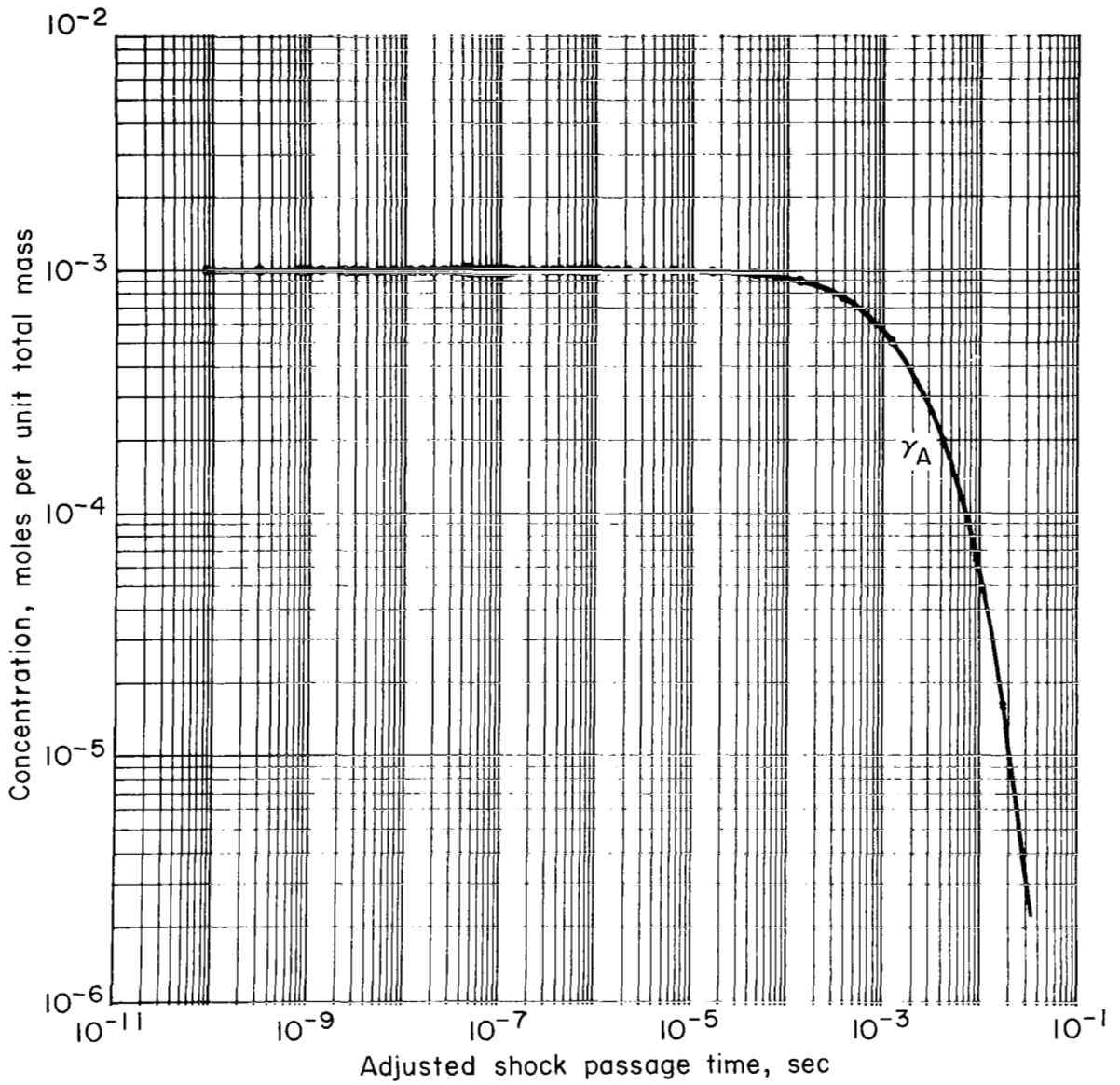


(a) Temperatures

Figure IV-6. Variables obtained from shock solutions versus adjusted laboratory time (associated parameters are listed along sixth row of table IV-1)

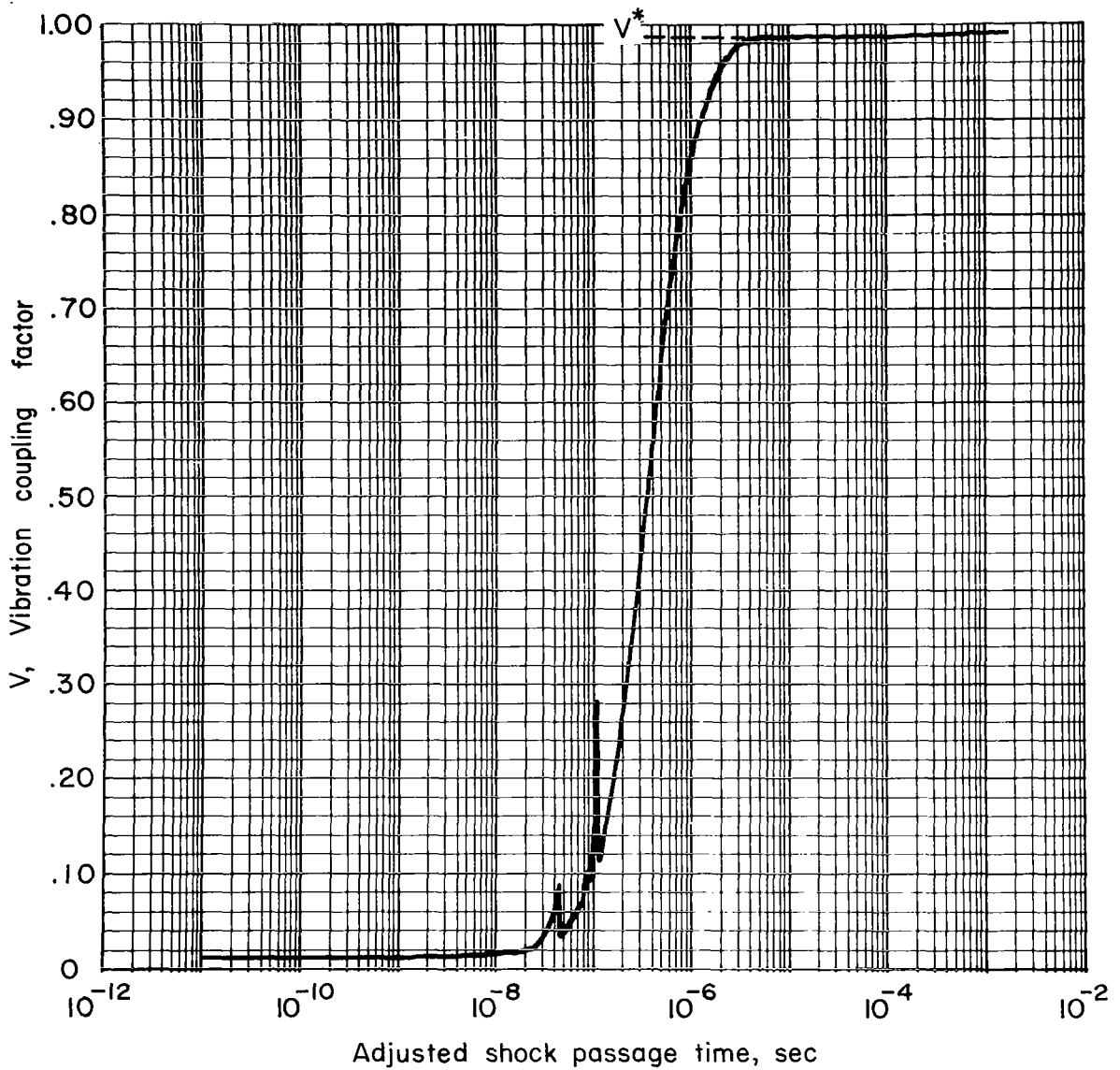


(b) Concentrations
 Figure IV-6 Continued



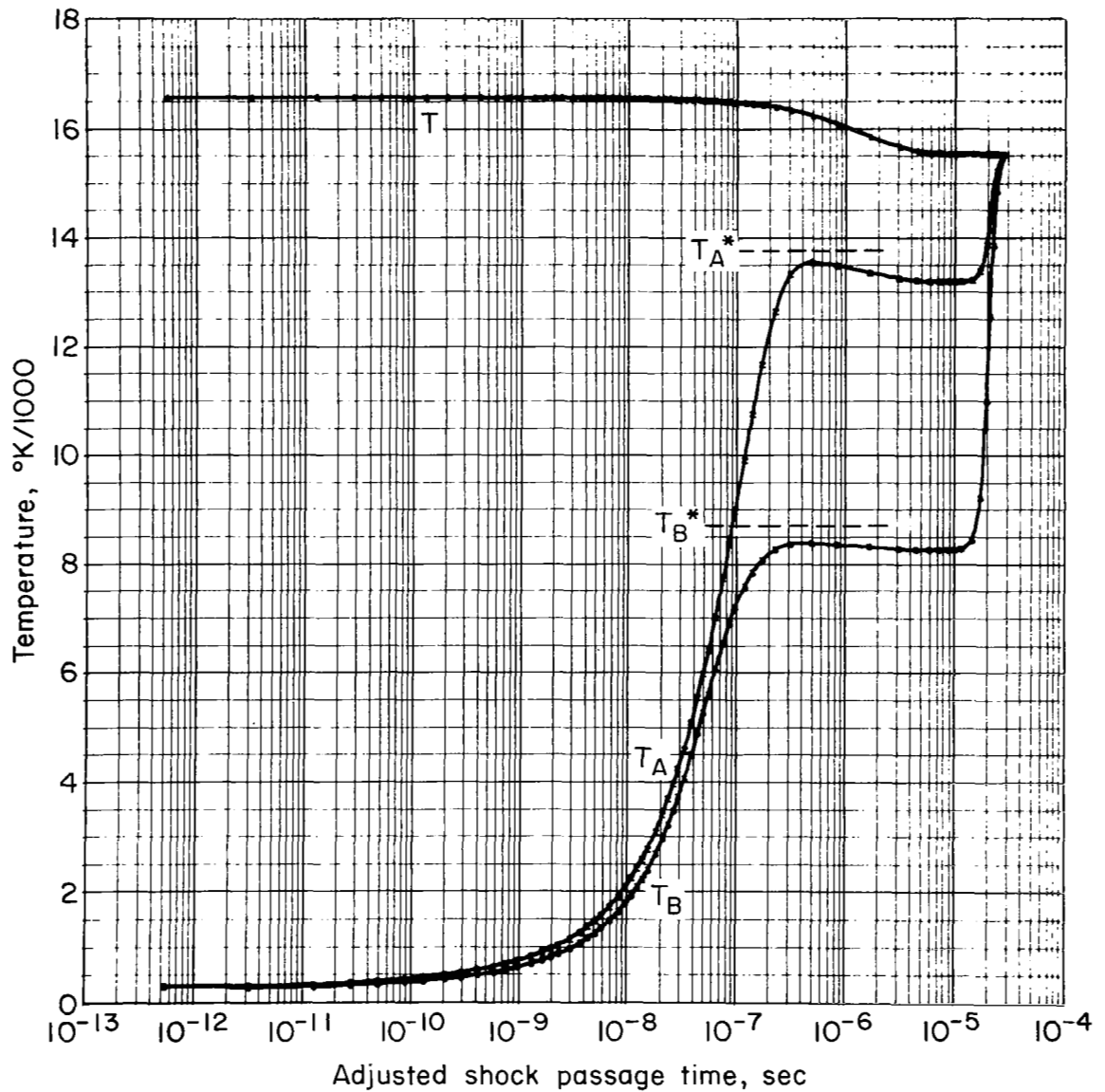
(c) Concentration, Lower States

Figure IV-6 Continued



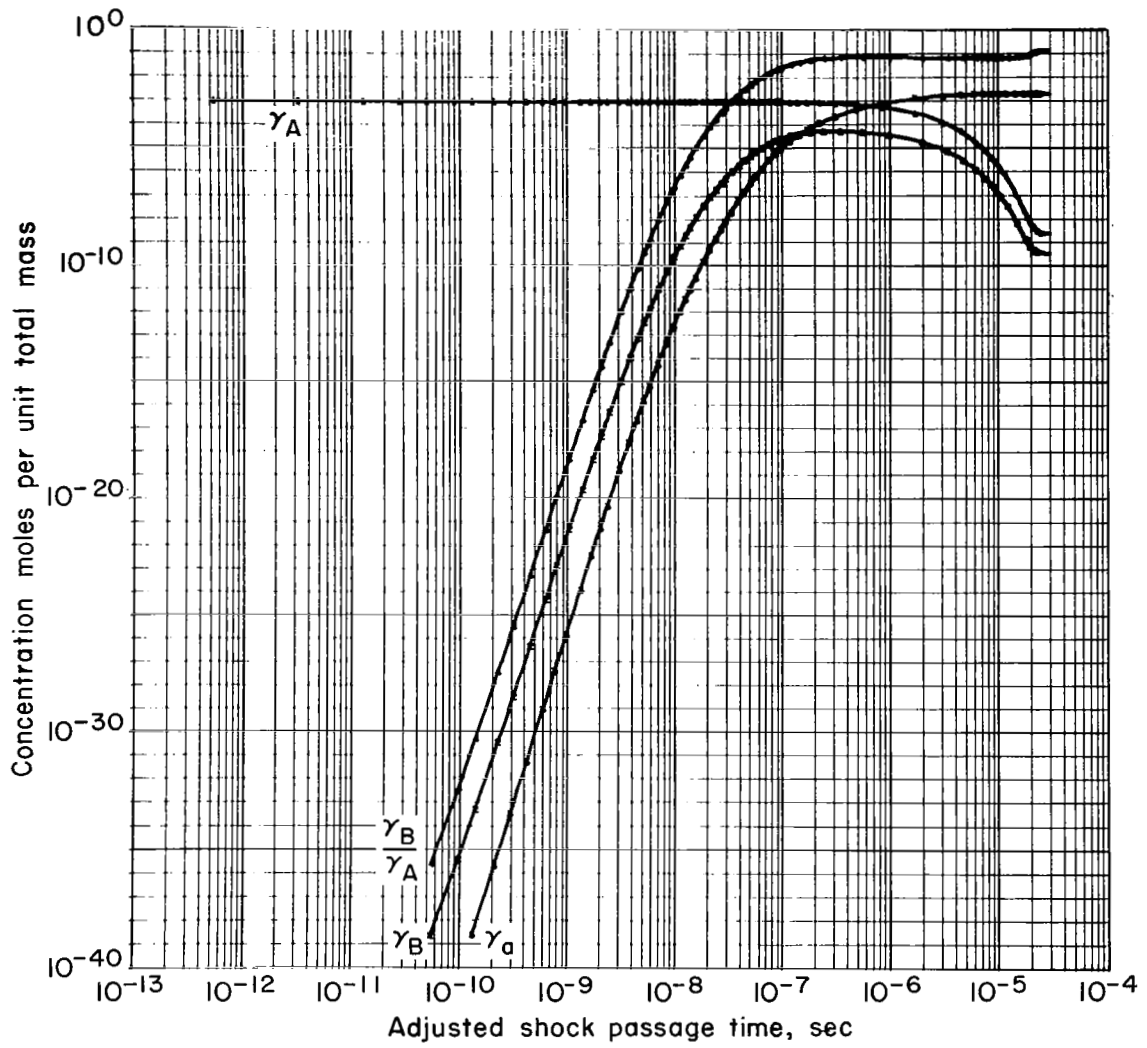
(d) Vibrational coupling factor

Figure IV-6 Continued



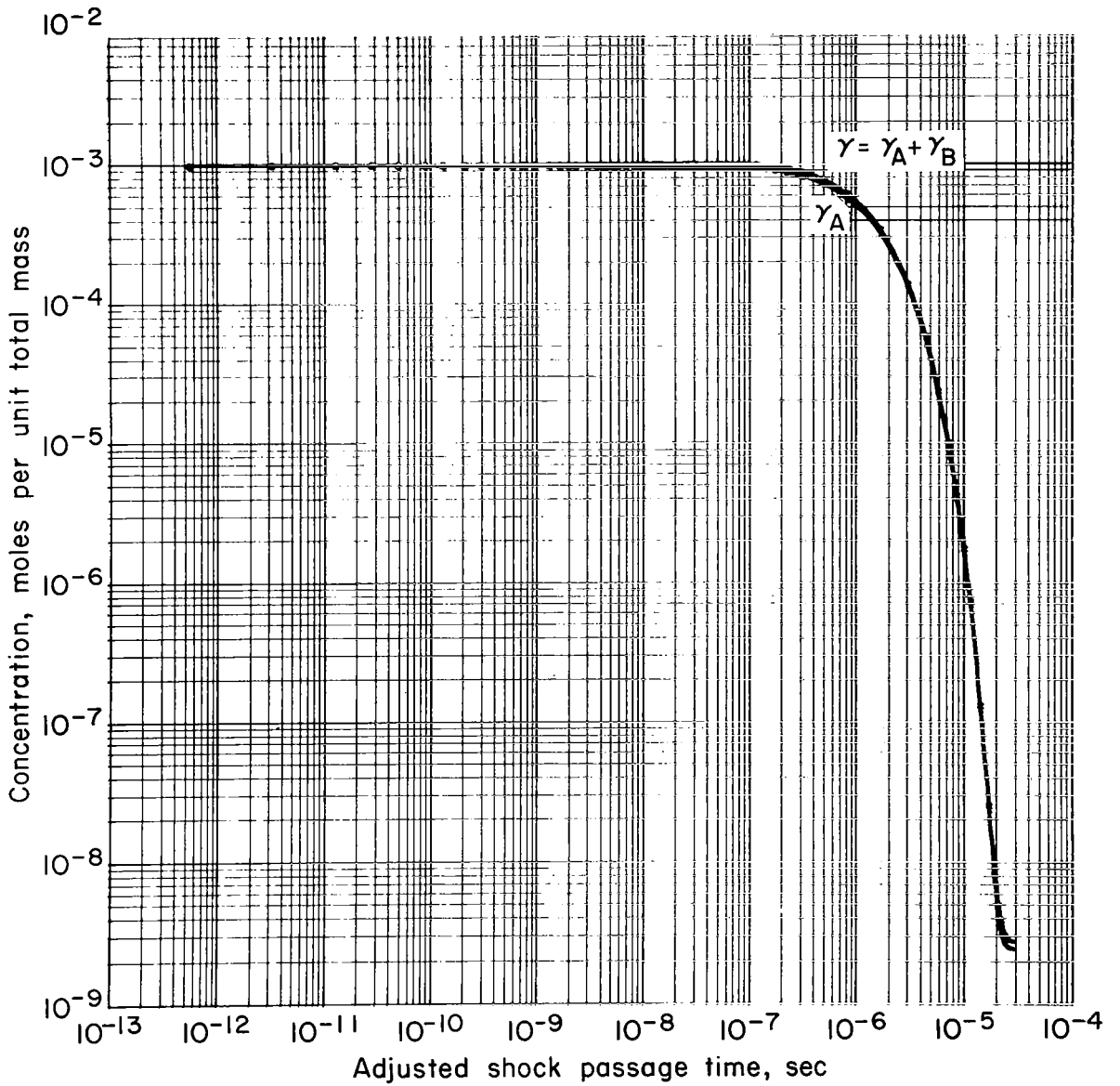
(a) Temperatures

Figure IV-7. Variables obtained from shock solutions versus adjusted laboratory time (associated parameters are listed along seventh row of table IV-1)



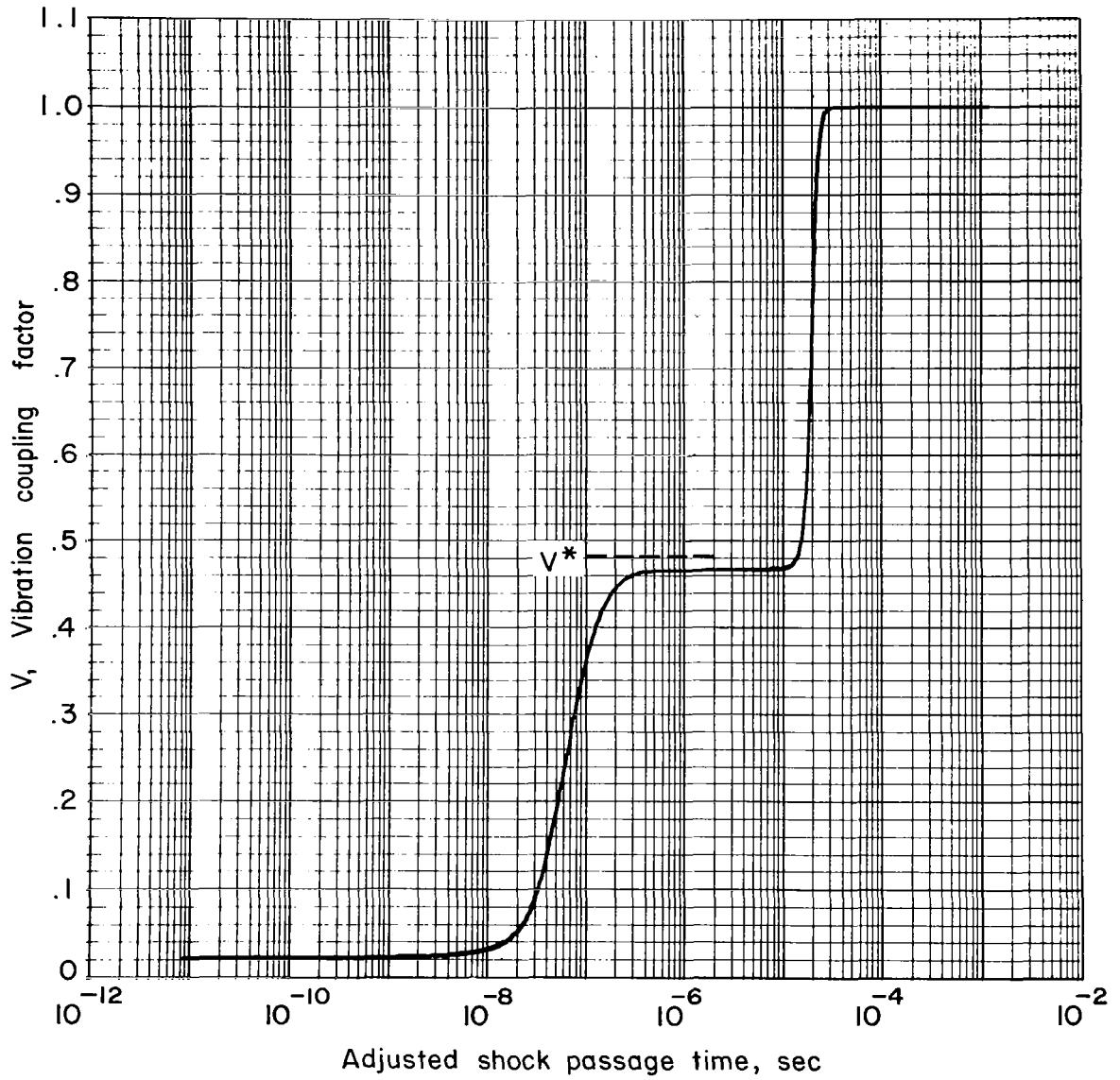
(b) Concentrations

Figure IV-7 Continued



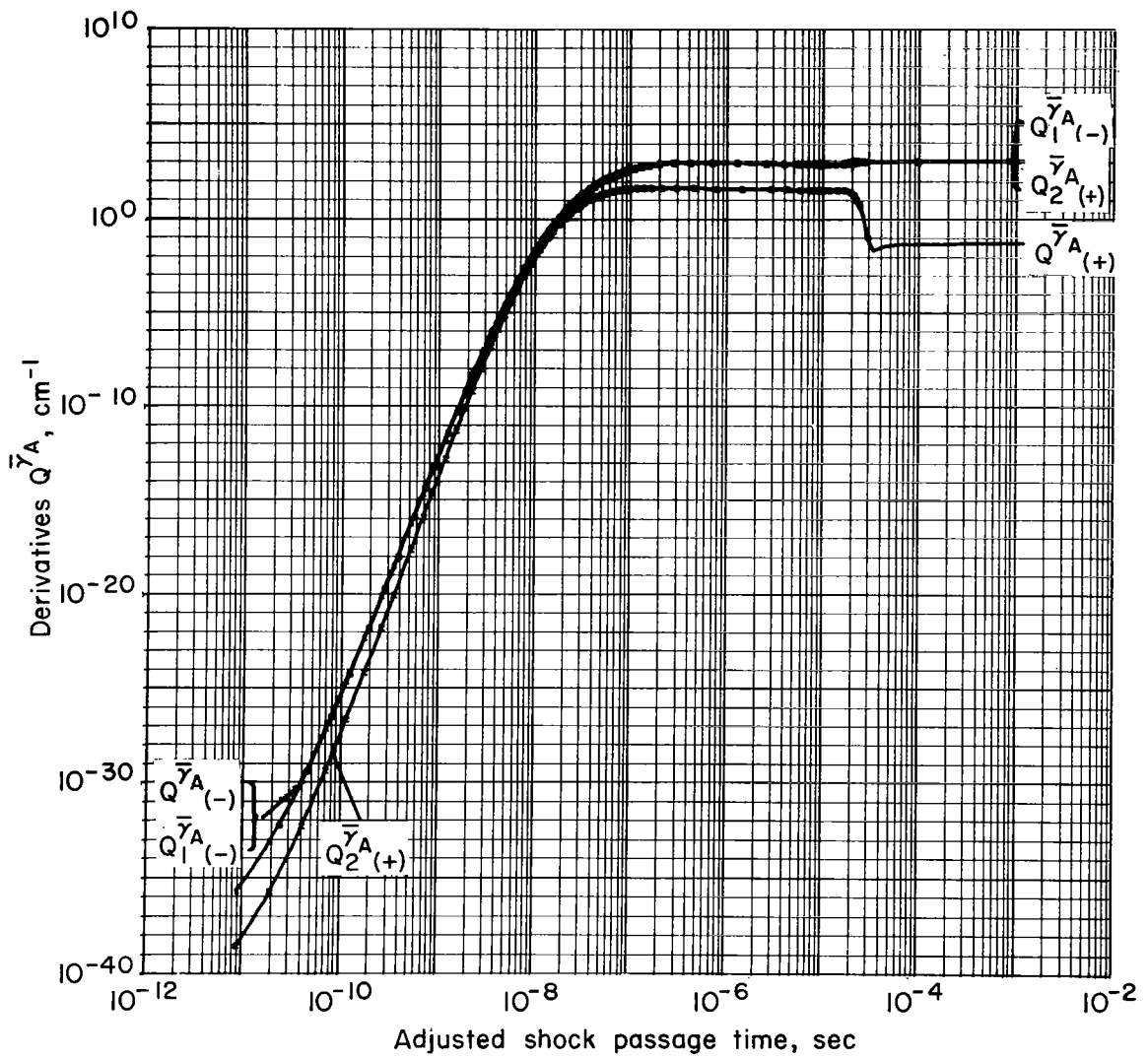
(c) Concentration, Lower States and Molecular

Figure IV-7 Continued



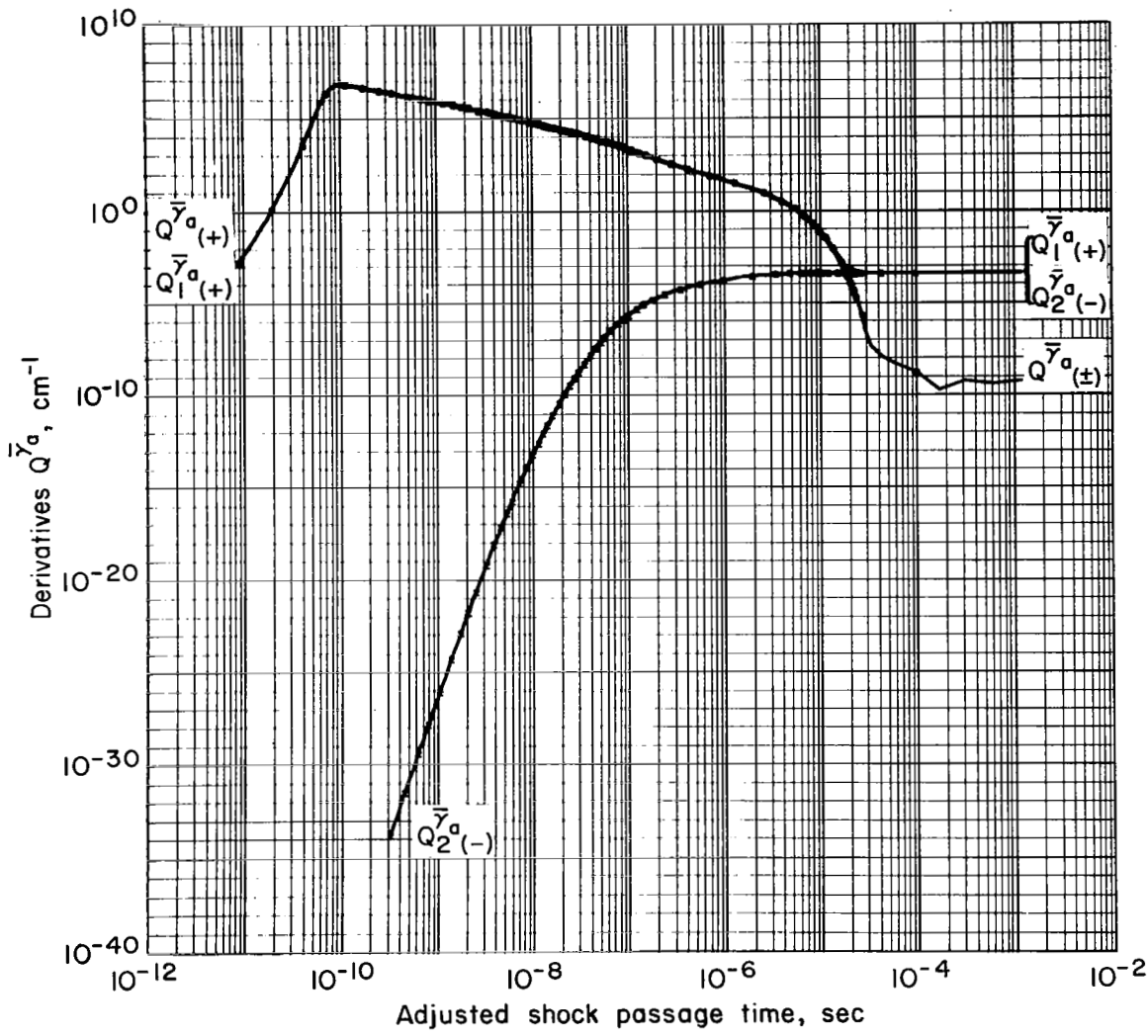
(d) Vibrational coupling factor

Figure IV-7 Continued



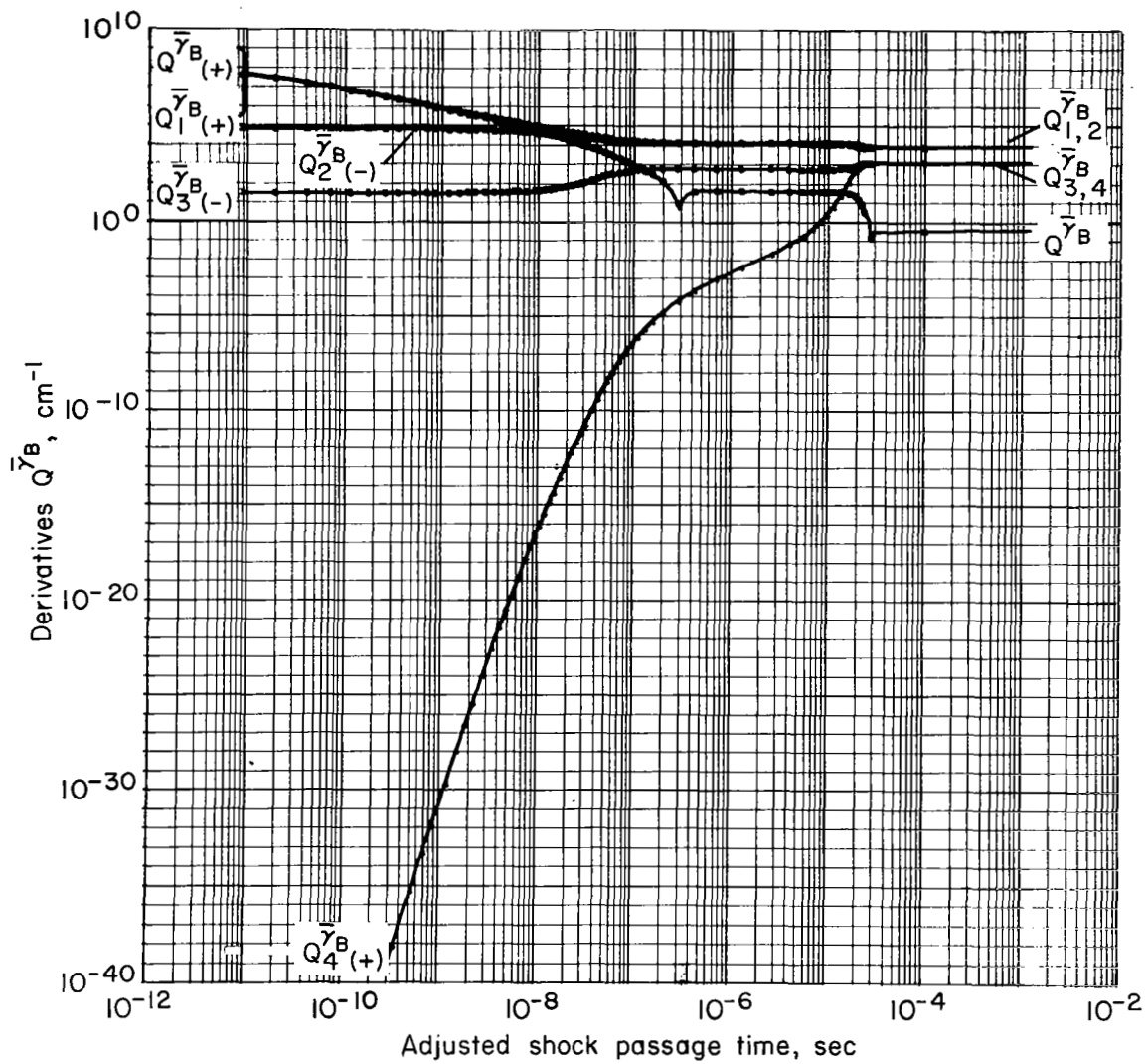
(e) Derivative, $\bar{Q}^{\bar{\gamma}_A}$, and component terms, $\bar{Q}_i^{\bar{\gamma}_A}$

Figure IV-7 Continued



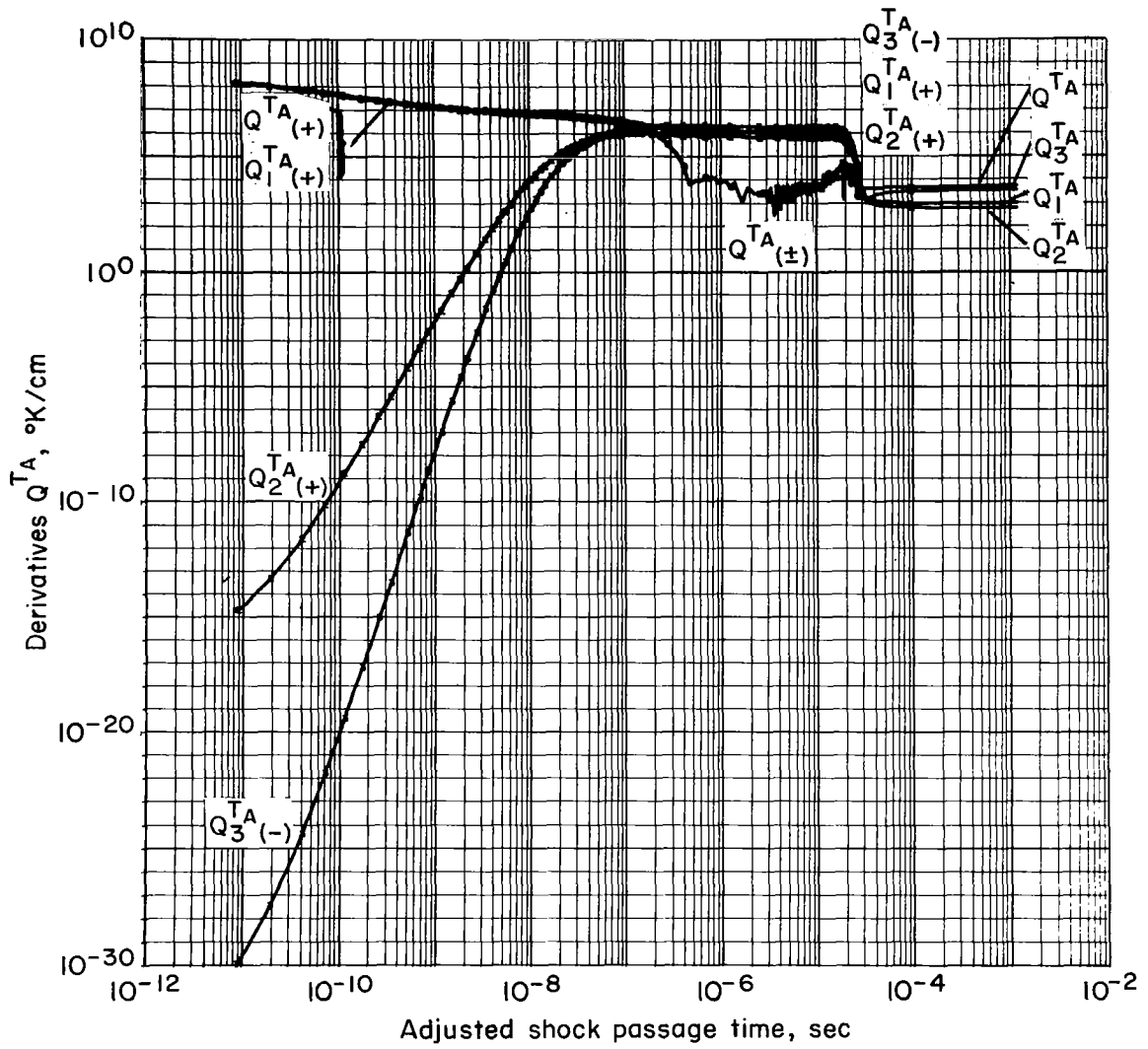
(f) Derivative, \bar{Q}_a , and component terms, \bar{Q}_1^a

Figure IV-7 Continued



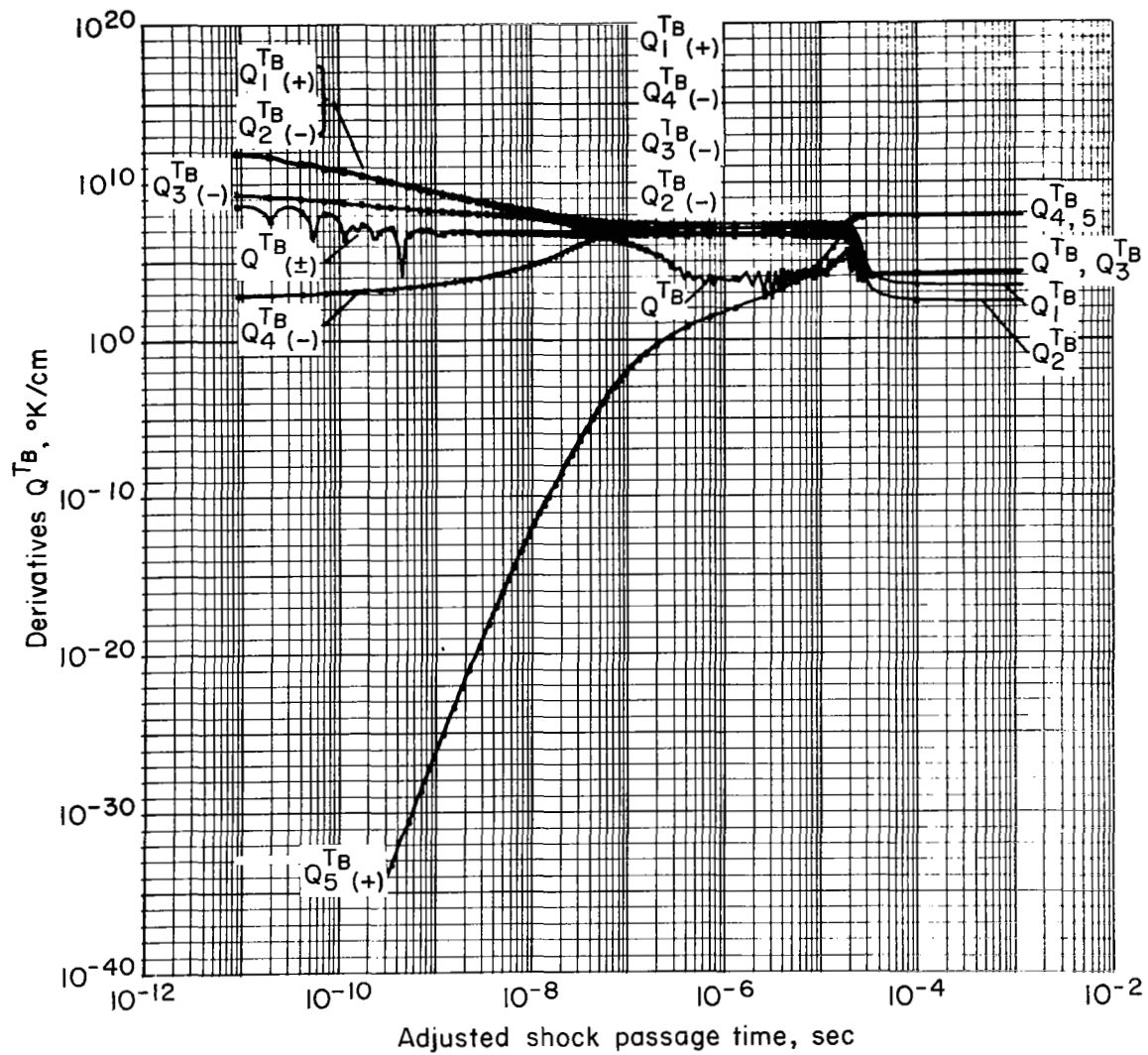
(g) Derivative, $\bar{Q}_{\bar{\gamma}_B}$, and component terms, $Q_{\bar{\gamma}_B,i}$

Figure IV-7 Continued



(h) Derivative, Q^{TA} , and component terms, Q_i^{TA}

Figure IV-7 Continued



(i) Derivative, Q^{TB} , and component terms, Q_i^{TB}

Figure IV-7 Continued

the effects of anharmonicity in the transition rates; in the case that such effects are negligible this parameter has a value that is unity. In figures IV-7 are also given the derivatives and, in addition, the component terms for comparison with the similar quantities of figure IV-1. The solutions for this latter case are analogous in some respects to those of the Marrone and Treanor model (58) in that no account is made for the more rapid transitions occurring in the upper vibrational levels. The closer level spacing for the B-states is still retained, however. One sees that the temperature T_B^* is perturbed to values much lower than T_A^* . This was also apparent in the quasi-steady solutions. The more interesting feature in the comparison of figures IV-1 and IV-7 is the very close similarity of the behavior of the separate terms contained in the derivatives. In particular, one may infer the importance of the Boltzmann factor in reducing the term $Q_2^T A$ in figures IV-1h and IV-4h. This term is relatively much smaller in the transient region for this case than in figure IV-1. One concludes that the effect of the Boltzmann factor is appreciable for the case of figure IV-1 and hence greatly reduces the effect of the small relaxation time τ_{A_2} . The relative dominance of $Q_1^T A$ and $Q_2^T A$ are interchanged in the quasi-steady region, but $Q_3^T A$ is still the major term. Thus, although anharmonicity has some effect on the solutions, it is not a large effect.

(IV-B-2). The Induction Time

In the preceding section the shock-wave structure was described in some detail, and the effects caused by changing the values of certain of the parameters were discussed. The section thus provided insight and familiarity with the model as regards normal-shock-wave flow. Here an additional comparison will be made with experimental data by using the experimental measurements of Wray (99) to check independently the evaluation of the parameters in the model equations. Wray measured the lag time before he observed molecular dissociation; this lag time is related to the elapsed time, after passage of a shock, during which the molecular oxygen concentration remains essentially constant (see, e.g., figs. IV-1c, 2c, etc.).

To obtain his values Wray (99), using ultraviolet absorption techniques, measured the intensity of the 1470 Å ultraviolet line during the passage of a shock wave. The absorption of this radiation, known as Schumann-Runge absorption (12, 99), is dependent on the number density of oxygen molecules in low-lying vibrational energy states. The radiation absorbed, measured after the shock wave passes some observational slit, is thus a measure of the molecular-oxygen concentration. The results reported by Wray were found by extrapolating back to the initial value the exponentially decreasing absorbed intensity, appropriately scaled. The shock-passage time associated with the intersection of the extrapolation and the initial value were defined by Wray as the "incubation" time. These results are denoted by Δt_w and shown in figure IV-8. The smooth curves were obtained from the solutions of the model equations. To obtain these theoretical results two types of induction times are defined. In one case the time, denoted Δt_1 , is the time for the concentration variable γ_A to decrease 0.1 percent. These results are plotted as curves (1) through (5). In the second case the straight-line portion of the oxygen-concentration curves is extrapolated back to the initial value, and the associated abscissa coordinate, denoted by Δt_2 , is taken as the second induction time. The curves (6) through (8) correspond to this procedure. Each of the pairs of curves (1) and (6), (2) and (7), and (5) and (8) are obtained from the same solution and are thus for identical values of the embedded parameters.

Curves (1) through (5) illustrate the effect on Δt_1 of using different values for the embedded parameters. From curves 1 and 2 we observe first that changing the value of T_U , the measure of how rapidly dissociation drops off for the lower vibrational levels in the preferential dissociation model (note definition in Appendix C), has no noticeable effect on Δt_1 . The reason is evident if one examines the separate derivative terms associated with the dissociation processes as given in the previous section. The effects of dissociation that depend on the parameter T_U are negligible within the time scale Δt_1 .

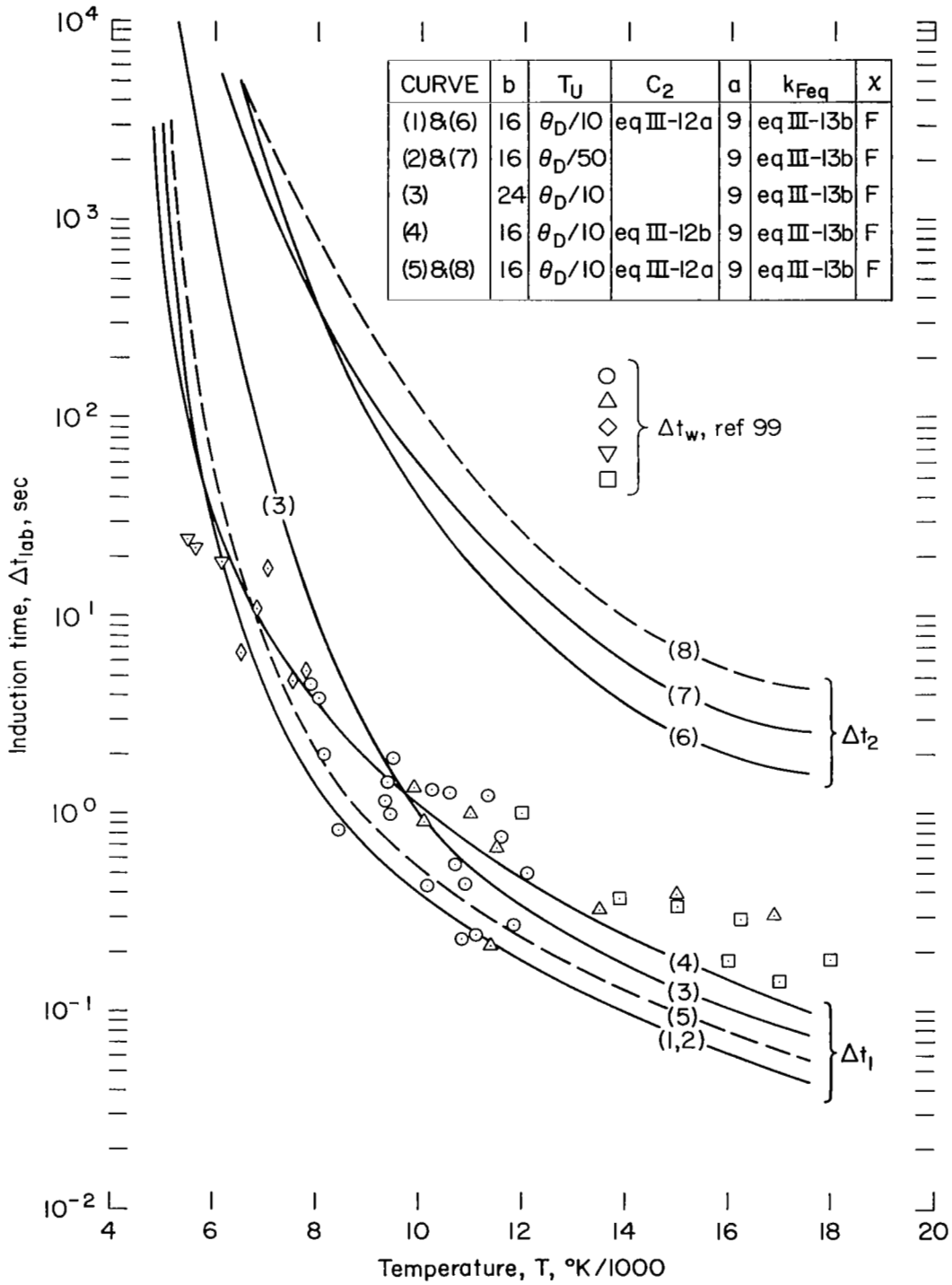


Figure IV-8. Induction time computed using two different methods and compared with experimental data of Wray

A comparison of curves (1) and (4) shows the effect of changing the parameter C_2 (see eq. III-12). The change in C_2 , as was pointed out previously, corresponds to an increase by a factor of 2 in the vibrational relaxation time at the higher temperatures. The effect is observed here as a similar increase in the induction time at the higher temperatures and little difference at the lower temperatures. A comparison of curves (1) and (3) shows that an increase of 50 percent in the level separation parameter b results in a 50 percent increase in the induction time at the higher temperatures and an order of magnitude increase at the lower temperatures. The result of using $\chi = 1$ rather than $\chi = \chi_F$ is shown in curve (5). In this case there is only a 20-percent effect.

The most interesting observation to make in figure IV-8 is that with the specified values for the parameters, the group of curves Δt_1 span values that nearly enclose Wray's data. More importantly, the temperature dependence of the computed values also agrees favorably with Wray's experimental data. The choice of the induction time Δt_1 , associated with a 0.1 percent differential decrease in the concentration variable γ_A , was made for several reasons: first, it was desirable to have a method for determining an induction time Δt that would not require considerable plotting and that would serve as a natural point at which the numerical calculations could be terminated without the necessity of computing the entire shock profile. Second, it was desirable to have a scheme that is readily applicable even when appreciable dissociation is not evidenced. The agreement, however, is accidental since the values assigned to the embedded parameters were chosen somewhat arbitrarily. It was later realized that the induction time Δt_1 is not directly relatable to the experimental time Δt_W obtained by Wray.[†]

[†]These results may, however, be of value in an experiment that does not involve extrapolation, but where small percentage changes in the initial molecular concentration of the lower states are measured.

The method for determining Δt_2 is similar to that used by Marrone and Treanor (58) but is difficult to apply unless there is considerable dissociation. As was mentioned, the Shumann-Runge absorption involves primarily the low lying vibrational levels of molecular oxygen. By taking this appropriately into account a measurement of induction time Δt can be obtained that would be directly relatable to Δt_w and would lie between Δt_1 and $\Delta t_2^{(11,12,13)}$. Because the low lying levels are most significantly populated, however, it is to be expected that an appropriate evaluation of an induction time, for comparison with Wray's data (99), would yield results that are close to the values Δt_2 . A comparison of Δt_2 and Δt_w is therefore the correct comparison for an assessment of the model equations.

Curves (6) through (8) show Δt_2 as calculated with different values for only a few of the embedded parameters. A comparison of curves (6) and (7) illustrates the effect on Δt_2 that results from changing the value of T_U . Although changing T_U had little effect on Δt_1 , here the effect is appreciable (causing the curves to differ by nearly a factor of 2 at the higher temperatures). The principal reason for the different behavior here is that the procedure for determining Δt_2 , described earlier, also depends on the slope of the curve for γ_A and hence on the rate of molecular dissociation. Reducing the value of T_U is equivalent to reducing the number of levels from which dissociation effectively occurs and hence reducing the rate of dissociation. The parameter Δt_2 therefore not only measures the transient time but is also dependent on the rate of dissociation. A comparison of curves (6) and (8) illustrates the effect of anharmonicity on the induction time Δt_2 ; in this case the effect is appreciable. Curve (8) is included only to illustrate the effect of using $\chi = 1$ rather than $\chi = \chi_F$.

The comparisons that have been made illustrate the differences due to changing the values of certain of the embedded parameters. A comparison of curves (6) and (7) with the induction time Δt_w of Wray, leads us to conclude that the model yields induction times that are about an order of magnitude too long. This is not too disturbing when one recalls that the initial values assigned

to b were arbitrary and the values used for T_U were found so as to depend on b . In this connection it is worthwhile to review briefly the procedure that led to the values assigned to the embedded parameters (see preceding chapter). The value of the separation b was chosen to yield a separation energy E_b that is roughly midway up the vibrational potential-energy well. Specifically, we have used $E_b/E_D = 0.544$ and 0.786 . These values were chosen arbitrarily, although they were thought to be reasonable on the basis of the results reported by Treanor (94), Shuler (84), and Keck and Carrier (48). The values for the remaining parameters, in particular T_U , were chosen (recall discussion in Chapter III) to provide a pre-exponential temperature dependence for the effective dissociation rate that would be in reasonable agreement with experiment. It was also noted that the small values of the parameter T_U that were required for the proper pre-exponential temperature behavior, led to the conclusion that dissociation occurs only from the very uppermost vibrational energy level (see also discussion in Appendix C). In this respect the preferential dissociation model is consistent with other theories (7, 48, 73, 84, 85) since it is strictly "ladder climbing." In the other theories vibrational excitation occurs stepwise and dissociation (or recombination) involves the very uppermost level only. In summary, a choice of b at the midpoint of the vibrational-energy well requires highly preferential dissociation in order to produce an appropriate pre-exponential temperature dependence, and the induction time that then results is about an order of magnitude too large. An opposite result was obtained (see (58)) from a non-preferential dissociation model in that the resulting induction times were more than an order of magnitude too small.

The parameters can be readjusted to yield more representative values for the oxygen molecule induction behind a normal-shock wave. Reducing the value of the separation parameter b will reduce the induction time. Such a change will yield a larger pre-exponential temperature factor for the effective dissociation rate constant (specifically, the vibrational coupling factor V) unless T_U is also increased. Increasing the value of T_U as b is reduced will maintain the present agreement of the temperature dependence of the vibrational

coupling factor and at the same time increase effectively the number of the uppermost vibrational energy levels from which dissociation occurs. One notes from figure IV-8 that larger values of T_U (compare curves (6) and (7)) also reduce the induction time and would thus effect more favorable agreement with experiment. After the appropriate value is found for b and T_U , dissociation will likely involve principally just a few of the very uppermost vibrational energy levels, and the ladder-climbing concept will probably still apply. That the Marrone and Treanor model (58) yields induction times (when $T_U = \infty$) that are too small while this model yields results that are too large provides confidence that the parameter values can be adjusted so as to obtain closer agreement with experimental data both as regards the temperature dependence of the effective dissociation rate and the induction time.

Before concluding this section there is one additional comment that should be made. In Appendix B the procedure used to account for the anharmonic effects associated with the transition rates is discussed. The procedure involves the use of two linear segments to approximate the rate-of-quantum-transfer relation. This two-segment approximation, although it may be considered superior to a single-segment Landau-Teller approach, is perhaps too coarse. Introducing another segment into the approximation (and thus another separation parameter of the same type as "a") will also have the effect of reducing the induction time. Such an improvement may be of value although it is not expected to have a large effect on the induction time.

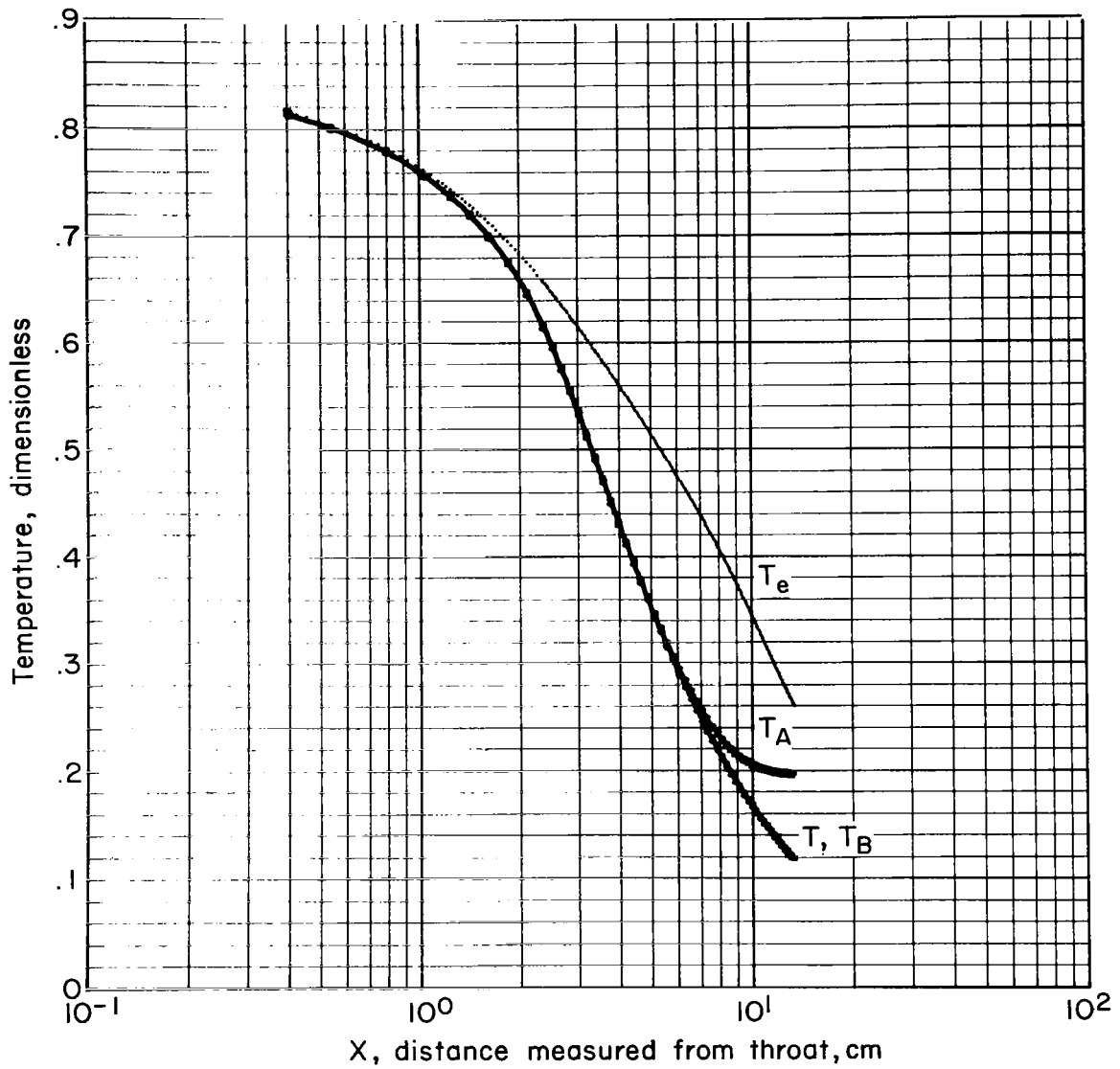
IV-C. Nozzle Flow

(IV-C-1) Example Solution

In this section the flow equations, given by equations (F16) of Appendix F, are solved by means of the implicit numerical-integration method (eqs. (E22)). The dimensionless streamtube area is obtained from $A(x) = 1 + (x/3.20)^2$, which represents an axisymmetric hyperbolic nozzle. At large distances ($x \gg 3.20$) the geometry is approximately that of a cone with a half angle of 10° . The gas is taken to be a mixture of 20 percent molecular oxygen with a diluent

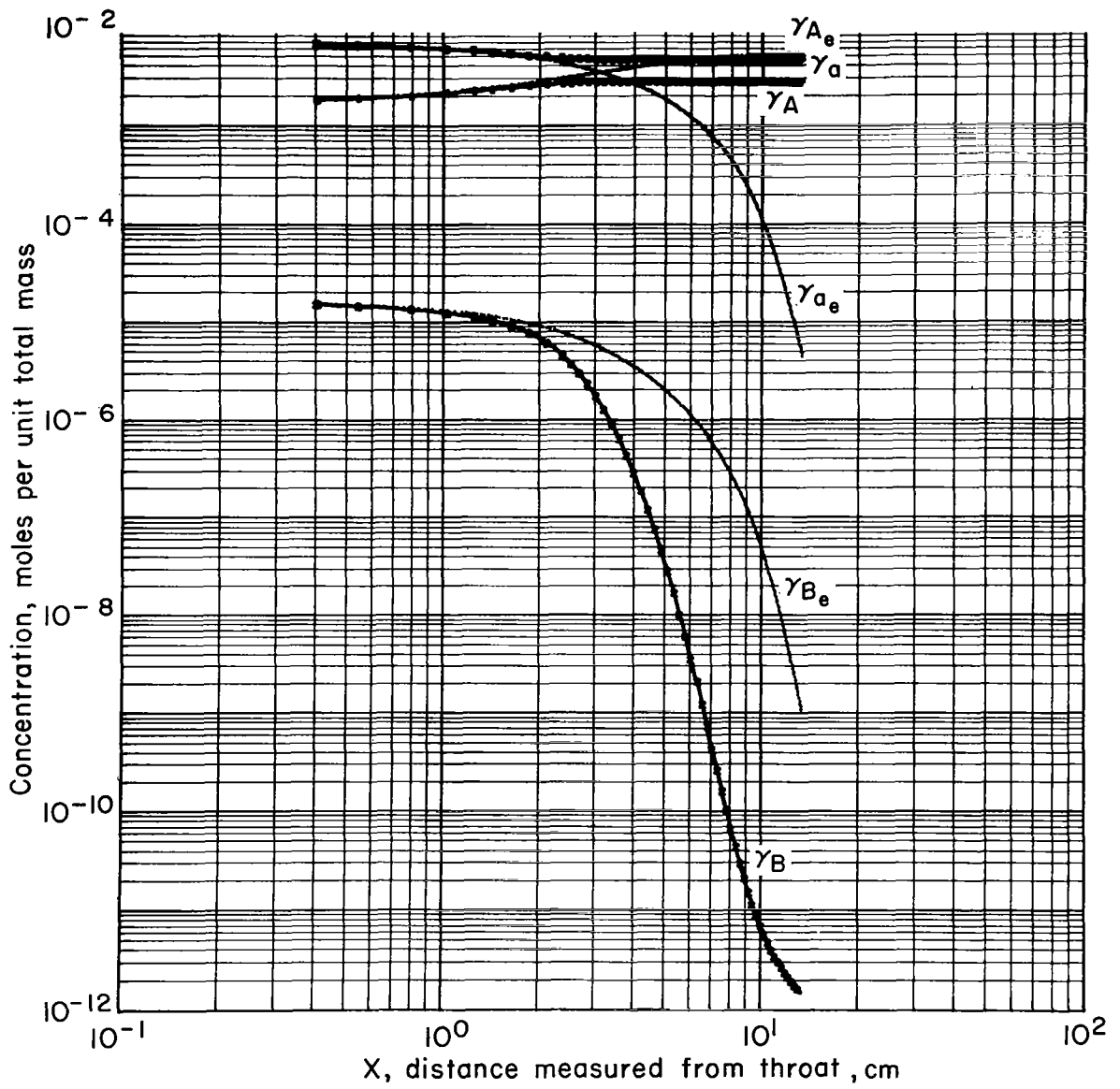
of 80 percent argon. For this calculation the effects of considering other than argon as a colliding partner are again considered negligible. (The solution is thus obtained from the same equations as in the previous section except that the fraction of the mixture that is molecular oxygen is greater and the stream-tube area is not constant.) Only one solution will be given; this solution applies to nozzle flow when the reservoir has a temperature of 8,000° K and a pressure of 3,000 atmospheres. The starting conditions for the integration procedure are obtained by assuming that the flow is in equilibrium (isentropic) up to and slightly beyond the throat. The solution includes some of the effects of recombination that occur before the atom-recombination processes freeze, as well as effects of the "cooling" of both the upper and lower vibrational energy states as a result of vibration-translation energy interchange. The solution also demonstrates that the vibrational temperatures and the kinetic temperature are all equal for a relatively large distance downstream of the throat. It will be shown that this characteristic allows one to estimate an effective vibrational relaxation time that is smaller than the relaxation time of Landau-Teller theory. Its value is quantitatively consistent with recent experimental data (98). It also turns out, however, that the smaller relaxation time (i.e., smaller as compared with the time obtained from Landau-Teller theory) is realized only when the vibrational temperatures are large. The nozzle solutions will be discussed in detail first, and later the procedure for estimating the characteristic vibrational relaxation time will be described.

The results of the calculations are plotted in figure IV-9. Figures IV-9a through IV-9g show nearly all the dependent integration variables (T , T_A , T_B , $\bar{\gamma}_A$, $\bar{\gamma}_B$, $\bar{\gamma}_a$, ρ , and v) together with the pressure p and the vibrational coupling factor V , which are found from the thermal equation of state (E3) and equation (C10), respectively. Also plotted in these figures are values computed for the equivalent case of equilibrium nozzle flow, where the rate constants are all assumed to be infinite. These values are subscripted with the letter e . The derivatives and their component terms are plotted in figures IV-9h through



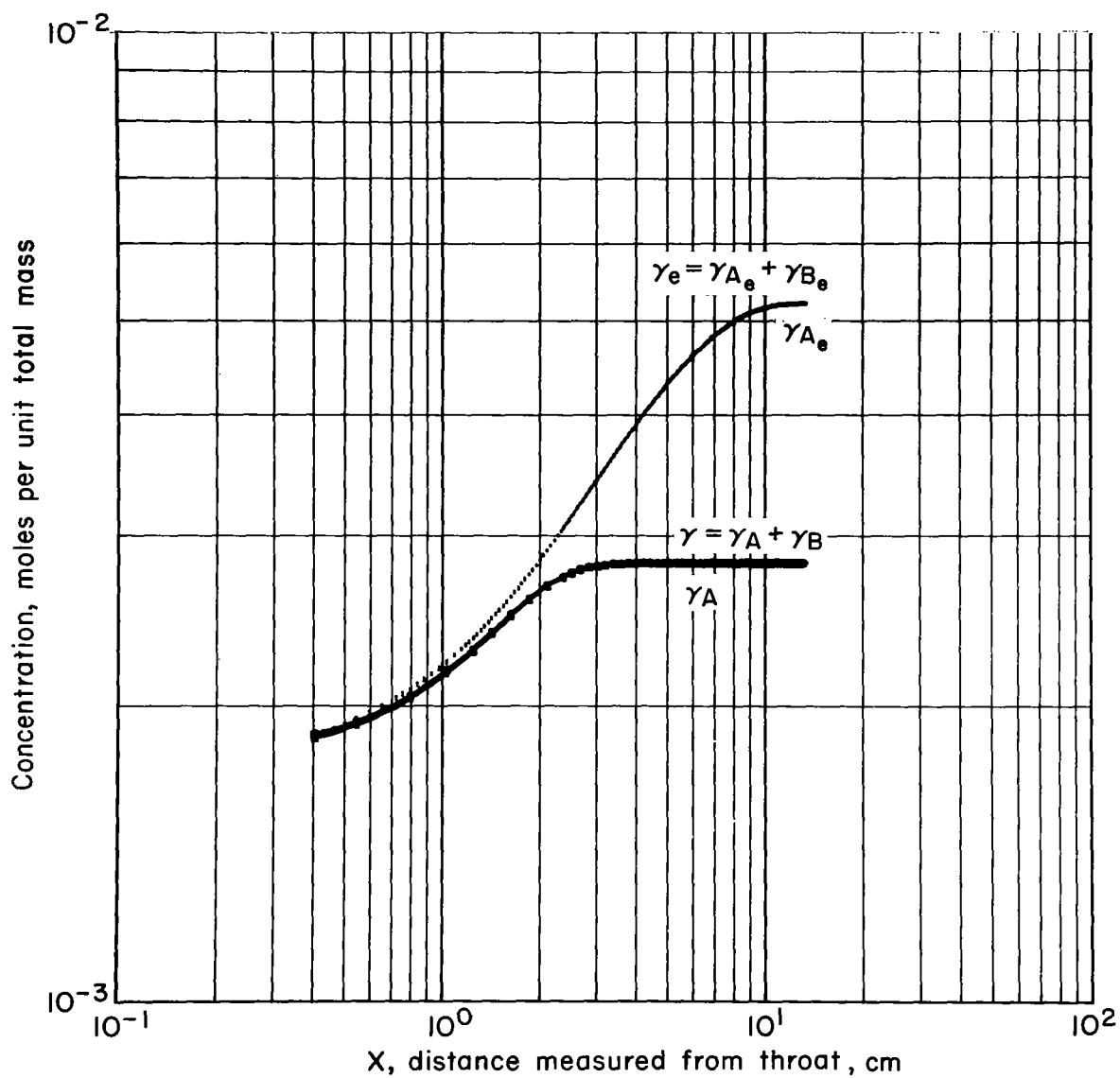
(a) Temperatures

Figure IV-9. Variables obtained from nozzle solution versus distance measured from the throat (associated parameters are the same as listed for figure IV-5)



(b) Concentrations

Figure IV-9 Continued

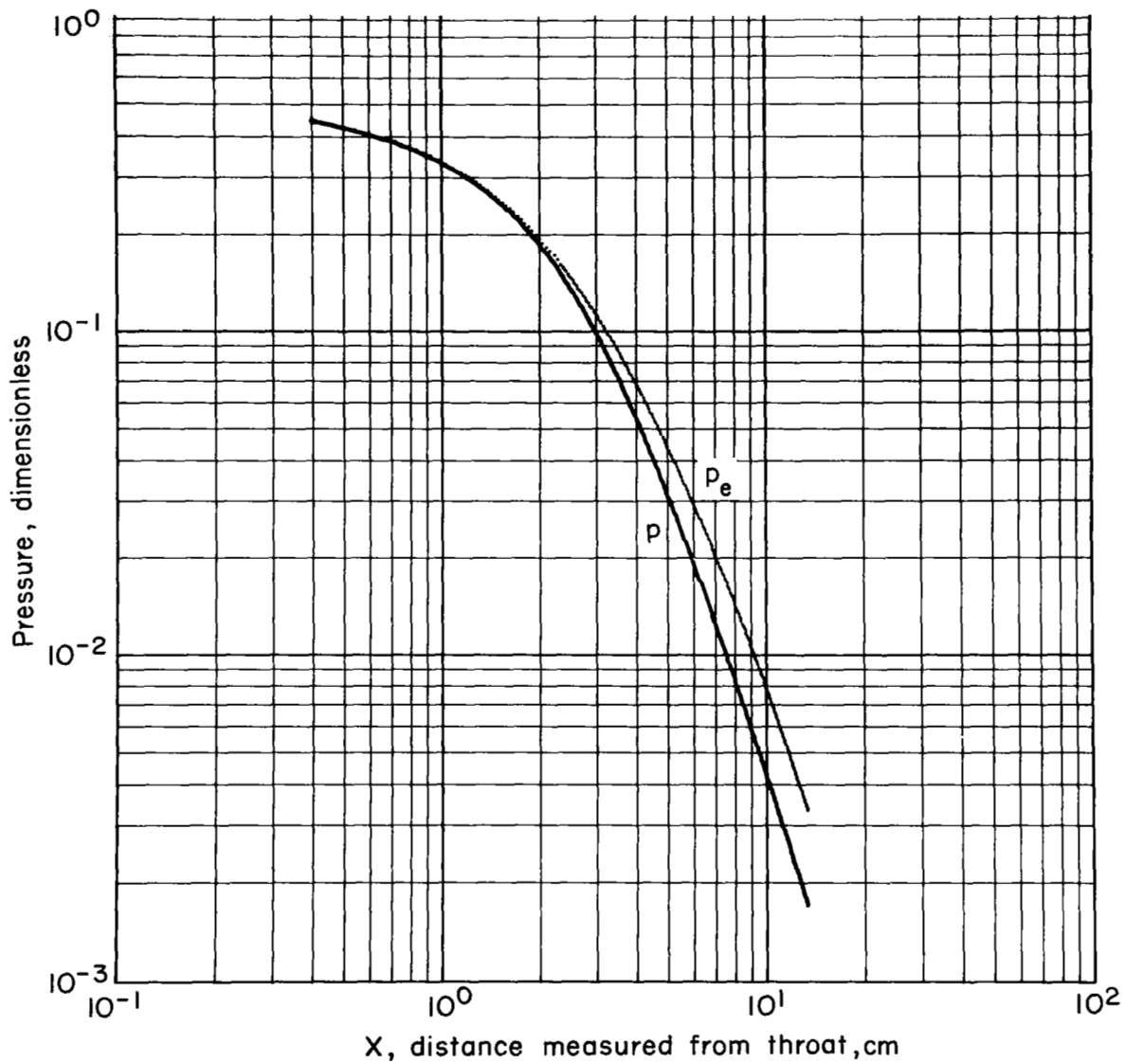


(c) Concentration, Lower States and Molecular
 Figure IV-9 Continued

IV-9l. The notation used in these figures is identical to that used previously (eqs. (IV-2) through (IV-7)).

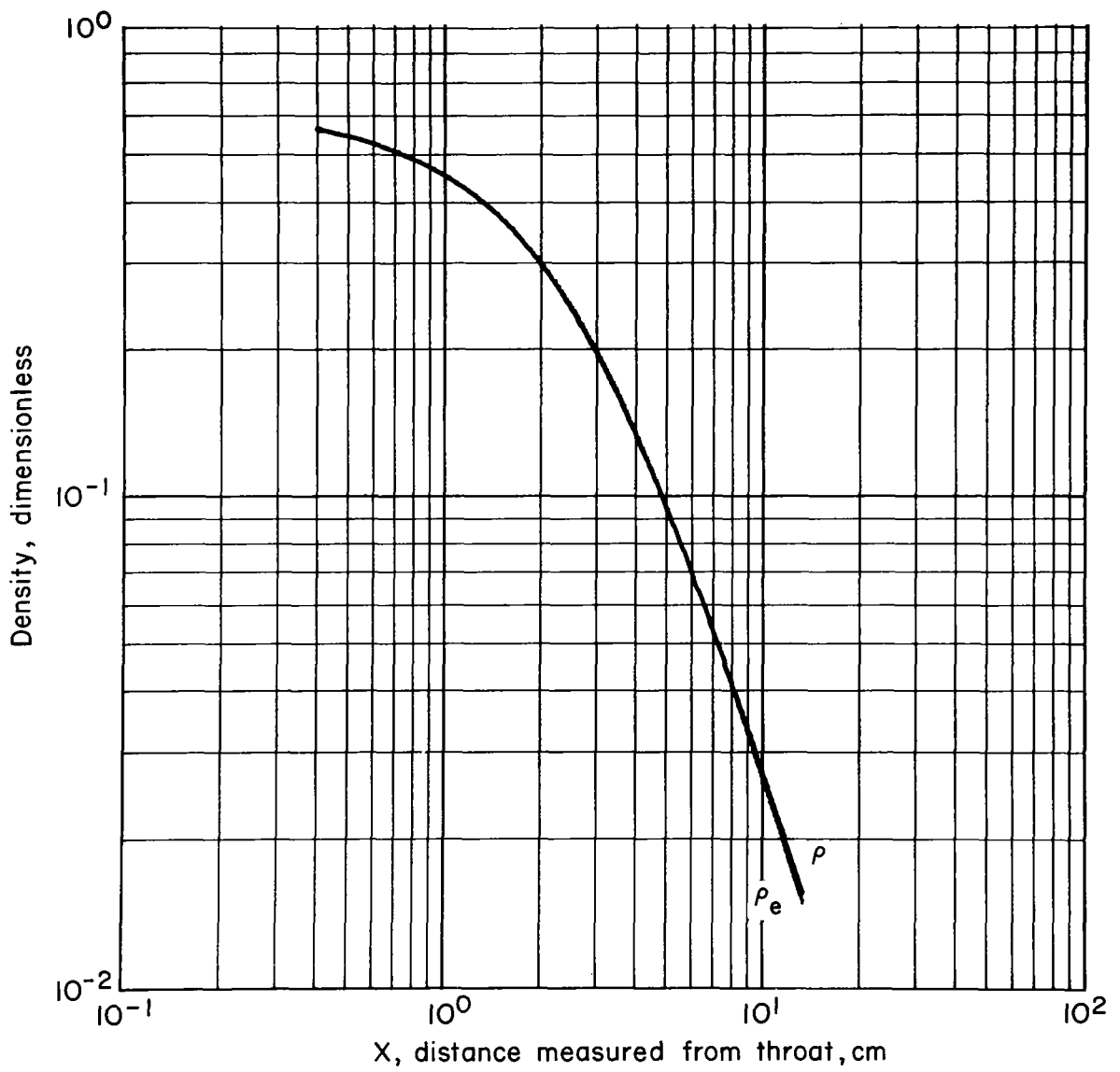
Beginning our discussion with figure IV-9a, we observe first that the temperatures T , T_A , and T_B are all equal to a distance of 7 centimeters downstream of the throat. At this point the lower state temperature T_A starts to differ from the other temperatures, and at 10 centimeters becomes constant (freezes). The upper-state temperature T_B and the kinetic temperature T continue to remain equal throughout the flow region shown. Other calculations (not shown) indicate that the upper-state temperature will also freeze when lower stagnation (reservoir) pressures are used. The freezing of T_B always occurs farther downstream than T_A . We also note in figure IV-9a that T , T_A , and T_B start to differ from their equivalent equilibrium-flow temperature at about 1 centimeter downstream of the throat. The flow is nonisentropic beyond this point. This is also evident from figures IV-9b and IV-9c, which show that the concentration variables γ_A , γ_B , and γ_a start to deviate from their equilibrium-flow values at about this point. At a distance of 3 centimeters we notice that recombination no longer occurs, as is evidenced by the constant atom concentration. The upper-state concentration variable continues to decrease throughout the entire flow region, but since its value is so small there is no noticeable increase of the lower-state concentration. Changes of the lower-state concentration occur only where atom recombination is observed. That the decreasing γ_B affects the lower states and is not caused by dissociation will be apparent when the derivatives are investigated.

The pressure, density, and velocity are compared with their equilibrium-flow equivalents in figures IV-9d through IV-9f. The pressure appears to be greatly affected by the chemical effects and not appreciably by the freezing of T_A , since the rapid freezing of the lower-state temperature T_A causes no further change of the pressure variable. Density, however, is affected by both the freezing of the chemical effects and of T_A . In particular, we have a



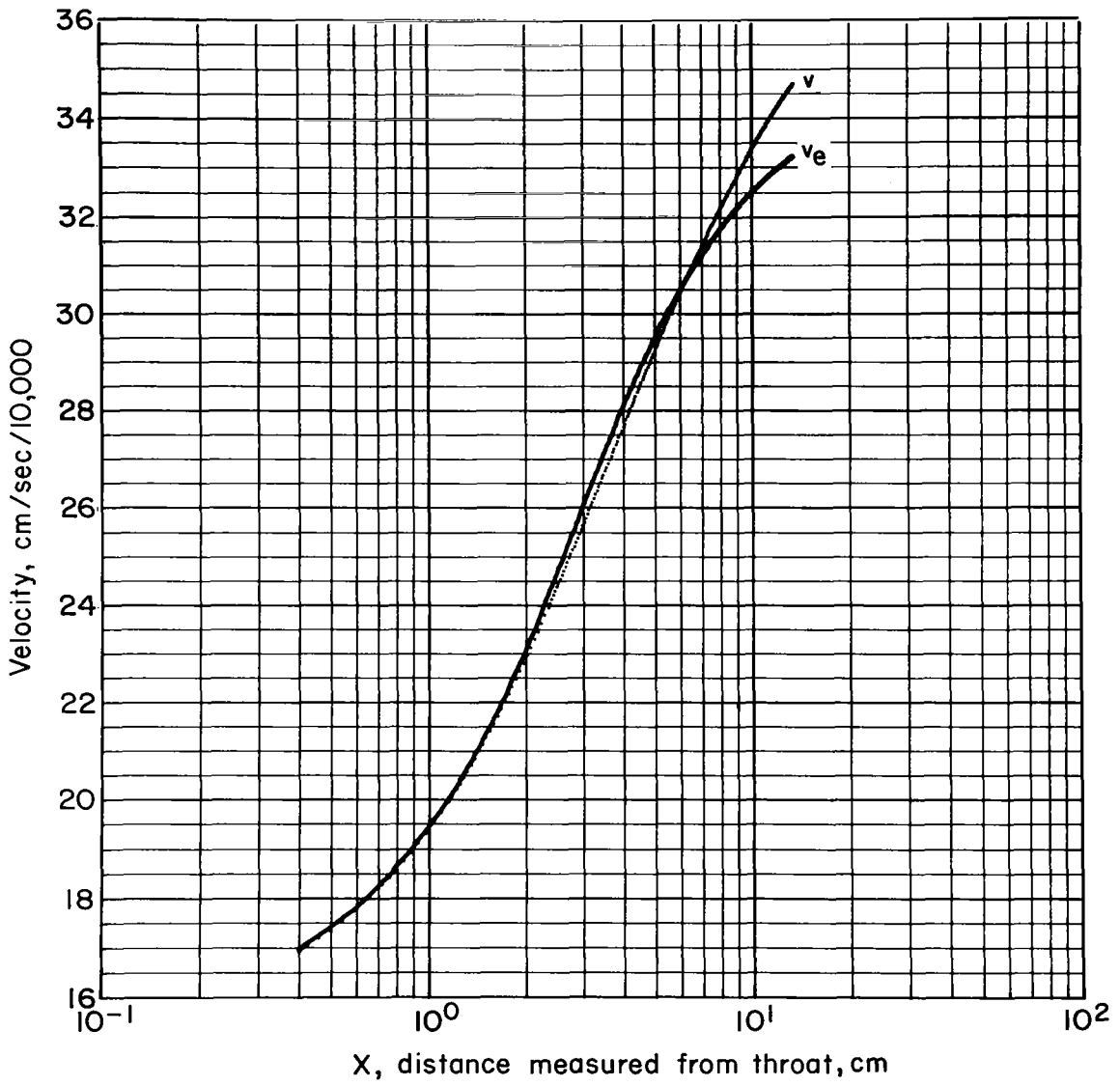
(d) Dimensionless static pressure

Figure IV-9 Continued



(e) Dimensionless static density

Figure IV-9 Continued



(f) Velocity

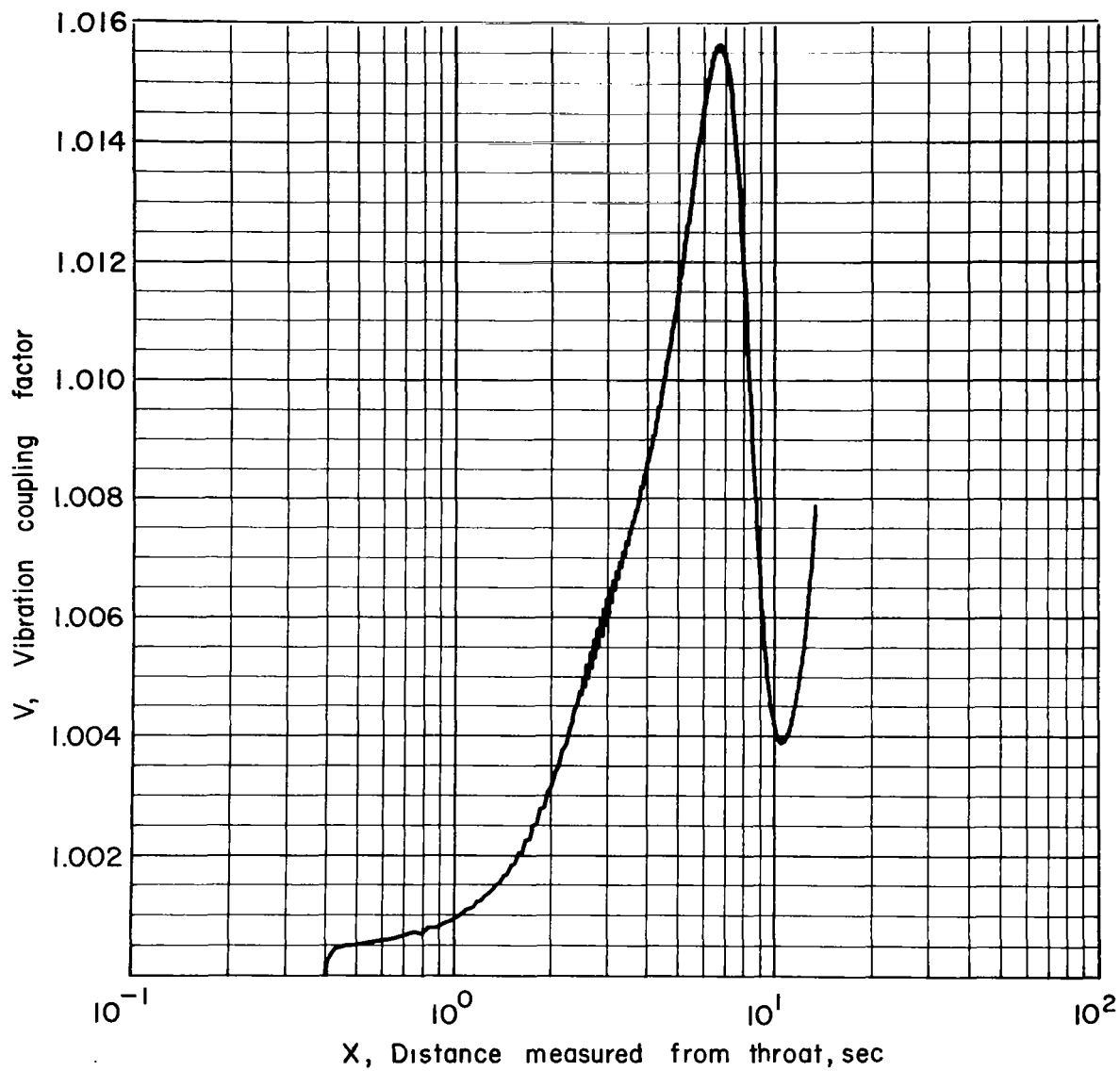
Figure IV-9 Continued

smaller flow velocity and larger mass density than is obtained on the assumption of complete equilibrium. (Notice that velocity is plotted with a linear scale while density is plotted with a logarithmic scale.)

Figure IV-9g shows the vibrational coupling factor V computed for the nozzle problem. This factor differs at most by only about 2 percent from unity and for all practical purposes has little effect on the flow. This is in contrast to the situation for normal-shock-wave flow, where this quantity was very important. There the coupling factor delayed the onset of dissociation. For the quasi-steady zone (see, e.g., Chapter III) this factor varied as $T^{-\frac{1}{2}}$ and such behavior is also not exhibited here.

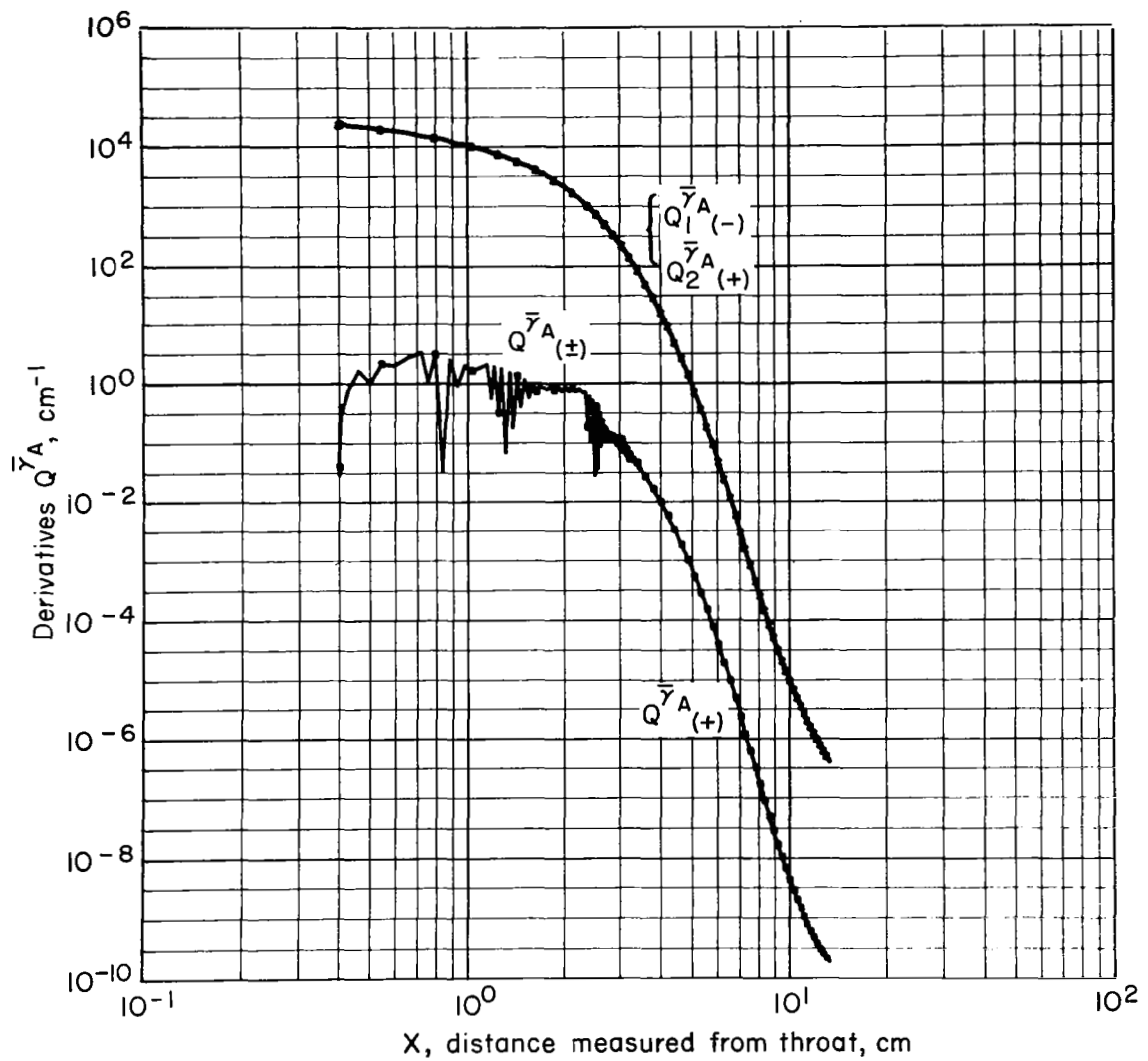
An understanding of the processes that occur during the expansion in the nozzle is, perhaps, more easily obtained by examining the various terms contained in the model rate equations, as was done for the shock-wave problem. The values of these terms are displayed in figures IV-9h through IV-9l). The labeling used for the curves is defined by equations (IV-2) through (IV-7); the Q -quantities without subscripts are the derivatives while the quantities with subscripts are the components of the derivatives. One general remark should be made about the apparent unstable behavior shown by the complete derivatives. As was mentioned earlier, the implicit method was used for these calculations, and a characteristic of implicit methods is to show such behavior for the complete derivatives (notice that the separate terms are smooth). This effect does not appear in the solutions where, as may be seen, the curves in figures IV-9a through IV-9f are quite smooth. Although there appears to be a slight noise effect superimposed on the curve representing the vibrational coupling factor in figure IV-9g, the fact is that the scale is greatly expanded and the noise amounts to only about 0.02 percent. The error of the calculation is about this order of magnitude (see discussion in Appendix E).

Figure IV-9h illustrates the behavior of $Q_{\tilde{\gamma}_A}$. Near the throat the gain and loss terms are nearly equal and result in a derivative that is small, although sufficiently large to cause about a 30-percent change in γ_A . As



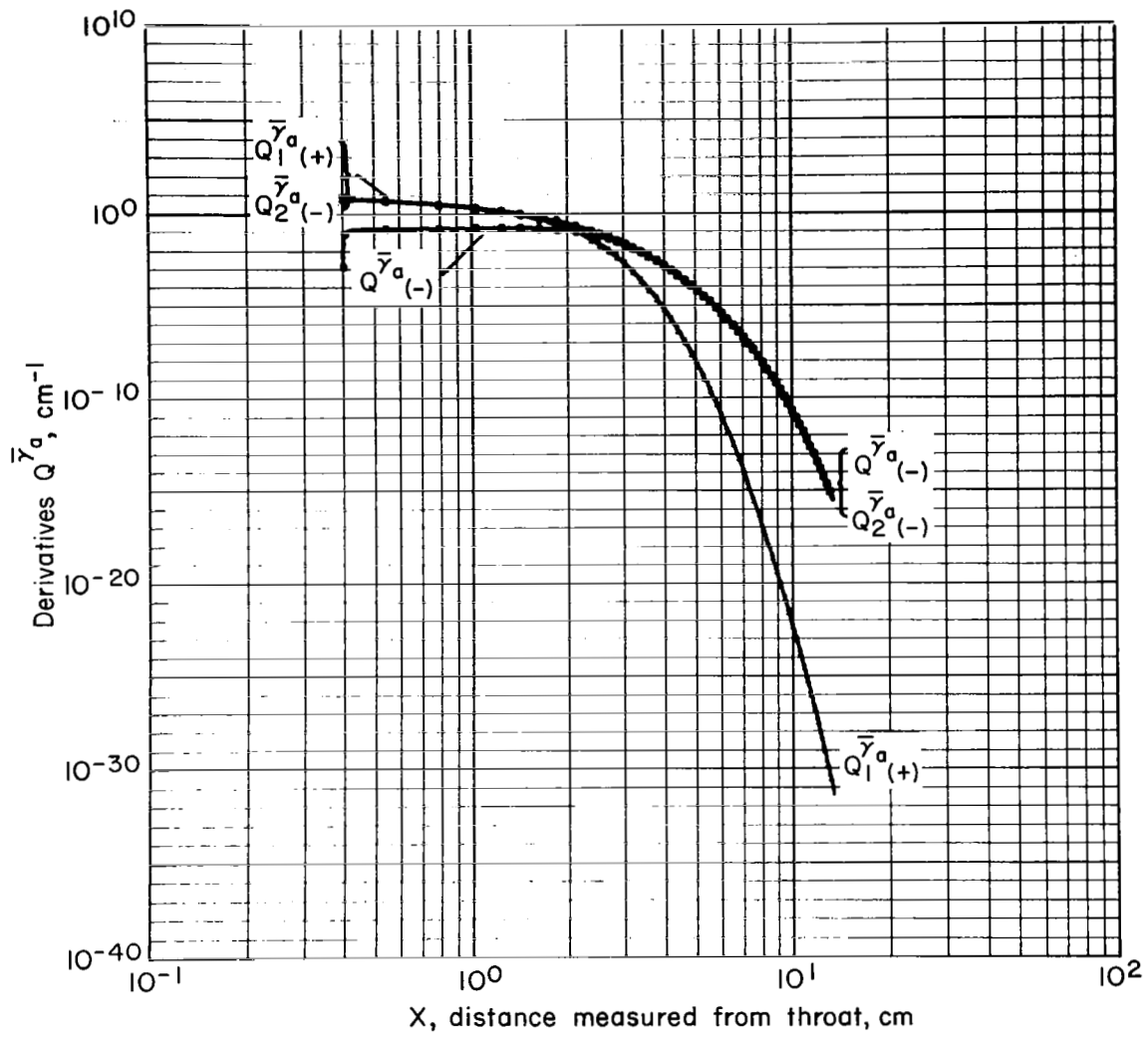
(g) Vibrational coupling factor

Figure IV-9 Continued



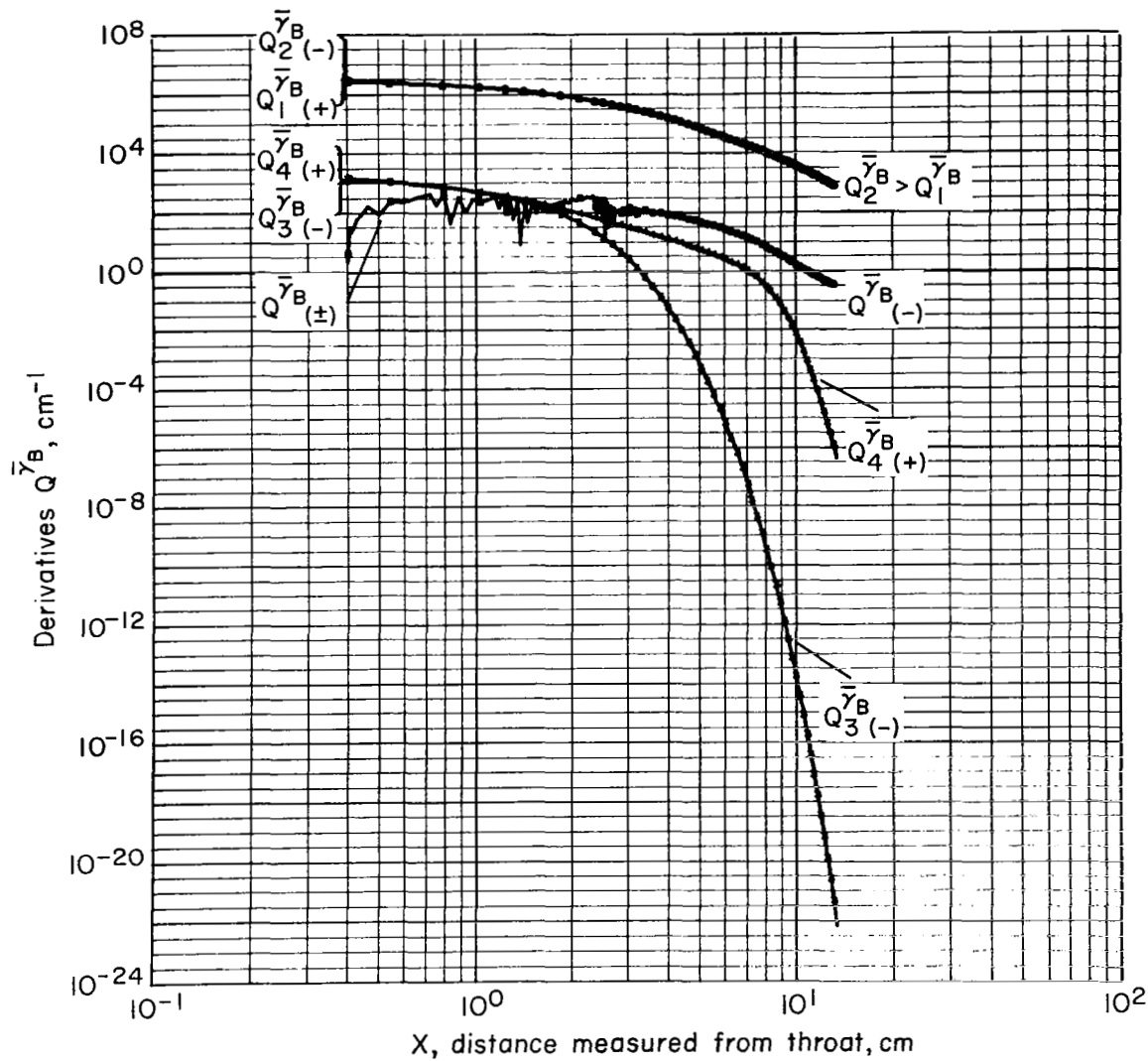
(h) Derivative, \bar{Q}_A , and component terms. \bar{Q}_i^A

Figure IV-9 Continued



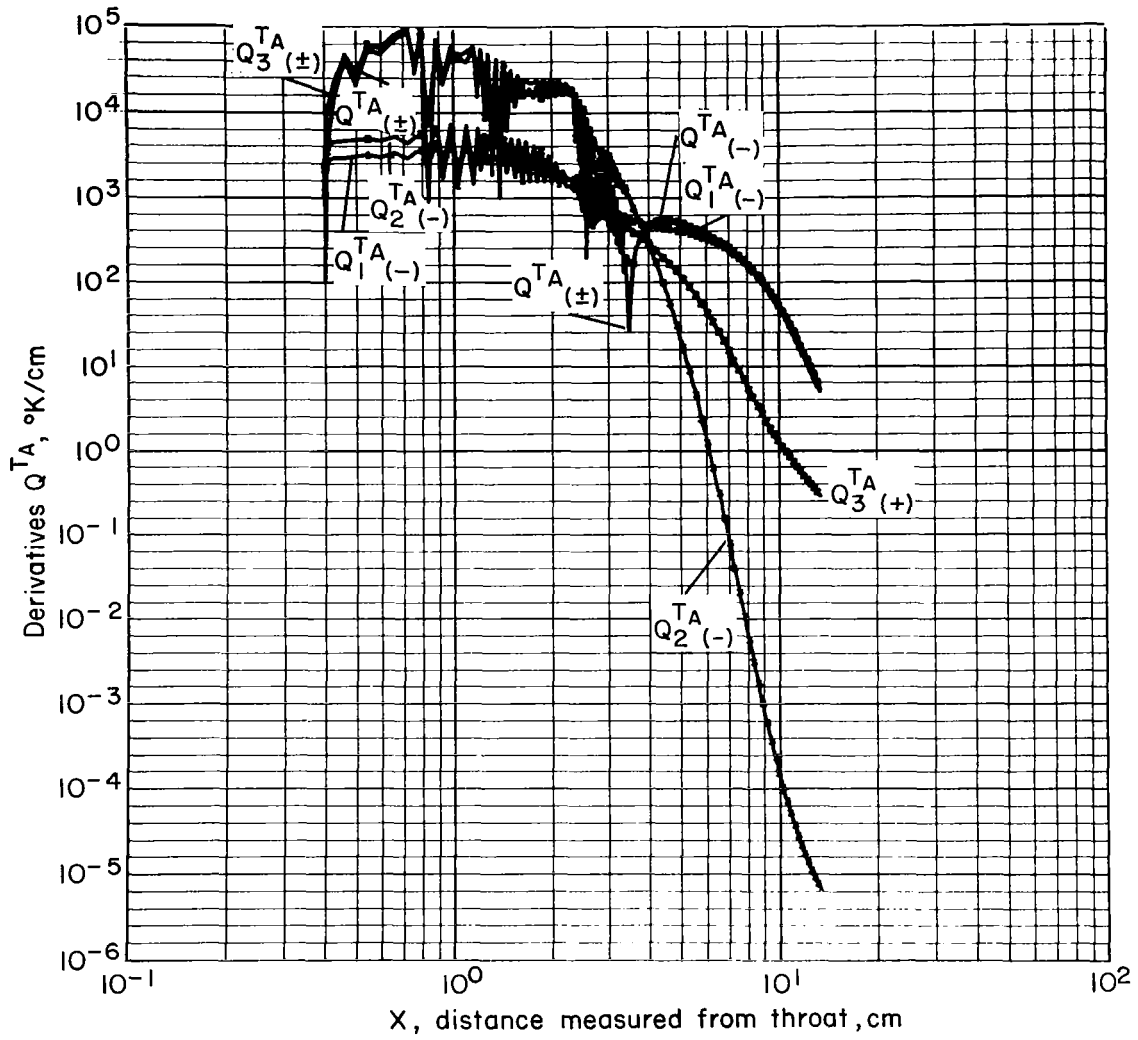
(i) Derivative, $\bar{Q}^{\bar{y}_a}$, and component terms, $Q_i^{\bar{y}_a}$

Figure IV-9 Continued



(j) Derivative, $Q \bar{y}_B$, and component terms, $Q_i \bar{y}_B$

Figure IV-9 Continued



(k) Derivative, Q^{TA} , and component terms, Q_i^{TA}

Figure IV-9 Continued

the temperature and density of the flow decrease the derivative decreases, and at distances downstream of the throat greater than about 3 centimeters, the derivative is so small that no further effect is observed for the value of the variable γ_A . This quantity is then said to be frozen.

In figure IV-9i are shown the derivative and component terms for the derivative $Q^{\bar{\gamma}_A}$. Here we observe that the behavior near the throat is similar in that the gain and loss terms are nearly equal, yielding smaller net values for the derivative. The derivative $Q^{\bar{\gamma}_A}$ is negative, indicating that atom recombination is occurring. This behavior continues downstream for about 2 centimeters, after which the gain term $Q_1^{\bar{\gamma}_A}$ rapidly decreases in value. Atom freezing occurs near the point where the value of $Q^{\bar{\gamma}_A}$ is approximately the same as that of its term $Q_1^{\bar{\gamma}_A}$. The chemical "sudden-freeze" behavior, discussed by Bray (14, 17) and resulting in his sudden-freeze approximation (14), is clearly evident here. The sudden-freeze, as normally applied, occurs where the dissociation term and the derivative have about the same values.

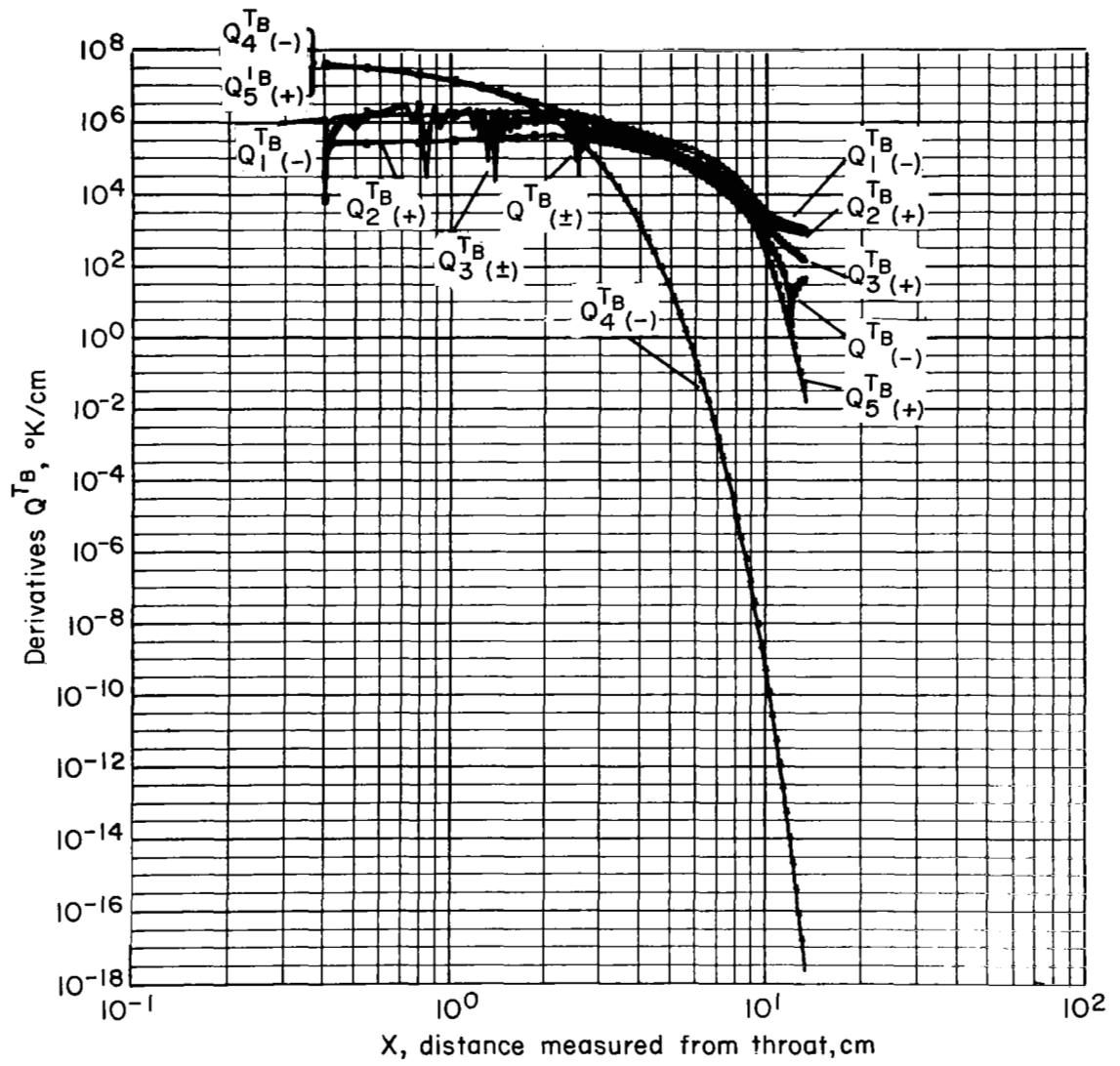
In figure IV-9j are exhibited the terms for the derivative $Q^{\bar{\gamma}_B}$. Because the net effects of the processes near the throat are the result of the small differences between the terms $Q_1^{\bar{\gamma}_B}$ and $Q_2^{\bar{\gamma}_B}$, and $Q_3^{\bar{\gamma}_B}$ and $Q_4^{\bar{\gamma}_B}$, it is difficult to separate the dominant processes. One can only infer that all of the terms are important. At distances greater than about 3 centimeters the dissociation and recombination terms $Q_3^{\bar{\gamma}_B}$ and $Q_4^{\bar{\gamma}_B}$, respectively, are small; and the continued decrease observed for the value of γ_B (see fig. IV-9b) is due to the transitions $\gamma_B \rightarrow \gamma_A$.

Figure IV-9k shows the behavior of the component terms for the vibrational-temperature derivative Q^{T_A} . The derivative oscillates erratically for this case, having both positive and negative values. The value at the peaks is about 10^5 °K/cm, while T_A itself varies between 4,000° and 6,000° K. This general behavior also occurred in the normal-shock problem (see fig. IV-1i), and for that case the comment was made that the upper states were in local thermodynamic equilibrium. The upper-state temperature derivative Q^{T_B} and its

component terms are displayed in figure IV-91 and we observe that oscillatory behavior is again evident. In the present nozzle problem both the upper and lower vibrational energy states are in local thermodynamic equilibrium, consequently, T_A and T_B are equal to the kinetic temperature T (fig. IV-9a). When the variable T_A freezes, at about 10 centimeters downstream of the throat, the associated derivative is small.

Turning to the component terms in the derivative, we observe that the term $Q_3^T A$, which represents energy addition to the lower states, is large. The vibrational relaxation terms $Q_1^T A$ and $Q_2^T A$, however, although appearing to be of smaller magnitude, also have a large effect on the relaxation processes. It is also interesting to note that when T_A becomes constant, the terms $Q_2^T A$ and $Q_3^T A$ are small relatively to the term $Q_1^T A$. We may conclude that the effect of anharmonicity is small when the dominant vibrational mode freezes, and the vibrational model yields results that are nearly the same as would be given by Landau-Teller theory. This point will be discussed further when the characteristic vibrational relaxation time associated with nozzle flows is introduced.

For the upper states we observe that although the dissociation term $Q_4^T B$ and the atom-recombination term $Q_3^T B$ are large relative to the derivative $Q^T B$, their net effect is small. The term $Q_1^T B$, representing vibrational relaxation in the upper states, is the dominant term as a result of the very small time scale associated with this equation (the associated equation is considered as being in local thermodynamic equilibrium). The "rate-limiting" term, $Q_2^T B$, appears to have only a small effect near the throat region, but it is very important after the lower-state temperature freezing occurs (about 7 cm downstream of the throat). On the basis of the calculation the significance of this term is difficult to assess. This term results from having different temperatures for the lower and upper groupings of energy states (see Chapter II); it may be related to the similar rate-limiting terms discussed by Pritchard and Bray (14, 71).



(l) Derivative, Q^{TB} , and component terms, Q_i^{TB}

Figure IV-9 Continued

This example of nozzle flow has been introduced to illustrate the behavior of the model equations for other than shock-wave flow. One important aspect of these solutions is that the upper vibrational energy states continue to relax even though atom recombination no longer occurs. If vibrational relaxation is governed by a single term analogous to that of Landau-Teller theory (e.g., as given in the Marrone-Treanor model (58)) a different effect is observed: All the energy states freeze simultaneously. Bray (14) commented that a study of the complete set of vibration-dissociation population equations (master equations) in which harmonic-oscillator transition quantities are used for the rate relations, will yield the same result; that is, the vibrational-population distribution can be represented as a continuous sequence of Boltzmann distributions described by a single vibrational temperature, and the freezing of all the energy-level populations occurs simultaneously. In his study (14) in which he allowed for multiple-level transitions for dissociations that occur above some upper vibrational energy level that he calls "rate-limiting," Bray obtained different behavior. The rate-limiting level or "bottle neck" freezes first, and subsequent vibrational relaxation is thereby prevented. For this case he commented that appreciable energy may be frozen in the upper vibrational energy levels. This effect was not observed for the solution presented here. In this case the upper vibrational energy states continue to relax even after the freezing of the lower energy states.

The reader will recall that in the previous section where the shock-wave flow was discussed, it was commented that the value used for the separation level b for the shock-wave solutions was probably too large. Reducing b might yield results analogous to the "bottle-neck" effect discussed by Bray. This speculation is based on the fact that the relative value of the rate limiting term $Q_2^T B$ is quite large for the case studied, particularly in the latter stages of the flow. As mentioned in the previous section, however, additional modification of the model equations may also be warranted in that more segments may be required for an approximation of the rate-of-quantum-transfer quantity introduced in Appendix B. It is not yet clear whether the bottle-neck effect will occur when the additional refinements are made.

(IV-C-2). Estimate of the Characteristic Vibrational Relaxation Time
Applicable for Nozzle Flows

One can estimate a characteristic vibrational relaxation time associated with the model equations for flows in which the upstream conditions are near local equilibrium. The procedure for obtaining this relaxation parameter is analogous to that described by Vincenti and Kruger (p. 236 in (97)). The study depends on the results given in the previous section in that we observed that the vibrational temperatures are equal to the kinetic temperature throughout the greater portion of the flow and, once freezing begins, it takes place quite rapidly. This effect allows us to answer in a very simple manner the question as to what effect anharmonicity has on the process of vibrational freezing.

We shall not include the dissociation and recombination terms in our investigation, since the effects being considered are largely independent of these processes. We base our investigation on equation (II-103a) of Chapter II and seek the characteristic vibrational relaxation time associated with this equation. Rewriting the equation, ignoring the last two terms, we have

$$\begin{aligned} \frac{dn\hat{q}(T_V)}{dt} = \frac{n}{Q_V(T_V)} & \left\{ \frac{Q_{A_1}(T_V)}{\tau_{A_1}} \hat{\Omega}_{A_1}(T, T_V) + \frac{Q_{A_2}(T_V)}{\tau_B} \hat{\Omega}_{A_2}(T, T_V) \left[1 - \frac{\hat{\Delta}(T)}{\hat{q}_{A_2}(T_V)} \right] \right. \\ & \left. + \frac{Q_B(T_V)}{\tau_B} \hat{\Omega}_B(T, T_V) \left[1 - \frac{\hat{\Delta}(T)}{\hat{q}_B(T_V)} \right] \right\} \end{aligned} \quad (IV-10)$$

We recall that the $\hat{\Omega}_i$ quantities measure the departure of the respective grouping of vibrational energy states from local equilibrium and are defined according to the relation

$$\hat{\Omega}_i(T, T_V) = \left[\hat{q}_i^\infty(T) - \hat{q}_i^\infty(T_V) \right] \mathcal{L}_i(T_V) \quad (IV-11)$$

Since we are concerned with only small departures from equilibrium, $q_i^\infty(T_V)$ may be expanded about the local value of the temperature T . We thus obtain the relation

$$\hat{\Omega}_i(T, T_V) = -\hat{C}_{V_i}^\infty(T) \Delta T \mathcal{L}_i(T_V) \quad (\text{IV-12})$$

where

$$T_V = T - \Delta T$$

and $\hat{C}_{V_i}^\infty(T) = d\hat{q}_i^\infty(T)/dT$ is the vibrational specific heat associated with an harmonic oscillator molecule having an infinite number of vibrational energy levels. (For a description of the notation the reader may refer to Chapter II or Appendix A.) The essential point is that for the flows having kinetic temperatures that are large compared with the vibrational temperature Θ_i associated with the level spacings, the above quantity is approximated by $k \Delta T \mathcal{L}_i(T_V)$ where k is Boltzmann's constant. In this relation the dependence on i is only through the truncation factor $\mathcal{L}_i(T_V)$. Equation (IV-10) may then be written

$$\begin{aligned} \frac{d(nT_V)}{dt} = \frac{n(T-T_V)}{\tau_{A_1}} & \left\{ \frac{Q_{A_1}(T_V)}{Q(T_V)} \mathcal{L}_{A_1}(T_V) + \frac{Q_{A_2}(T_V)}{Q(T_V)} \mathcal{L}_{A_2}(T_V) \frac{\tau_{A_1}}{\tau_B} \left[1 - \frac{\Delta(T)}{\hat{q}_{A_2}(T_V)} \right] \right. \\ & \left. + \frac{Q_B(T_V)}{Q(T_V)} \mathcal{L}_B(T_V) \frac{\tau_{A_1}}{\tau_B} \left[1 - \frac{\hat{\Delta}(T)}{\hat{q}_B(T_V)} \right] \right\} \quad (\text{IV-13}) \end{aligned}$$

When equation (IV-10) is displayed in this form, the characteristic vibrational relaxation time, denoted by τ_V , is readily recognized. We have

$$\frac{1}{\tau_V} = \frac{1}{\tau_{A_1}} \left\{ \frac{Q_{A_1}(T)}{Q_V(T)} \mathcal{L}_{A_1}(T) + \frac{Q_{A_2}(T)}{Q_V(T)} \mathcal{L}_{A_2}(T) \frac{\tau_{A_1}}{\tau_B} \left[1 - \frac{\hat{\Delta}(T)}{\hat{q}_{A_2}(T)} \right] \right. \\ \left. + \frac{Q_B(T)}{Q_V(T)} \mathcal{L}_B(T) \frac{\tau_{A_1}}{\tau_B} \left[1 - \frac{\hat{\Delta}(T)}{\hat{q}_B(T)} \right] \right\} \quad (\text{IV-14})$$

The effect of anharmonicity insofar as the model equations are concerned may be easily inferred from this relation. Landau-Teller theory yields the vibrational relaxation time τ_{A_1} . A study of the quantity in braces (equivalent to a study of the ratio τ_{A_1}/τ_V) thus allows one to examine the effect of anharmonicity in causing deviations from Landau-Teller theory. Such deviations have been experimentally observed (see, e.g., 43, 44, 45, 78, 79, 98).

In figure IV-10 are plotted the ratio τ_{A_1}/τ_V and the contribution of each of the three separate terms to this ratio. The ratio is functionally dependent on the separation parameters a and b , and on the temperature-dependent parameter $\chi(T)$ (see list of equations at the end of Appendix B). The quantity $\hat{\Delta}(T)$ and the ratio τ_{A_1}/τ_B are directly dependent on this parameter. The values of these quantities for the curves plotted are 9, 16, and $\chi = \chi_F$, respectively. One observes that anharmonicity causes a reduction by a factor of between 1/3 and 1/4 of the characteristic vibrational time τ_V as compared with the time obtained from Landau-Teller. This reduction (maximum curve value) occurs at relatively large vibrational temperatures, that is, at $T_V \approx 8,000^\circ \text{K}$ (or $T_V/\Theta_{A_1} \approx 3.6$ where $\Theta_{A_1} = 2234$). At the lower temperatures, $T_V \sim \Theta_{A_1}$, the model yields results equivalent to Landau-Teller theory (8,49).

An investigation of the various terms illustrates the effect of the contributions of the various groupings of energy states on the net effect of anharmonicity. The first term is associated with the lowest grouping of vibrational energy states, A_1 ; the second term is for the states, denoted A_2 , that are midway up in energy; and the last term is the contribution associated with the uppermost grouping of vibrational states, denoted B . A close investigation of the various terms shows that the population factors $Q_i(T)/Q_V(T)$ have an important

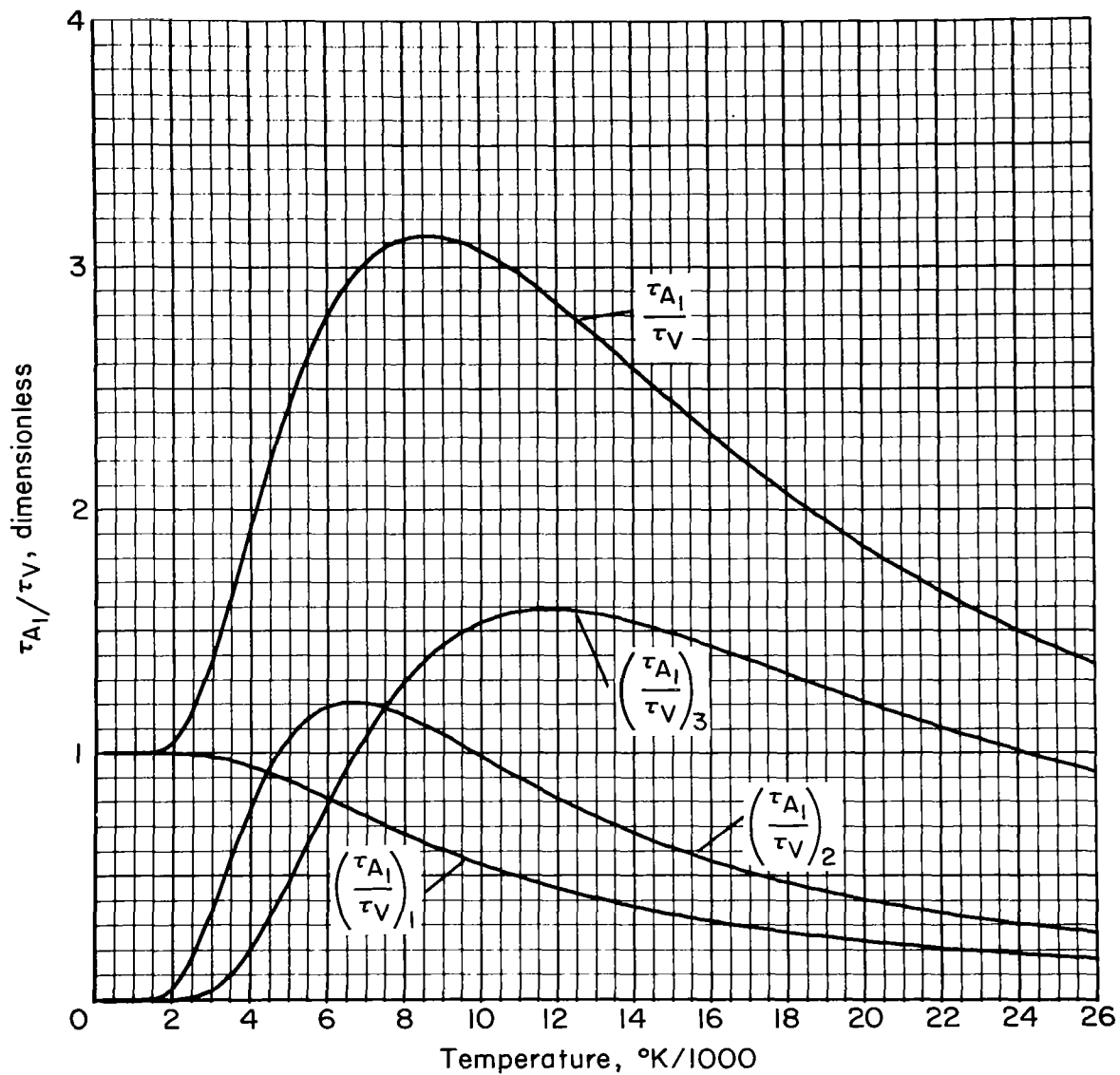


Figure IV-10. Anharmonicity effects from model equations compared with Landau-Teller theory; characteristic vibrational relaxation time

influence on the magnitude of the contributions. Although this is not explicitly shown, it turns out that changing the value of b changes the relative magnitude of $(\tau_{A_1}/\tau_V)_2$ and $(\tau_A/\tau_V)_3$ but has no effect on their sum. Increasing the value of the anharmonicity parameter χ (see Appendix B), however, increases the net effect of anharmonicity, and, accordingly, reducing χ reduces this effect. Also, it may be shown that setting $\chi = 1$ results in a ratio τ_{A_1}/τ_V of unity, indicating that the model is equivalent to Landau-Teller theory in this case. Reducing the value of the parameter a has the effect of making the parameter χ effective over a greater number of vibrational energy states (see Appendix B) and thus increases the net effect of anharmonicity. On the whole, the effects of anharmonicity are only crudely approximated by the model equations, a point that is best exemplified by figures B-4 and B-5 of Appendix B. Introducing additional segments for an approximation of the "rate-of-quantum-transfer" relation would yield more accurate relations for the ratio τ_{A_1}/τ_V . If as many segments are introduced as there are energy levels, in principle a precise value for the quantity τ_{A_1}/τ_V could be obtained. (Such an approach may not be justified, since the values of the transition rates $k_{i,i\pm 1}$ that would appear in the equation are still not certain.) It is expected, however, that with the values of $k_{i,i\pm 1}$ used in this paper more accurate computation of τ_{A_1}/τ_V will not yield results that are greatly different from those reported here.

CHAPTER V

RÉSUMÉ

With the master equations as a basis, a simplified mathematical model has been derived that is useful for studying the effects of vibration-dissociation coupling in fluid flows. The effects of changing the values of the various parameters contained within the equations has been investigated. Results have been given for the quasi-steady zone behind a normal shock wave, for the structure of the complete shock-wave profile, and for the flow in a nozzle. It has been shown that the equations contain the minimum structure required to obtain agreement with existing experimental data. As more refined experimental measurements become available, additional complication of the model rate equations may be necessary. The formalism is sufficiently general that modifications can readily be accomplished.

The most important results of this study are the recognition of the necessary modifications required to Landau-Teller theory to account for

- (1) The finite number of vibrational energy levels,
- (2) Molecular anharmonicity as regards both the energy-level spacing and the collisional transition rates,
- (3) Non-Boltzmann population distributions.

To take account of (1) the Landau-Teller equation was modified by the addition of a "truncation factor." In regard to (2), the "collisional rate of quantum transfer" was approximated by linear functions. The results yield more rapid vibrational relaxation of the upper energy states and closer energy-level separation in these states. To approximate (3) the distribution of energy was represented in terms of two vibrational temperatures, one for the lower energy states and one for the upper states.

The thermodynamic quantities that result (partition functions, energy, and specific heat) accurately approximate the equivalent quantities computed on the basis of spectroscopically determined data. The temperature dependence of the

pre-exponential factor in the effective dissociation rate is accurately represented. The assignment of values to the parameters in the model equations to effect agreement with experimental values of the induction time behind a normal shock wave is by trial and error. This process was not carried to completion and as a result values of the induction time too large by a factor of 10 were computed with the preliminary choice of parameters. The procedure for the required readjustment of the parameters has been discussed. The present results show qualitative agreement of the characteristic vibrational relaxation time associated with nozzle flows (expanding flow) in that this time is about a factor of 1/4 of that given by Landau-Teller theory. The equations reduce to the form of Landau-Teller theory when the temperatures are not too large.

Although further adjustments of the parameters are indicated, the present study shows that agreement with available experimental data can be achieved with a single assignment of values for the embedded parameters. These parameters (a , $b(T_U)$ and λ) depend only on the choice of species in a mixture. This is in contrast to simpler models where different values were required for the parameters in order to effect agreement with different experimental results.

The fact that the model equations can readily be solved in conjunction with the equations of flow has been demonstrated. The numerical integration procedure that was used is also discussed.

APPENDIX A
THERMODYNAMIC QUANTITIES

The thermodynamic quantities (partition functions, internal energies, specific heats, etc.) that are used to obtain the solutions described in the text are given in this section. Of these functions, those that pertain to the internal energy modes — translation, rotation, and electronic excitation — are listed for the reader's convenience with little comment. These functions are commonly used, and if supplementary information is desired, the reader can refer to other references (see, e.g., 9, 59, 97). The functions relating to the vibrational energy mode, however, are discussed more extensively, because of their bearing on the vibrational model that is the subject of this thesis, and because they are not commonly used.

(A-1). General Relations

In the list of relations that follow, the subscripts T , R , E , and V refer, respectively, to the translational, rotational, electronic, and vibrational parts of the indicated quantities. To abbreviate notation the integers 1, 2, 3, and 4, respectively, may be used in place of the above subscripts. The subscript j denotes the species for which the quantity is defined. The symbols appearing in the various relations are defined in the list of symbols. In the case of the relations referring to the vibrational mode, the additional subscripts A_1 , A_2 , and B indicate groupings of vibrational energy states to which the molecule belongs. In the list that follows the quantities are separated according to their type, the "complete" quantity of each type is listed first and the component parts are listed thereafter.

Partition Functions

$$Q_j = \prod_i Q_{i,j} \quad (\text{A1a})$$

$$\begin{aligned} Q_{T,j} &= V \tilde{Q}_{T,j} \\ &= V \left(\frac{m_j k T}{2 \pi \hbar^2} \right)^{\frac{3}{2}} \end{aligned} \quad (\text{A1b})$$

$$Q_{R,j} = \left(\frac{T}{\Theta_{R,j}} \right)^{a_j - 1} \quad (\text{A1c})$$

$$Q_{E\ell,j} = \sum_{\ell} g_{E\ell,\ell,j} \exp \left(- \frac{\Theta_{E\ell,\ell,j}}{T} \right) \quad (\text{A1d})$$

$$Q_{V,j} = Q_{A_1,j}(T) + Q_{A_2,j}(T) + Q_{B,j}(T) \quad (\text{A1e})$$

(The last equation applies in the case of vibrational equilibrium only; see eqs. (A14) for a description of the formulas.)

Internal Energies

$$e_j = \sum_i e_{i,j} \quad (\text{A2a})$$

$$= R_0 T^2 \frac{\partial \ln Q_j}{\partial T} \quad (\text{A2b})$$

$$e_{T,j} = \frac{3}{2} R_0 T \quad (\text{A2c})$$

$$e_{R,j} = R_0 T (a_j - 1) \quad (\text{A2d})$$

$$e_{E\ell,j} = R_0 \sum_{\ell} \frac{g_{E\ell,\ell,j}}{Q_{E\ell,j}} \Theta_{E\ell,\ell,j} \exp \left(- \frac{\Theta_{E\ell,\ell,j}}{T} \right) \quad (\text{A2e})$$

$$e_{V,j} = \left[Q_{A_1,j}(T) q_{A_1,j}(T) + Q_{A_2,j} q_{A_2,j}(T) + Q_{B,j}(T) q_{B,j}(T) \right] / Q_{V,j}(T) \quad (\text{A2f})$$

(The last equation applies in the case of vibrational equilibrium only; see eqs. (A30), (A38), and (A39) for a description of the formulas.)

Enthalpy

$$h_j = e_j + R_o T + h_j^o \quad (A3)$$

Specific Heats at Constant Volume

$$(c_v)_j = \left(\frac{\partial e_j}{\partial T} \right)_V \quad (A4a)$$

$$= \sum_i (c_v)_{i,j} \quad (A4b)$$

$$(c_v)_{T,j} = \frac{3}{2} R_o \quad (A4c)$$

$$(c_v)_{R,j} = R_o(a_j - 1) \quad (A4d)$$

$$(c_v)_{E\ell,j} = R_o \left[\sum_{\ell} \frac{g_{E\ell,\ell,j}}{Q_{E\ell,j}} \left(\frac{\Theta_{E\ell,\ell,j}}{T} \right)^2 \exp \left(- \frac{\Theta_{E\ell,\ell,j}}{T} \right) - \left(\frac{e_{E\ell,j}}{R_o T} \right)^2 \right] \quad (A4e)$$

$$(c_v)_{V,j} = \frac{R_o}{Q_{V,j}} \left\{ Q_{A_1} \left[\frac{(c_v)_{A_1,j}}{R_o} + \left(\frac{q_{A_1,j}}{R_o T} \right)^2 \right] + Q_{A_2} \left[\frac{(c_v)_{A_2,j}}{R_o} + \left(\frac{q_{A_2,j}}{R_o T} \right)^2 \right] \right. \\ \left. + Q_B \left[\frac{(c_v)_{B,j}}{R_o} + \left(\frac{q_{B,j}}{R_o T} \right)^2 \right] - \left(\frac{q_{V,j}}{R_o T} \right)^2 \right\} \quad (A4f)$$

(The last equation applies in the case of vibrational equilibrium only; see last section for description of the formulas.)

Specific Heats at Constant Pressure

$$(c_p)_j = \left(\frac{\partial h_j}{\partial T} \right)_p \quad (A5a)$$

$$= (c_v)_j + R_o \quad (A5b)$$

Temperature Derivative of the Specific Heats

(Note: Asterisk denotes that vibrational contribution is excluded)

$$\frac{d}{dT}(c_p)_j^* = \frac{d}{dT}(c_v)_j^* = \sum_{i=1}^3 \frac{d}{dT}(c_v)_{i,j} \quad (\text{A6a})$$

$$\frac{d}{dT}(c_v)_{T,j} = 0 \quad (\text{A6b})$$

$$\frac{d}{dT}(c_v)_{R,j} = 0 \quad (\text{A6c})$$

$$\begin{aligned} \frac{d}{dT}(c_v)_{E\ell,j} = \frac{R_o}{T} \left\{ -\frac{2(c_v)_{E\ell,j}}{R_o} + \sum_{\ell} \frac{g_{E\ell,\ell,j}}{Q_{E\ell,j}} \left(\frac{\Theta_{E\ell,\ell,j}}{T} \right)^3 \exp\left(-\frac{\Theta_{E\ell,\ell,j}}{T}\right) \right. \\ \left. - \frac{e_{E\ell,\ell,j}}{R_o T} \left[\frac{3(c_v)_{E\ell,j}}{R_o} + \left(\frac{e_{E,\ell,j}}{R_o T} \right)^2 \right] \right\} \quad (\text{A6d}) \end{aligned}$$

Entropy Function

The contribution of each internal energy mode to the entropy can also be defined. Such relations, however, are not useful in this paper and will not be given here. The entropy associated with a specific species, say j , will be used and is

$$\frac{S_j}{R_o} = \ln\left(\frac{\tilde{Q}_j}{N_o}\right) + 1 + \frac{e_j}{R_o T} - \ln\left(\frac{p_j}{R_o T}\right) \quad (\text{A7})$$

where the quantity \tilde{Q}_j denotes that the volume V (see eq. (A1b)) is omitted from the translational partition function prior to the formation of the product denoted by equation (A1a). The variable p_j denotes the partial pressure associated with the species j ($p_j = m_j kT$).

Equilibrium Constant

A general form for a chemical equation (see, e.g., 97) is

$$\sum_j \nu_{ij} M_j = \sum_j \nu'_{ij} M_j \quad i = 1, \dots, R \quad (\text{A8a})$$

where the ν_{ij} and ν'_{ij} are the stoichiometric coefficients associated with the reactants and products, respectively, and M_j (chemical symbol) denotes the j th species. In terms of this notation the equilibrium constant $\kappa_i(T)$, associated with the i th reaction, is:

$$\kappa_i(T) = \prod_j \left(\frac{Q_j}{N_o V} \right)^{\beta_{ij}} \exp \left(- \sum_j \frac{\beta_{ij} h_j^o}{R_o T} \right) \quad (A8b)$$

$$= \prod_j \left(\frac{\tilde{Q}_j}{N_o} \right)^{\beta_{ij}} \exp \left(- \sum_j \frac{\beta_{ij} h_j^o}{R_o T} \right) \quad (A8c)$$

where

$$\beta_{ij} = \nu'_{ij} - \nu_{ij} \quad (A8d)$$

and h_j^o is the heat of formation of the j th species.

(A-2). Derivation of the Relations for the Vibrational Mode

Early researchers (see, e.g., 8, 30, 36, 62) assumed that a molecule could be described as a harmonic oscillator with an infinite number of vibrational energy levels. Such a description is attractive because of the simple thermodynamic relations that result (see, e.g., 97). These relations are reasonably valid provided that the temperature T assigned to the vibrational mode (the subscript V on T denoting vibrational temperature is dropped in this section since it only complicates the notation) is very small compared with the characteristic dissociation temperature Θ_D ($\approx E_{N-1}/k$). At temperatures comparable to or higher than the characteristic dissociation temperature, such a description fails since the vibrational partition function and the vibrational energy increase with increasing temperature without limit. It follows, in particular, that at high temperatures the amount of energy contained in the vibrational mode exceeds the energy required for dissociation.

Later researchers (see, e.g., 32, 82, 90) remedied this problem by truncating the number of vibrational levels so that the energy of the uppermost level

and the dissociation energy were approximately equal. The thermodynamic relations that result for this "truncated harmonic oscillator" are also simple; however, the effect of truncating the number of vibrational energy levels is to over-compensate in the opposite sense at the higher temperatures (4, 58) in that the vibrational partition function and the energy function are too small.

In this section a vibrational model is developed that includes a representative number of vibrational energy levels and the effect of molecular anharmonicity, thus yielding more accurate values for the vibrational quantities. The model also retains some of the simplicity characteristic of the harmonic-oscillator models. The development evolves naturally from the approach taken in the text to study the effects of vibration-dissociation coupling (see Chapter II). The model still contains some of the shortcomings of other models (36, 58, 93) in that the effects of vibration-rotation coupling are not considered. The lack of reliable values of the rate parameters pertinent to rotation precluded the addition of rotation-vibration relaxation effects into the rate equations (see Appendix B); consequently, it is questionable whether it is of value to include these effects in the thermodynamic quantities. For an explanation of some of the effects of vibration-rotation coupling, the reader is referred to the papers by Bauer and Tsang (4) and Bauer (5).

The approach taken in developing the thermodynamic quantities for the vibrational energy mode is to assume that molecules can be split according to vibrational energy into two separate groups, a lower and an upper, in the same manner as described in Chapter II of the text. The separation level is denoted by a (see fig. A-1). The lower group of molecular energy states has relatively large energy spacing; in fact, it has the spacing commonly ascribed to the vibrational mode of harmonic-oscillator models (e.g., see 97). The upper group of energy levels has a reduced energy spacing. The number of vibrational energy levels is truncated so that the uppermost level has an energy corresponding to the dissociation limit. An additional separation b is introduced to make the thermodynamic quantities derived here identical with the quantities required in the text. As far as the derivations in this section are

concerned, this separation may be assumed at any arbitrary position within the upper group of vibrational levels. The set of energy levels in figure A-1 illustrates the placement of the levels for the model molecule. The levels are numbered consecutively starting with zero. The separation levels a and b are labeled, and the A₁, A₂, and B groupings of energy states are indicated at the left-hand margin. For a Morse oscillator the vibrational energy E_v for the *v*th level is given by references 9, 40.

$$(E_v)_M = \hbar \omega_0 v \left[1 - (x_0)_M v \right] \quad v = 0, 1, \dots, N_M$$

where

$$(x_0)_M = \frac{\hbar \omega_0}{4D_0}$$

$$N_M = 1/2 (x_0)_M \tag{A10a}$$

The best values for E_v, from spectroscopic data, are based on the relation

$$(E_v)_H = \hbar \left[\omega_0 v - \omega_0 (x_0)_H v^2 + \omega_0 (y_0)_H v^3 \right] \quad v = 0, 1, \dots, N_H \tag{A10b}$$

where the constants ω_0 , $\omega_0(x_0)_H$, and $\omega_0(y_0)_H$ are given, for example, by Herzberg (40), and N_H is defined as the largest integer such that E_{N_M} ≤ D₀. It is worthwhile to point out that the Morse-oscillator model is known to contain too many vibrational energy levels (see, e.g., 58), and the partition functions that result are therefore too large at the higher temperatures.

The value commonly assigned as the vibrational energy-level spacing for harmonic-oscillator models is E_{A₁}, defined by the relation[†]

$$E_{A_1} = (E_1)_H - (E_0)_H \approx \hbar \omega_0 \left[1 - (x_0)_M \right] \tag{A10c}$$

We will utilize this quantity as well as an additional level spacing E_{A₂}, the upper level spacing, defined analogously by

[†]The differences in E_{A₁}, depending on whether (x₀)_M or (x₀)_H is the anharmonicity coefficient used in equation (A10c), are insignificant for most practical purposes.

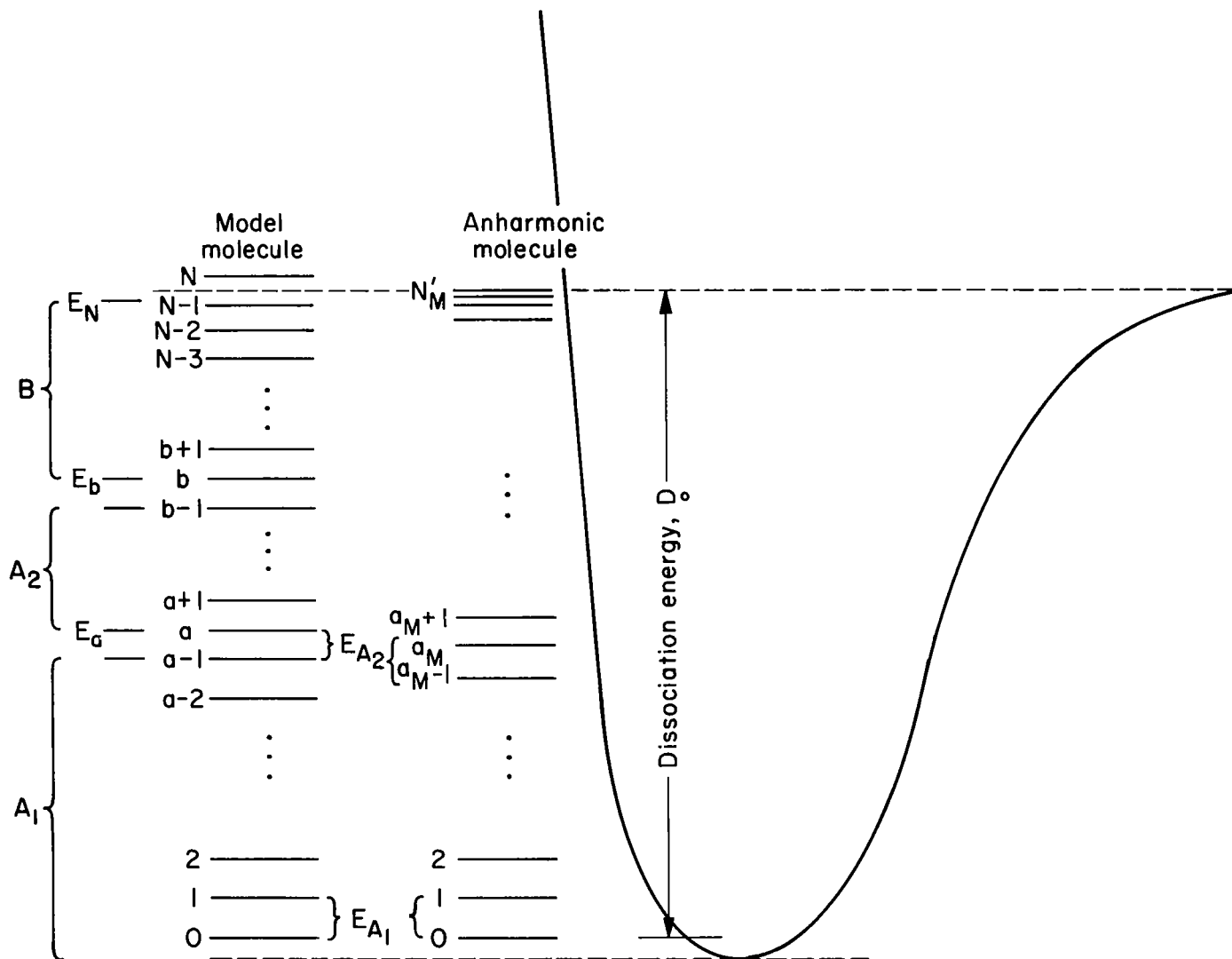


Figure A-1. Diagram showing relative placement of vibrational energy levels for model as compared to anharmonic-oscillator molecules

$$\begin{aligned}
E_{A_2} &= E_B = (E_a)_M - (E_{a-1})_M \\
&= \hbar\omega_0 \left[1 - 2a(x_0)_M \right]
\end{aligned} \tag{A10d}$$

Here it is important to use the Morse oscillator harmonic constant, $(x_0)_M$ that yields smaller energy-level spacing than would be obtained from $(x_0)_H$ in order to compensate partially for the fact that the levels are spaced even closer near the top of the potential well. Although this evaluation of E_{A_2} results in only a qualitatively correct level spacing, it will be shown later to lead to good agreement of the thermodynamic quantities as compared with those obtained from equation (A10b).

The energies at the separation levels are given by

$$E_a = (a - 1)E_{A_1} + E_{A_2} \tag{A11a}$$

$$E_b = E_a + (b - a)E_{A_2} \tag{A11b}$$

$$E_N = E_b + (N - b)E_{A_2} \tag{A11c}$$

where the constants a , b , and N are defined as the largest integers that satisfy the relations

$$a = \left[(E_a)_M - (E_{A_2} - E_{A_1}) \right] / E_{A_1} \tag{A11d}$$

$$b = a + \left[(E_b)_M - (E_a)_M \right] / E_{A_2} \tag{A11e}$$

$$N = b + \left[D_0 - (E_b)_M \right] / E_{A_2} \tag{A11f}$$

The quantities $(E_a)_M$, $(E_b)_M$, and D_0 are specified. In terms of these relations the energies for the various levels for the model are given by

$$E_v = E_{A_1} v \quad v \leq a - 1 \tag{A12a}$$

$$= E_a + E_{A_2}(v - a) \quad a \leq v \leq b - 1 \tag{A12b}$$

$$= E_b + E_{A_2}(v - b) \quad b \leq v \leq N - 1 \tag{A12c}$$

The important thing to observe is that the thermodynamic quantities for the vibrational degrees of freedom are defined in terms of three parameters, E_{A_1} , E_{A_2} (or E_a), and N (or D_0). The Morse oscillator contains two parameters, ω_0 and $(x_0)_M$ (or D_0), and the truncated harmonic oscillator also contains two parameters E_{A_1} and N_{HO} (or D_0). The constants ω_0 and E_{A_1} insure that the various models have proper low-temperature dependence, and the inclusion of D_0 , directly or indirectly, insures that the energy cutoff is accounted for. The model has one additional parameter, E_{A_2} (or E_a), that lies between the lowest and highest levels of the potential well and improves the behavior at intermediate temperatures.

(A-2a). Partial Vibrational Partition Functions

The partition functions corresponding to the various grouping of energy levels can be evaluated in terms of parameters defined previously. The partial partition function is defined by the sum

$$Q_i(T) = \sum_{v=\ell_{i_1}}^{\ell_{i_2}-1} \exp\left(-\frac{E_v}{kT}\right) \quad (A13)$$

where ℓ_{i_1} and ℓ_{i_2} are the appropriate bounds corresponding to the grouping of energy levels indicated by the subscript i . The subscript j , denoting a specific molecular species, is omitted from what follows to simplify the notation. Substituting the appropriate values for the energy E_v (eqs. (A12)) into the preceding equation, we obtain

$$\begin{aligned} Q_{A_1}(T) &= \sum_{v=0}^{a-1} \exp\left(-\frac{E_{A_1} v}{kT}\right) \\ &= \frac{1 - \exp\left(-\frac{a E_{A_1}}{kT}\right)}{1 - \exp\left(-\frac{E_{A_1}}{kT}\right)} \end{aligned} \quad (A14a)$$

$$\begin{aligned}
Q_{A_2} &= \exp\left(-\frac{E_a}{kT}\right) \sum_{v=a}^{b-1} \exp\left[-\frac{(v-a)E_{A_2}}{kT}\right] \\
&= \exp\left(-\frac{E_a}{kT}\right) Q'_{A_2}(T)
\end{aligned} \tag{A14b}$$

$$\begin{aligned}
Q_B(T) &= \exp\left(-\frac{E_b}{kT}\right) \sum_{v=b}^{N-1} \exp\left[-\frac{(v-b)E_{A_2}}{kT}\right] \\
&= \exp\left(-\frac{E_b}{kT}\right) Q'_B(T)
\end{aligned} \tag{A14c}$$

where the primed quantities are defined by

$$Q'_{A_2}(T) = \frac{1 - \exp\left[-\frac{(b-a)E_{A_2}}{kT}\right]}{1 - \exp\left(-\frac{E_{A_2}}{kT}\right)} \tag{A15}$$

$$Q'_B(T) = \frac{1 - \exp\left[-\frac{(N-b)E_{A_2}}{kT}\right]}{1 - \exp\left(-\frac{E_{A_2}}{kT}\right)} \tag{A16}$$

The primes attached to the thermodynamic quantities Q_{A_2} and Q_B denote that the relevant partition functions are evaluated relative to their separate zeroth states, E_a and E_b , respectively, and not to the molecular ground state E_0 .

The fractional population of molecules that have vibrational energy corresponding to some specific level within a grouping of levels (say, for example, the v th level within the B grouping of levels) is represented by

$$\frac{n_v}{n_B} = \frac{\exp\left(-\frac{E_v}{kT}\right)}{Q_B(T)} = \frac{\exp\left[-\frac{(v-b)E_{A_2}}{kT}\right]}{Q'_B(T)} \tag{A17}$$

$b \leq v \leq N-1$

Furthermore, given the total vibrational partition function

$$Q_v(T) = Q_{A_1}(T) + Q_{A_2}(T) + Q_B(T) \tag{A18}$$

we can obtain the fractional number of molecules in any group as a ratio of the partial partition function and the total partition function. For example, the number of molecules in the A_2 -grouping of states relative to the total number of molecules is given by

$$\frac{n_{A_2}}{n} = \frac{Q_{A_2}(T)}{Q_V(T)} \quad (\text{A19})$$

These ratios are important, for example, when the initial values for the numerical integration are required. It is necessary to point out that the latter ratio is valid only for vibrational equilibrium, while the former ratio (eq. (A17)) is always valid provided the appropriate vibrational temperature characteristic of the grouping of states (T_B for the example cited) is assigned.

In figure (A2) the molecular vibrational partition functions are compared for molecular oxygen, computed on the basis of four different models, plotted as a function of temperature. The curve labeled "Morse" was obtained from equation (A13) with values of E_V computed from equation (A10a). The curve labeled "Herzberg" was obtained in a similar manner, but with E_V computed from equation (A10b) and with values for the anharmonicity coefficients, x_0 and y_0 , obtained from reference 40. Equation (A1c) was used (with internal parameters having values $a = 9$, $b = 16$, $N = 32$, $\Theta_{A_1} = 2234$, and $\Theta_{A_2} = 1800$) and the plotted result is labeled "Model." The evaluation of equation (A14a) ($a = 26$ and $\Theta_{A_1} = 2234$) yields the curve labeled "Truncated Harmonic Oscillator."

The Morse oscillator contains too many energy levels which, furthermore, are spaced too close together near the top of the potential well. Consequently, its partition function is generally conceded (see, e.g., 58) to be too large. The truncated harmonic oscillator, having relatively large level spacing for the upper vibrational levels, has too few vibrational energy levels and a partition function that is therefore too small (see, e.g., 4). The model introduced in this paper is in reasonable agreement with the Herzberg result that excludes any effect of rotation (as used here). As pointed out earlier, it is perhaps unwarranted to come to any specific conclusion as to the validity of any one of the

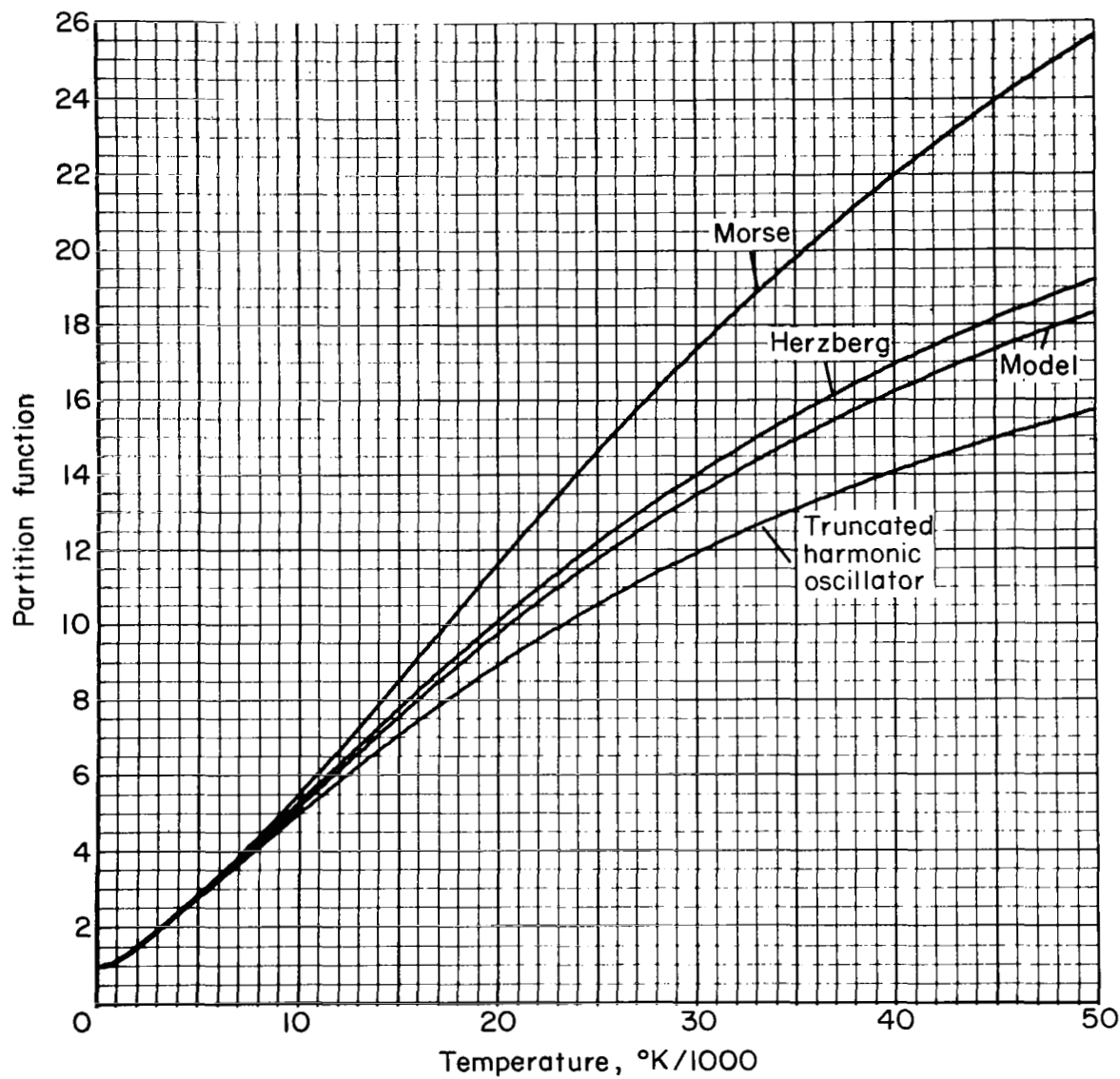


Figure A-2. Comparison of vibrational partition function computed using different models

models for flow calculations, since in all cases the effects of rotation have not been considered and these effects may be large, particularly at the higher temperatures (see, e.g., 4).

(A-2b). Partial Vibrational Energy Functions

The average vibrational energy associated with molecules in the i th grouping of energy states is defined by

$$\hat{q}_i(T) = \sum_{v=\ell_{i_1}}^{\ell_{i_2}-1} E_{v_i} \frac{n_v}{n_i} \quad (\text{A20})$$

The quantity $q_i(T)$ is readily related to the partition functions defined in the previous section by the following procedure. With the substitution of the appropriate ratio for n_v/n_i (e.g., see text preceding eq. (A17)), the preceding equation can be written

$$\begin{aligned} \hat{q}_i(T) &= \sum_{v=\ell_{i_1}}^{\ell_{i_2}-1} \frac{E_{v_i} \exp\left(-\frac{E_{v_i}}{kT}\right)}{Q_i(T)} \\ &= \frac{kT^2 \partial \ln Q_i(T)}{\partial T} \end{aligned} \quad (\text{A21})$$

The above definition is consistent with that normally encountered in statistical mechanics (e.g., see 73) and is convenient in practice since it gives the vibrational energy directly by differentiation of the partition function.

Substituting the expressions for the partition functions into the preceding equation yields

$$\hat{q}_{A_1}(T) = \frac{E_A \exp\left(-\frac{E_{A_1}}{kT}\right)}{1 - \exp\left(-\frac{E_{A_1}}{kT}\right)} - \frac{a E_{A_1} \exp\left(-\frac{a E_{A_1}}{kT}\right)}{1 - \exp\left(-\frac{a E_{A_1}}{kT}\right)} \quad (\text{A22})$$

$$\hat{q}_{A_2}(T) = E_a + \hat{q}'_{A_2}(T) \quad (\text{A23})$$

$$\hat{q}_B(T) = E_b + \hat{q}'_B(T) \quad (\text{A24})$$

where

$$\hat{q}'_{A_2}(T) = \frac{E_{A_2} \exp\left(-\frac{E_{A_2}}{kT}\right)}{1 - \exp\left(-\frac{E_{A_2}}{kT}\right)} - \frac{(b - a) E_{A_2} \exp\left[-\frac{(b - a) E_{A_2}}{kT}\right]}{1 - \exp\left[-\frac{(b - a) E_{A_2}}{kT}\right]} \quad (\text{A25})$$

$$\hat{q}'_B(T) = \frac{E_{A_2} \exp\left(-\frac{E_{A_2}}{kT}\right)}{1 - \exp\left(-\frac{E_{A_2}}{kT}\right)} - \frac{(N - b) E_{A_2} \exp\left[-\frac{(N - b) E_{A_2}}{kT}\right]}{1 - \exp\left[-\frac{(N - b) E_{A_2}}{kT}\right]} \quad (\text{A26})$$

These expressions can be modified to obtain an alternate form that is also useful. The first terms in equations (A22), (A25), and (A26) represent the expressions that one would obtain for an infinite harmonic oscillator (harmonic oscillator containing an infinite number of levels). The second terms are important only at the higher temperatures and, in effect, limit the values of the first terms. This may be shown in the following manner, with equation (A22) as an example. Dividing the right-hand side by the first term and retaining it as a factor, we obtain[†]

$$\hat{q}_{A_1}(T) = \frac{E_{A_1} \exp\left(-\frac{E_{A_1}}{kT}\right)}{1 - \exp\left(-\frac{E_{A_1}}{kT}\right)} \left\{ 1 - \exp\left[-\frac{(a - 1) E_{A_1}}{kT} - \ln\left(\frac{Q_{A_1}(T)}{a}\right)\right] \right\} \quad (\text{A27})$$

[†]All quantities defined in this and the next section contain factors having the functional form $1 - \exp(\alpha)$. This form is convenient for the accurate evaluation of the thermodynamic quantities. Because it is not possible to evaluate $1 - \exp(\alpha)$ accurately for all possible arguments on an electronic computer having only a finite number of significant digits, the following relation is used when the arguments are small ($\alpha < 10^{-3}$)

$$1 - \exp(\alpha) \approx -\alpha \left\{ 1 + \frac{\alpha}{2} \left[1 + \frac{\alpha}{3} \left(1 + \frac{\alpha}{4} \right) \right] \right\}$$

When the right-hand quantity is expanded, the equation is seen to be simply a truncated Taylor's-series expansion of the quantity on the left.

Because of their frequent occurrence in the text, it is worthwhile to assign symbols to the separate factors in this equation. We first define

$$\hat{q}_{A_1}^{\infty}(T) = \frac{E_{A_1} \exp\left(-\frac{E_{A_1}}{kT}\right)}{1 - \exp\left(-\frac{E_{A_1}}{kT}\right)} \quad (\text{A28})$$

As mentioned previously, this quantity is the vibrational energy of a harmonic oscillator containing an infinite number of equally spaced energy levels with a spacing E_{A_1} . The second factor in equation (A28) will be called the "truncation factor" for reasons that will be explained, and is symbolized as follows:

$$\mathcal{L}_{A_1}(T) = \left\{ 1 - \exp\left[-\frac{(a-1)E_{A_1}}{kT} - \ln\left(\frac{Q_{A_1}}{a}\right)\right] \right\} \quad (\text{A29})$$

In terms of these functions equation (A27) is then simply

$$\hat{q}_{A_1}(T) = \hat{q}_{A_1}^{\infty}(T) \mathcal{L}_{A_1}(T) \quad (\text{A30})$$

Before proceeding it is worthwhile to discuss the above functions. In figure A-3 dimensionless equivalents of these functions (with internal parameters having values $a = 9$ and $\Theta_{A_1} = 2234$ representative of molecular oxygen) are plotted as functions of temperature. Also indicated on the abscissa scale are the dimensionless units T/Θ_{A_1} . Dimensionless quantities are plotted so that all three of the quantities can be plotted conveniently on one graph. At low temperatures, $T \ll \Theta_{A_1}$, the infinite-harmonic-oscillator energy function increases nearly exponentially with temperature. At sufficiently high temperatures, $T \gg \Theta_{A_1}$, the function can be approximated by $\hat{q}_{A_1}^{\infty}(T) \approx kT$ (or $\hat{q}_{A_1}^{\infty}(T)/kT \approx 1$ as indicated in the figure). The function continues to increase without bound with increasing temperature. Because of this characteristic, nontruncated harmonic-oscillator models are limited in their usefulness to fluid flows that have relatively low temperatures, $T < a\Theta_{A_1}$.

As regards the truncation factor, at low temperatures this factor is unity (as indicated by the constant slope in the figure that is approximately Q_{A_1}/Θ_{a-1}) and remains nearly unity for all practical purposes until the second

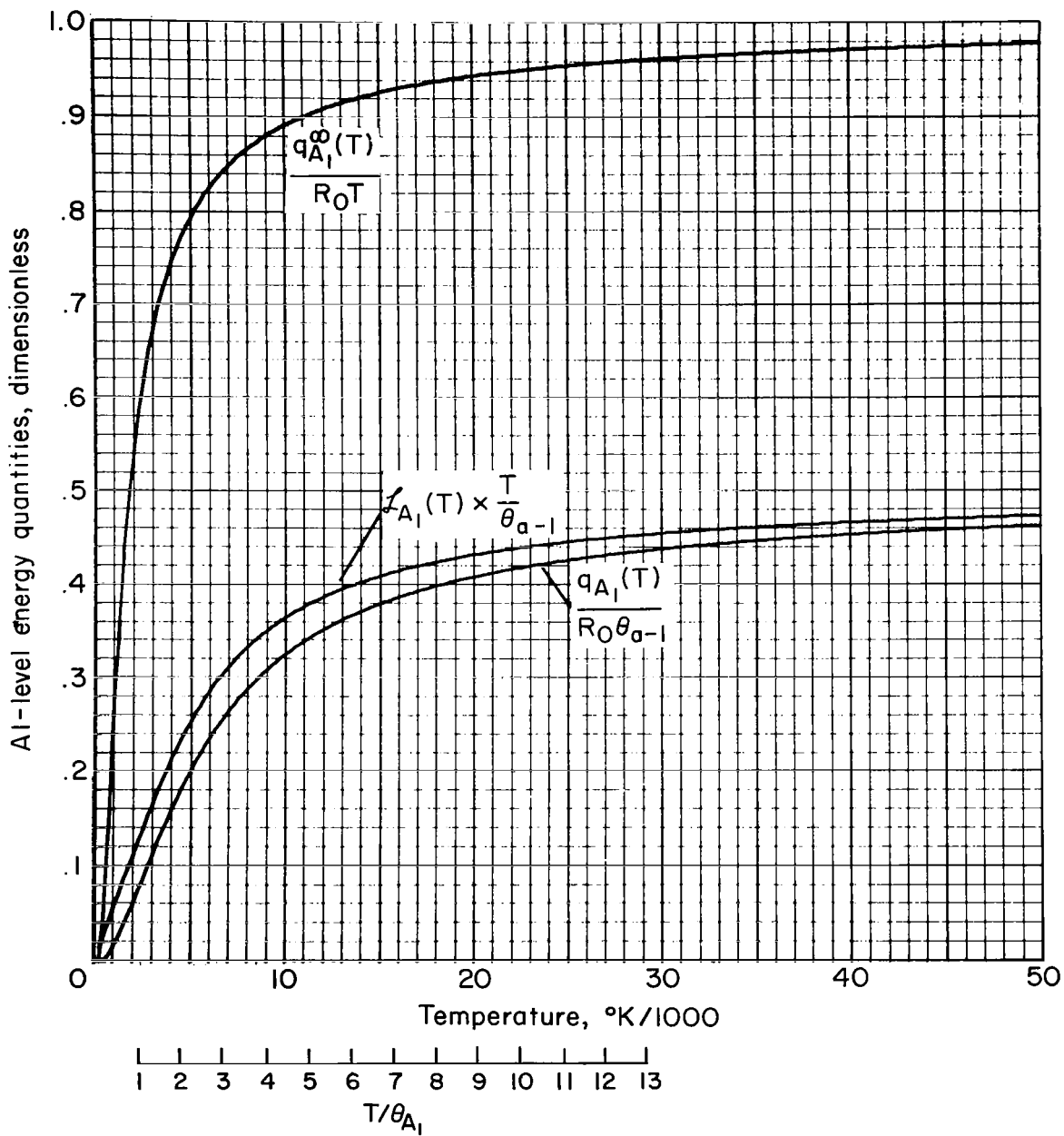


Figure A-3. Dimensionless plot of the component factors required for the model vibrational energy function

term becomes important, that is, when $T \sim (a - 1)\Theta_{A_1} = \Theta_{a-1}$ (the dimensionless quantity increases linearly in this region because of the factor T). At higher temperatures, $T > \Theta_{a-1}$, the truncation factor may be accurately approximated by $\Theta_{a-1}/2T$ (from the figure we observe that $\mathcal{L}_{A_1}(T)T/\Theta_{a-1} \sim \frac{1}{2}$). The maximum value of the product $\hat{q}_{A_1}(T) = \hat{q}_{A_1}^\infty(T) \mathcal{L}_{A_1}(T)$ at these extreme temperatures is given by $k\Theta_{a-1}/2$, a constant (this is implied in the figure as a result of the approximate value $\hat{q}_{A_1}(T)/k\Theta_{a-1} \sim \frac{1}{2}$).

One can obtain similar functions for each grouping of energy levels. There results

$$\mathcal{L}'_{A_2}(T) = 1 - \exp\left[-\frac{(b - a - 1)\Theta_{A_2}}{T} - \ln\left(\frac{Q'_{A_2}(T)}{b - a}\right)\right] \quad (\text{A31})$$

$$\mathcal{L}'_B(T) = 1 - \exp\left[-\frac{(N - b - 1)\Theta_{A_2}}{T} - \ln\left(\frac{Q'_B(T)}{N - b}\right)\right] \quad (\text{A32})$$

With the defining relations

$$\hat{q}_{A_2}^\infty(T) \equiv \frac{E_{A_2} \exp\left(-\frac{\Theta_{A_2}}{T}\right)}{1 - \exp\left(-\frac{\Theta_{A_2}}{T}\right)} \quad (\text{A33})$$

$$\hat{q}_B^\infty(T) \equiv \hat{q}_{A_2}^\infty(T) \quad (\text{A34})$$

the primed values of the vibrational-energy functions take the form

$$\hat{q}'_{A_2}(T) = \hat{q}_{A_2}^\infty(T) \mathcal{L}'_{A_2}(T) \quad (\text{A35})$$

$$\hat{q}'_B(T) = \hat{q}_B^\infty(T) \mathcal{L}'_B(T) \quad (\text{A36})$$

The corresponding quantities for the unprimed vibrational energy functions are given by

$$\hat{q}_{A_2}(T) = \hat{q}_{A_2}^\infty(T) \mathcal{L}_{A_2}(T) \quad (\text{A37})$$

$$\hat{q}_B(T) = \hat{q}_B^\infty(T) \mathcal{L}_B(T) \quad (\text{A38})$$

where

$$\mathcal{L}_{A_2}(T) = \mathcal{L}'_{A_2}(T) + \frac{E_a}{\hat{q}_{A_2}^\infty(T)} \quad (\text{A39})$$

$$\mathcal{L}_B(T) = \mathcal{L}'_B(T) + \frac{E_b}{\hat{q}_B^\infty(T)} \quad (\text{A40})$$

When each grouping of vibrational energy states has the same vibrational temperature, the vibrational energy per molecule (including all groupings of vibrational energy states) can be written

$$\begin{aligned} \hat{q}_V(T) &= \frac{n_{A_1}}{n} \hat{q}_{A_1}(T) + \frac{n_{A_2}}{n} \hat{q}_{A_2}(T) + \frac{n_B}{n} \hat{q}_B(T) \\ &= \frac{1}{Q_V(T)} [Q_{A_1}(T) \hat{q}_{A_1}(T) + Q_{A_2}(T) \hat{q}_{A_2}(T) + Q_B(T) \hat{q}_B(T)] \end{aligned} \quad (\text{A41a})$$

or, in the case that only A_1 and A_2 states are to be combined,

$$\hat{q}_A(T) = \frac{1}{Q_A(T)} [Q_{A_1}(T) \hat{q}_{A_1}(T) + Q_{A_2}(T) \hat{q}_{A_2}(T)] \quad (\text{A41b})$$

Figure A-4 shows the results from equation (A41a) for molecular oxygen. Also included are the corresponding quantities computed from three other vibrational models. These quantities are obtained by differentiation (see eq. (A21)) of the relations displayed in figure A-2. The curve labeled "Morse" has values that are large and the curve labeled "truncated harmonic oscillator" has values that are small relative to the curves labeled "Herzberg" and "Model." The general behavior of the various models is thus the same here as in figure A-2. The energy quantity agrees very closely (differing at most by about 2 percent) with the Herzberg result.

To conclude this section it will be shown that, in the limit as the spacings E_{A_2} and E_{A_1} become equal, the total vibrational energy tends to a function recognized as that for a truncated harmonic oscillator with equal energy-level spacing. When the appropriate values of the product expressions for the energy

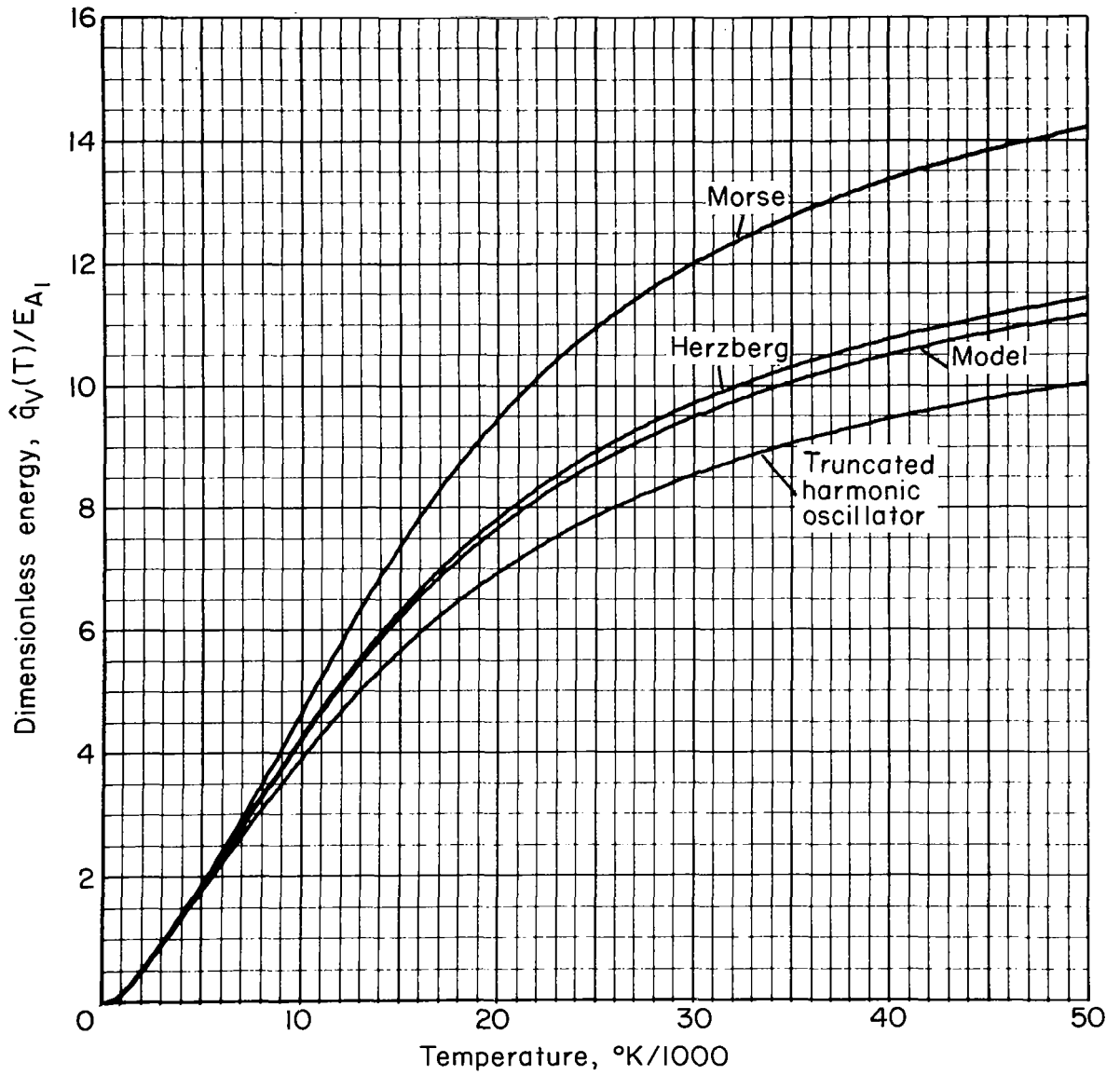


Figure A-4. Comparison of the vibrational energy function computed using different models

functions (noting $q_V^\infty = q_{A_1}^\infty = q_{A_2}^\infty = q_B^\infty$ when $E_{A_1} = E_{A_2}$) are substituted into equation (A41), we have

$$\hat{q}_V(T) = \hat{q}_V^\infty(T) \left[\frac{Q_{A_1}(T) \mathcal{L}_{A_1}(T) + Q_{A_2}(T) \mathcal{L}_{A_2}(T) + Q_B(T) \mathcal{L}_B(T)}{Q_V(T)} \right] \quad (\text{A42})$$

The expression in brackets is the truncation factor for the function $q_V(T)$. Substitution of the appropriate expressions for the truncation factor and simplification of the result yields

$$\mathcal{L}_V(T) = 1 - \exp \left[-\frac{(N-1)E_{A_1}}{kT} - \ln \left(\frac{Q_V(T)}{N} \right) \right] \quad (\text{A43})$$

This is identical to $\mathcal{L}_{A_1}(T)$ with N substituted for the parameter a as one would expect.

(A-2c). Partial Vibrational Specific Heats

The contribution of the vibrational internal energy mode to the specific heat at constant volume is found from the temperature derivative of the average vibrational energy. Consistent with the relations defined in the previous sections, there will be three separate contributions, A_1 , A_2 , and B , depending on the specific grouping of vibrational-energy states considered. Additional quantities corresponding to the specific energy of a non-truncated harmonic oscillator will also be introduced and such quantities will be superscripted ∞ similarly to the analogous energy quantities. Truncation factors \mathcal{L}_i will also be introduced.

The temperature differentiations are readily found and the resulting specific-heat quantities are as follows:[†]

$$c_{V_{A_1}}(T) = c_{V_{A_1}}^\infty(T) \mathcal{L}_{A_1}(T) \quad (\text{A44a})$$

$$c_{V_{A_2}}(T) = c_{V_{A_2}}^\infty(T) \mathcal{L}_{A_2}(T) \quad (\text{A44b})$$

[†]These functions also contain the functional forms $1 - \exp(\alpha)$; see footnote in previous section.

$$c_{v_B}(T) = c_{v_{A_2}}^{\infty}(T) \xi_B(T) \quad (\text{A44c})$$

$$= c_{v_B}^{\infty}(T) \xi_B(T) \quad (\text{A44d})$$

where

$$c_{v_{A_1}}^{\infty}(T) \equiv \frac{dq_{A_1}^{\infty}(T)}{dT} = \frac{R_0 \left(\frac{\Theta_{A_1}}{T}\right)^2 \exp\left(-\frac{\Theta_{A_1}}{T}\right)}{\left[1 - \exp\left(-\frac{\Theta_{A_1}}{T}\right)\right]^2} = R_0 \left[\frac{q_{A_1}^{\infty}(T)}{R_0 T}\right]^2 \exp\left(\frac{\Theta_{A_1}}{T}\right) \quad (\text{A45a})$$

$$c_{v_{A_2}}^{\infty}(T) \equiv \frac{dq_{A_2}^{\infty}(T)}{dT} = R_0 \left[\frac{q_{A_2}^{\infty}(T)}{R_0 T}\right]^2 \exp\left(\frac{\Theta_{A_2}}{T}\right) \quad (\text{A45b})$$

$$\xi_{A_1}(T) = 1 - \exp\left[-\frac{(a-1)}{T} \Theta_{A_1} - 2 \ln\left(\frac{Q_{A_1}(T)}{a}\right)\right] \quad (\text{A46a})$$

$$\xi_{A_2}(T) = 1 - \exp\left[-\frac{(b-a-1)}{T} \Theta_{A_2} - 2 \ln\left(\frac{Q'_{A_2}(T)}{b-a}\right)\right] \quad (\text{A46b})$$

$$\xi_B(T) = 1 - \exp\left[-\frac{(N-b-1)}{T} \Theta_{A_2} - 2 \ln\left(\frac{Q'_B(T)}{N-b}\right)\right] \quad (\text{A46c})$$

We note that the primed and unprimed values of the specific heat are equal, that is, the specific heat is not affected by the ground-state reference energy.

If consecutive pairs of energy groups, or all the energy states collectively, have the same temperature, they may be readily combined. For example, the specific heat of the combined A_1 and A_2 states can be obtained by differentiating equation (A41b) with respect to temperature. The results

$$c_{v_A}(T) = R_0 \left\{ \frac{Q_{A_1}}{Q_A} \left[\frac{c_{v_{A_1}}}{R_0} + \left(\frac{q_{A_1}}{R_0 T}\right)^2 \right] + \frac{Q_{A_2}}{Q_A} \left[\frac{c_{v_{A_2}}}{R_0} + \left(\frac{q_{A_2}}{R_0 T}\right)^2 \right] - \left(\frac{q_A}{R_0 T}\right)^2 \right\} \quad (\text{A47a})$$

If all the energy states have the same temperature, the total vibrational specific heat is given by

$$c_{vV}(T) = R_o \left\{ \frac{Q_A}{Q_V} \left[\frac{c_{vA}}{R_o} + \left(\frac{q_A}{R_o T} \right)^2 \right] + \frac{Q_B}{Q_V} \left[\frac{c_{vB}}{R_o} + \left(\frac{q_B}{R_o T} \right)^2 \right] - \left(\frac{q_V}{R_o T} \right)^2 \right\} \quad (A47b)$$

The behavior of the vibrational specific heat (assuming that the vibrational energy may be defined in terms of a single temperature, eq. (A47b)) is exhibited for molecular oxygen in figure A-5. This is a dimensionless plot of the temperature derivatives of the energy functions displayed in figure A-4. The curves for the Morse and Herzberg models are obtained from equations very similar to equation (A4e), the electronic contribution of the specific heat, except that for the vibrational model the degeneracy g is unity and in place of the electronic excitation temperature $\Theta_{E\ell}$ we use the vibrational temperature E_v/k , where as before E_v is obtained from either equation (A10a) or equation (A10b). The Model results are found from equation (A4f) or equation (A47b).

These quantities display the same relative characteristics observed in figures A-2 and A-4. The curves for the Morse and Herzberg results show a slight anomalous behavior (the slight indentation of the curves between the temperatures 4,000° and 7,000° K; also the model curve crosses the Herzberg curve at the temperature 7,000° K). The Morse and Herzberg quantities are computed as differences of terms obtained by summation. The anomalous behavior is attributed to a slight loss of numerical significance for these quantities resulting from the procedure used in their computation. Since they are not used for the computations given in the text, it was not felt worthwhile to make them more accurate. The model results, however, are accurately computed.

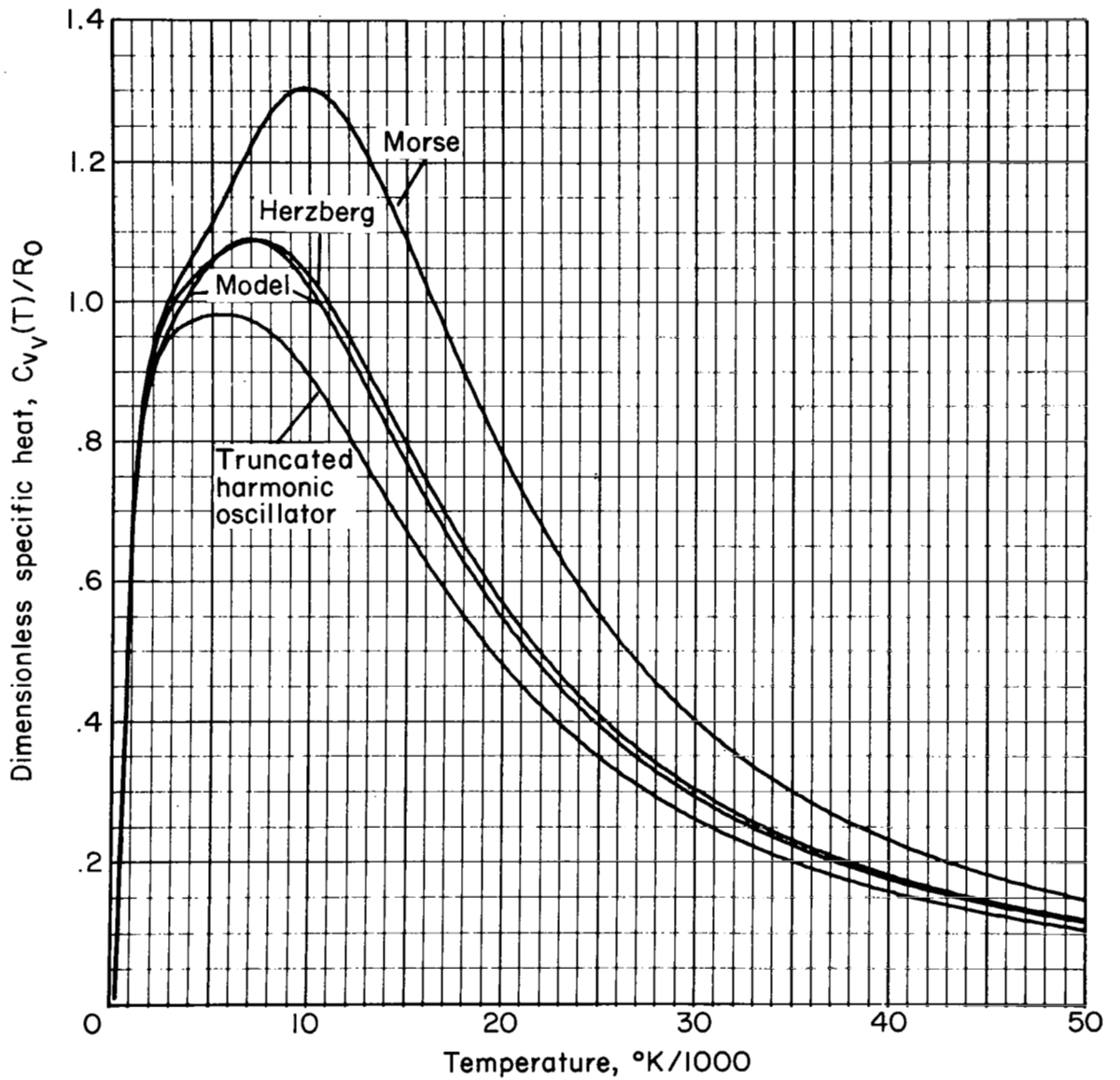


Figure A-5. Comparison of the vibrational specific heat computed using different models

APPENDIX B

VIBRATIONAL TRANSITION RATES

In Chapter II values are required for the vibrational transition rates $k_{v-1,v}$, or, more specifically, for the parameters $k_{1,0}^{(1)}$, $k_{1,0}^{(2)}$, $\chi(T)$, and the level separation a . The latter quantities are those used for the approximate rate relations (II-45) through (II-48) developed in the text. Obtaining these quantities requires the introduction of an approximation for a special quantity "the collisional rate of vibrational quantum transfer." The linear vibrational models that have had widespread utility, for example, the Landau-Teller (49) or Bethe-Teller vibrational relaxation model (8) described in Chapter I approximate this quantity, in effect, in terms of a temperature-dependent linear function of the vibrational-energy-level number v . Such a relation is unsatisfactory since it does not take into account the effect of the more rapid transitions that occur for vibrationally excited molecules. It will be shown that a more accurate relation can be obtained if at least 2 connected linear functions are used for the "rate-of-quantum-transfer" quantity.

In the next section a discussion will be given of the transition rates applicable for anharmonic-oscillator models, and the results of several different theories will be compared. In the last section the procedure for approximating the transition-rate relations will be introduced.

(B-1). Transition Rates, Analytical Form

It will be shown that the vibrational transition rates, applicable for vibration-translation energy interchange involving atom-molecule collisions, may be represented in general by

$$k_{v-1,v} = v k_{0,1}(T) G(T, v; x_0) \quad (\text{B1a})$$

$$k_{v,v-1} = \exp(E_{v,v-1}/kT) k_{v-1,v} \quad (\text{B1b})$$

$$= v k_{1,0}(T) G(T, v; x_0) \exp\left\{ [E_{v,v-1} - E_{1,0}]/kT \right\} \quad (\text{B1c})$$

where

$$v = 1, 2, \dots, N - 1$$

$$E_{v,v-1} = E_v - E_{v-1} \quad (\text{B1d})$$

and x_0 is the anharmonicity coefficient ($x_0 = 0$ for harmonic oscillators), v is the vibrational quantum number, E_v is the energy of the vibrational level designated v , $k_{0,1}$ and $k_{1,0}$ are the rates for transitions between the ground state and the first excited state of a molecule, and G is a factor that accounts for the effect of molecular anharmonicity on the values of the transition rates. The above formulations display the effect of anharmonicity explicitly through the function G . For example, setting G equal to unity (i.e., $G(T, v; 0) = 1$) yields the Landau-Teller transition rates (46, 49) for harmonic oscillators.

One may speculate on the functional behavior of the anharmonicity factor G . Since the low-lying molecular states are nearly equally spaced and the effects of anharmonicity are therefore small, G should be approximately unity for values of v near unity. The energy-level spacing decreases for the higher vibrational energy states as a result of molecular anharmonic effects, and we may expect the rate of interchange of vibrational energy occurring during atom-molecule collisions to increase. We may therefore expect that G is a monotonically increasing function of v . In this section the G factor will be evaluated from the transition rates given by Keck and Carrier (48). It will be shown that the factor differs very little from a similar G -factor obtained from transition rates derived by Nikitin (65) and used by Bray and Pratt (18). The rates given by Keck and Carrier are based on quantum-mechanical treatment of the collision processes, while the Nikitin formula, obtained from a perturbation treatment of the Landau-Teller results (49), is based on a semiclassical approach to the collision problem. In both cases the rates are described as being only qualitatively correct (see, e.g., 18); their main shortcoming is that they apply to nonrotating molecules; that is, they do not include the effects of vibration-rotation coupling. The effects of this mechanism may be important at the higher temperatures (see, e.g., 4, 5, 85), effectively increasing the rate

of energy interchange. Completely reliable values for the rate parameters describing the molecular kinetics, particularly the rotational processes, are not available.

The rates given by Keck and Carrier (48) are for a nonrotating quantized Morse oscillator, for which the potential energy is given by (see 48 or 49)

$$V_M(r) = D_e \left\{ 1 - \exp[-\beta(r - r_0)] \right\}^2 \quad (\text{B2})$$

The vibrational transition rates are written

$$k_{v-1,v} = k_{0,1} \frac{a_v f(\omega_v \tau)}{a_1 f(\omega_1 \tau)} \quad (\text{B3})$$

This formulation differs from reference 48 only in the notation and the fact that the factors independent of v in that reference have been lumped together here in the coefficient $k_{0,1}$. (The present representation is useful since the factor $k_{0,1}$ appears explicitly. This factor may be found from experimental data as in Chapter III or its value can be estimated from the following relations.) The expressions given in equation (B3) are defined as follows:

$$k_{0,1} = \frac{Z(m,n) f(\omega_1 \tau) a_1}{mn} \quad (\text{B3a})$$

where

$$Z(m,n) = d_{n,m}^2 \bar{c} mn \quad (\text{B3b})$$

is the bimolecular collision rate,

$$a_v = \frac{2\mu_3}{\Theta\mu_{12}} \frac{2Nv}{(2N - v)} \quad (\text{B3c})$$

is the resonance transition probability for a Morse oscillator,

$$f(x) = x^2 \int_0^\infty e^{-y} \operatorname{csch}^2(xy^{-1/2}) dy \quad (\text{B3d})$$

is the adiabaticity factor,

$$\omega_v \approx kT(E_v - E_{v-1})/\hbar = \omega_0 \left(1 - \frac{v}{N} \right) \quad (\text{B3e})$$

is the angular frequency of the transition,

$$E_v \approx \Theta_0 v \left[1 - \frac{v}{2N} \right] = \Theta_0 v [1 - x_0 v] \quad (\text{B3f})$$

is the energy (ergs per particle) of the vibrational level designated v , $\Theta_0 = \frac{\hbar \omega_0}{kT}$ is the ground-state level spacing divided by kT , $d_{n,m}^2$ is the kinetic cross section for collisions between molecules n and collision partners m , and n and m are the concentrations of colliding partners and molecules. The constant μ_3 is the reduced mass for the collision, μ_{12} is the reduced mass for the molecules, $\tau = \pi L \sqrt{\mu_3 / 2kT}$ is the effective collision time for an exponential interaction potential $V_3 = V_0 \exp(-r_3/L)$, and $\omega_0 = \beta \sqrt{2D_e / \mu_{12}}$ is the angular frequency of the transition between the ground and first excited vibrational states. The quantity $\bar{c} = \sqrt{8kT / \pi \mu_3}$ is the mean speed for collisions of molecules and collision partners, and N is approximately equal to the number of vibrational levels in the potential well. This notation has also been altered somewhat from that of Keck and Carrier (48) to conform with the notation of this thesis. For $x \gg 1$, the adiabaticity factor, equation (B3d), can be evaluated by the method of steepest descent and is found to be

$$f(x) \approx f_1(x) = 8 \left(\frac{\pi}{3} \right)^{1/2} x^{7/3} \exp(-3x^{2/3}) \quad (\text{B4a})$$

By numerical integration and curve fitting, Keck and Carrier (48) obtained the expression

$$f(x) \approx f_2(x) = \frac{1}{2} \left[3 - \exp\left(-\frac{2x}{3}\right) \right] \exp\left(-\frac{2x}{3}\right) \quad (\text{B4b})$$

which they point out is accurate ($\pm 20\%$) for $0 \leq x \leq 20$, and bridges the gap between impulsive and adiabatic energy exchange.

It will be shown here that equation (B4a) can be related to the rate relation found by Nikitin (65). On this basis, the G -function, defined by equation (B4a), can be written

$$\begin{aligned}
G_1(T, v; x_e) &= \frac{a_v}{v a_1} \left(\frac{\omega_v}{\omega_1} \right)^{7/8} \exp \left[-3 \tau^{2/3} (\omega_v^{2/3} - \omega_1^{2/3}) \right] \\
&= \exp \left\{ -\ln \left(1 - \frac{v-1}{2N-1} \right) + \frac{7}{3} \left(1 - \frac{v-1}{N-1} \right) + 3(\omega_0 \tau)^{2/3} \left(1 - \frac{1}{N} \right)^{2/3} \right. \\
&\quad \left. \times \left[1 - \left(1 - \frac{v-1}{N-1} \right)^{2/3} \right] \right\} \tag{B5}
\end{aligned}$$

We obtain an approximation for G that is valid when v is small compared with the total number of levels, N , by the substitution of the approximations $\ln(1 \pm \delta) \approx \pm \delta$, $(1 \pm \delta)^{2/3} \approx 1 \pm \frac{2}{3} \delta$, and $\frac{11}{12} \sim 1$ where δ in this case is some small number $\delta < 1$. The G -function can then be represented by

$$G(T, v; x_0) = \exp \left\{ 2 \frac{(v-1)}{N} \left[(x_0 \tau)^{2/3} - 1 \right] \right\} \tag{B6a}$$

$$= \exp \left\{ 4 x_0 (v-1) \left[(x_0 \tau)^{2/3} - 1 \right] \right\} \tag{B6b}$$

where the subscript has been dropped in order to differentiate the expressions denoted by equations (B5) and (B6). The second of the two equations follows from the fact that for a Morse oscillator the number of energy levels is given by $N = 1/2 x_0$ (see, e.g., 9, 40, or 48), that is, the anharmonicity coefficient x_0 is determined from

$$x_0 = \frac{\hbar \omega_0}{4D} = \frac{1}{2N} \tag{B7}$$

The factor $\omega_0 \tau$ may be written in a more convenient form such that its temperature dependence is explicitly displayed. We first introduce a dimensionless constant defined by

$$\varphi_0 = \left[\left(\frac{\pi L}{\hbar} \right)^2 \frac{\mu_3 \hbar \omega_0}{2} \right]^{1/3} \tag{B8}$$

In terms of this quantity we then obtain

$$(\omega_0 \tau)^{2/3} = \varphi_0 \left(\frac{\hbar \omega_0}{kT} \right)^{1/3} \tag{B9}$$

The G-function may then be written

$$\begin{aligned} G(T, v; x_0) &= \exp \left\{ 4 x_0 (v - 1) \left[\varphi_0 \left(\frac{\hbar \omega_0}{kT} \right)^{1/3} - 1 \right] \right\} \\ &= \exp \left\{ \alpha_F (v - 1) \right\} \end{aligned} \quad (\text{B10})$$

where

$$\alpha_F = 4 x_0 \left[\varphi_0 \left(\frac{\hbar \omega_0}{kT} \right)^{1/3} - 1 \right] \quad (\text{B10a})$$

is introduced to further abbreviate the notation.

The expression in equation (B10) is relatively simple in outward appearance. When substituted into the equation for the transition rates, equation (B1a), it yields an expression very similar to the following relation obtained by Nikitin (65):

$$\begin{aligned} (k_{v-1, v})_{\text{Nikitin}} &= v k_{0,1} \exp \left[4 x_0 (v - 1) \varphi_0 \left(\frac{\hbar \omega_0}{kT} \right)^{1/3} \right] \\ &= v k_{0,1} G_{\text{Nikitin}} \end{aligned} \quad (\text{B11a})$$

where

$$G_{\text{Nikitin}} = \exp \left[4 x_0 (v - 1) \varphi_0 \left(\frac{\hbar \omega_0}{kT} \right)^{1/3} \right] \quad (\text{B11b})$$

We observe that

$$G_{\text{Nikitin}} = G \exp [4 x_0 (v - 1)] \quad (\text{B12})$$

The relations thus differ only at the higher vibrational energy levels; at the uppermost level, where $v = N$ (recall $x_0 = 1/2 N$), they differ by a factor e^2 . Because these expressions are only qualitatively correct at these high vibrational levels, factors of order e^2 are certainly not unreasonable.

It is interesting to compare the G-functions obtained from the adiabaticity factors (eqs. (B4a) and (B4b) with the function of equation (B10). This comparison is shown in figure B-1, where the parameters have been evaluated for oxygen (see constants in Appendix G). The solid-line curves are plots of

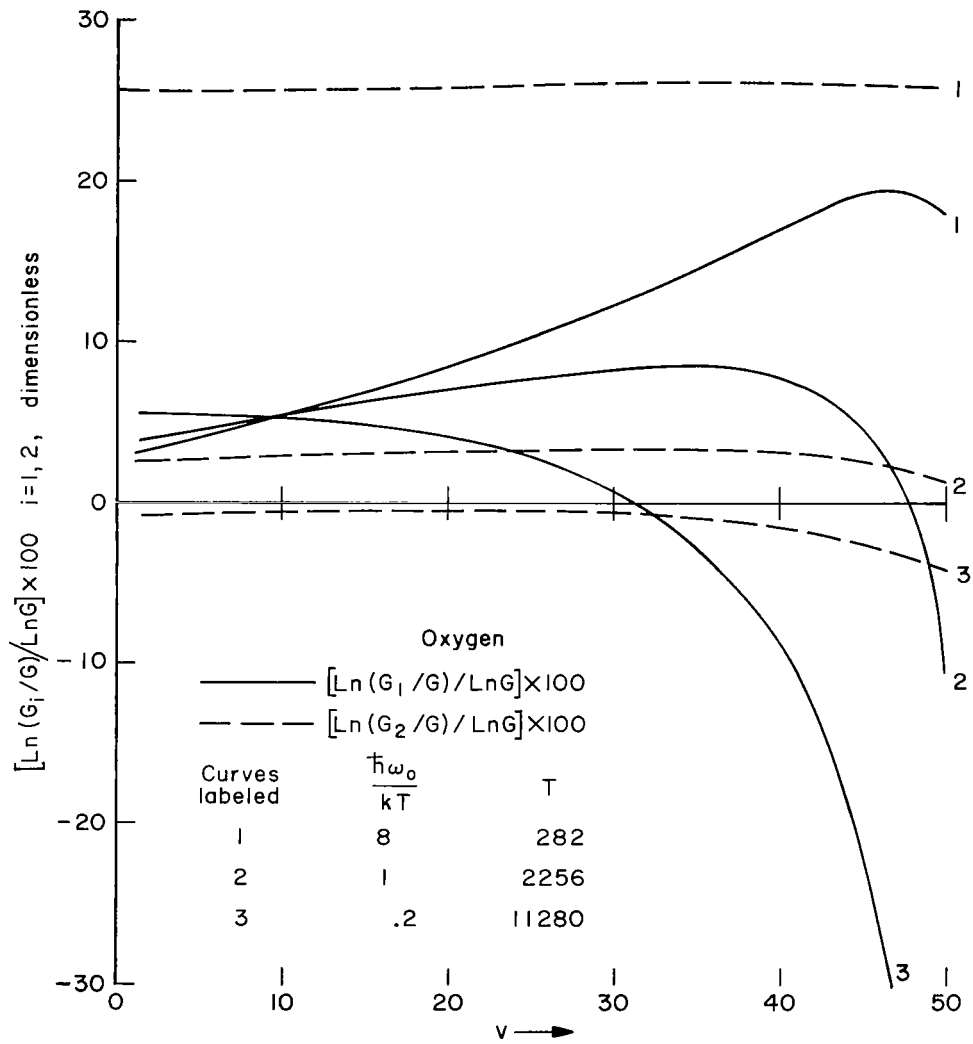


Figure B-1. Plot showing relative deviation of the rate anharmonicity coefficients computed using different adiabaticity factors

$[\ln G_1 - \alpha_F(v-1)]/\alpha_F(v-1)$, and the dotted curves are plots of $[\ln G_2 - \alpha_F \times (v-1)]/\alpha_F(v-1)$; in both figures the vibrational number v is plotted along the abscissa. The plots are made for three different temperatures that yield values of $\hbar\omega_0/kT$ of 8, 1, and 0.02, and the corresponding curves are labeled 1, 2, and 3, respectively. In effect, the plots illustrate deviations of the G -functions from exponentials whose arguments vary linearly in v and inversely in the one-third power of the temperature. Such functional behavior is exhibited by horizontal lines in the figure. The solid-line curves, corresponding to the adiabaticity factor f_1 of equation (B4a), deviate significantly from such functional behavior, especially when the vibrational number v is large. Under these conditions the parameter $\omega_v\tau$ (see eq. (B3e) and discussion) is small (of order unity), and the quantum-mechanical and semiclassical derivations leading to these quantities are questionable. Keck and Carrier (48) introduced the adiabaticity factor f_2 of equation (B4b) to formulate more accurately the correct behavior of the transition rates for the smaller values of $\omega_v\tau$. The dotted curves corresponding to this adiabaticity factor are nearly horizontal. These curves, however, exhibit a strong low-temperature dependence that is suspect. When v is small and the temperatures are lowest, the dotted curves correspond to percentage deviations from zero that are quite large (25 to 30 percent), and we observe that the quantity $\omega_v\tau$ has its largest values. In this case we expect that the solid-line curves are perhaps more accurate. This supposition follows since at relatively low temperatures and for the smallest values of v the solid-line curves are equivalent to the Landau-Teller $k_{0,1}$ transition rates for which there is good experimental agreement. Also, for this case, there is close agreement with the Nikitin formula (eq. (B11)). We shall consider that the G -factor to be used in equation (B1) is given by equation (B10) for all temperatures and for the complete spectrum of values of the vibrational quantum number v .

(B-2). Approximating the Transition Rates

From the relations of the previous section, one can see that a vibrational-relaxation model containing transition rates that vary linearly with the

vibrational quantum number v cannot account for the rapid relaxation that occurs in the upper vibrational levels. Linearly varying rates, such as result from the study of collisions of atoms and harmonic-oscillator molecules (Landau-Teller (49) and Jackson and Mott (46)), are very attractive, because the resulting relations greatly simplify the energy-moment equations derived from the master equations. This is exemplified by the analysis in Chapter II (see also, Bethe and Teller (8) and also p. 198 of Vincenti and Kruger (97)). To account properly for the nonlinear effects resulting from molecular anharmonicity, one has the choice either of developing a relatively complex model based on nonlinear rate constants that are only qualitatively correct or of introducing approximations and thus extending the utility of the existing models. Such models have heretofore been remarkably successful in describing vibrational relaxation at the lower temperatures and have had considerable appeal in flow-field calculations because of their relative simplicity. A procedure will be introduced here whereby one can utilize the advantages of linearly varying rate relations, but still account qualitatively for the more rapid relaxation occurring in the upper states.

The essential problem is one of correctly approximating T_1 and T_2 in equations (II-49). This can be accomplished by appropriately approximating the quantities

$$E_{v,v-1} \quad k_{v,v-1} \quad (B13a)$$

$$E_{v+1,v} \quad k_{v,v+1} \quad (B13b)$$

by linear functions (note that $E_{v,v-1}$ is defined by eq. (B1d)). These relations represent the rate of transfer of vibrational quanta as a result of collisions (vibration-translation energy interchange). If one assumes a harmonic oscillator then the energy differences $E_{v,v-1}$ and $E_{v+1,v}$ are constant and the transition rates are given by $v k_{1,0}$ and $(v+1)k_{0,1}$, respectively. These relations have been basic in previous models. For a Morse oscillator the energy differences between successive vibrational energy levels are not constant, but vary linearly with the vibrational number v and, furthermore, the transition rates

depend exponentially on v (see eq. (B10)). A single linear relation is therefore not satisfactory. We shall therefore approximate the above relations by two linear segments, as exemplified in figure B-2.

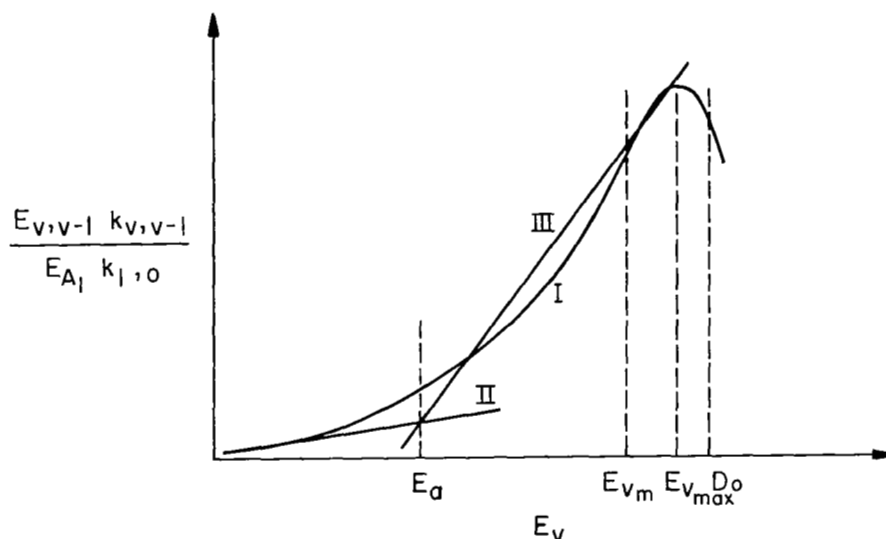


Figure B-2. Approximation scheme for including anharmonic effects

The ordinate is the product under consideration made dimensionless by the factor $(E_{A_1} k_{1,0})^{-1}$ and the abscissa is the vibrational energy E_v ; the smooth curve I is the function to be approximated. We observe that this curve attains a maximum very near the dissociation energy D_0 . This maximum is a result of the Morse oscillator equations and is probably not a real effect. The curve I will here be approximated by the two straight-line segments II and III that intersect near the separation E_a . The plot (and the approximations) is found with the vibrational energy E_v as the independent variable rather than the vibrational number v for two reasons: First, the variation of the quantity $E_{v,v-1} k_{v,v-1}$ is least in this case; and second, the thermodynamic energy quantities $q_1(T_1)$ (see Appendix A) are more accurately included. The segment II appropriate to the lower states (with energy less than E_a) is the vibrational-relaxation function obtained from Landau-Teller theory (8, 49). At relatively low temperatures only these states are appreciably populated. Since existing low-temperature theories have been successful in their description of vibrational

relaxation, particularly behind shock waves, there is no reason to alter this function. The segment III applicable to the upper states requires a different approach. This segment lies between a point on the smooth curve (with a coordinate E_{v_m}) that lies near the curve maximum and the intersection of the segment I at the separation E_a . The value of the curve maximum depends on the temperature T . The value (a constant) of E_a is chosen somewhat arbitrarily and will be discussed later. The procedure is described in detail later, and compared with others by means of figures at the end of this section.

From the above discussion the required relations can readily be found:

$$(E_{v,v-1} k_{v,v-1})_{\text{approx.}} = v k_{1,0} E_{A_1} \quad 0 \leq v \leq a \quad (\text{B14a})$$

$$(E_{v,v-1} k_{v,v-1})_{\text{approx.}} = E_{A_2} k_{1,0} \left[(v - a) \chi_R(T) + a \frac{E_{A_1}}{E_{A_2}} \right] \quad a \leq v \leq N \quad (\text{B14b})$$

where

$$\chi_R(T) = \frac{k_{1,0}^{(2)}}{k_{1,0}^{(1)}} = \frac{\left[E_{v,v-1} \frac{k_{v,v-1}}{k_{1,0}} \right]_{v=v_{mR}} - a E_{A_1}}{E_{v_{mR}} - E_a} \quad (\text{B14c})$$

is the slope of curve III shown in the sketch and the parameter a is an integer evaluated in such a manner that $(a - 1) E_{A_1} + E_{A_2} = E_a$ (see Appendix A). The quantity v_{mR} depends on the temperature; its value is obtained as an approximation to the actual coordinate v_{max} at which $E_{v,v-1} k_{v,v-1}$ is a maximum. The procedure will be discussed shortly.

The above relations are associated with rates of transfer of vibrational energy for transitions in the "backward" direction, that is, from the level v to $v-1$. Equivalent expressions for transitions in the "forward" direction, $E_{v,v-1} k_{v-1,v}$, are found by requiring that the model equations have the proper behavior at equilibrium. At equilibrium we have $n_v k_{v,v-1} = n_{v-1} k_{v-1,v}$ which follows as a consequence of "detailed balancing" or "microscopic reversibility" (e.g., see 97, 100). For the model equations, there results

$$\frac{k_{v-1,v}}{k_{v,v-1}} = \left(\frac{n_v}{n_{v-1}} \right)_{\text{equilibrium}} \quad (\text{B15a})$$

$$= \exp\left(-\frac{\Theta_{A_1}}{T}\right) \quad 1 \leq v \leq a \quad (\text{B15b})$$

$$= \exp\left(-\frac{\Theta_{A_2}}{T}\right) \quad a \leq v \leq N \quad (\text{B15c})$$

The required rate parameters, of the form given by equations (II-45) in the text, are obtained by dividing equation (B14a) by E_{A_1} and equation (B14b) by E_{A_2} . We obtain

$$k_{v,v-1} = v k_{1,0}^{(1)} \quad 1 \leq v \leq a \quad (\text{B16a})$$

$$k_{v,v-1} = (v - a) k_{1,0}^{(2)} + k_{a,a-1}^{(2)} \quad a \leq v \leq N \quad (\text{B16b})$$

where

$$k_{1,0}^{(1)} = k_{1,0} \quad (\text{B16c})$$

$$k_{1,0}^{(2)} = k_{1,0}^{(1)} \chi_R(T) \quad (\text{B16d})$$

$$k_{a,a-1}^{(2)} = k_{1,0}^{(1)} a \frac{E_{A_1}}{E_{A_2}} \quad (\text{B16e})$$

The reverse rates (eqs. (B15)) are unchanged.

To obtain the coordinate v_m required in the above rate relations we need the derivative with respect to the energy E_v . With Morse-oscillator values for the energy spacing ($E_{v,v-1} = \hbar\omega_0[1 - x_0(2v - 1)]$) and equations (B1) and (B10) for the transition rates, the energy derivative of the product of interest is given by

$$\frac{\partial}{\partial E_v} \ln[E_{v,v-1} k_{v,v-1}]_{T=\text{const.}} = \left[\frac{-\frac{2x_0}{1 - x_0(2v - 1)} + \frac{1}{v} + \alpha_F(T) - \frac{2\hbar\omega_0 x_0}{KT}}{\hbar\omega_0[1 - 2x_0 v]} \right] \quad (\text{B17})$$

To simplify notation we define

$$\alpha_R(T) = \alpha_F(T) - \frac{2 \hbar \omega_0 x_0}{kT} \quad (\text{B18a})$$

$$= 4 x_0 \left[\varphi_0 \left(\frac{\hbar \omega_0}{kT} \right)^{1/3} - \frac{\hbar \omega_0}{2 kT} - 1 \right] \quad (\text{B18b})$$

The quadratic equation in the variable v_{\max} that results when the above derivative is set equal to zero is easily solved. The solution is given by

$$v_{\max}(T) = \frac{1}{2} \left[\left(-\frac{2}{\alpha_R} + \frac{1}{2x_0} + \frac{1}{2} \right) + \sqrt{\left(-\frac{2}{\alpha_R} + \frac{1}{2x_0} + \frac{1}{2} \right)^2 + \frac{4(1+x_0)}{2x_0\alpha_R}} \right] \quad (\text{B19})$$

The root with the negative radical is discarded because negative values of v_{\max} are meaningless.

Since we are seeking only approximate relations, it is not worthwhile to use the complicated expression given above. A simpler one is obtained as follows. Neglecting the terms $1/2$ as compared with the terms $1/x_0$ and $1/\beta$ and x_0 as compared with unity, we have

$$v_{\max} \approx \frac{1}{2} \left[-\frac{2}{\alpha_R} + \frac{1}{2x_0} + \frac{1}{2x_0} \sqrt{1 + \left(\frac{4x_0}{\alpha_R} \right)^2} \right] \quad (\text{B20})$$

The ratio $4x_0/\alpha_R$ is always less than 1 for the temperatures of interest. We can approximate the radical using the first two terms of a binomial expansion and obtain for v_{\max} the approximate quantity

$$v_{m_1}(T) = \frac{1}{2x_0} \left[1 - \frac{2x_0}{\alpha_R(T)} \left(1 - \frac{2x_0}{\alpha_R(T)} \right) \right] \quad (\text{B21})$$

An alternative, less accurate formulation is obtained if terms of order $(2x_0/\alpha_R)^2$ are neglected:

$$v_{m_2}(T) = \frac{1}{2x_0} \left[1 - \frac{2x_0}{\alpha_R(T)} \right] \quad (\text{B22})$$

The quantities v_{\max} , v_{m_1} , and v_{m_2} are plotted versus temperature in figure B-3. We see that v_{m_1} is always greater than v_{\max} and differs most at a temperature of about $24,000^\circ\text{K}$, where the error is about one vibrational level (or about 3 percent). The approximate quantity v_{m_2} is always less than v_{\max} and differs at most from the correct value, v_{\max} , by about five vibrational levels (about 13 percent error). The product $E_{v,v-1} k_{v,v-1}$ actually increases relatively slowly with increasing v until it reaches its maximum and then decreases very rapidly (e.g., see fig. B-2). The most accurate value, v_{m_1} , yields values for $E_{v,v-1} k_{v,v-1}$ in the rapidly decreasing region ($v_{m_1} > v_{\max}$) and the least accurate value, v_{m_2} , yields values for the product quantity in the slowly increasing region ($v_{m_2} < v_{\max}$). Consequently, whether one uses v_{m_1} or v_{m_2} to represent v_{\max} actually makes little difference in the value of the quantity $E_{v,v-1} k_{v,v-1}$ that is of interest. We shall therefore use the simpler relation v_{m_2} when values of v_{m_r} are required. The quantities $(E_{v,v-1} k_{v,v-1})/(E_{1,0} k_{1,0})$, $(E_{v+1,v} k_{v,v+1})/(E_{1,0} k_{1,0})$ and their approximated equivalents are plotted versus dimensionless vibrational energy, E_v/E_{A_1} , in figures B-4. The product relations appropriate for the "forward" transitions are labeled (f) and the "reverse" quantities are labeled (r). Figure B-4a is for a temperature ratio T/Θ_{A_1} of unity ($\Theta_{A_1} = 2234^\circ\text{K}$), and figures B-4b, B-4c, and B-4d are for ratios of 2, 5, and 10, respectively.

Discussing figure B-4a first, one notes that in this case the approximating method is extremely poor. It is obvious that the approximate rates have values that are too large in the region adjacent to and above the separation point ($E_v/E_{A_1} \approx 9$) and the forward rate is not large enough at the higher levels. It may be shown, however, (e.g., see Chapter III and IV) that for normal-shock waves the upper levels are not appreciably populated at these temperatures and, therefore, the large differences between the approximate and Morse relations have little effect in the application of the approximate rates. At successively higher temperatures, illustrated by figures B-4b, B-4c, and B-4d (note that the ordinate scale changes in these figures), the approximate relations improve as regards their difference from the Morse relations, and the difference between

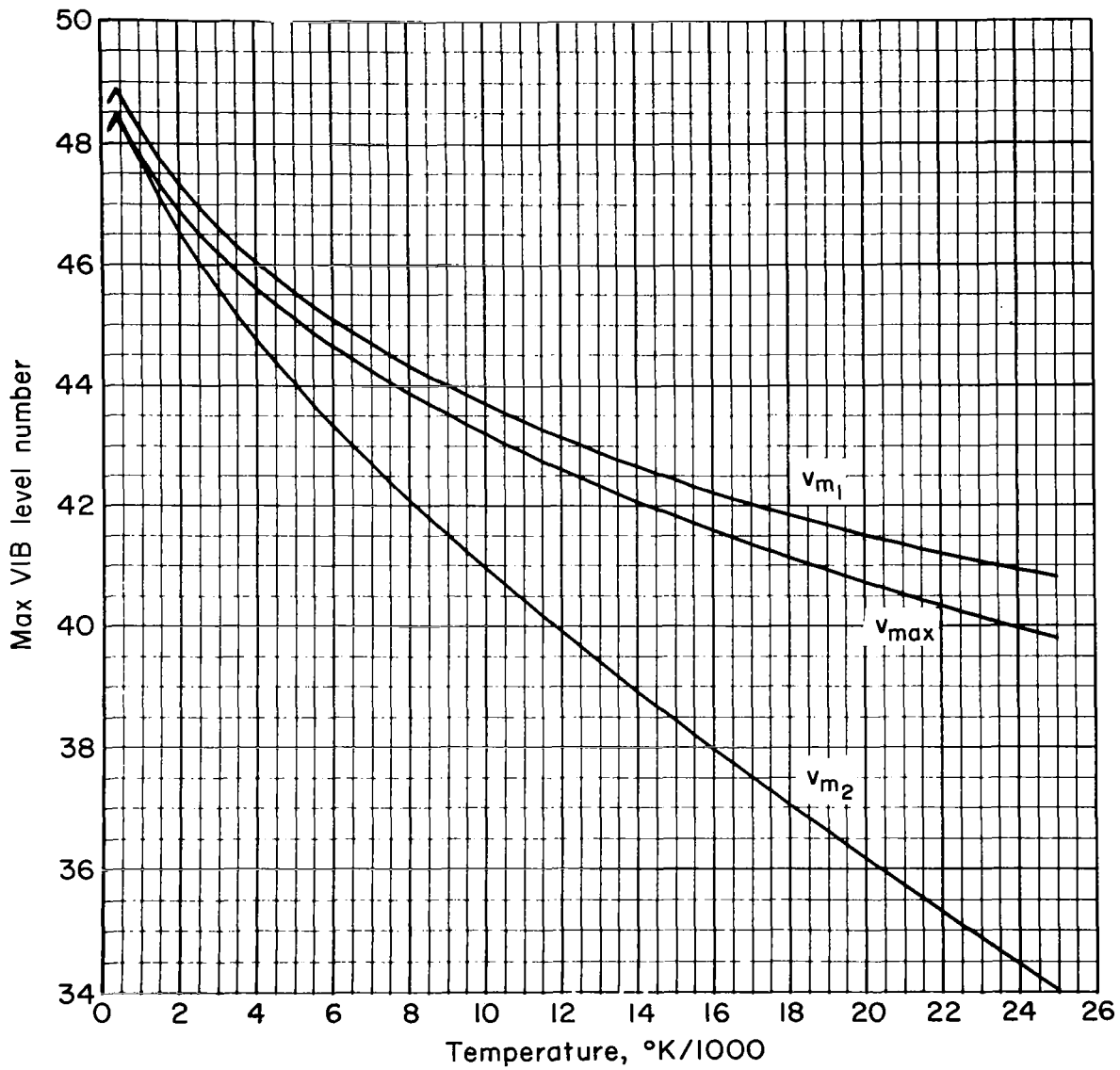
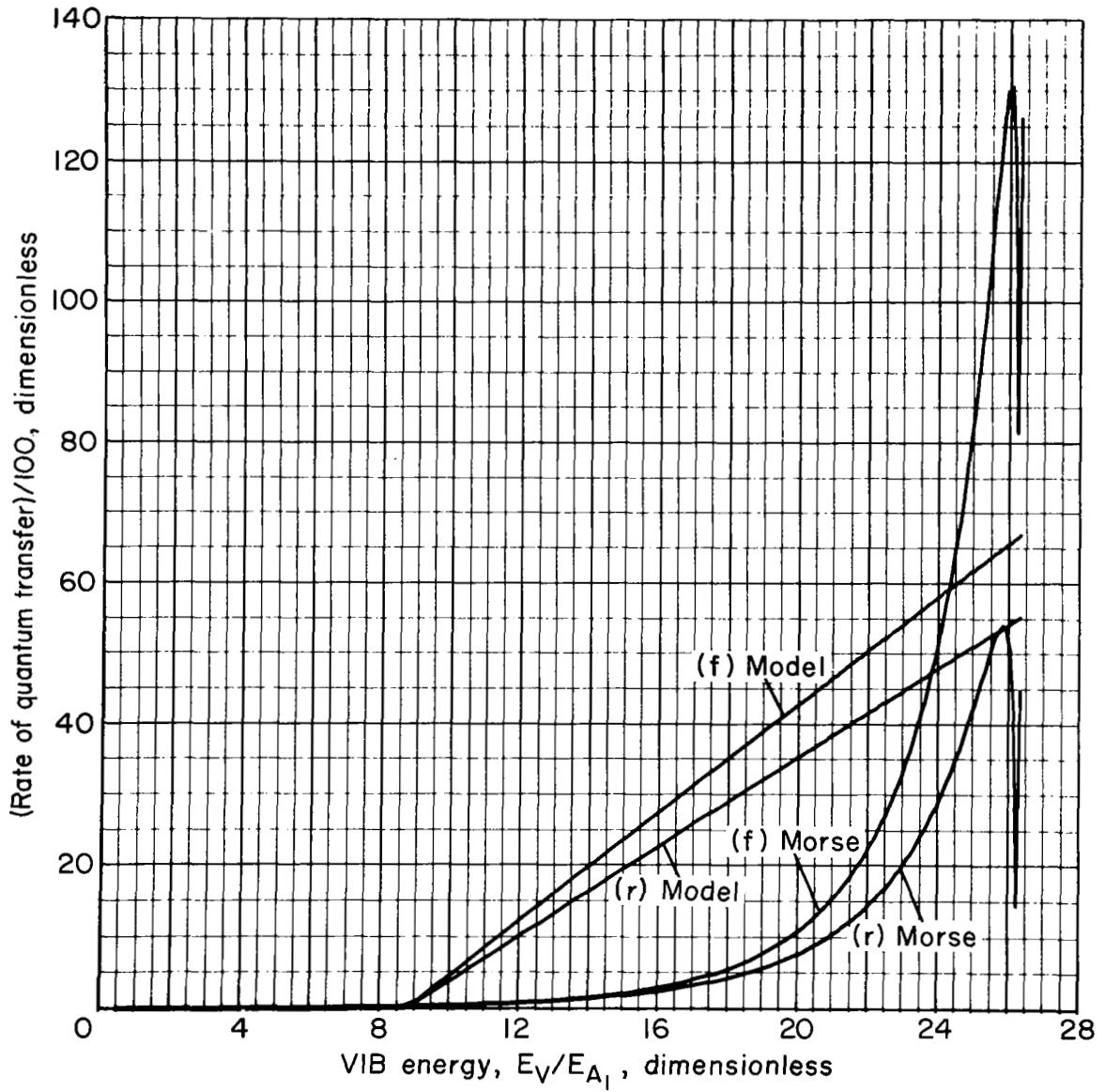
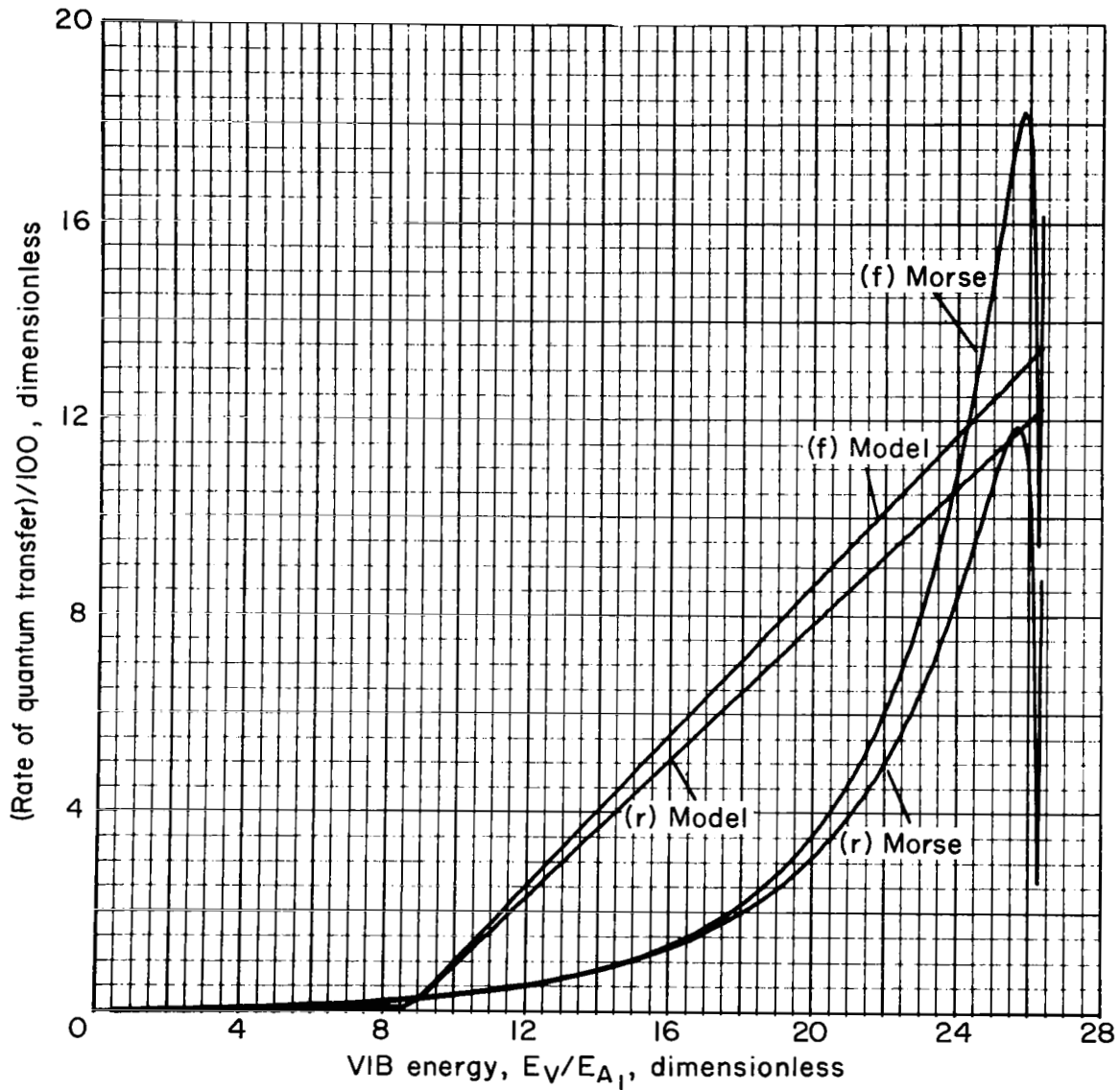


Figure B-3. Comparison of the vibrational energy level computed by different methods that yields a maximum "rate of vibrational quantum transfer"



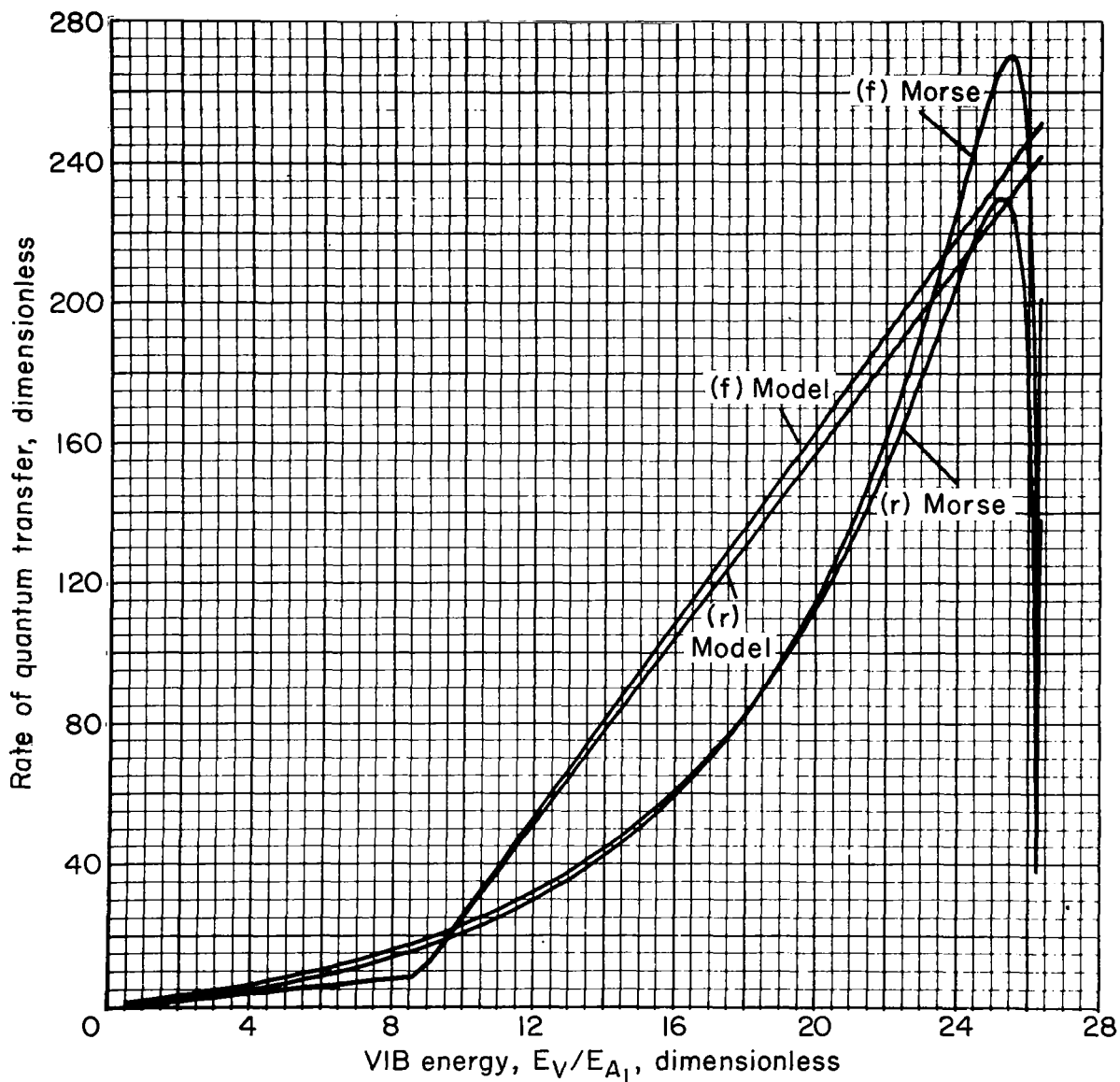
(a) $T = \Theta_{A_1}$

Figure B-4. Comparison of the "rate-of-quantum-transfer quantity," (χ_R)



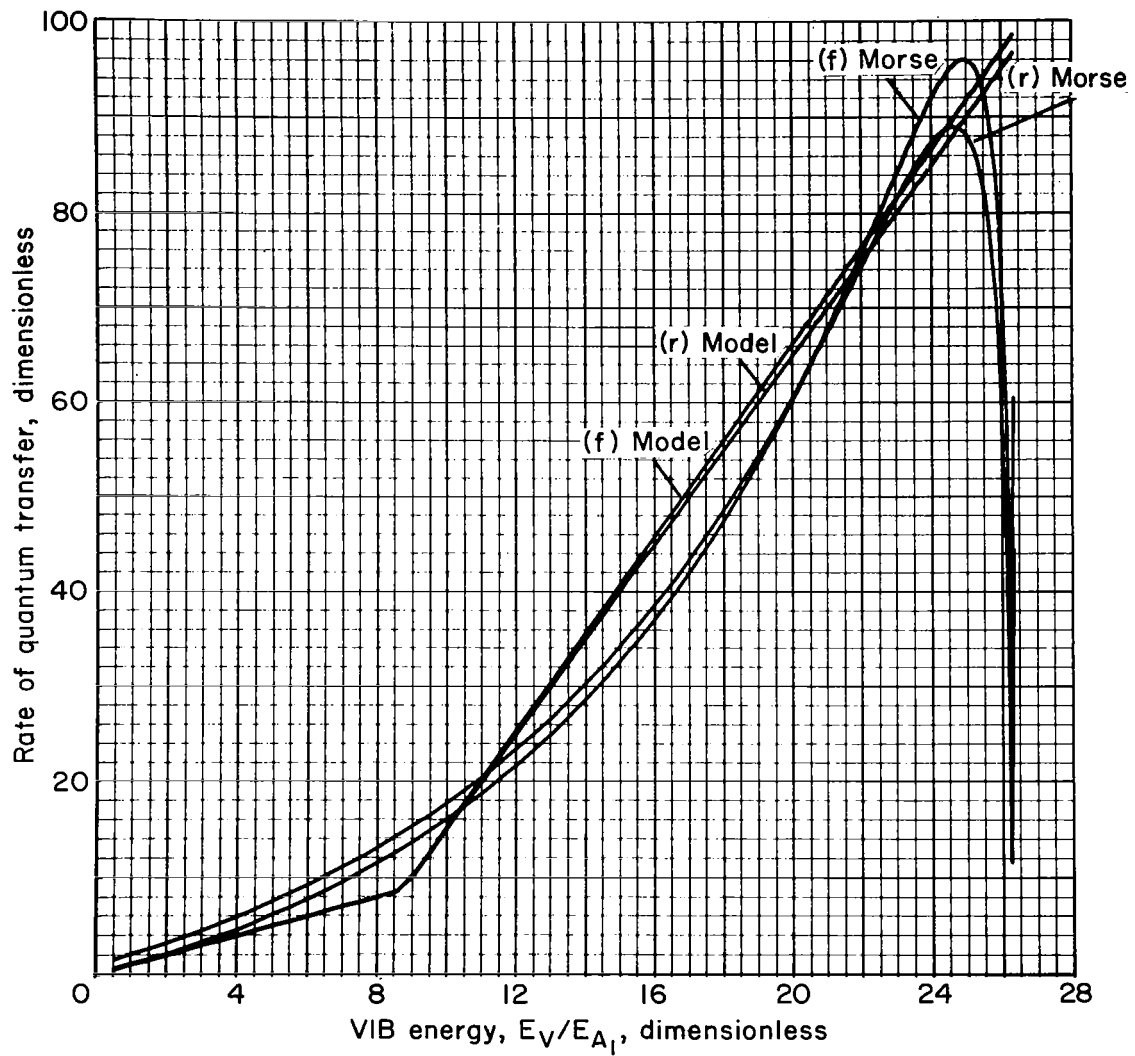
(b) $T = 2 \Theta_{A_1}$

Figure B-4 Continued



(c) $T = 5 \Theta_{A_1}$

Figure B-4 Continued



(d) $T = 10 \Theta_{A_1}$

Figure B-4 Continued

the forward rate relations also becomes less. For nozzle flow where the temperatures are high, the rates are therefore accurately approximated. Freezing of the vibrational mode generally occurs before the lower temperatures are reached.

The value of the separation E_a , at which the lower linear segment intersects the upper segment, was chosen so that the value of the approximate rates found for the lower segment, differ only by a factor of about 2 from the Morse values. This choice is somewhat arbitrary, and E_a may be determined on the basis of other criteria when such approximations are worthwhile, for example, when more reliable values of the quantities being approximated are available. Then it may also be advisable to make the separation E_a temperature dependent. It may also be worthwhile to introduce additional segments for these approximations (see Chapters III and IV).

To assess the effect of the approximating procedure for the upper states, it is convenient to have a different set of relations from those just described. Such relations are obtained by following a procedure similar to that used to obtain equations (B14) through (B22). Rather than being based on the reverse rates, however, the approximating procedure is based here on the forward rates. It turns out that the resulting equations are very similar, except that in equations (B14b) and (B16d) χ_R is replaced by χ_F , where

$$\chi_F(T) = \frac{\left[\frac{E_{v,v-1} k_{v-1,v}}{k_{0,1}} \right]_{v=v_{m_F}} \exp\left(\frac{\Theta_{A_2} - \Theta_{A_1}}{T}\right) - a E_{A_1}}{E_{v_{m_F}} - E_a} \quad (\text{B23a})$$

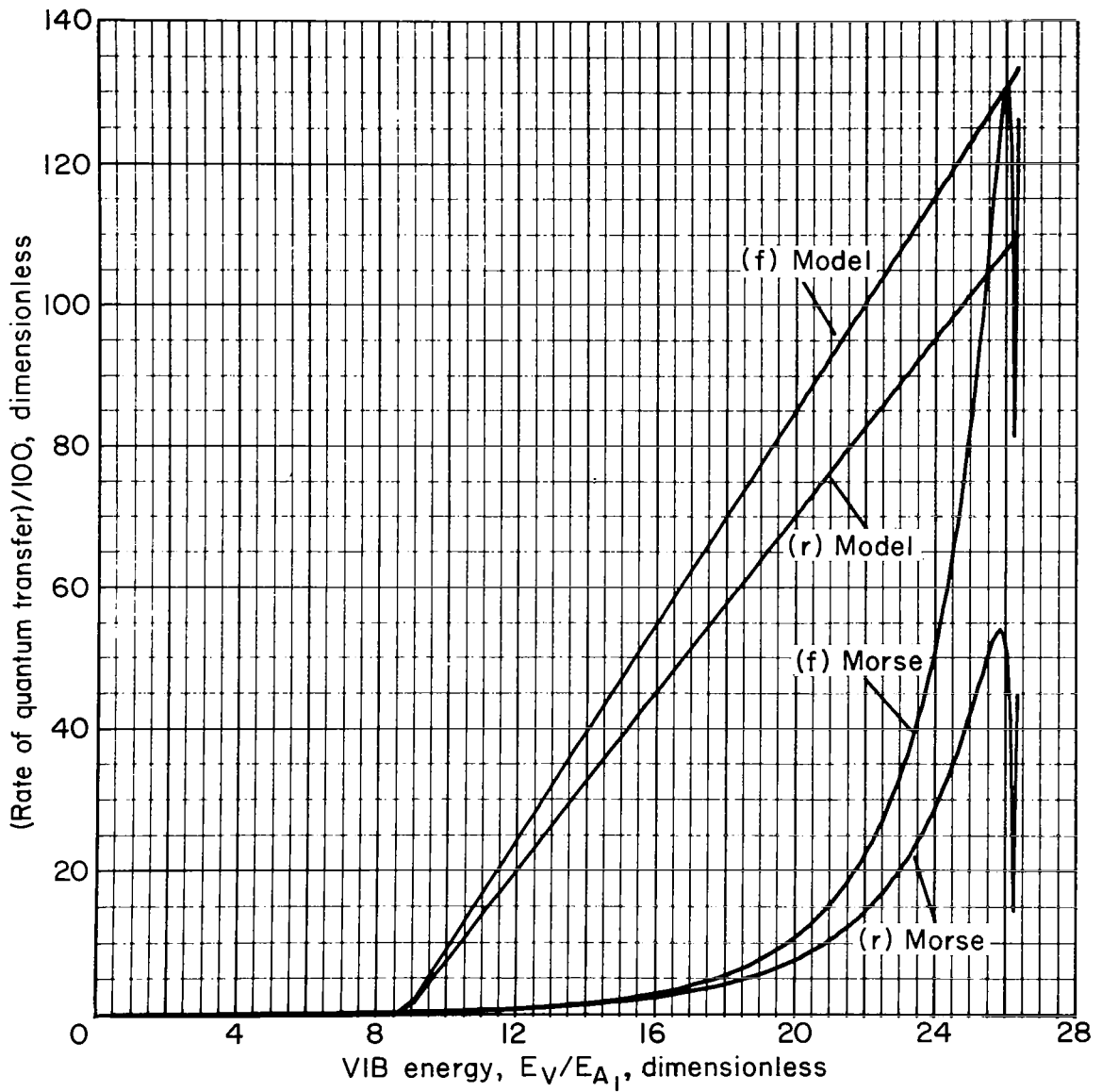
$$= \frac{\left[\frac{E_{v,v-1} k_{v,v-1}}{k_{1,0}} \exp\left(\frac{\Theta_{A_2}}{T}\right) \right]_{v=v_{m_F}} - a E_{A_1}}{E_{v_{m_F}} - E_a} \quad (\text{B23b})$$

and

$$v_{m_F} = \frac{1}{2x_0} \left[1 - \frac{2x_0}{\alpha_F(T)} \right]$$

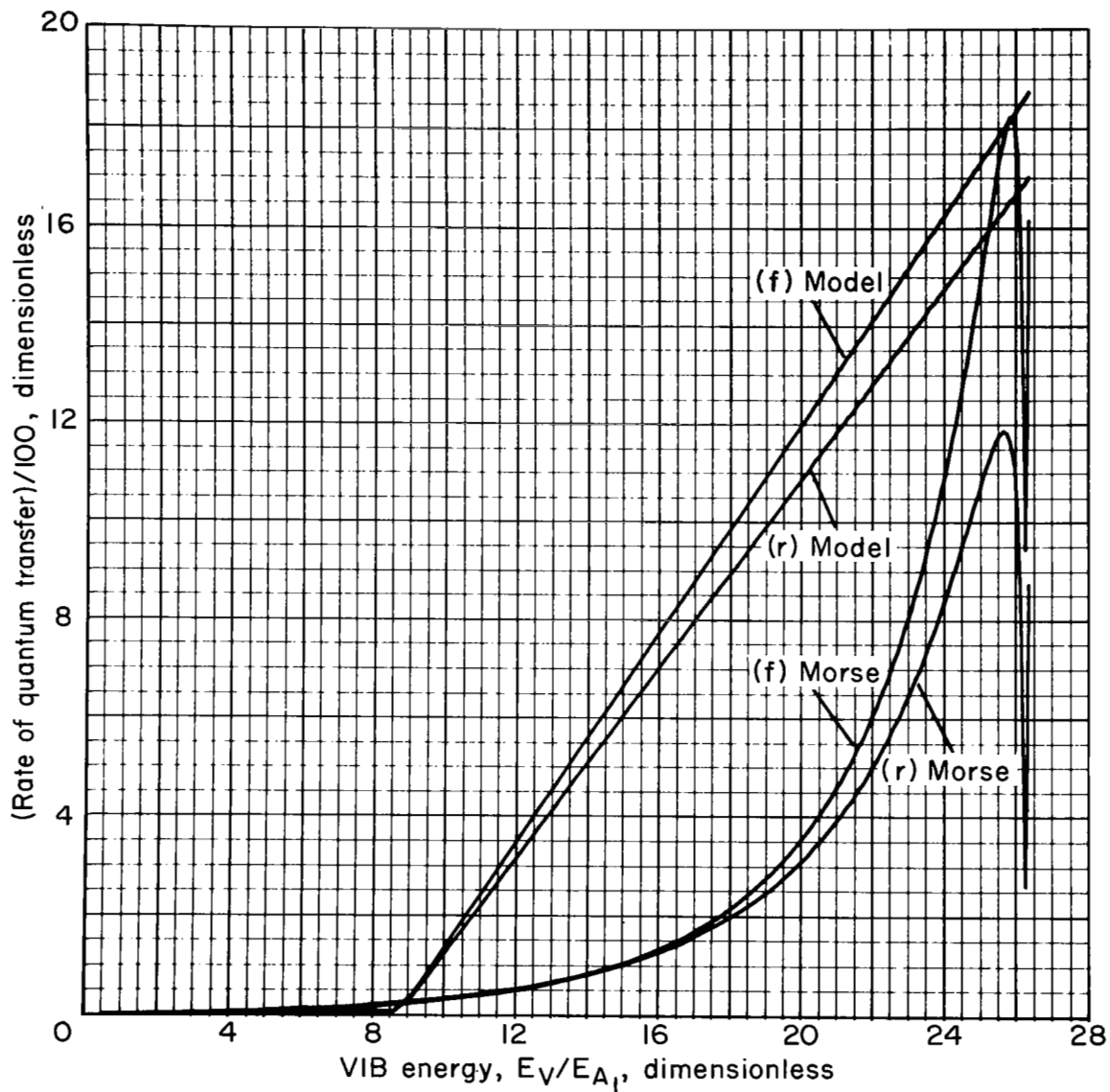
The results from replacing χ_R by χ_F is illustrated in figures B-5. The labeling has the same meaning as in the previous figures. Here we observe that the curves labeled $(f)_{\text{Model}}$ intersect near the maximum of the curves $(f)_{\text{Morse}}$ where in the previous four figures the curves labeled $(r)_{\text{Model}}$ intersected near the maximum of those labeled $(r)_{\text{Morse}}$. Temperature dependence is similar in that the behavior at low temperatures (see fig. B-5a) results in a relatively poor approximation. We also note that the differences between the curves subscripted "Model" and those subscripted "Morse" become less at the higher temperatures, and the approximated rate relations are more accurate.

The quantities χ_R and χ_F are plotted versus temperature in figure B-6, and their differences may be observed by a comparison of these curves. We see that the differences are greatest at the lower temperatures (about a factor of 4 at about 1000° K) and become less at the higher temperatures. At about 24,000° K, χ_R and χ_F are approximately equal. It is worth pointing out again that the χ quantities, defined as the ratio $k_{i,0}^{(2)}/k_{i,0}^{(1)}$ (see eq. (B16d)), are also a measure of the effect of molecular anharmonicity on the rate processes. For a harmonic oscillator we have $\chi_F = \chi_R = 1$, since in this case both $E_{v,v-1}$ and $k_{v-1,v}$ are linear functions of v . It then follows that for those temperatures where the $\chi(T)$ are large, the effect of molecular anharmonicity is expected to be greatest; conversely, when the $\chi(T)$ are small, the effects of anharmonicity are least. We thus observe in figure B-6 that the effects of molecular anharmonicity are greatest at the lower temperatures; although they still exist at the higher temperatures, they are greatly reduced. This result is not unexpected if one considers that when $kT \gg E_{v,v-1}$ (regardless of v) then the effect of the smaller level spacing is essentially lost in the collision process. This should not imply that the rate of energy transfer is less at higher temperatures. The quantity $\chi(T)$ does not include the effect of $k_{i,0}^{(1)}$ (see, e.g., eq. B14a); $k_{i,0}^{(1)}$ increases with increasing temperature.



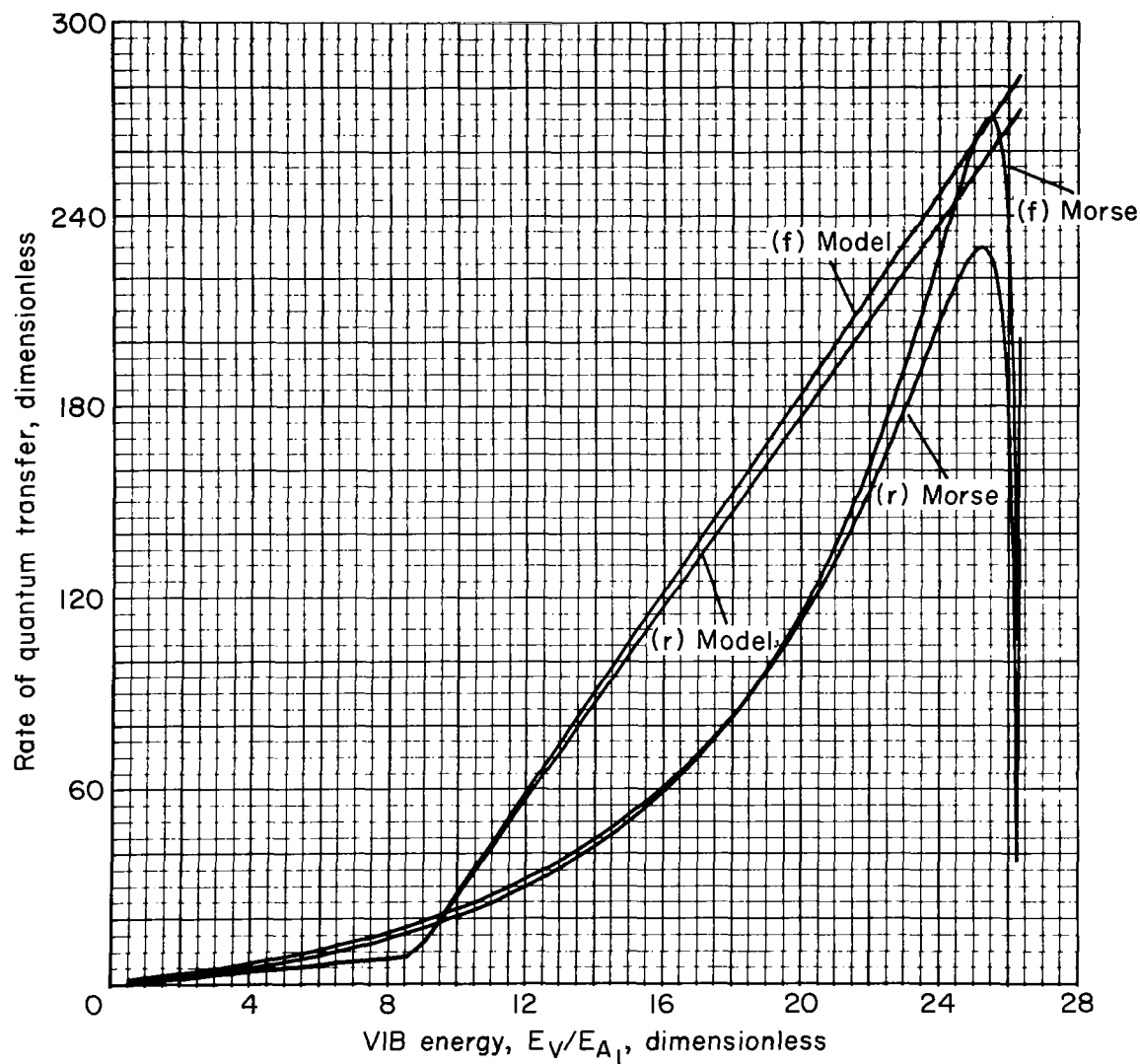
(a) $T = \Theta_{A_1}$

Figure B-5. Comparison of the "rate of quantum transfer" quantity, (χ_F)



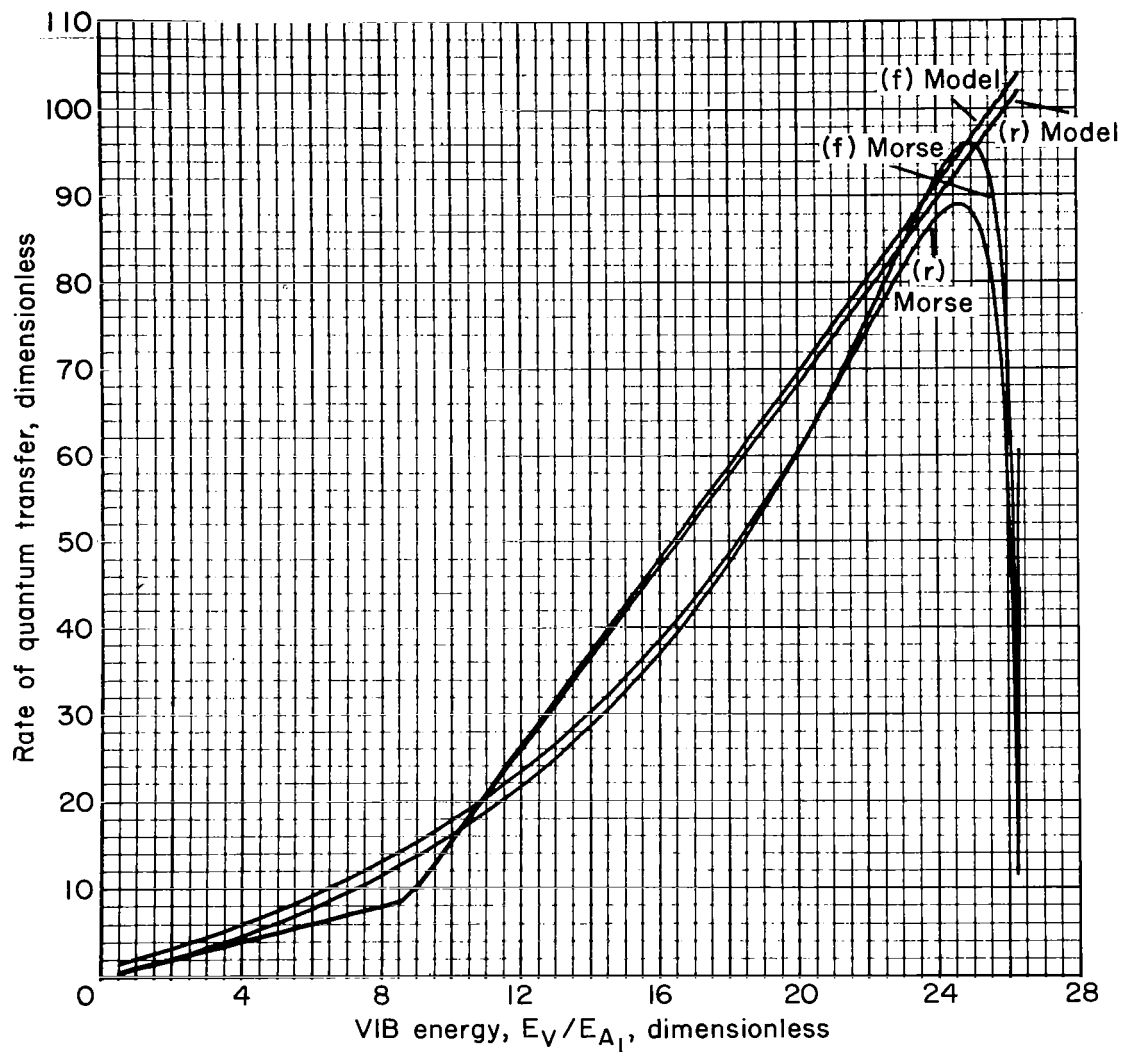
(b) $T = 2\theta_{A_1}$

Figure B-5 Continued



(c) $T = 5 \Theta_{A_1}$

Figure B-5 Continued



(d) $T = 10 \Theta_{A_1}$

Figure B-5 Continued

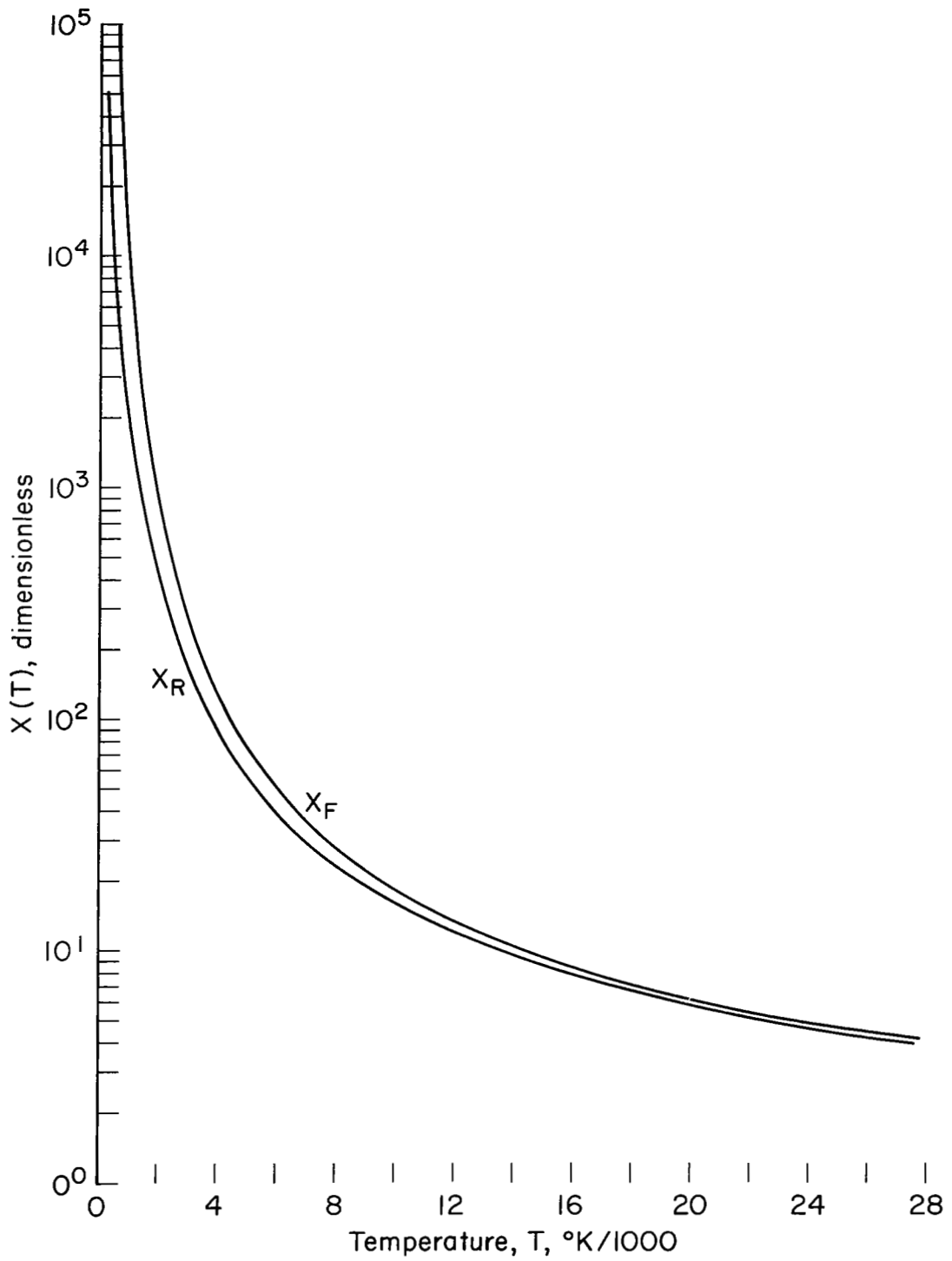


Figure B-6. Plots of the parameter $\chi(T)$ versus temperature

To conclude this section, the rate parameters defined in Chapter II by equations (II-39), (II-56), (II-68), and (II-73) will be rewritten in terms of the quantities derived here. We obtain

$$k_{\text{R}}^{(1)}(T_{\text{B}}, T) = \frac{k_{\text{b}, \text{b}-1}(T)}{Q_{\text{B}}'(T_{\text{B}})} \quad (\text{B24a})$$

$$\begin{aligned} k_{\text{F}}^{(1)}(T_{\text{A}}, T) &= \frac{k_{\text{b}-1, \text{b}}(T)}{Q_{\text{A}}(T_{\text{A}})} \exp\left(-\frac{E_{\text{b}-1}}{kT_{\text{A}}}\right) \\ &= \frac{k_{\text{b}, \text{b}-1}(T)}{Q_{\text{A}}(T_{\text{A}})} \exp\left[\frac{E_{\text{A}_2}}{k}\left(\frac{1}{T_{\text{A}}} - \frac{1}{T}\right) - \frac{E_{\text{b}}}{kT_{\text{A}}}\right] \end{aligned} \quad (\text{B24b})$$

$$\begin{aligned} \tau_{\text{A}_1} &= \left\{ m \hat{k}_{1,0}^{(1)} \left[1 - \exp\left(-\frac{E_{\text{A}_1}}{kT}\right) \right] \right\}^{-1} \\ &= \left\{ \rho \gamma_{\text{m}} k_{1,0}^{(1)} \left[1 - \exp\left(-\frac{E_{\text{A}_1}}{kT}\right) \right] \right\}^{-1} \end{aligned} \quad (\text{B25a})$$

$$\begin{aligned} \tau_{\text{B}} &= \left\{ m \hat{k}_{1,0}^{(2)} \left[1 - \exp\left(-\frac{E_{\text{A}_2}}{kT}\right) \right] \right\}^{-1} \\ &= \left\{ \rho \gamma_{\text{m}} k_{1,0}^{(2)} \left[1 - \exp\left(-\frac{E_{\text{A}_2}}{kT}\right) \right] \right\}^{-1} \end{aligned} \quad (\text{B25b})$$

$$\frac{\tau_{\text{A}_1}}{\tau_{\text{B}}} = \chi(T) \frac{1 - \exp\left(-\frac{E_{\text{A}_2}}{kT}\right)}{1 - \exp\left(-\frac{E_{\text{A}_1}}{kT}\right)} \quad (\text{B25c})$$

$$\Delta(T) = E_{\text{a}} \left[1 - \frac{\chi^{-1}(T)}{1 - \left(1 - \frac{E_{\text{A}_2}}{E_{\text{A}_1}}\right)/a} \right] \quad (\text{B26})$$

where

$$\frac{k_{\text{b}, \text{b}-1}}{k_{1,0}^{(1)}(T)} = (b - a) \chi(T) + a \frac{E_{\text{A}_1}}{E_{\text{A}_2}} \quad (\text{B27})$$

and where $\chi(T)$ is given by either

$$\begin{aligned} \chi_R(T) &= \frac{\left[E_{v,v-1} \frac{k_{v,v-1}}{k_{1,0}} \right]_{v=v_{mR}} - a E_{A_1}}{E_{v_{mR}} - E_a} \\ &= \frac{\left[E_{v,v-1} v \exp[(v-1)\alpha_R] \right]_{v=v_{mR}} - a E_{A_1}}{E_{v_{mR}} - E_a} \end{aligned} \quad (B28a)$$

or

$$\begin{aligned} \chi_F(T) &= \frac{\left[E_{v,v-1} \frac{k_{v-1,v}}{k_{0,1}} \right]_{v=v_{mF}} \exp\left(\frac{\Theta_{A_2} - \Theta_{A_1}}{T}\right) - a E_{A_1}}{E_{v_{mF}} - E_a} \\ &= \frac{\left\{ E_{v,v-1} v \exp\left[(v-1)\alpha_F + \frac{\Theta_{A_2} - \Theta_{A_1}}{T}\right] \right\}_{v=v_{mF}} - a E_{A_1}}{E_{v_{mF}} - E_a} \end{aligned} \quad (B28b)$$

where

$$v_{mR} = \frac{1}{2x_0} \left[1 - \frac{2x_0}{\alpha_R} \right] \quad (B29a)$$

$$v_{mF} = \frac{1}{2x_0} \left[1 - \frac{2x_0}{\alpha_F} \right] \quad (B29b)$$

The temperature-dependent parameters α_F and α_R are defined by equations (B10a) and (B18b).

APPENDIX C

PREFERENTIAL DISSOCIATION MODEL OF MARRONE AND TREANOR

Marrone and Treanor (58) introduced a model that yields the vibrational-level dissociation rates in a useful and rational manner. Their model, referred to as the "preferential dissociation model", is relatively simple and introduces few parameters into the problem of vibration-dissociation coupling. Furthermore, it is consistent with recent theoretical and experimental evidence that the dissociation probability is higher for higher vibrational levels. The derivation given here is slightly different from that in the original paper, the most significant difference being that here the level dissociation rates $\hat{k}_{v,N}$ are assumed to be negligibly small for all vibrational levels below some level designated b . No such level was introduced in the original model. The final equations remain very similar to those of Marrone and Treanor.

In the derivation a function p_v is introduced that represents the fraction of dissociation events taking place from the v th level. Thus the sum of p_v over all levels is equal to 1. The function p_v is given by

$$p_v = \frac{\hat{k}_{v,N} n_{v,m}}{\hat{k}_{F,N} n_{B,m}} \quad (C1)$$

where

$$\hat{k}_{F,N} n_{B,m} = \sum_{v=b}^{N-1} \hat{k}_{v,N} n_{v,m} \quad (C2)$$

From collision theory (e.g., see p. 215 in 97), one obtains

$$p_v = C \frac{Z(n_{v,m})}{Z(n_{B,m})} \frac{M(D-E_v)}{M(D-E_b)} \frac{f(n_{v,m})}{f(n_{B,m})} \quad (C3)$$

where the various quantities are defined as follows:

$Z(m,n)$ bimolecular collision rate associated with a mixture of gas particles m and n $\left(n_m n_n d_{nm}^2 \left(\frac{8\pi kT}{\mu_{mn}} \right)^{\frac{1}{2}} \right)$;

$M(e)$ activation or energy factor, that is, the fractional number of collisions with line-of-center kinetic energy greater than the activation energy $e \left(\exp\left(-\frac{e}{kT}\right) \right)$;

$f(n,m)$ steric factor, that is, the fraction of sufficiently energetic collisions between the gas particles m and n that actually result in a dissociation;

C normalizing constant evaluated such that $\sum_{v=b}^{N-1} p_v = 1$.

If we assume that the collision diameter of a molecule is unaffected by its vibrational state, then we have $Z(n_v, m)/Z(n_B, m) = n_v/n_B$. Furthermore, if the molecular population in the vibrational energy states is described by a Boltzmann distribution, the population ratio n_v/n_B is given by $\exp(-E_v/kT_B)/Q_B(T_B)$, where $Q_B(T_B)$ is the vibrational partition function associated with the upper states evaluated at the vibrational temperature, T_B , associated with these states (see Appendix A). The activation factor (e.g., see p. 218 in (97)) is given by $\exp(-e/kT)$ provided only the kinetic energy of the relative motion along the line of centers between two colliding particles is active in promoting a reaction requiring an activation energy e . The key to Marrone and Treanor's preferential dissociation model (58) is the hypothesis that the ratio of steric factors in equation (C3) increases exponentially with increasing vibrational quantum number; that is,

$$\frac{f(n_v, m)}{f(n_B, m)} = \exp\left(-\frac{D_0 - E_v}{kT_U}\right) \quad (C4)$$

where T_U (with dimensions of temperature), describes how rapidly the dissociation probability drops off for low values of v .

With the above relations substituted into equation (C3), we obtain an alternative representation for p_v as follows:

$$p_v = C \frac{\exp \left[-\frac{E_v}{k} \left(\frac{1}{T_B} - \frac{1}{T} - \frac{1}{T_U} \right) \right]}{Q_B(T_B) \exp(E_b/kT)} \exp \left(-\frac{D_0}{kT_v} \right) \quad (C5)$$

The normalizing constant C is readily evaluated as

$$C = \frac{Q_B(T_B)}{Q_B(T_F)} \exp(E_b/kT) \exp(D_0/kT_U) \quad (C6)$$

and the quantity T_F is defined by

$$\frac{1}{T_F} = \frac{1}{T_B} - \frac{1}{T} - \frac{1}{T_U} \quad (C7)$$

The final form for p_v is obtained by the substitution of C into equation (C5) to obtain

$$p_v = \frac{\exp \left(-\frac{E_v}{kT_F} \right)}{Q_B(T_F)} \quad (C8)$$

This expression is very similar to that obtained by Marrone and Treanor. At equilibrium we note that $T_F = -T_U$ and $(p_v)_{eq} = \exp(E_v/kT_U)/Q_B(-T_U)$. In the case that $T_U \sim \infty$, we have $p_v = \exp(-E_v/kT_m)/Q_B(T_m)$ where $1/T_m = 1/T_B - 1/T$. This corresponds to nonpreferential dissociation (equal probability that dissociation occurs from any B-state vibrational level; see, e.g., 58 or 93). For the other extreme case where $T_U < T, T_B$, we have $p_v = \exp(E_v/kT_U)/Q_B(-T_U)$. We may approximate $Q_B(-T_U)$ by $\exp(E_b/kT_U) \exp[(N-b-1)E_{A_2}/kT_U]$ (see Appendix A), and after introducing the appropriate relations for E_b and E_v in terms of Θ_{A_2} from Appendix A, we have $p_v \approx \exp[(v-N+1)\Theta_{A_2}/T_U]$ where $N-1 \geq v \geq b$. In the limit that T_U is small compared to Θ_{A_2} we note that p_v is negligibly small for all v except $v = N-1$. This case corresponds

to highly preferential dissociation—in essence, dissociation involving only the very uppermost bound vibrational state N-1.

Substitution of the probability factor p_v into equation (C1) yields an expression for the level dissociation probability $\hat{k}_{v,N}$. This expression, however, is not yet useful since it introduces still another parameter into the problem, that is, the effective dissociation rate \hat{k}_F . We can relate \hat{k}_F to the quantity $\hat{k}_{F\text{eq.}}(T)$, the dissociation rate constant that would exist with vibrational equilibrium at the local translational temperature T . By definition the level dissociation rate, $\hat{k}_{v,N}$, depends only on the translational temperature and, hence, is independent of the number of molecules in any of the B grouping of vibrational levels, that is, the vibrational temperature T_B . It follows then from equation (C1), that the level transition probability may be defined by either of the following pair of equations:

$$\hat{k}_{v,N} = (\hat{k}_F)_{\text{eq}} (p_v)_{\text{eq}} \frac{Q_B(T)}{\exp\left(-\frac{E_{B,v}}{kT}\right)} \quad (\text{C9a})$$

$$= \hat{k}_F p_v \frac{Q_B(T_B)}{\exp\left(-\frac{E_{B,v}}{kT_B}\right)} \quad (\text{C9b})$$

Equating these relations, we obtain

$$V(T_B, T) \equiv \frac{\hat{k}_F}{\hat{k}_{F\text{eq.}}} = \frac{Q_B(T)}{Q_B(T_B)} \frac{(p_v)_{\text{eq}}}{p_v} \exp\left[\frac{E_{B,v}}{k}\left(\frac{1}{T} - \frac{1}{T_B}\right)\right] \quad (\text{C10a})$$

$$= \frac{Q_B(T)Q_B(T_F)}{Q_B(T_B)Q_B(-T_U)} \quad (\text{C10b})$$

The factor $V(T_B, T)$ thus defined is called the "vibrational coupling factor." At equilibrium, where $T_B = T$, we have $V(T, T) = 1$. The parameter $\hat{k}_{F\text{eq.}}(T)$ is, as already mentioned, the equilibrium dissociation rate.

The level recombination rate expression $\hat{k}_{N,v}(T)$ is obtained by invoking "detailed balancing," that is, by assuming that $\hat{k}_{N,v}(T)$ is not affected by the degree of vibrational nonequilibrium. The appropriate expression can be found by requiring that the rate at which vibrationally excited molecules are formed as a result of atom recombination (and having energy corresponding to the v th quantum state) be identically equal to the rate that such molecules are dissociated (at equilibrium). There results

$$\hat{k}_{N,v}(T) = (\hat{k}_{v,N})_{\text{eq}} \left(\frac{n_v}{n_a^2} \right)_{\text{eq}} \quad (\text{C11a})$$

$$= \frac{(\hat{k}_{v,N})_{\text{eq}}}{\hat{\kappa}_B(T)} \left(\frac{n_v}{n_B} \right)_{\text{eq}} = \frac{\hat{k}_F(T)_{\text{eq}}}{\hat{\kappa}_B(T)} (p_v)_{\text{eq}} \quad (\text{C11b})$$

where $\kappa_B(T)$ is the "partial" thermodynamic equilibrium constant associated with the reaction and is defined by

$$\hat{\kappa}_B(T) = \left(\frac{n_a^2}{n_B} \right)_{\text{eq}} = \left(\frac{n_a^2}{n} \right)_{\text{eq}} \left(\frac{n}{n_B} \right)_{\text{eq}} \quad (\text{C12})$$

The "partial" equilibrium constant $\kappa_B(T)$ is not the same as the thermodynamic equilibrium constant normally encountered in studies of diatomic molecular dissociation, but differs by the factor $n/n_B = Q(T)/Q_B(T)$; that is,

$$\hat{\kappa}_B(T) = \frac{Q_v(T)}{Q_B(T)} \hat{\kappa}(T) \quad (\text{C13a})$$

$$= \frac{Q_v(T)}{Q_B(T)} \hat{\kappa}(T) \exp\left(\frac{E_b}{kT}\right) \quad (\text{C13b})$$

where $Q_v(T)$ is the complete vibrational partition function associated with the diatomic molecular species and $\hat{\kappa}(T)$ is the normally encountered equilibrium constant (e.g., see eq. (A6)).

To recapitulate, the form of the equations representing the level dissociation and recombination rates will be set down. These equations, obtained by appropriate substitution of equations (C9) and (C10), are as follows:

$$\hat{k}_{v,N} = \hat{k}_F p_v \frac{n_B}{n_v} \quad (C14a)$$

$$= \hat{k}_{F\text{eq.}(T)} p_v V(T_B, T) \frac{n_B}{n_v} \quad (C14b)$$

$$\hat{k}_{N,v} = \frac{\hat{k}_{F\text{eq.}(T)}}{\kappa_B(T)} (p_v)_{\text{eq}} \quad (C14c)$$

where p_v is defined by equation (C8).

APPENDIX D

A STUDY OF THE EFFECT OF THE TRUNCATION FACTOR: PROBLEM OF UNCOUPLED VIBRATIONAL RELAXATION

The simplicity of the Landau-Teller vibrational relaxation equation as obtained by Bethe and Teller (see Chapter I and also (8)) is noteworthy. Furthermore, as a result of the theoretical investigations of Rubin, Montroll, and Shuler (62, 75, 76, 81) and the favorable agreement with experiment the equation has received widespread acceptance. Some investigators, however, (e.g., 57, 58) have altered the original formulation by the use of accurate thermodynamic vibrational-energy quantities with the aim of generalizing the equation to account (1) for the effects of anharmonicity on the vibrational energy and (2) for the fact that there are only a finite number of vibrational energy levels. Such generalizations have been heuristic in that no attempt was made to justify their use in a formal manner on the basis of the master equations. Such "improvements" are questionable and, furthermore, may lead to erroneous conclusions (57) concerning the effects of anharmonicity.

To exemplify this the differences obtained by the inclusion of the truncation factor in the vibrational relaxation terms will be investigated for the problem of uncoupled vibrational relaxation. The effects to be discussed are somewhat hypothetical in that when the differences are sufficiently large the effects of dissociation would also be important and should not really be ignored. We are concerning ourselves then only with the study of the vibrational relaxation terms.

We shall compare vibrational relaxation as given by the previously used equation

$$\frac{dq_V(T_V)}{dt} = \frac{q_V(T) - q_V(T_V)}{\tau(T)} \quad (D1)$$

with that given by

$$\begin{aligned} \frac{dq_V(T_V)}{dt} &= \frac{[q_V^\infty(T) - q_V^\infty(T_V)]}{\tau} \mathcal{L}_V(T_V) \\ &= \frac{\left[q_V(T) \frac{\mathcal{L}_V(T_V)}{\mathcal{L}_V(T)} - q_V(T_V) \right]}{\tau(T)} \end{aligned} \quad (D2a)$$

which is the relaxation equation obtained in Chapter II, except that the effects of anharmonicity are ignored and only the truncation factor is included (see eq. (II-106)). In this equation the function q_V is that given by equation (A42). Its value of $N = 26$ yields a characteristic dissociation temperature Θ_D that is approximately correct for molecular oxygen ($\Theta_D = 59,368^\circ \text{K}$). It must be emphasized that the effect of anharmonicity is not being taken into account in this investigation. The comparisons that will be made would show even larger differences if such effects were accounted for in the manner discussed in Chapter II.

Equation (D1) can be readily integrated to obtain

$$\left(\frac{t}{\tau}\right)_2 = -\text{Log} \left[\frac{q_V(T_V) - q_V(T)}{q_V(T_0) - q_V(T)} \right] \quad (D3)$$

where T_0 is the initial temperature (i.e., the temperature at $t/\tau = 0$). We can also solve equation (D2a) formally by quadrature as follows:

$$\left(\frac{t}{\tau}\right)_1 = \int_{T_0}^{T_V} \frac{c_V(x) dx}{q_V(T) \frac{\mathcal{L}_V(x)}{\mathcal{L}_V(T)} - q_V(x)} \quad (D4)$$

This integral can be evaluated numerically.

The solutions are compared in figures D-1 and D-2. Here the abscissa is the dimensionless time t/τ and the ordinate is the dimensionless vibrational temperature T_V/T . The dashed-line curves are obtained from equation (D3) and the solid-line curves from equation (D4) with the integration done numerically using an electronic computer. We shall presume that our problem is that of studying uncoupled vibrational relaxation behind a normal-shock wave (of course, ignoring effects of dissociation) in a dilute mixture of oxygen molecules in an inert diluent of argon atoms. The fluid temperature T is impulsively changed by the shock wave from ambient T_0 upstream of the shock to some large constant value T immediately downstream of the shock. For shock temperatures of $T = 4000^\circ \text{K}$ (not plotted), there is little perceptible difference between the two solutions. At the higher shock temperatures, however, the introduction of the truncation factor causes more rapid vibrational relaxation. This is illustrated by the fact that the solid-line curves are closer to the equilibrium asymptote ($T_V/T = 1$) than the dashed line curves regardless of the time t/τ . This is perhaps better illustrated by the following table, where the relaxation time required for the solutions to approach to 10 percent of their equilibrium value is compared.

Table D-1
Comparison of characteristic 90-percent relaxation time

T	$(t/\tau)_1$	$(t/\tau)_2$
8,000	2.12	2.28
12,000	1.94	2.51
16,000	1.75	2.75

We see that the stronger shocks (indicated by the larger values for T) yield the greater differences. There is nearly a factor of 2 difference in the last case listed. These differences occur only because the ratio $\mathcal{L}_V(T_V)/\mathcal{L}_V(T)$ is not unity (see discussion in Chapter II). Changing the functions q_V in equation (D3) affects primarily the driving force $q_V(T_V) - q_V(T)$ and would be expected to have only a negligible effect on the relaxation time. Hence, it may

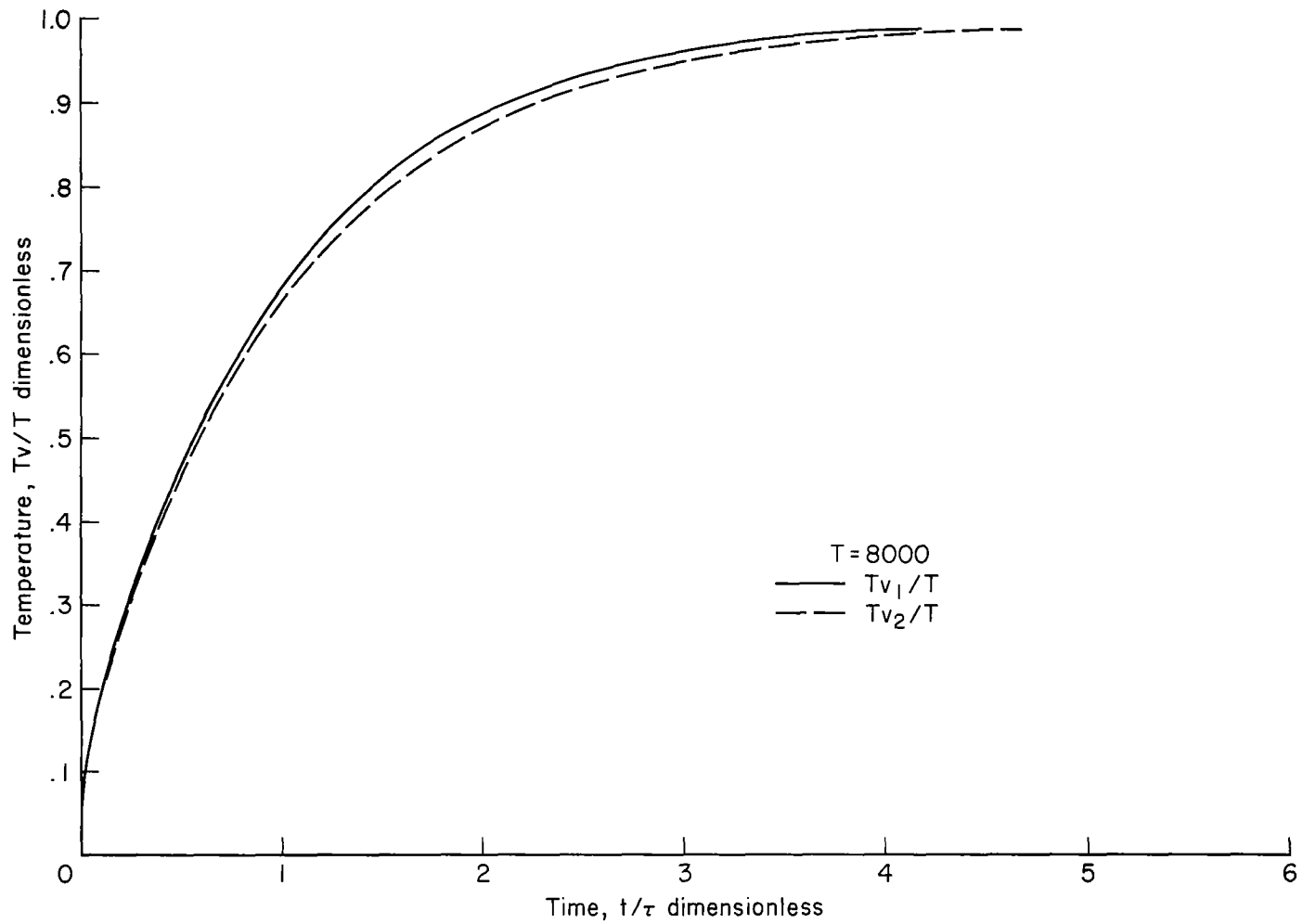
be anticipated that investigations, such as that conducted by Maillie and Hsu (57), will show only a minor effect of "anharmonicity."

The present model contains a number of terms of the type given by equation (D2a) (e.g., see eq. II-95). The parameter a , which is equivalent to N in the case of the first term of equation (II-95a), has values less than 26, and the differences exemplified in table D2 are even greater. Figures D-2 illustrate the differences when $a = 11$. (The quantity q_V has the same functional form as given above except that the parameter N is denoted instead by a ; compare, e.g., eq. (A27) and (A42).) In this case we obtain the characteristic relaxation times given by the following table, where the values have the same meaning as previously:

Table D-2
Comparison of characteristic 90-percent relaxation time.

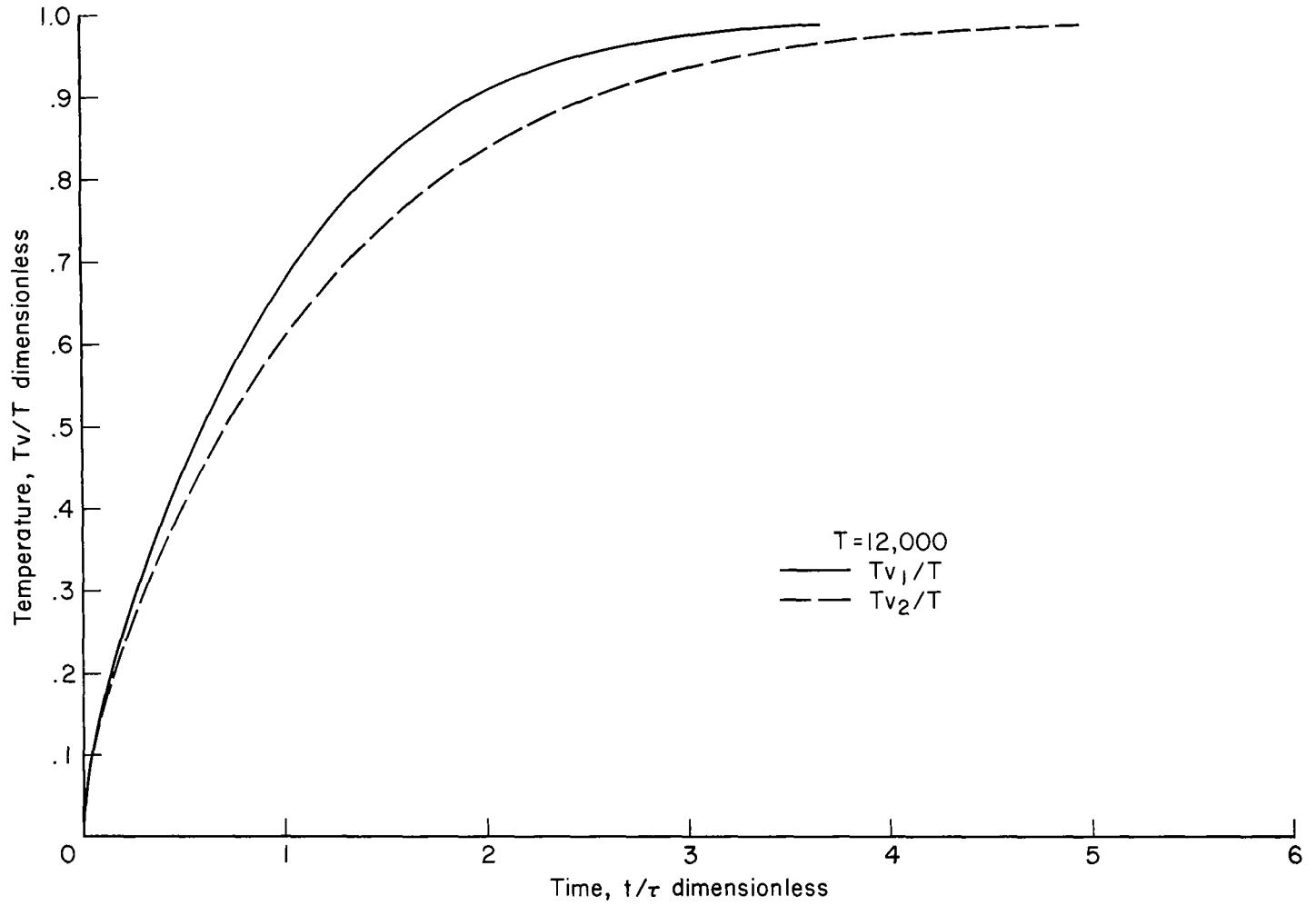
T ($^{\circ}\text{K}$)	$(t/\tau)_1$	$(t/\tau)_2$
8,000	1.50	2.40
16,000	0.98	3.60

At the higher temperature the values differ by nearly a factor of four and the effect of the truncation factor is even greater.



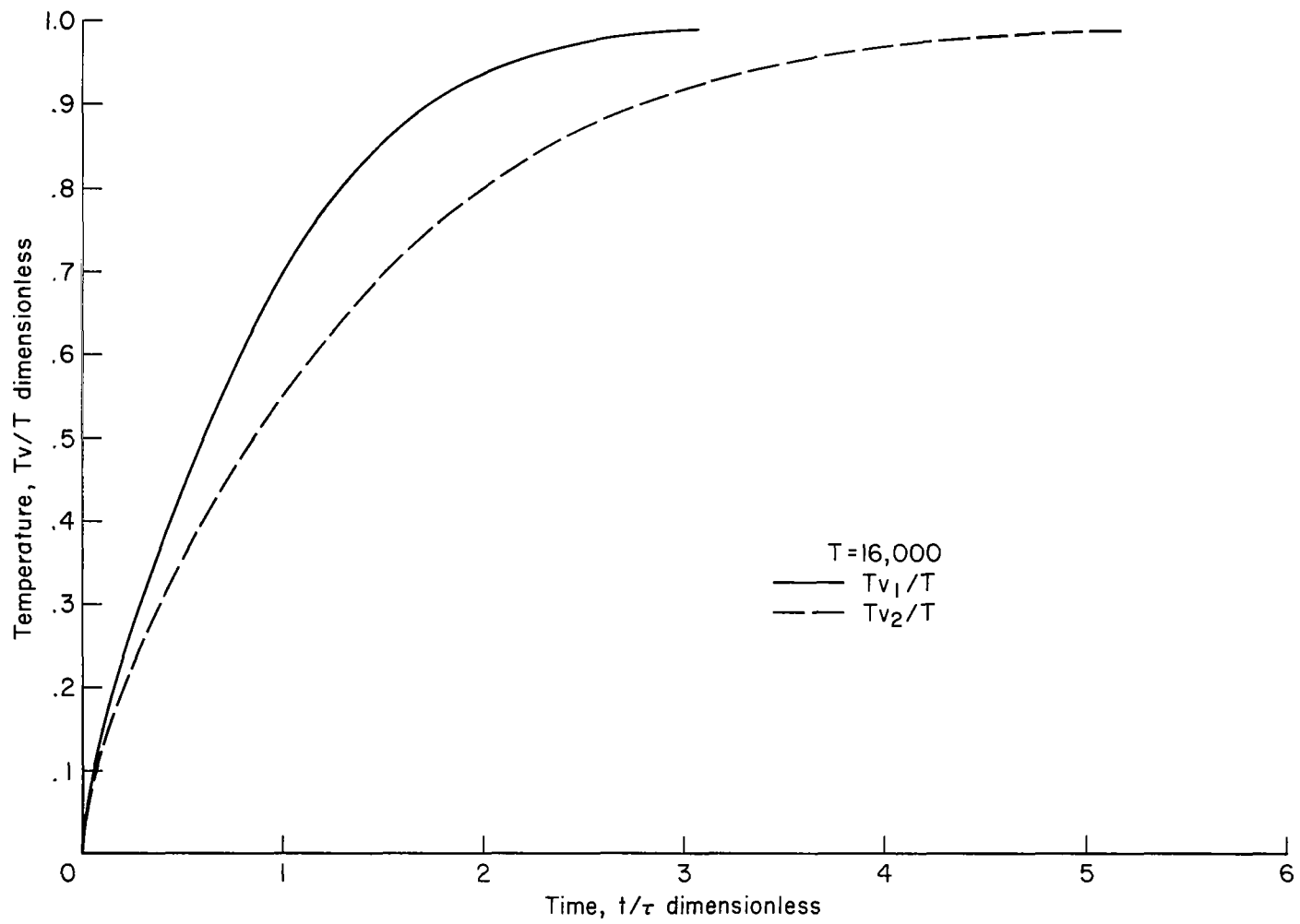
(a) $T = 8,000^\circ \text{K}$

Figure D-1. Comparison of relaxation behavior for case of uncoupled vibrational relaxation where a representative number of vibrational energy states are included



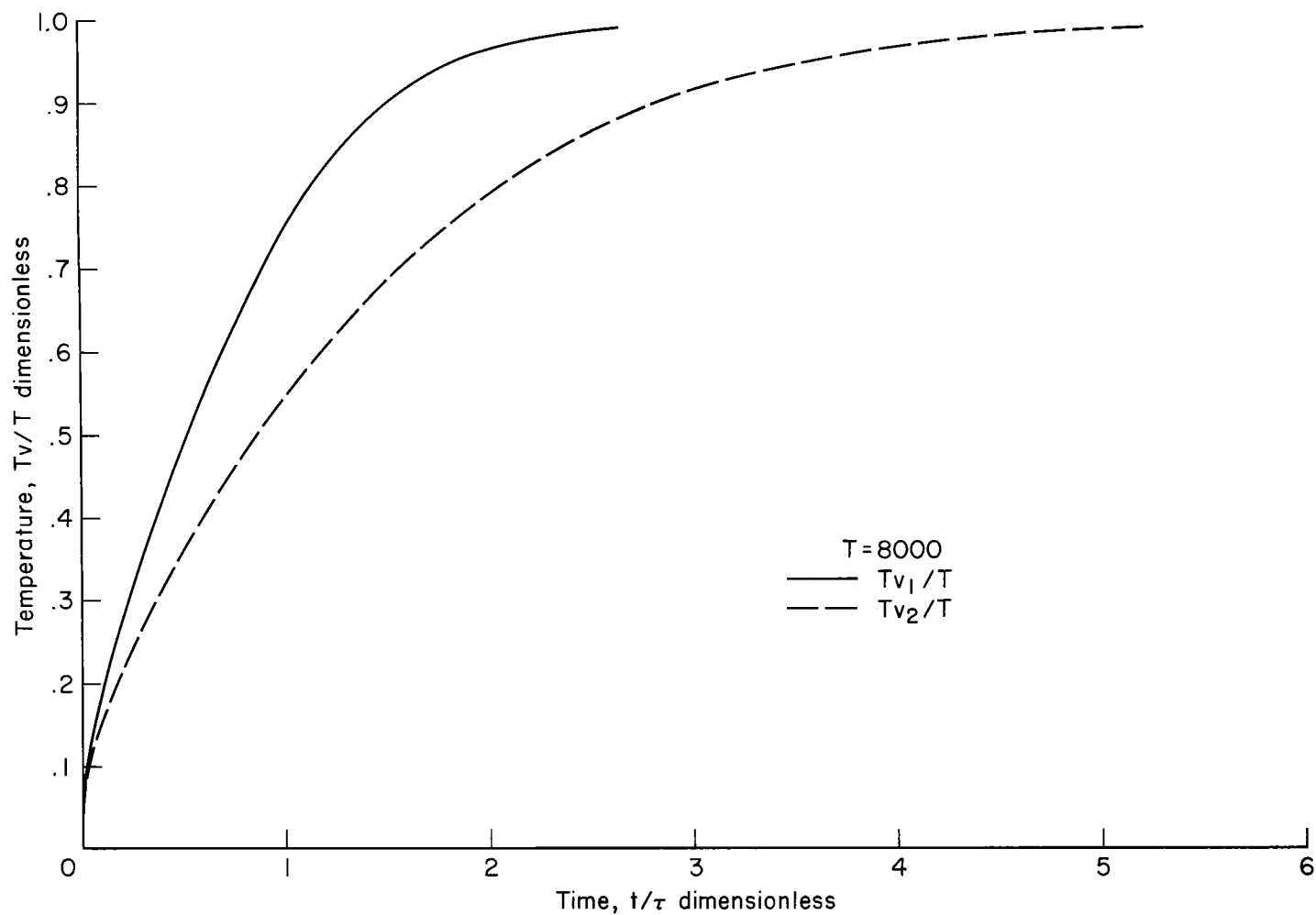
(b) $T = 12,000^\circ \text{K}$

Figure D-1 Continued



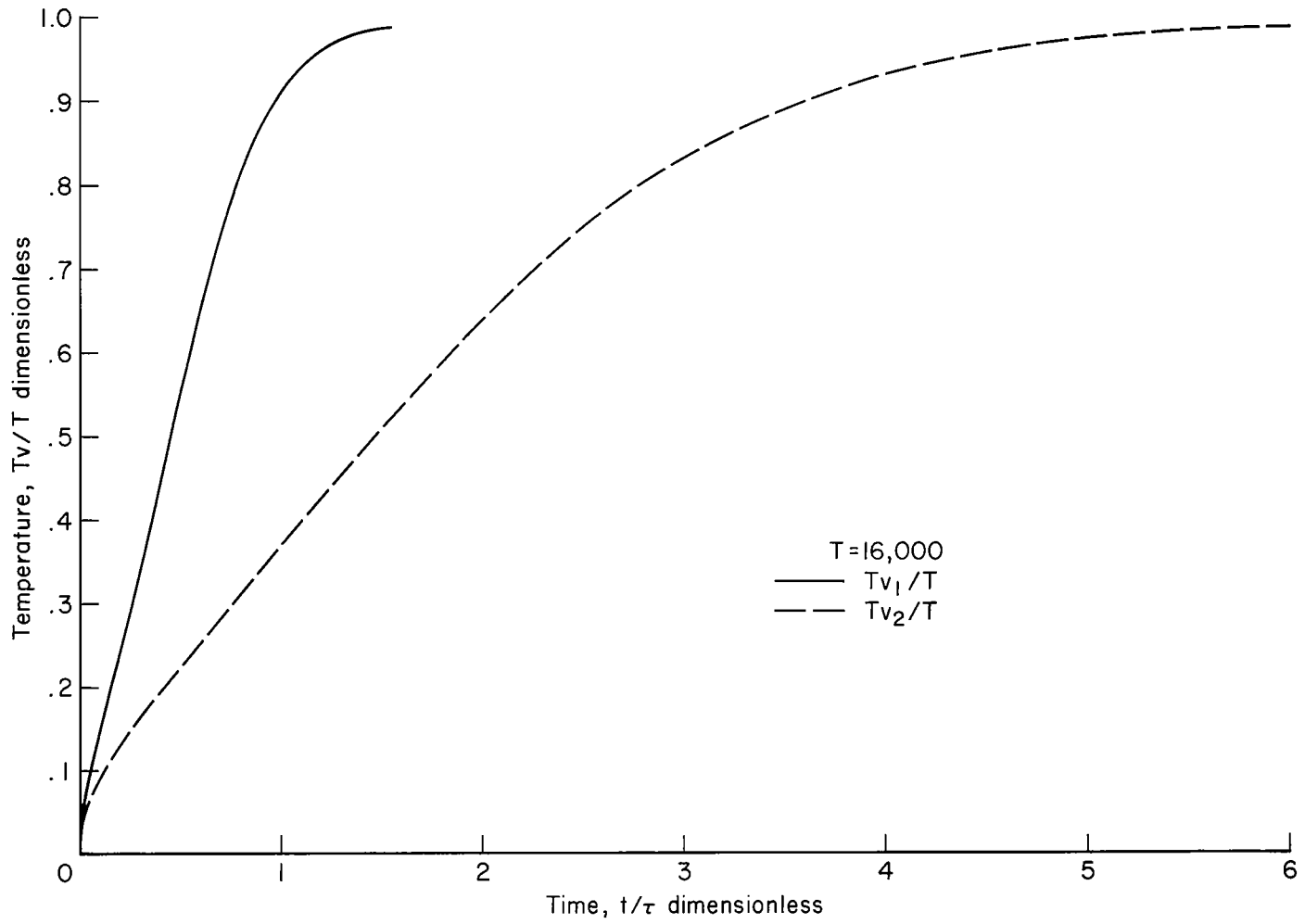
(c) $T = 16,000^\circ \text{K}$

Figure D-1 Continued



(a) $T = 8,000^\circ \text{K}$

Figure D-2. Comparison of relaxation behavior for uncoupled vibrational relaxation where only a portion of the vibrational energy states are included



(b) $T = 16,000^\circ \text{K}$

Figure D-2 Continued

APPENDIX E

DEVELOPMENT OF THE NUMERICAL PROCEDURE FOR SOLVING THE MODEL AND FLUID-FLOW EQUATIONS[†]

(E-1). Introductory Comments

The differential equations that describe the internal properties of the model molecule were derived in Chapter II; special solutions not requiring integration were obtained and discussed in Chapter III. To obtain the "complete" solutions described in Chapter IV necessitates a coupling of the model rate equations with the fluid-flow equations and requires a fairly involved numerical procedure for integrating these equations. In particular, the model equations will here be coupled with the one-dimensional fluid-dynamic equations to obtain a system of nine first-order nonlinear ordinary differential equations. A discussion will then be given of the numerical procedure used to integrate these equations.

It is beyond the scope of this paper to analyze the model equations for all possible flow fields. One can infer the behavior along streamlines in a complex flow field, however, by reasoning from the results obtained for shock waves and nozzle flow. Furthermore, considerable data are available for such one-dimensional and quasi-one-dimensional flows, and results may be compared quantitatively both with experimental data and with other vibration-dissociation models. Although the time-independent one-dimensional fluid problem is one of the simplest to attack, such studies are not without difficulty (18, 29, 77). The major problem is that of integrating a system of equations containing greatly

[†]The author wishes to draw attention to the many valuable discussions he has had with his colleagues Mr. Harvard Lomax and Dr. Harry E. Bailey, of NASA Ames Research Center, concerning the numerical integration of the model equations given in this paper. The numerical work was undertaken while they were completing the research for several papers that are now published (51, 52, 53, 53a, 54). The discussion here may be considered a brief summary of the material relevant to this work and contained in those papers.

different time constants. This problem is often referred to as that of integrating "stiff" equations (29, 25); the reason for this designation will be apparent later.

(E-2). Fluid-Flow Equations

The model equations to be integrated are given by equations (II-110). These equations must be solved together with the fluid-dynamic equations to compute the properties of flow fields subject to vibration-dissociation coupling. We make the following basic assumptions:

- (1) The flow is steady, one-dimensional, inviscid, nonconductive, and nonradiating.
- (2) The fluid behaves as a mixture of perfect gases.

The equations for conservation of mass, momentum, and energy, respectively, are then

$$\rho v A(x) = M \quad (\text{E1a})$$

$$v dv + \frac{dp}{\rho} = 0 \quad (\text{E1b})$$

$$h + \frac{v^2}{2} = h_t \quad (\text{E1c})$$

where ρ and v are the mass density and speed of the fluid, and $A(x)$ is the cross-sectional area of a streamtube or a channel, a known function of the distance x measured along the flow, h is the specific enthalpy, and M and h_t are constants. In derivative form with x as the independent variable the equations are

$$\rho A \frac{dv}{dx} + v A \frac{d\rho}{dx} = -\rho v \frac{dA}{dx} \quad (\text{E2a})$$

$$\rho v \frac{dv}{dx} + \frac{dp}{dx} = 0 \quad (\text{E2b})$$

$$v \frac{dv}{dx} + \frac{dh}{dx} = 0 \quad (\text{E2c})$$

These constitute three equations for the four unknowns v , p , ρ , and h . To complete the set we must introduce additional relations specifying the thermochemical state of the gas. These are given by the thermal equation of state

$$p = \rho R_0 T \sum_j \gamma_j \quad (\text{E3a})$$

$$= \rho R Z T \quad (\text{E3b})$$

$$= \sum_i n_i k T \quad (\text{E3c})$$

and the caloric equation of state

$$h = \sum_j \gamma_j h_j \quad (\text{E4})$$

where R_0 is the universal gas constant (gas constant per mole), $R = R_0 \sum_j (\gamma_j)_0$ is the low-temperature specific gas constant (gas constant per unit mass), T is the local or "translational" temperature of the gas, $Z = \sum_j \gamma_j / \sum_j (\gamma_j)_0$ is the compressibility factor, γ_j is a measure of the concentration in units of moles per unit mass of gas, and the concentration variable subscripted 0 means "evaluated at low temperatures." The enthalpy per mole, h_j , is defined according to

$$h_j = R_0 T + e_j^*(T) + q_j(T_j) + h_{0j} \quad (\text{E5a})$$

$$= h_j^*(T) + \frac{\epsilon_j}{\gamma_j} \quad (\text{E5b})$$

where $e_j(T)$ is the internal energy per mole and h_{0j} is the heat of formation per mole (see Appendix G for values). The asterisk (*) is applied only when the subscript j denotes a molecular species and only when the vibrational

energy is considered separately in the internal energy or enthalpy. In this case the variable q_j , already defined, represents the vibrational energy per mole, and the variable ϵ_j the vibrational energy per unit mass. The functions $e_j(T)$ and their asterisk equivalents $e_j^*(T)$ are defined in Appendix A.

In general, we can consider the nonequilibrium thermochemical state to be specified by the two state variables ρ and T and the nonequilibrium variables γ_j and ϵ_j . In terms of these variables the equations of state have the functional form

$$p = p(\rho, T, \gamma_j) \quad (\text{E6a})$$

$$h = h(T, \gamma_j, \epsilon_j) \quad (\text{E6b})$$

With the state equations we can eliminate p and h from equations (E2). By introducing the rate equations (II-114) and (II-110), we then obtain the following complete set of differential equations:

$$\begin{aligned} \rho A \frac{dv}{dx} + v A \frac{d\rho}{dx} &= -\rho v A_x \\ \rho v \frac{dv}{dx} + \frac{\partial p}{\partial \rho} \frac{d\rho}{dx} + \frac{\partial p}{\partial T} \frac{dT}{dx} + \frac{\partial p}{\partial \gamma_A} \frac{d\gamma_A}{dx} + \frac{\partial p}{\partial \gamma_B} \frac{d\gamma_B}{dx} + \frac{\partial p}{\partial \gamma_a} \frac{d\gamma_a}{dx} &= 0 \\ v \frac{dv}{dx} + \frac{\partial h}{\partial T} \frac{dT}{dx} + \frac{\partial h}{\partial \gamma_A} \frac{d\gamma_A}{dx} + \frac{\partial h}{\partial \gamma_B} \frac{d\gamma_B}{dx} + \frac{\partial h}{\partial \epsilon_A} \frac{d\epsilon_A}{dx} + \frac{\partial h}{\partial \epsilon_B} \frac{d\epsilon_B}{dx} + \frac{\partial h}{\partial \gamma_a} \frac{d\gamma_a}{dx} &= 0 \\ \frac{d\gamma_A}{dx} &= Q^{\gamma_A} \\ \frac{d\gamma_B}{dx} &= Q^{\gamma_B} \\ \frac{d\epsilon_A}{dx} &= Q^{\epsilon_A} \\ \frac{d\epsilon_B}{dx} &= Q^{\epsilon_B} \\ \frac{d\gamma_a}{dx} &= Q^{\gamma_a} \end{aligned} \quad (\text{E7})$$

The Q's, with appropriate superscripts, denote the right-hand side of the rate equations (II-110), divided by the velocity v . These equations are written for one-dimensional flows in general. The results for flow behind a normal shock are obtained by setting the cross-sectional area constant, so that $dA/dx = A_x = 0$.

Equations (E7) can be written in matrix-vector form if the vector \vec{w}^* is introduced such that its transpose is $\vec{w}^{*T} = (v, \rho, T, \gamma_A, \gamma_B, \epsilon_A, \epsilon_B, \gamma_a)$, the vector \vec{c}^* such that $\vec{c}^{*T} = (\rho v A_x, 0, 0, Q^{\gamma_A}, Q^{\gamma_B}, Q^{\epsilon_A}, Q^{\epsilon_B}, Q^{\gamma_a})$, and the matrix $[B^*]$ having elements that are the coefficients of the derivatives $d\vec{w}^*/dx$. The result is

$$[B^*] \frac{d\vec{w}^*}{dx} = \vec{c}^* \quad (E8)$$

In the general case the matrix $[B^*]$ will become singular when the velocity v has the value corresponding to the local speed of sound a_f (e.g., see Appendix F). For this reason it is advantageous to introduce a new independent variable s defined such that

$$\frac{dx}{ds} \equiv x' = \sigma' \det ([B^*]) \quad (E9)$$

there σ is an arbitrary scaling constant that is equal to 1.0×10^{-20} for normal-shock flow and equal to -1.0×10^{-20} for nozzle flow. If we multiply both sides of equation (E8) by the product $\det ([B^*]) [B^*]^{-1}$ and use equation (E9),

$$\frac{d\vec{w}^*}{ds} \equiv \vec{w}^{*'} \equiv \vec{F}^* = \det ([B^*]) [B^*]^{-1} \vec{c}^* \quad (E10)$$

where $\det ([B^*]) [B^*]^{-1}$ is the adjoint of $[B^*]$. Finally, we define the new vectors \vec{w} and \vec{F} with one element more than their starred counterparts according to

$$\vec{w}^T = (\vec{w}^{*T}, x) \quad (E11a)$$

that is,

$$\vec{w}^T = (v, \rho, T, \gamma_A, \gamma_B, \epsilon_A, \epsilon_B, \gamma_a, x) \quad (\text{E11b})$$

and, further,

$$\vec{F}^T = (\vec{F}^*T, \det([B^*])) \quad (\text{E11c})$$

The explicit representations for the elements of these vectors are given in Appendix F, along with a minor alteration that facilitates the integration of the equations. With the abbreviated notation we then have a set of nine simultaneous equations represented in vector form by

$$\frac{d\vec{w}}{ds} \equiv \vec{w}' = \vec{F}(\vec{w}) \quad (\text{E12})$$

In this there is no explicit dependence of \vec{F} on the independent variable s ; that is, the equations may be described as being autonomous. These equations and their dependent variables are analogous to the set of equations and variables investigated by Lomax and Bailey (53, 53a). The equations are first-order, non-linear, ordinary differential equations and, in general, are not easily solved. In the next section the difficulties associated with these equations will be discussed, and the numerical procedure required for their solution will be described.

(E-3). Review of the Numerical Integration Methods

The equations described in the previous section, equations (E12), have features not unlike those of similar equations encountered in the study of effects of chemical nonequilibrium in fluid flow. Considerable research and computer time has been spent on the numerical integration of such systems of equations, and many different methods have been developed for this purpose (63, 68, 69, 95). These methods fall into two principal categories.

In one, the nonlinear differential equations are reduced to nonlinear difference equations by the substitution of difference-differential expressions for the derivatives, and the equations that result are then solved numerically (27, 28, 29, 30, 31, 32, 95). In the other, the differential equations are first linearized locally, and the resulting linearized form is solved either exactly (63, 68, 69, 72), approximately (26), or by finite-difference methods (96). On reviewing these methods one observes that three basic considerations occur regarding a comparison of the methods: accuracy, stability, and efficiency. The precise definitions of these terms are given in references 53, 53a, and 54. Rather than involve the present discussion with the intricacies of these definitions, it suffices to state that (1) a numerical method is accurate if it produces a solution that would agree with an analytical solution (if one could be obtained) within a controllable error (i.e., an error that may presumably be made small by reducing the size of the difference interval); (2) a method is stable if its solution does not diverge; and (3) a method is more efficient than other numerical methods if it requires less computer time to obtain the same numerical solution, numerical error being roughly the same.

From the experience gained with the various methods, instability appears to be the most troublesome problem in nonequilibrium studies in which conventional integration methods are used. An unstable method can often be made stable by reducing the integration step size (29). This, however, often decreases the efficiency of the method (many steps are required while the dependent variables change by only very small amounts). One also finds that methods that are always stable may not always be the most efficient or even the most accurate. The interplay of stability, accuracy, and efficiency is thus extremely important in numerical integration methods. Such considerations form the subject of three recently published papers by Lomax and by Lomax and Bailey (53, 53a, 54). Their recommended procedures will be followed here. Since an understanding of a few of their findings is essential for the proper utilization of the numerical procedure to be described, it is worthwhile to digress and discuss their theories briefly.

Lomax and Bailey have concentrated their investigations primarily on coupled linear ordinary differential equations. They also discuss, however, how their results extend to certain nonlinear systems; specifically, those that may be characterized as quasi-linear (i.e., in which the highest order derivative is linear). The equations of the previous section are of this type. To apply their theories it is advantageous first to obtain a linearized form of equations (E12). Consider the set of autonomous equations

$$\frac{d\vec{w}}{ds} = \vec{w}' = \vec{F}(\vec{w}) \quad (\text{E13})$$

where the elements, say F_i , have no explicit dependence on the independent variable s . If the right-hand side of the equation, F_i , is expanded about a local point, referenced as n where $s = nh$, we obtain

$$w'_i = (F_i)_n + \sum_j (w_j - w_{jn}) \left(\frac{\partial F_i}{\partial w_j} \right)_n + 0[(\vec{w} - \vec{w}_n)^2] \quad (\text{E14})$$

We define

$$a_{ij} = \left(\frac{\partial F_i}{\partial w_j} \right)_n \quad (\text{E15})$$

as the elements of the matrix $[A]_n$, where the subscript n signifies that the quantities are evaluated at the discrete reference point denoted by n . If $w = w_{n+1}$ we note that the higher-order terms in $\vec{w} - \vec{w}_n$ can be written $h^2[\vec{w}_{n+1} - \vec{w}_n]^2/h^2$ or $h^2[w'_n]^2$ plus terms of order $0(h^3)$. Thus in vector-matrix form we have

$$\vec{w}' = [A]_n \vec{w} + (\vec{F})_n - [A]_n \vec{w}_n + 0(h^2) \quad (\text{E16})$$

The above equation is, after higher-order terms are neglected, a locally linearized form of the original equations. Further, since the original equations were autonomous, the linearized equations have constant coefficients.

Equations (E16) are readily solved (e.g., see 54) and the homogeneous solution may be written[†]

$$w_i = \sum_j C_{ij} \exp(\lambda_j s) \quad (\text{E17})$$

where the C_{ij} are constants depending on the initial conditions and that λ_j are the eigenvalues associated with the system of equations; that is, they are the solutions of the characteristic equations $[A_{ij} - \lambda_j \delta_{ij}] = 0$ (δ_{ij} is the Kronecker delta function such that $\delta_{ij} = 1$ or 0 for $j = i$ or $j \neq i$). It is typical of equations for nonequilibrium flow that in certain regions of a flow field the eigenvalues λ_j are large, negative, real numbers and some are much smaller in magnitude than others. (These characteristics are also found in the differential equations that describe the dynamics of "stiff" springs. For this reason systems of equations having such properties are often referred to as "stiff" equations (25)).

To facilitate explanation of the problem, consider a system of two differential equations with eigenvalues represented, for example, by $(\lambda_1)_n = -1000\mu$ and $(\lambda_2)_n = -\mu$, respectively. In the integration of equations with such eigenvalues, two cases can occur. (1) If the effect of $(\lambda_1)_n$ over the small region where $\exp(-1000\mu s)$ is significant and is to be resolved, then we must perform our calculations at points spaced very close together. (2) If the value of s is large enough that $\exp(-1000\mu s)$ is negligible compared with $\exp(-\mu s)$, then we need use only the much coarser spacing that resolves $\exp(-\mu s)$. However, if the integration is carried out numerically with many of the conventional integration schemes (e.g., "explicit" methods such as the fourth-order Runge-Kutta method), violent instabilities occur for the coarse spacing. Lomax and Bailey

[†]A different relation is required when the eigenvalues λ_j are not all distinct. This point is considered in reference 54 but will be ignored here as not particularly essential either to the discussion or to the analysis. The eigenvalues are not actually required in the numerical methods, but are only monitored occasionally as a check on the integration procedure. This point will be made clear in the discussion.

(51, 53, 53a) refer to those like $(\lambda_1)_n$ as "parasitic" eigenvalues and those like $(\lambda_2)_n$ as "driving" eigenvalues.

Just how the eigenvalues affect the various numerical methods can be understood from the paper by Lomax (54). He shows in a rigorous manner that if each equation of the set of differential equations is operated on by identical linear difference-differential operators (we define such operations as "the numerical method") then the numerical method "detects" the eigenvalues of the differential equations and the success or failure of the method is measured by

- (1) Its accuracy in resolving the eigenvalue for which it is most accurate.
- (2) Its stability with respect to the eigenvalue for which it is most unstable.

Briefly, we may say that linear numerical methods, in effect, "decouple" the system of equations, and one needs only to determine whether a method has the ability to resolve the effects produced by the separate eigenvalues. The accuracy and stability criteria of a number of numerical methods are cataloged by Lomax and by Lomax and Bailey in references 53 and 54. The efficiency of a few of the more useful methods in the integration of stiff equations, is discussed in reference 54. Lomax and Bailey conclude that at least two types of difference-differential operators are required for rapid integration of the equations of non-equilibrium flow. Two satisfactory methods are the explicit and implicit methods described in the following discussion.

The explicit method used by Lomax and Bailey (53) with considerable success,[†] and employed to obtain the solutions of Chapter IV, is referred to as either an "Euler predictor with a modified Euler corrector" or as a

[†] Lomax and Bailey (51, 52, 53, 53a, 54) do not extol any particular method or combination of methods as being universal techniques. On the contrary, they have investigated and reported on the merits of a number of methods.

"second-order Runge-Kutta method". The method is defined by the difference-differential equations

$$\vec{w}_{n+1}^{(1)} = \vec{w}_n + h \vec{F}(\vec{w}_n)$$

$$\vec{w}_{n+1} = \vec{w}_n + \frac{h}{2} [\vec{F}(\vec{w}_{n+1}^{(1)}) + \vec{F}(\vec{w}_n)]$$
(E18)

The quantity h is the interval size and the superscript in parentheses denotes the iteration number. (The superscripts are omitted from the symbols that represent the final values of the dependent difference variables. Note the omission of (2) on \vec{w}_{n+1} in the second equation above.) Equations (E18) have a truncation error $(\lambda h)^3/6$ when applied to linear equations and a real stability boundary of -2.0 (see (54) for the definitions associated with the terminology and for a discussion on these given values). If $\lambda h > -2.0$ then numerical instability will not occur. We may exemplify this further by returning to the "two-eigenvalue" problem discussed earlier. We see that stability will be assured provided the integration interval size is the smaller of the two values $(h_1)_n < 2 \times 10^{-3}/\mu$ and $(h_2)_n < 2/\mu$. The smaller value, of course, is $(h_1)_n$ and is the interval based on the "parasitic" eigenvalue. Also the effect of truncation error on the dependent variables is, to a great extent, determined by the "driving" eigenvalue. Although the solution values are little affected by the parasitic eigenvalue, stability depends on this eigenvalue, and if the effect of the parasitic eigenvalue could be ignored, a three-order-of-magnitude increase in interval size would be possible, in principle. Implicit methods have such desired characteristics.

The implicit method used by Lomax and Bailey (53) is the "modified Euler method" defined by the difference-differential equation

$$\vec{w}_{n+1} = \vec{w}_n + \frac{h}{2} [\vec{F}(\vec{w}_{n+1}) + \vec{F}(\vec{w}_n)]$$
(E19)

This equation contains derivatives that must be evaluated in terms of the unknown dependent variables \vec{w}_{n+1} . Application of this equation is facilitated by the following procedure. If we substitute $\vec{w}_{n+1} = \frac{d\vec{w}_{n+1}}{ds}$ given by equation (E16) for $\vec{F}(\vec{w}_{n+1})$, the equation can also be written

$$\vec{w}_{n+1} = \vec{w}_n + \frac{h}{2} \{ [A]_n \vec{w}_{n+1} + (\vec{F})_n - [A]_n \vec{w}_n \} = 0(h^3) \quad (\text{E20})$$

or we can combine terms and obtain the set of simultaneous equations given by

$$[I] - \frac{h}{2} [A]_n (\vec{w}_{n+1} - \vec{w}_n) = h \vec{F}_n + 0(h^3) \quad (\text{E21})$$

where $[I]$ is the unit matrix (matrix with diagonal elements of unity and off diagonal elements of zero). These equations may be readily solved for the unknown quantities \vec{w}_{n+1} , with the result[†]

$$\vec{w}_{n+1} = \vec{w}_n + h \left[[I] - \frac{h}{2} [A]_n \right]^{-1} \vec{F}_n \quad (\text{E22})$$

Although, the equation may now be considered explicit since the unknown quantities are now related to quantities that are readily evaluated, we shall continue to refer to this method, and as well as methods requiring the evaluation of the Jacobian matrix A , as implicit. It can be shown (53,54) that the above method is unconditionally stable for all real negative values of λh . (The truncation error is $(\lambda h)^3/12$ when applied to linear equations. See 54.)

[†]In practice the matrix inversion that yields equation (E22) may cause machine "overflows" if the matrix $\left[[I] - \frac{h}{2} [A]_n \right]$ is not first properly scaled. This is easily done. If we let $[S]$ be a diagonal matrix of which the elements are the reciprocals of the maximum-valued elements of the row vectors of the matrix to be scaled, then $S_{ij} \left[[I] - \frac{h}{2} [A]_n \right]_{ij} \leq 1$ and inversion difficulties are not encountered. Thus, in practice, the inversion procedure given by

$$\vec{w}_{n+1} = \vec{w}_n + h \left\{ [S] \left[[I] - \frac{h}{2} [A]_n \right] \right\}^{-1} [S] \vec{F}_n \quad (\text{E23})$$

is to be preferred. Equations (E22) and (E23) are exactly equivalent.

With the use of the implicit method we have gained "stability" when the parasitic eigenvalues are important, but at the expense of additional computational complexity. Specifically, the elements of the Jacobian matrix, a_{ij} , must be computed. Although additional computer time is required to advance a step with the implicit method, considerable saving in the computational time required to obtain the entire solution may be obtained since large step sizes are possible. In particular, the intervals are large relative to those required for explicit methods that are dominated by stability criteria.

The application of the implicit method is made considerably easier if one obtains the matrix elements by numerical rather than analytical differentiation. The procedure to use is that suggested by Lomax and Bailey (53) and is indicated by the formula[†]

$$a_{ij} \equiv \frac{\partial F_i}{\partial w_j} \approx \frac{\Delta F_i}{\Delta w_j} = \frac{F_i(1.01 \times w_j) - F_i(0.99 \times w_j)}{0.02 \times w_j} \quad (\text{E24})$$

[†]Some of the individual elements, a_{ij} , obtained by numerical differentiation, may not agree with the similar elements obtained by evaluation of the relations found by analytical differentiation. This occurs when there are large-magnitude differences between the individual terms. For example, if

$$\left. \begin{aligned} F_i &\equiv \sum a'_{i,j} w_j \\ \text{where} \quad |a'_{i,k} w_k| &\leq 10^{-9} |a'_{i,k-1} w_{k-1}| \end{aligned} \right\} \quad (\text{E25})$$

one obtains "numerically" $a_{ik} = 0$ and "analytically" $a_{ik} = a'_{i,k}$ using an electronic computer with an eight digit mantissa. The full implication of this difference is not yet understood, and the disagreement is pointed out only as a potential source of difficulty. Actually, neither the author nor Lomax and Bailey (53) encountered any difficulties from equation (E24) (except when trying to compare matrix elements). Considerable time was expended and difficulty experienced, however, in trying to evaluate and use analytically obtained matrix elements. The Jacobian matrix contains 81 nontrivial elements for the case studied in Chapter IV, and only a few are identical zero.

One additional numerical parameter requires some discussion. This is the interval size "h" contained in both integrating methods. During the course of a numerical integration the interval size was allowed to vary in a manner similar to that discussed by Lomax and Bailey, but according to the following specific criteria.

- (1) If for all variables w_j we have $[(w_j)_n - (w_j)_{n-1}]/(w_j)_{n-1} \leq 0.025 \epsilon$, then the interval for the next point was doubled, that is, $h_{n+1} = 2h_n$,
- (2) If for any variable w_j , say w_k , we have $[(w_k)_n - (w_k)_{n-1}]/(w_k)_{n-1} > 0.1 \epsilon$, then the interval size h_n was halved and the $(\bar{w})_n$ were recomputed.
- (3) If neither condition (1) nor condition (2) was satisfied, then the variables $(\bar{w})_{n+1}$ for the next point were computed with unchanged interval, that is, $h_{n+1} = h_n$.

For most calculations $\epsilon = 0.5$ was used. With this scheme it turns out that any reasonable "initial value" h_1 may be used for starting the integration procedure. The above criteria were more stringent than the conditions used by Lomax and Bailey (53) where $\epsilon = 1.0$. These criteria were required to assure sufficient accuracy for the cases investigated.

The importance of using a combination of explicit and implicit methods can be illustrated by plots of the eigenvalues and of certain key parameters based on these eigenvalues for a few of the cases discussed in Chapter IV. In particular, we shall exhibit the effects that occur when the stability criteria are not satisfied. Figures E-1 show the eigenvalues and the parameters $|\lambda_{\min} h|$ and $|\lambda_{\max} h|$ corresponding to the solutions given by figure IV-1 of Chapter IV. The similar figures E-2 correspond to the solution of figure IV-6. The abscissa scale here is the same as that in the figures in Chapter IV. The eigenvalues were computed for every third point of the solutions. In figure E-1 the transient, quasi-steady, and final relaxation regions are again labeled by the numerals 1, 2, and 3, respectively. In obtaining the solutions the first 125 points were computed with the explicit method, equation (E18), and the remaining points (roughly, between 200 and 250 points) were computed with the implicit method, equation (E22). The "switch point," at which the integration method was changed,

is indicated on these figures by a dashed vertical line. One observes that the equations are quite "stiff" throughout the entire flow region, since all the large-magnitude eigenvalues are negative and are very large compared with the driving eigenvalues. The driving eigenvalues are the very small quantities having values of order 10^{-5} to 10^{-6} in figure E-1 and 10^{-6} to 10^{-7} in figure E-2. The precise values of these small eigenvalues are not to be trusted, since there is some doubt as to whether the computer program can accurately compute eigenvalues having values seven orders of magnitude less than the largest eigenvalue. One may be sure, however, that the small eigenvalues are no greater than those shown. (Note also that the small eigenvalues are distributed less randomly as the largest eigenvalue becomes smaller.)

The fact that the equations are "stiff" appears to be a characteristic of vibration-dissociation coupling and may explain the computational difficulty experienced in references 18 and 77. Such behavior is usually not observed for shock-wave flow governed only by chemical relaxation (note the solutions exhibited in (53)), and explicit methods are then quite satisfactory. Actually the implicit method could well have been used throughout the entire flow region for the shock-wave cases that were investigated for this thesis; however, only a very small amount of computer time was expended in using the explicit method. Although, it may appear on the bases of the figures, that a large fraction of the entire flow region was computed with the explicit method, the reader is to be reminded that the variables are plotted with a logarithmic abscissa scale.

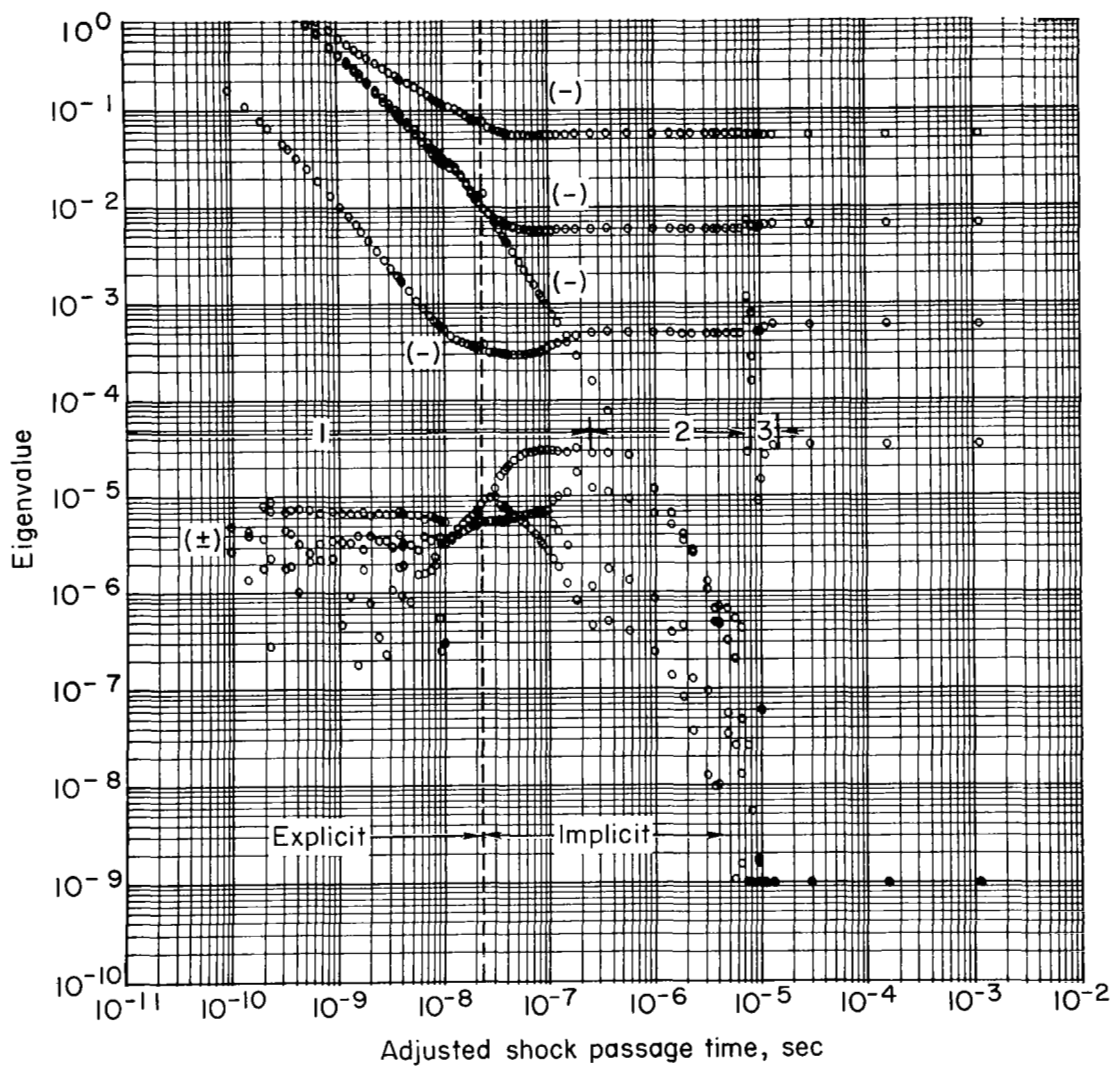
The figures show that the eigenvalues vary primarily in the transient region and remain relatively constant in the other regions. Another feature to note is that figures E-1 and E-2 exemplify strong and weak shock waves, respectively, and there is roughly an order-of-magnitude difference in the eigenvalues. The strong shock wave has parasitic eigenvalues with the larger values. The general character of the locus of eigenvalue points remains relatively unchanged independently of the strength of the shock wave.

The effect of exceeding the stability criteria may be observed in figures E-1b and E-2b, particularly the latter figure. A comparison of these figures with

figures IV-1 and IV-6 shows that whenever the quantity $|\lambda_{\min} h|$ exceeds the stability criterion (i.e., whenever $|\lambda_{\min} h| > 2$), then unstable behavior is exhibited in the solutions. This is particularly evident in a comparison of figures E-2b and IV-6, where $\epsilon = 0.75$ rather than $\epsilon = 0.50$ was used to find the interval size. The most dramatic effect, which exemplifies the value of implicit methods for overcoming numerical instability, is the almost immediate damping of unstable behavior directly after switching methods. Since the stability criterion no longer applies, there is then a rapid increase in the size of the integration interval. This is shown in figures E-1b and E-2b by the rapid increase in the value of $|\lambda_{\min} h|$.

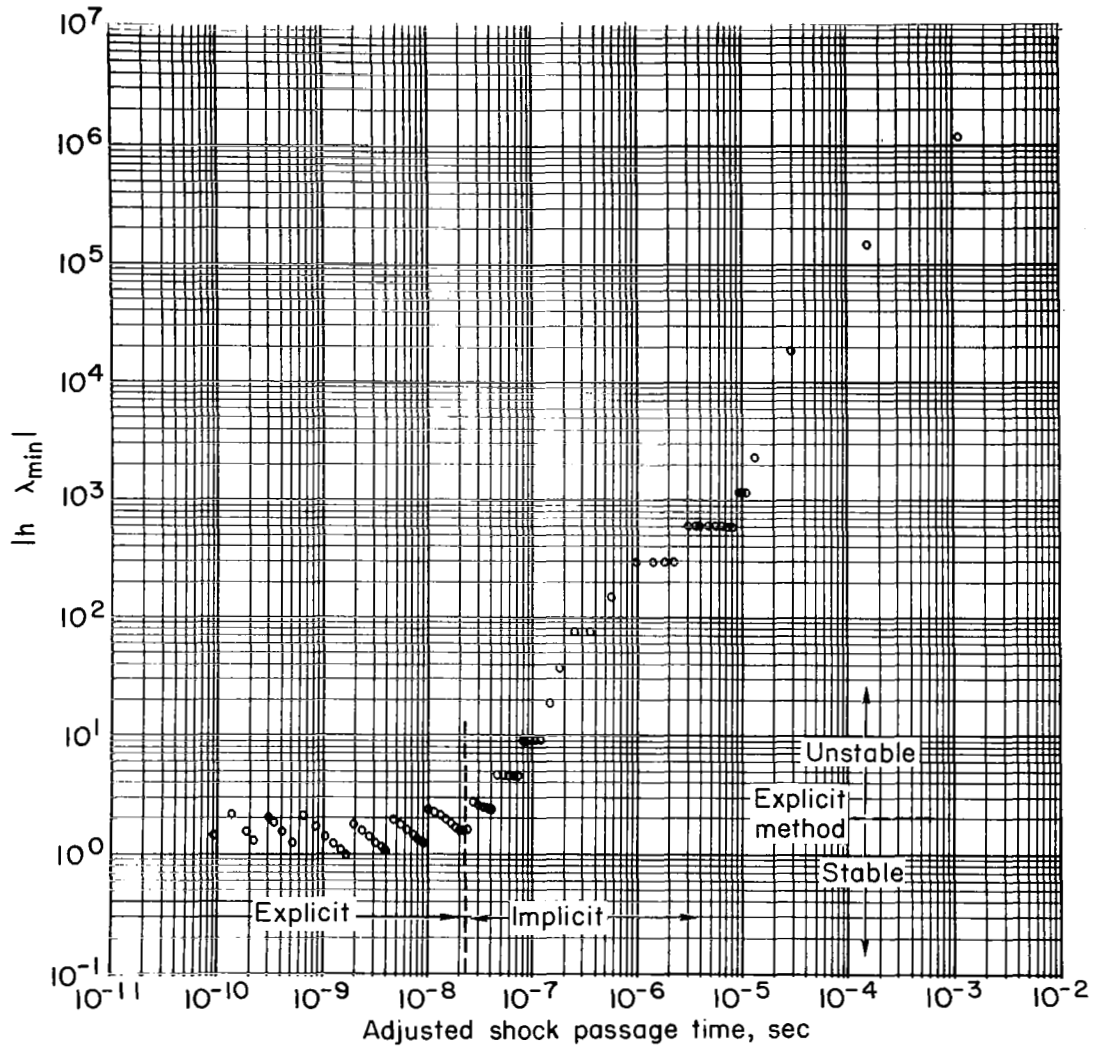
Figures E-1c and E-2c are plots of the quantity $|\lambda_{\max} h|$, which is a measure of the influence of truncation error on the solutions (for a detailed description of this quantity, see (53)). So long as this parameter remains less than 0.01 we may be reasonably confident that the truncation error has little effect on the final values of the solutions. This condition is slightly violated, but not to the extent one would expect an error greater than 0.01 percent.

Figure E-3b shows the parameters for nozzle flow. Here the sign of the scaling constant σ (see eq. E9) is changed, and the sign of the eigenvalues is changed accordingly. The parasitic eigenvalues are now positive, and the role of the parameters $|\lambda_{\min} h|$ and $|\lambda_{\max} h|$ is interchanged. The implicit method was used exclusively for obtaining the nozzle-flow solutions; as a result, the stability criterion, $|\lambda_{\max} h|$, is always greater than 2. The "error" criterion, $|\lambda_{\min} h|$, reaches a maximum value of 0.12 about 1-centimeter downstream of the throat, indicating that the maximum error due to numerical truncation effects is slightly greater than 0.01 percent. Everywhere else in the flow the error is much less. It should be mentioned again that the values of the stability and error parameters depend on the value of ϵ in the procedure described for determining the step size.



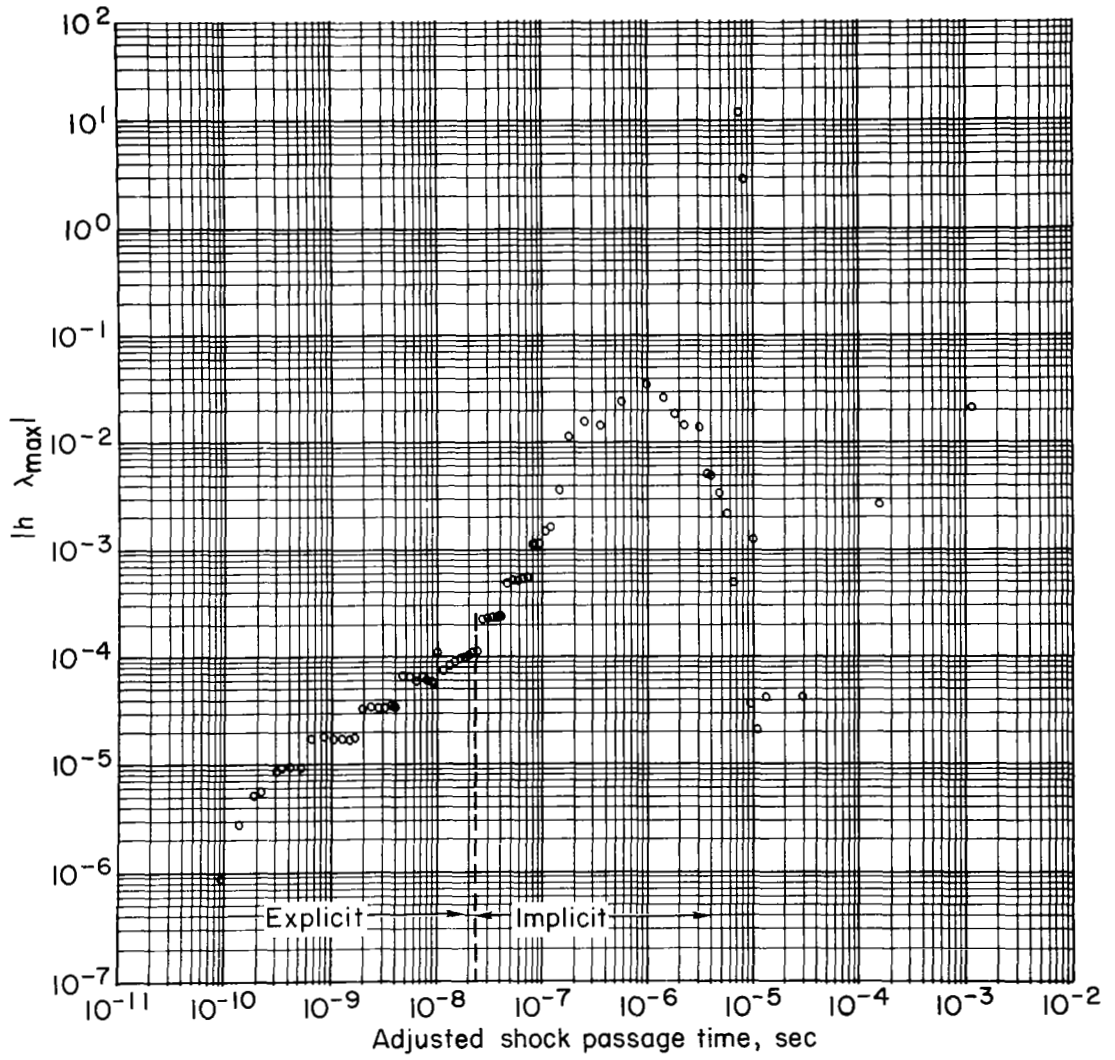
(a) Eigenvalues, λ

Figure E-1. Parameters characterizing the numerical aspects of shock wave solutions, versus adjusted shock passage time (associated model parameters are listed along first row of table IV-1)



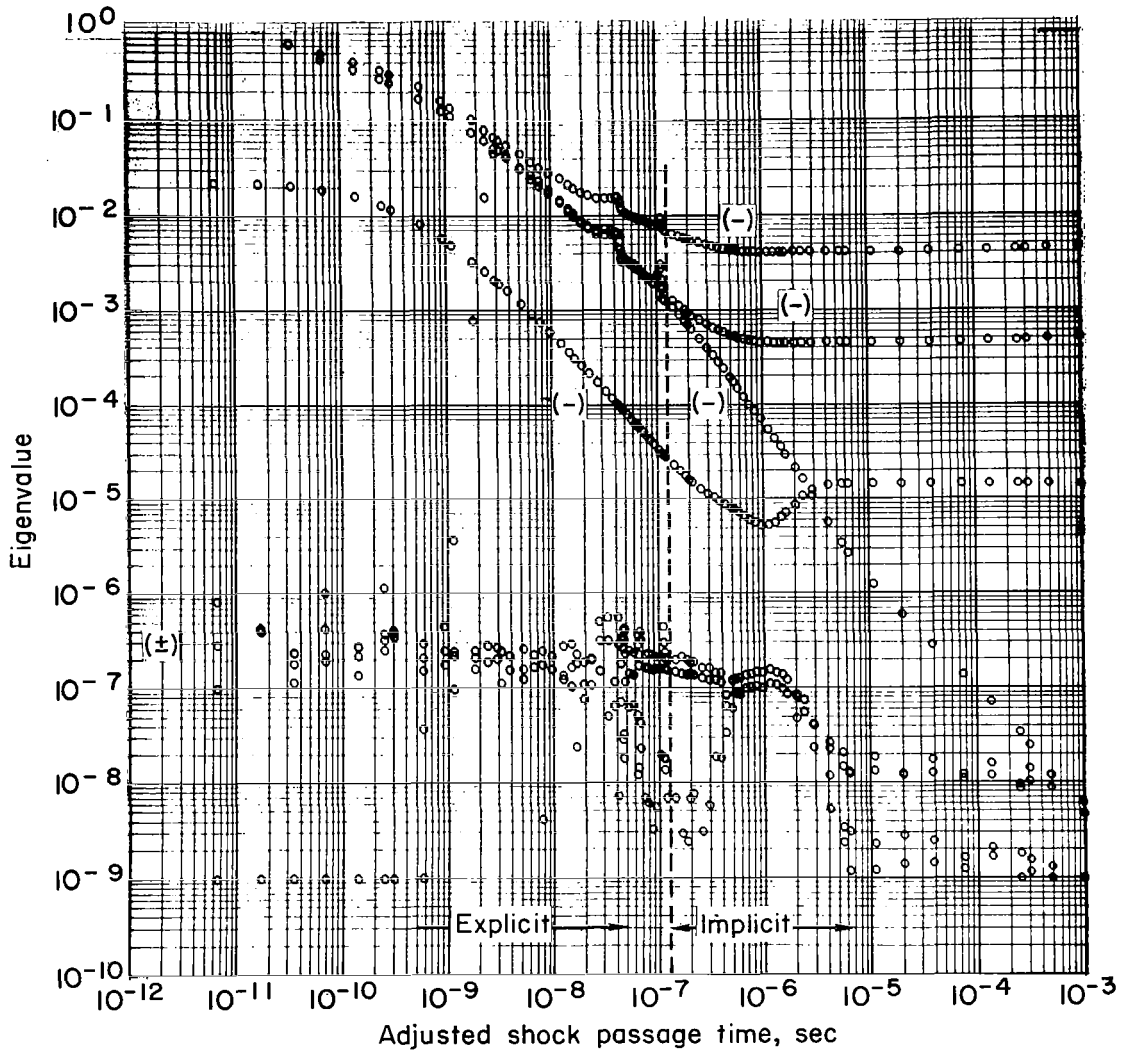
(b) $|\lambda_{\min} h|$

Figure E-1 Continued



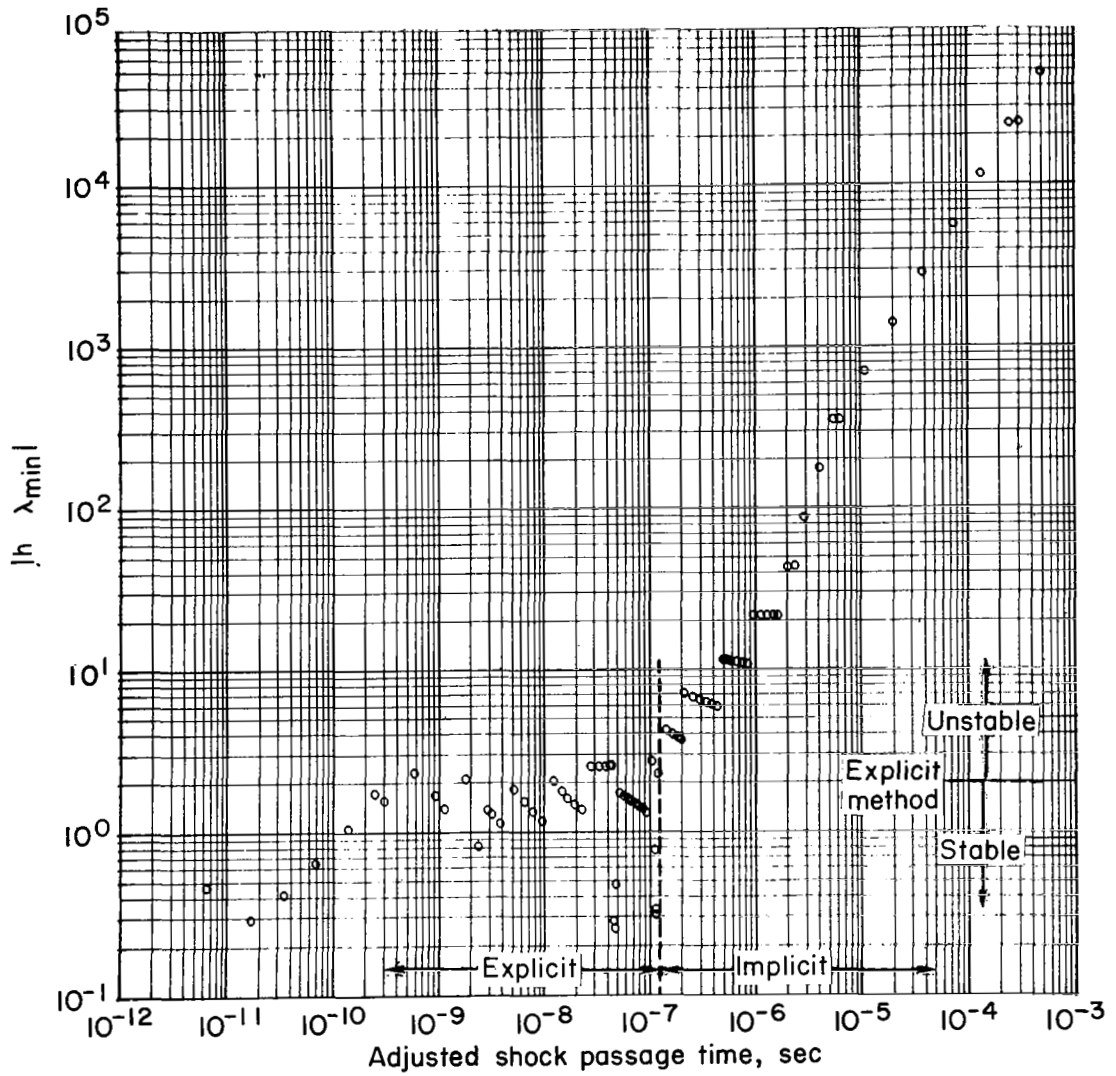
(c) $|\lambda_{\max} h|$

Figure E-1 Continued



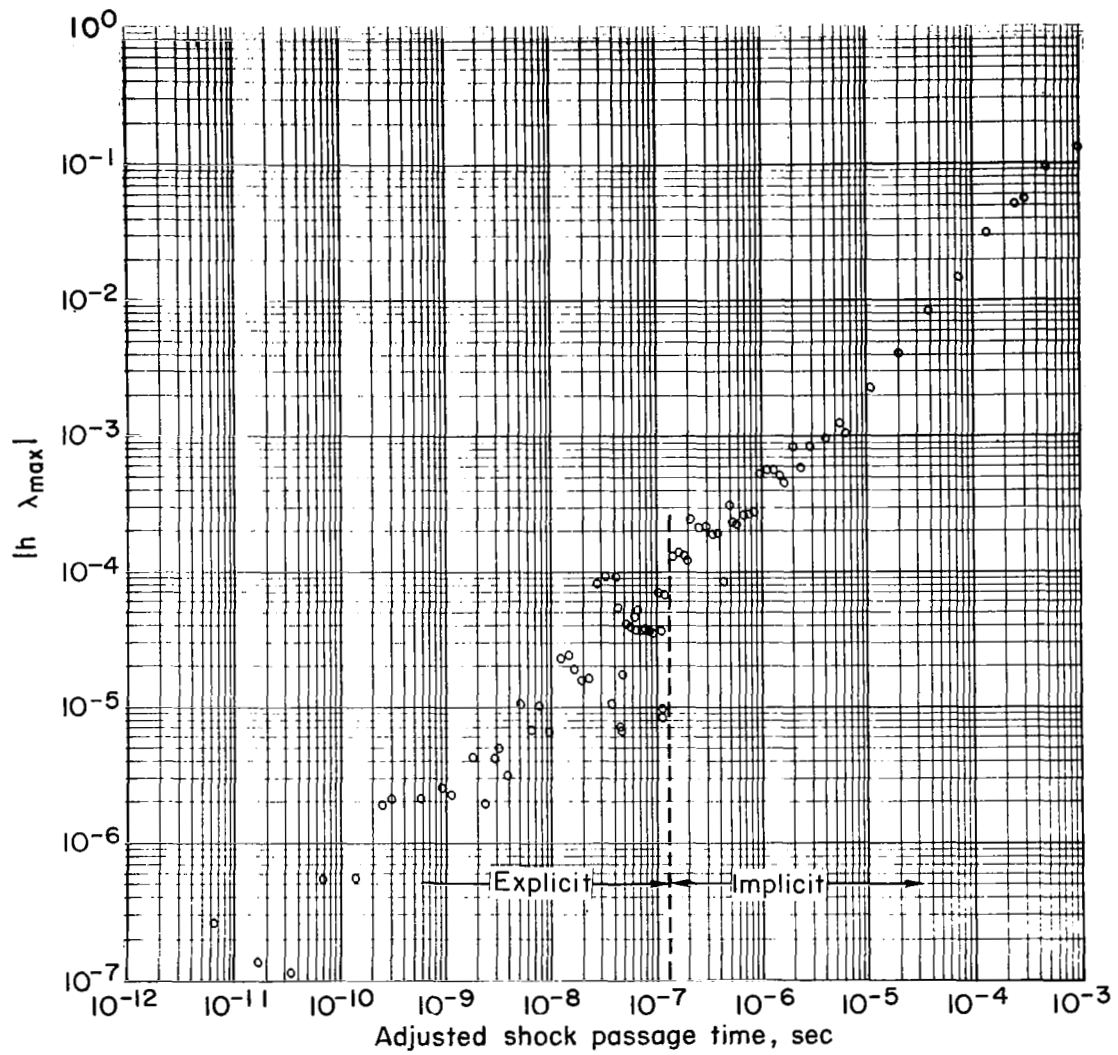
(a) Eigenvalues, λ

Figure E-2. Parameters characterizing the numerical aspects of shock wave solutions, versus adjusted shock passage time (associated model parameters are listed along the sixth row of table IV-1)



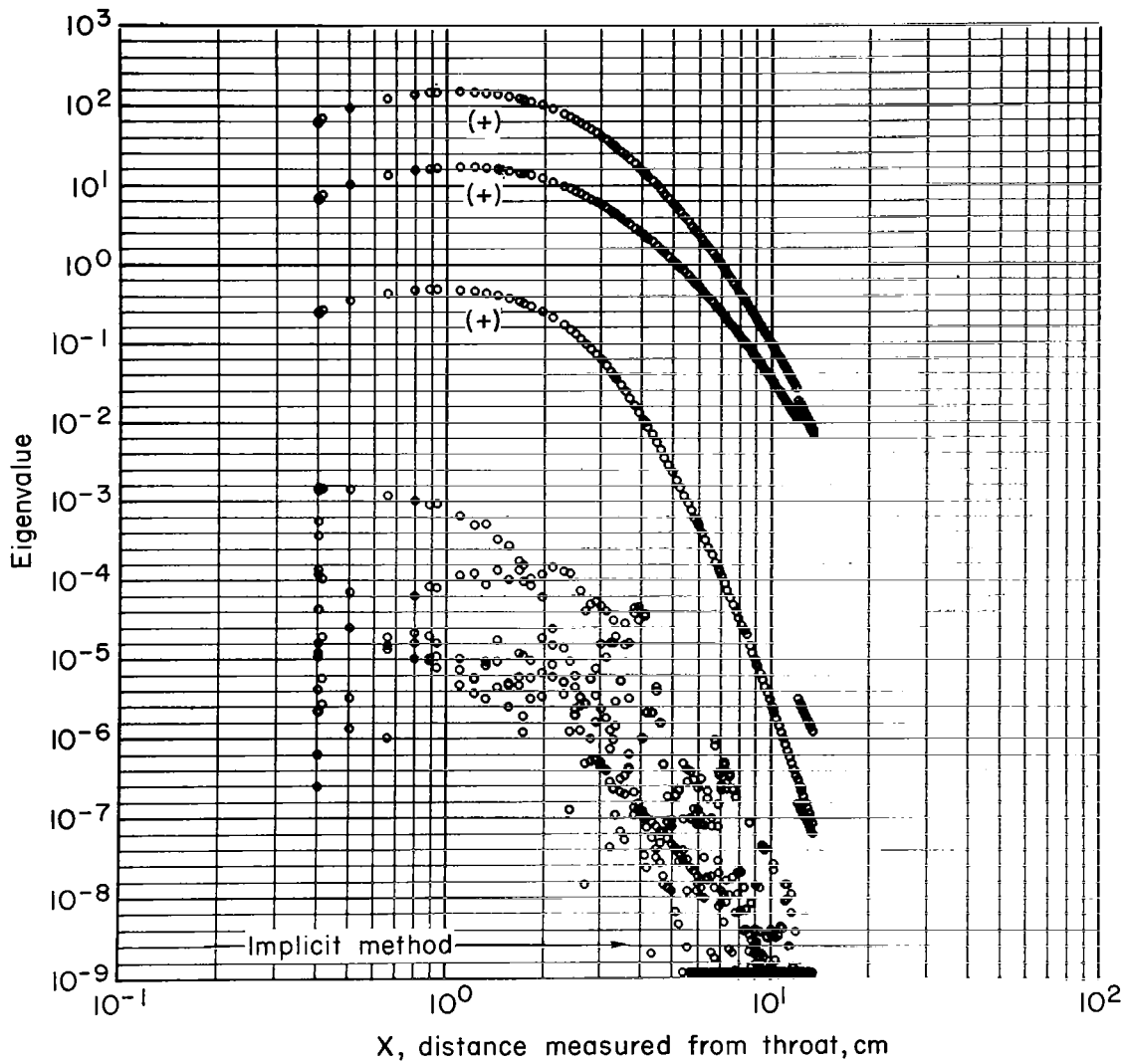
(b) $|\lambda_{\min} h|$

Figure E-2 Continued



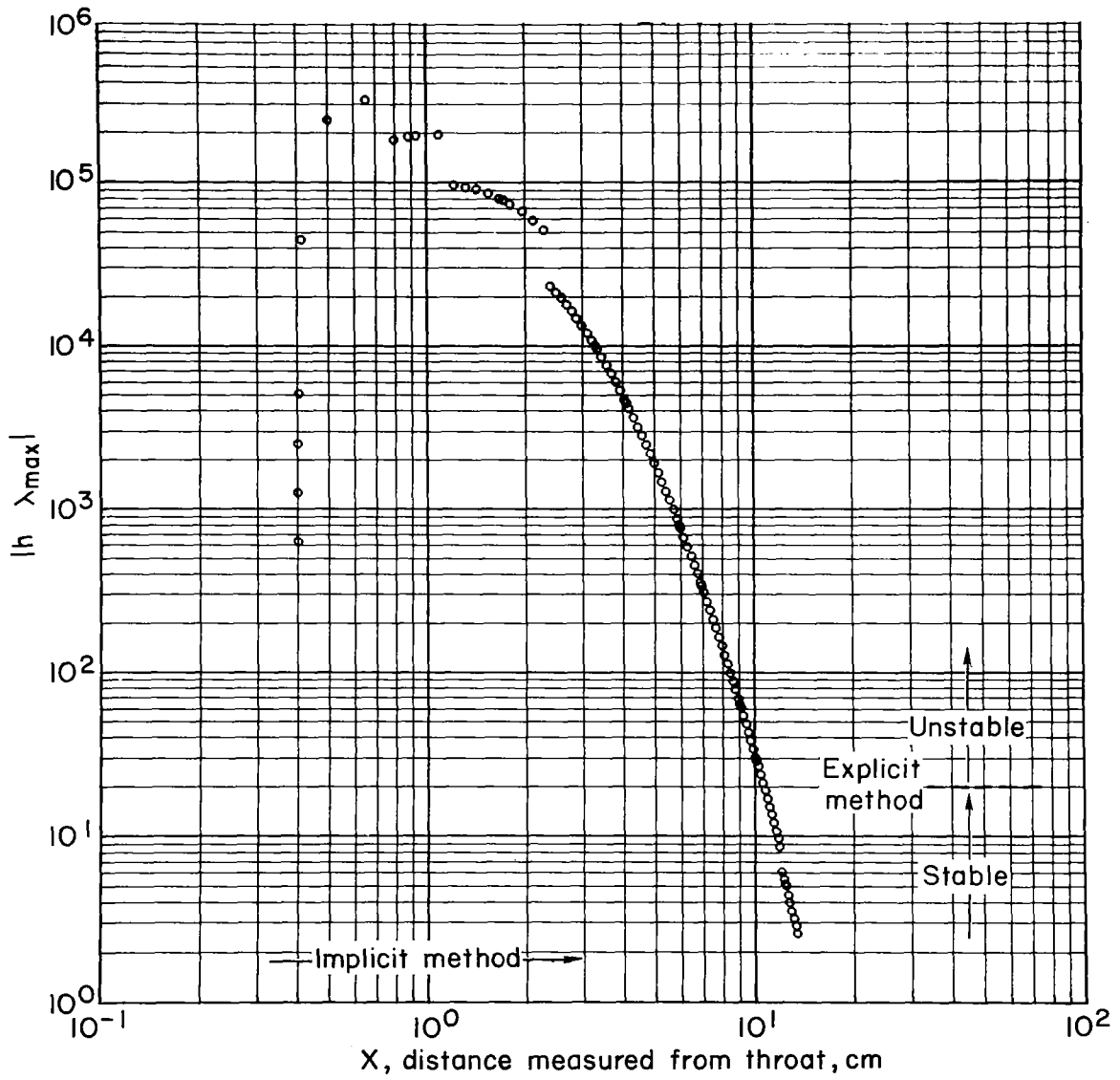
(c) $|\lambda_{\max} h|$

Figure E-2 Continued



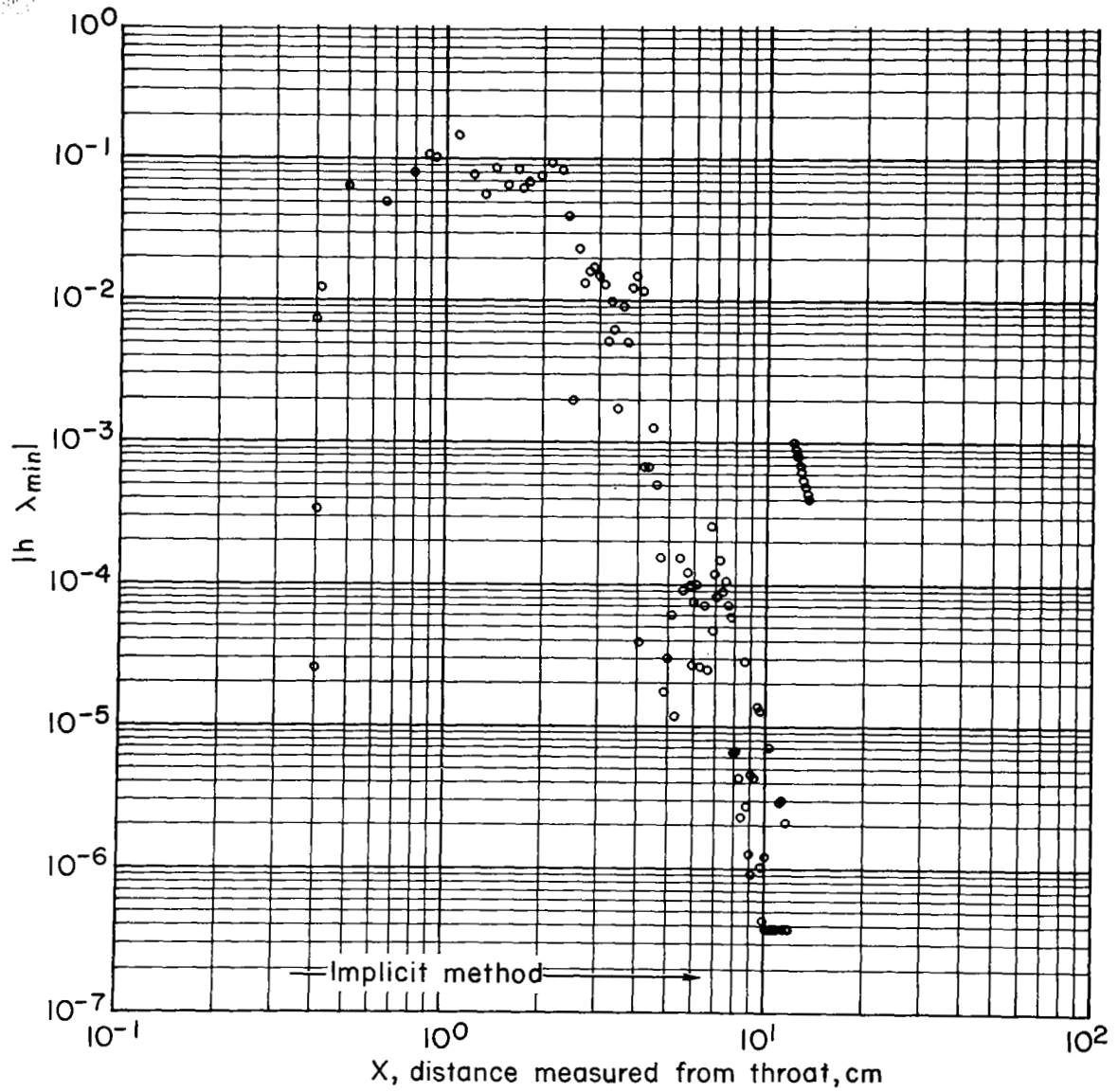
(a) Eigenvalues, λ

Figure E-3. Parameters characterizing the numerical aspects of nozzle solutions versus distance along nozzle (associated model parameters are those of figure IV-5)



(b) $|\lambda_{\max} h|$

Figure E-3 Continued



(c) $|\lambda_{\min} h|$

Figure E-3 Continued

APPENDIX F

EXPLICIT FORMULATION OF THE FLOW EQUATIONS

The procedure for obtaining the differential equations of one-dimensional flow was described in Appendix E, and the required equations were given implicitly. Here the explicit formulation of these equations is set down. The singular behavior of the coefficient matrix $[B^*]$ (see Appendix E) is also discussed.

The set of equations required to describe one-dimensional flow with vibration-dissociation coupling are given by equation (E8), where the coefficient matrix $[B^*]$ is defined by

$$[B^*] = \begin{bmatrix} \rho A & uA & 0 & 0 & 0 & 0 & 0 & 0 \\ \rho u & \frac{\partial p}{\partial \rho} & \frac{\partial p}{\partial T} & \frac{\partial p}{\partial \gamma_A} & \frac{\partial p}{\partial \gamma_B} & 0 & 0 & \frac{\partial p}{\partial \gamma_a} \\ u & 0 & \frac{\partial h}{\partial T} & \frac{\partial h}{\partial \gamma_A} & \frac{\partial h}{\partial \gamma_B} & \frac{\partial h}{\partial \epsilon_A} & \frac{\partial h}{\partial \epsilon_B} & \frac{\partial h}{\partial \gamma_a} \\ 0 & 0 & 0 & 1 & 0 & 0 & 0 & 0 \\ 0 & 0 & 0 & 0 & 1 & 0 & 0 & 0 \\ 0 & 0 & 0 & 0 & 0 & 1 & 0 & 0 \\ 0 & 0 & 0 & 0 & 0 & 0 & 1 & 0 \\ 0 & 0 & 0 & 0 & 0 & 0 & 0 & 1 \end{bmatrix} \quad (F1)$$

In general, chemically reacting systems with vibrational equilibrium also exhibit similar coefficient matrices in that most of the diagonal elements are unity (see, e.g., 53, 53a).

The matrix of minors and the determinant of such matrix systems are readily evaluated. (This is the same as saying that such systems of equations

are easily solved.) That this is true can be demonstrated as follows: We may partition the matrix $[B^*]$ into square submatrices according to

$$[B^*] = \begin{bmatrix} [A] & [B] \\ [0] & [I] \end{bmatrix} \quad (F2)$$

The determinant of such a system can be written

$$\det [B^*] = \det [A] \times \det [I] - \det [B] \times \det [0] \quad (F3)$$

However, the determinant of the submatrix $[0]$, the null matrix, is zero and the determinant of the matrix $[I]$, the identity or unit matrix, is unity. Hence, the problem of obtaining the determinant of the high-order coefficient matrix is reduced to a simpler problem of obtaining the determinant of the lower order submatrix $[A]$. The result is given by

$$\det [B^*] \equiv \det [A] = \det \begin{bmatrix} \rho A & \mu A & 0 \\ \rho \mu & \frac{\partial p}{\partial \rho} & \frac{\partial p}{\partial T} \\ u & 0 & \frac{\partial h}{\partial T} \end{bmatrix} = A \left(\rho \frac{\partial p}{\partial \rho} \frac{\partial h}{\partial T} + u^2 \frac{\partial p}{\partial T} - \rho u^2 \frac{\partial h}{\partial t} \right) \quad (F4)$$

The singular behavior of $[B^*]$ is particularly important, since it is the source of integration difficulties. It will only be demonstrated here that such behavior exists when the flow velocity v is equal to the "frozen" value of the speed of sound. We first introduce the following relations: the specific heat at constant pressure

$$c_p = \frac{\partial h}{\partial T_p} \quad (F5a)$$

the isentropic exponent

$$\gamma = \frac{c_p}{c_v} \quad (F5b)$$

the frozen speed of sound

$$a_f = \sqrt{\gamma R Z T} \quad (\text{F5c})$$

and the identity

$$c_p - c_v = R Z \quad (\text{F5d})$$

We can evaluate the determinant of the coefficient matrix (F4), in terms of these quantities. The result is

$$\det [B^*] = \rho A \left[\frac{\partial h}{\partial T} \left(\frac{\partial p}{\partial \rho} - u^2 \right) + \frac{u^2}{\rho} \frac{\partial p}{\partial T} \right] \quad (\text{F6a})$$

$$= \rho A [c_p (R Z T - u^2) + R Z u^2] \quad (\text{F6b})$$

$$= \rho A (c_p - R Z) \frac{c_p R Z T}{c_p - R Z} - u^2 \quad (\text{F6c})$$

$$= \rho A c_v [\gamma R Z T - u^2] \quad (\text{F6d})$$

$$= \rho A c_v [a_f^2 - u^2] \quad (\text{F6e})$$

We observe that the determinant $[B^*]$ is zero when the flow velocity is equal to the frozen speed of sound a_f (see, e.g., 97). This singular point may be identified as a saddle-point singularity and is the source of considerable computation difficulty near the throat of a nozzle (see, e.g., (53a)).

The adjoint matrix is required before an explicit form of the flow equations can be given (e.g., note eq. (E10)). An expression for this matrix is readily

obtained once the matrix of minors is given. With the "partitioning scheme" described earlier, the matrix of minors is readily evaluated. We obtain

$$\text{Minor } [B^*] = \begin{bmatrix} \frac{\partial p}{\partial \rho} \frac{\partial h}{\partial T} & u \left(\rho \frac{\partial h}{\partial T} - \frac{\partial p}{\partial T} \right) & -u \frac{\partial p}{\partial \rho} & 0 & 0 & 0 & 0 & 0 \\ uA \frac{\partial h}{\partial T} & \rho A \frac{\partial h}{\partial T} & -u^2 A & 0 & 0 & 0 & 0 & 0 \\ uA \frac{\partial p}{\partial T} & \rho A \frac{\partial p}{\partial T} & \beta A & 0 & 0 & 0 & 0 & 0 \\ uA \frac{\partial(p,h)}{\partial(T,\gamma_A)} & \rho A \frac{\partial(p,h)}{\partial(T,\gamma_A)} & \beta \gamma_A A & |B^*| & 0 & 0 & 0 & 0 \\ -uA \frac{\partial(p,h)}{\partial(T,\gamma_B)} & -\rho A \frac{\partial(p,h)}{\partial(T,\gamma_B)} & -\beta \gamma_B A & 0 & |B^*| & 0 & 0 & 0 \\ uA \frac{\partial(p,h)}{\partial(T,\epsilon_A)} & \rho A \frac{\partial(p,h)}{\partial(T,\epsilon_A)} & \beta \epsilon_A A & 0 & 0 & |B^*| & 0 & 0 \\ -uA \frac{\partial(p,h)}{\partial(T,\epsilon_B)} & -\rho A \frac{\partial(p,h)}{\partial(T,\epsilon_B)} & -\beta \epsilon_B A & 0 & 0 & 0 & |B^*| & 0 \\ uA \frac{\partial(p,h)}{\partial(T,\gamma_a)} & \rho A \frac{\partial(p,h)}{\partial(T,\gamma_a)} & \beta \gamma_a A & 0 & 0 & 0 & 0 & |B^*| \end{bmatrix} \quad (\text{F7})$$

where

$$\beta_f \equiv \beta \frac{\partial h}{\partial f} + \frac{\partial p}{\partial f} u^2 \quad (\text{F8a})$$

$$f = \gamma_A, \gamma_B, \epsilon_A, \epsilon_B, \gamma_a$$

$$\beta \equiv \rho \left[\frac{\partial p}{\partial \rho} - u^2 \right] = p - \rho u^2 \quad (\text{F8b})$$

$$\frac{\partial(p,h)}{\partial(T,f)} \equiv \begin{bmatrix} \frac{\partial p}{\partial T} & \frac{\partial h}{\partial T} \\ \frac{\partial p}{\partial f} & \frac{\partial h}{\partial f} \end{bmatrix} = \frac{\partial p}{\partial T} \frac{\partial h}{\partial f} - \frac{\partial h}{\partial T} \frac{\partial p}{\partial f} \quad (\text{F8c})$$

$$f = \gamma_A, \gamma_B, \epsilon_A, \epsilon_B, \gamma_a$$

The adjoint matrix $[B^*]^{-1} \det [B^*]$ is obtained from the matrix of minors in the following straightforward manner: First, multiply each element of the matrix of minors by the factor $(-1)^{i+j}$, which changes the sign of alternate elements. (The resulting matrix is called the cofactor of $[B^*]$.) Second, interchange rows and columns; that is, obtain the transpose of the cofactor. The resulting matrix is the adjoint matrix of $[B^*]$ and is given by

$$\text{Adj} [B^*] = [B^*]^{-1} \det [B^*] =$$

$$\begin{bmatrix} \frac{\partial p}{\partial \rho} \frac{\partial h}{\partial T} & -uA \frac{\partial h}{\partial T} & uA \frac{\partial p}{\partial T} & -uA \frac{\partial(p,h)}{\partial(T,\gamma_A)} & -uA \frac{\partial(p,h)}{\partial(T,\gamma_B)} & -uA \frac{\partial(p,h)}{\partial(T,\epsilon_A)} & -uA \frac{\partial(p,h)}{\partial(T,\epsilon_B)} & -uA \frac{\partial(p,h)}{\partial(T,\gamma_a)} \\ -u \rho \left(\frac{\partial h}{\partial T} - \frac{\partial p}{\partial T} \right) & \rho A \frac{\partial h}{\partial T} & -\rho A \frac{\partial p}{\partial T} & \rho A \frac{\partial(p,h)}{\partial(T,\gamma_A)} & \rho A \frac{\partial(p,h)}{\partial(T,\gamma_B)} & \rho A \frac{\partial(p,h)}{\partial(T,\epsilon_A)} & \rho A \frac{\partial(p,h)}{\partial(T,\epsilon_B)} & \rho A \frac{\partial(p,h)}{\partial(T,\gamma_a)} \\ -u \frac{\partial p}{\partial \rho} & u^2 A & \beta A & -A\beta_{\gamma_A} & -A\beta_{\gamma_B} & -A\beta_{\epsilon_A} & -A\beta_{\epsilon_B} & -A\beta_{\gamma_a} \\ 0 & 0 & 0 & |B^*| & 0 & 0 & 0 & 0 \\ 0 & 0 & 0 & 0 & |B^*| & 0 & 0 & 0 \\ 0 & 0 & 0 & 0 & 0 & |B^*| & 0 & 0 \\ 0 & 0 & 0 & 0 & 0 & 0 & |B^*| & 0 \\ 0 & 0 & 0 & 0 & 0 & 0 & 0 & |B^*| \end{bmatrix} \quad (\text{F9})$$

The derivative vector \vec{F}^* , equation (E10), is obtained from the vector-matrix product $\text{adj} [B^*] \vec{c}$. The elements of the resulting vector are the derivatives that are required. Explicitly they are as follows:

$$F_1^* = -puA_x \frac{\partial h}{\partial T} - uA \sum_{\ell} \frac{\partial(p,h)}{\partial(T,\ell)} Q^{\ell} \quad (\text{F10a})$$

$$F_2^* = u^2 \rho^2 A_x \left(\frac{\partial h}{\partial T} - RZ \right) + \rho A \sum_{\ell} \frac{\partial(p,h)}{\partial(T,\ell)} Q^{\ell} \quad (\text{F10b})$$

$$F_3^* = u^2 p A_x - A \sum_{\ell} \beta_{\ell} Q^{\ell} \quad (\text{F10c})$$

$$F_4^* = |B^*| Q^{\gamma_A} \quad (\text{F10d})$$

$$F_5^* = |B^*| Q^{\gamma_B} \quad (\text{F10e})$$

$$F_6^* = |B^*| Q^{\epsilon_A} \quad (\text{F10f})$$

$$F_7^* = |B^*| Q^{\epsilon_B} \quad (\text{F10g})$$

$$F_8^* = |B^*| Q^{\gamma_a} \quad (\text{F10h})$$

where $\ell = 1, 2, \dots, 5$ denotes the nonequilibrium variables $\gamma_A, \gamma_B, \epsilon_A, \epsilon_B$, and γ_a , respectively. This formulation is useful in that its symmetry suggests the generalization required for more complex systems, for example, chemical systems with additional reacting species. In such cases there will be additional rate equations (Q quantities); one additional equation is required for each additional dependent species-concentration variable.

The complete system of equations, denoted by the vector \vec{F} (see eq. (E11c) in the text), is obtained by adding one more element to the set \vec{F}^* to obtain

$$\vec{F}^T = \left(\vec{F}^{*T}, \det [B^*] \right) \quad (\text{F11})$$

An alternative representation of the first three rate equations, equations (F10 a, b, and c) is useful. We first introduce the identities

$$H_1 \equiv R_0 T \left(Q^{\gamma_A} + Q^{\gamma_B} + Q^{\gamma_a} \right) \quad (\text{F12a})$$

$$H_2 = h_{\gamma_a}^* Q^{\gamma_A} + h_{\gamma_B}^* Q^{\gamma_B} + Q^{\epsilon_A} + Q^{\epsilon_B} + h_{\gamma_a} Q^{\gamma_a} \quad (\text{F12b})$$

In terms of these relations the summation quantities in the first three equations may be written

$$\sum_{\ell} \frac{\partial(p, h)}{\partial(T, \ell)} = \rho \left(RZH_2 - \frac{\partial h}{\partial T} H_1 \right) \quad (F13a)$$

$$\sum_{\ell} \beta_{\ell} Q^{\ell} = \rho \left[(RZT - u^2) H_2 - u^2 H_1 \right] \quad (F13b)$$

Substitution of these quantities into the relevant equations (F10) yields

$$F_1 = F_1^* = -\rho u A \left[\frac{\partial h}{\partial T} \left(RZT \frac{d \ell nA}{dx} - H_1 \right) + RZH_2 \right] \quad (F14a)$$

$$F_2 = F_2^* = \rho^2 A \left[u^2 \left(\frac{\partial h}{\partial T} - RZ \right) \frac{d \ell nA}{dx} + RZH_2 - \frac{\partial h}{\partial T} H_1 \right] \quad (F14b)$$

$$F_3 = F_3^* = \rho A \left[u^2 RZT \frac{d \ell nA}{dx} - (RZT - u^2) - u^2 H_1 \right] \quad (F14c)$$

These equations rather than equations (F10 a, b, and c) were used to obtain the results reported in Chapter IV.

One additional change was made. In practice it was found that equations (F14), the associated rate equations, and the choice of dependent variables indicated by equation (E11b) of Appendix E are not always easily solved on an electronic computer that is limited to arithmetic operations involving numbers between certain fixed bounds. These bounds are of order 10^{-38} and 10^{38} for an IBM 7094 electronic computer when the single-precision arithmetic option is employed. The reason for the difficulties that occur can be illustrated as follows: In the flow field immediately behind a shock wave the dependent variable γ_B is proportional to $\exp(-E_b/kT_B)$ ($T_B = 300^\circ$ K immediately behind the shock), and for values of E_b/k greater than $26,000^\circ$ K, γ_B is less than 10^{-38} and its value is rounded to zero by the computer. Since this variable occurs as a product in the rate equation Q^{ϵ_B} , equation (F10g) (see also eq.

(II-110d) in the text), considerable difficulty is then encountered until the temperature T_B is sufficiently large that $\exp(-E_b/kT_B) > 10^{-38}$. Similar problems are experienced with the dependent variable γ_a . In addition, these variables also change rapidly in the transient region behind the shock, increasing in an exponential manner more than 33 orders of magnitude (see, e.g., fig. IV-1). The integration methods actually involve low-degree polominal "fitting." Consequently, many points and a corresponding large amount of computer time were required to advance through the transient region. Another problem was that of determining the temperature T_B in the transient region. If γ_B is identically zero then so is ϵ_B and T_B is then indeterminant. All these problems were alleviated by introducing the dependent variables $\bar{\gamma}_A, \bar{\gamma}_B, T_A, T_B, \bar{\gamma}_a$ in place of $\gamma_A, \gamma_B, \epsilon_A, \epsilon_B, \gamma_a$ where

$$\bar{\gamma}_A = \ell n \gamma_A \quad (F15a)$$

$$\bar{\gamma}_B = \ell n \gamma_B \quad (F15b)$$

$$\bar{\gamma}_a = \ell n \gamma_a \quad (F15c)$$

The appropriate rate equations for these more convenient variables can be obtained by inspection. They are as follows:

$$F_1 = -\rho u A \left[\frac{\partial h}{\partial T} \left(R Z T \frac{d \ell n A}{dx} - H_1 \right) + R Z H_2 \right] \quad (F16a)$$

$$F_2 = \rho^2 A \left[u^2 \left(\frac{\partial h}{\partial T} - R Z \right) \frac{d \ell n A}{dx} + R Z H_2 - \frac{\partial h}{\partial T} H_1 \right] \quad (F16b)$$

$$F_3 = \rho A \left[u^2 R Z T \frac{d \ell n A}{dx} - (R Z T - u^2) H_2 - u^2 H_1 \right] \quad (F16c)$$

$$\bar{F}_4 = |B^*| Q^{\bar{\gamma}_A} \quad (F16d)$$

$$\bar{F}_5 = |B^*| Q^{\bar{\gamma}_B} \quad (F16e)$$

$$\bar{F}_6 = |B^*| Q^{T_A} \quad (F16f)$$

$$\bar{F}_7 = |B^*| Q^{T_B} \quad (F16g)$$

$$\bar{F}_8 = |B^*| Q^{\bar{\gamma}_a} \quad (F16h)$$

$$\bar{F}_9 = |B^*| \quad (F16i)$$

The quantities H_1 and H_2 are evaluated according to equations (F12), where

$$Q^{\epsilon_A} = \gamma_A \left[Q^{\bar{\gamma}_A} q_A(T_A) + c_{v_A}(T_A) Q^{T_A} \right] \quad (F17a)$$

$$Q^{\epsilon_B} = \gamma_B \left[Q^{\bar{\gamma}_B} q_B(T_B) + c_{v_B}(T_B) Q^{T_B} \right] \quad (F17b)$$

The rate quantities $Q^{\bar{\gamma}_A}$, $Q^{\bar{\gamma}_B}$, Q^{T_A} , Q^{T_B} , and $Q^{\bar{\gamma}_a}$ are obtained from equations (II-113) (note eq. (II-114)). The rate equations represented by \bar{F} were integrated to yield the results discussed in Chapter IV.

APPENDIX G

PHYSICAL CONSTANTS AND OTHER REQUIRED PARAMETERS

The fundamental physical constants required for the analysis are listed here for the reader's convenience. Also given are the assigned values of other constants used throughout the work. The reader is referred to the text for an explanation of the listed values. We have used c.g.s units throughout.

(1) Physical Constants

Avagadro's number	$N_0 = 6.02486 \times 10^{23}$	(g-mole) ⁻¹
Planck's constant	$h = 6.62517 \times 10^{-27}$	erg-sec
	$\hbar = 1.05443 \times 10^{-27}$	erg-sec
Boltzmann constant	$k = 1.38044 \times 10^{-16}$	erg °K ⁻¹
Universal gas constant	$R_0 = 8.31662 \times 10^7$	erg (g-mole) ⁻¹ °K ⁻¹

(2) Other required parameters

(a) Molecular oxygen

Anharmonicity separation	$a = 9$	(see Appendix A and B)
Temperature separation	$b = 16$	(see Chapters III and IV)
Number of energy levels	$N = 32$	(see Appendix A)
Lower states energy level separation	$\Theta_{A_1} = 2234.3^\circ \text{K}$	(see Appendix A)
Upper states energy level separation	$\Theta_{A_2} = \Theta_B = 1800.2^\circ \text{K}$	(see Appendix A)
	$\Theta_a = 19,675^\circ \text{K}$	(see Appendix A)
	$\Theta_b = 32,276^\circ \text{K}$	(see Appendix A)
Model dissociation temperature	$\Theta_{N-1} = 59,280^\circ \text{K}$	(see Appendix A)

Characteristic dissociation temperature $\Theta_D = 59,368^\circ\text{K}$ (see Appendix A)

Characteristic rotational temperature $\Theta_{R,O_2} = 2.07\sigma^\circ\text{K}$ (see eq. (A2d))
 where σ (symmetry factor) is 2

$(E_0)_M = 2256^\circ\text{K}$ (see eq. (A10a))

$(\chi_0)_M = .00962$ (see eq. (A10a))

Oxygen molecular mass $m_{O_2} = 32$ g/mole

Heat of formation $h^\circ_{O_2} = 0$ (see eq. (E5a))

Electronic excitation parameters (Eq. (A1d))

l	$g_{E_{l,l,O_2}}$	$\Theta_{E_{l,l,O_2}} (^\circ\text{K})$
1	3	0

$\varphi_0 |_{O_2-O_2} = 5.2587$ (Eq. (B8))

$\varphi_0 |_{O_2-O} = 4.5939$

$\varphi_0 |_{O_2-Ar} = 5.4454$

(b) Atomic oxygen

Mass $m_O = 16$ g/mole

Heat of formation $h^\circ_O/R_O = 29690^\circ\text{K}$ (Eq. (E5a))

Electronic excitation parameters (Eq. (A1d))

l	$g_{E_{l,l,O}}$	$\Theta_{E_{l,l,O}} (^\circ\text{K})$
1	5	0
2	3	228.0
3	1	325.8
4	5	22825
5	1	48609
6	5	106112
7	3	110166
8	19	126051
9	8	137878
10	84	142875

(c) Argon

Mass $m_{\text{Ar}} = 39.944 \text{ g/mole}$

Heat of formation $h_{\text{Ar}}^{\circ} = 0$ (Eq. (E5a))

Electronic excitation parameters (Eq. (A1d))

l	$g_{E_{l,l,Ar}}$	$\Theta_{E_{l,l,Ar}}(^{\circ}\text{K})$
1	1	0
2	5	93144
3	3	93751

(3) The following table was often used for converting various energy units in references and is reproduced here because of its usefulness.

Table G-1
Energy Unit Conversion Factors

Unit	cm^{-1}	erg/molecule	cal/mole	ev	$^{\circ}\text{K}$	erg/mole
1 cm^{-1}	1	$(hc)=1.98618 \times 10^{-16}$	2.863	1.23976×10^{-4}	$(hc/k)=1.43880$	$(hcN)=1.19665 \times 10^8$
1 erg/molecule	$(hc)^{-1}=5.03479 \times 10^{15}$	1	1.441×10^{16}	6.24196×10^{11}	$(k^{-1})=7.24407 \times 10^{15}$	$(N)=6.02486 \times 10^{-23}$
1 cal/mole	.3493	6.938×10^{-17}	1	4.331×10^{-5}	.5026	4.18×10^7
1 ev	8.06608×10^3	1.60206×10^{-12}	2.309×10^4	1	1.16054×10^4	9.65219×10^{11}
1 $^{\circ}\text{K}$	$(k/hc)=.69502$	$(k)=1.38044 \times 10^{-16}$	1.990	8.6164×10^{-5}	1	$(kN=R_0)=8.31696 \times 10^7$
1 erg/mole	$(hcN)^{-1}=8.35666 \times 10^{-9}$	$(N^{-1})=1.65979 \times 10^{-24}$	2.392×10^{-8}	1.03603×10^{-12}	$(kN)^{-1}=1.20236 \times 10^{-8}$	1

N Avagadro's number
 c Speed of light
 k Boltzmann constant
 h Planck's constant
 R₀ Universal gas constant

REFERENCES

1. Appleton, J. P., "A Shock Tube Study of the Vibrational Relaxation of Nitrogen Using Vacuum Ultra-Violet Light Absorption," A. C. Electronics D.R.L., TR 67-01 D (1967).
2. Appleton, J. P., and Steinberg, M., "Vacuum-Ultraviolet Absorption of Shock-Heated Vibrationally Excited Nitrogen," J. Chem. Phys., 46, 1521 (1967).
3. Bauer, S. H., "The Role of Rotation in the Dissociation of Diatoms," Abstract no. 20, Division of Physical Chemistry, Meeting of American Chemical Society, San Francisco, 1958.
4. Bauer, S. H., and Tsang, S. C., "Mechanisms for Vibrational Relaxation at High Temperatures," Phys. of Fluids, 6, 182 (1963).
5. Bauer, E., "The Excitation of Electronic and Other Degrees of Freedom in a Hypersonic Shock Wave in Air," Institute for Defense Analysis, Research and Engineering Support Division, Research paper P-311 (1967).
6. Bazley, N. W., Montroll, E. W., Rubin, R. J., and Shuler, K. E., "Studies in Nonequilibrium Rate Processes. III The Vibrational Relaxation of a System of Anharmonic Oscillators," J. Chem. Phys., 28, 700 (1958) and 29, 1185 (1958).
7. Benson, S. W., and Fueno, T., "Mechanism of Atom Recombination by Consecutive Vibrational Deactivations," J. Chem. Phys., 36, 1597 (1962).
8. Bethe, H. A., and Teller, E., "Deviations from Thermal Equilibrium in Shock Waves," U.S. Ballistic Res. Lab. Rep. X-117 (1941).
9. Bond, J. W., Watson, K. M., and Welch, J. A., Atomic Theory of Gas Dynamics, Addison-Wesley (1965).
10. Bradley, J. N., Shock Waves in Chemistry and Physics, John Wiley and Sons, Inc. (1962).

11. Brau, Charles A., "Approximate Calculation of Dissociation Rates and Incubation Times," *J. Chem. Phys.*, 47, 3076 (1967).
12. Brau, C. A., Keck, J. C., and Carrier, G. F., "Transient Phenomena in Dissociative Reactions," *Phys. of Fluids*, 9, 1885 (1966) see also Avco Everett Res. Lab. Res. Rep. 243 (1966).
13. Brau, C. A., "On the Stochastic Theory of Dissociation and Recombination of Diatomic Molecules in Inert Diluents," *J. Chem. Phys.*, 47, 1153 (1967).
14. Bray, K. N. C., "Coupling Between Atomic Recombination and Vibrational Relaxation in Expanding Gas Flows," University of Southampton, Dept. of Aeronautics and Astronautics Rep. no. 260 (1964).
15. Bray, K. N. C., "Vibrational Relaxation of Anharmonic Oscillator Molecules," Massachusetts Institute of Technology, Fluid Mech. Lab. Pub. No. 67-3 (1967).
16. Bray, K. N. C., "Vibrational Relaxation of Anharmonic Oscillator Molecules: Relaxation Under Isothermal Conditions," *Journal Phys. B. (Proc. Phys. Soc.)*, 1, 705 (1968).
17. Bray, K. N. C., "Atomic Recombination in a Hypersonic Wind-Tunnel Nozzle," *J. Fluid Mech.* 6, 1 (1959).
18. Bray, K. N. C., and Pratt, N. H., "Conditions for Significant Gas Dynamically Introduced Vibration-Recombination Coupling," 11th Sym. (International) on Combustion, The Combustion Institute, pg. 23 (1967).
19. Camac, M., and Vaughn, A., "O₂ Dissociation Rates in O₂-Ar Mixtures," *J. Chem. Phys.*, 34, 460 (1961).
20. Camac, Morton, "O₂ Vibration Relaxation in Oxygen-Argon Mixtures," *J. Chem. Phys.*, 34, 448 (1961).
21. Carrington, Tucker, "Transition Probabilities in Multilevel Systems: Calculation from Impulsive and Steady-State Experiments," *J. Chem. Phys.*, 35, 807 (1961).

22. Clarke, J. F., and McChesney, M., *The Dynamics of Real Gases*, Butterworths (1964).
23. Cottrell, T. L., and McCoubrey, *Molecular Energy Transfer in Gases*, Butterworths (1961).
24. Crawford, B. L., Jr., and Dinsmore, H. L., "Vibrational Intensities: I. Theory of Diatomic Infra-Red Bands," *J. Chem. Phys.*, 18, 983 (1950).
25. Curtiss, C. F., and Hirschfelder, J. O., "Integration of Stiff Equations," *Proc. Natl. Acad. Sci. U.S.*, 38, 235 (1952).
26. DeGroat, J. J., and Abbett, M. J., "A Computation of One-Dimensional Combustion of Methane," *AIAA J.*, 3, 381 (1965).
27. Dresser, H. S., French, E. P., and Webb, H. G., Jr., "Computer Program for One-Dimensional Nonequilibrium Reacting Gas Flow," Air Force Flight Dynamics Laboratory, Wright Patterson A.F.B., AFFDL-TR-67-75 (1967).
28. Emanuel, G., "A General Method for Numerical Integration Through a Saddle-Point Singularity with Application to One-Dimensional Nonequilibrium Nozzle Flow," Arnold Engineering Development Center, Rept. AEDC-TDR-64-29 (1964).
29. Emanuel, G., "Problems Underlying the Numerical Integration of the Chemical and Vibrational Rate Equations in Near-Equilibrium Flow," Arnold Engineering Development Center, Rept. AEDC-TDR-63-82 (1963).
30. Emanuel, G., and Vincenti, W. G., "Method for Calculation of the One-Dimensional Nonequilibrium Flow of a General Gas Mixture Through a Hypersonic Nozzle," Arnold Engineering Development Center, Rept. AEDC-TDR-62-131 (1962).
31. Garr, L. J., Marrone, P. V., Joss, W. W., and Williams, M. J., "Inviscid Nonequilibrium Flow Behind Bow and Normal Shock Waves, Part III the Revised Normal Shock Program," Cornell Aeronautical Lab., CAL Rept. No. QM-1626-A-12 (III) (1966), and (II) (1963).

32. Gavril, B. D., "Generalized One-Dimensional Chemical Reacting Flows with Molecular Vibrational Relaxation," General Applied Science Laboratories, Inc. TR no. 426 (1964).
33. Gerry, E. T., and Leonard, D. A., "Measurement of the 10.6μ CO₂ Laser Transition Probability and Optical Broadening Cross Section," Applied Phys. Letters, 8, 227 (1966).
34. Gilmore, F. R., Bauer, E., and McGowan, J. W., "A Review of Atomic and Molecular Excitation Mechanisms in Nonequilibrium Gases up to 20,000 °K." Rand Corp., Memorandum RM-5202 ARPA (1967).
35. Greenblatt, M., "The Coupling of Vibrational Relaxation and Dissociation," Von Karman Institute for Fluid Dynamics, Rhode-Saint-Genese, Belgium, Tech. Note 19 (1964).
36. Hammerling, P., Teare, J. D., and Kivel, B., "Theory of Radiation from Luminous Shock Waves in Nitrogen," Phys. of Fluids, 2, 422 (1959).
37. Heaps, H. S., and Herzberg, G., "Intensity Distribution in the Rotation-Vibration Spectrum of the OH Molecule," Z. Physik, 133, 48 (1952).
38. Heims, S. P., "Moment Equations for Vibrational Relaxation with Dissociation," J. Chem. Phys., 38, 603 (1963).
39. Herman, R. C., and Shuler, K. E., "Intensities of Vibration-Rotation Bands," J. Chem. Phys., 21, 373 (1953), see also 22, 954 (1954).
40. Herzberg, Gerhard, Molecular Spectra and Molecular Structure, D. Van Nostrand Co. (1950).
41. Herzfeld, K. F., and Litovitz, T. A., Absorption and Dispersion of Ultrasonic Waves, Academic Press (1959).
- 41a. Hindelang, Franz J., "Coupled Vibration and Dissociation Relaxation Behind Strong Shock Waves in Carbon Dioxide," NASA TR R-253 (1967).

42. Hocker, L. O., Kovacs, M. A., Rhodes, C. K., Flynn, G. W., and Javan, A., "Vibrational Relaxation Measurements in CO₂ Using an Induced-Fluorescence Technique," *Phys. Rev. Letters*, 17, 233 (1966).
43. Holbeche, T. A., "Spectrum-Line-Reversal Temperature Measurements Through Unsteady Rarefaction Waves in Vibrationally Relaxing Oxygen," *Nature*, 203, 476 (1964).
44. Hurle, I. R., Russo, A. L., and Hall, G. J., "Spectroscopic Studies of Vibrational Nonequilibrium in Supersonic Nozzle Flows," *J. Chem. Phys.*, 40, 2076 (1964).
45. Hurle, I. R., and Russo, A. L., "Spectrum-line Reversal Measurements of Free-Electron and Coupled N₂ Vibrational Temperatures in Expansion Flows," *J. Chem. Phys.*, 43 4434 (1965).
46. Jackson, J. M., and Mott, N. F., "Energy Exchange Between Inert Gas Atoms and a Solid Surface," *Proc. Roy. Soc. London, Series A*, 137, 703 (1932).
47. Keck, James C., "Variational Theory of Reaction Rates," M.I.T. Fluid Mechanics Lab., Pub. no. 66-1 (1966).
48. Keck, J. C., and Carrier, G., "Diffusion Theory of Nonequilibrium Dissociation and Recombination," *J. Chem. Phys.*, 43, 2284 (1965) and also AVCO-Everett Res. Lab. Rept. 212 (1965).
49. Landau, L., and Teller, E., "Zur Theorie Der Schalldispersion," *Physikalische Zeitschrift der Sowjetunion* 10, 34 (1936).
50. Lockheed Missiles and Space Co. (no author listed) S-C 4020 Manual, L.M.S.C., Sunnyvale, Calif. (1965).
51. Lomax, Harvard, "Stable Implicit and Explicit Numerical Methods for Integrating Quasi-Linear Differential Equations with Parasitic-Stiff and Parasitic-Saddle Eigenvalues," NASA TN D-4703 (1968).
52. Lomax, Harvard, "On the Construction of Highly Stable, Explicit, Numerical Methods for Integrating Coupled Ordinary Differential Equations with Parasitic Eigenvalues," NASA TN D-4547 (1968).

53. Lomax, H., and Bailey, H. E., "A Critical Analysis of Various Numerical Integration Methods for Computing the Flow of a Gas In Chemical Non-equilibrium," NASA TN D-4109 (1967).
- 53a. Lomax, H., Bailey, H. E., and Fuller, F. B., "On Some Numerical Difficulties in Integrating the Equations for One-Dimensional Nonequilibrium Flow," NASA TN D-5176 (1969).
54. Lomax, Harvard, "An Operational Unification of Finite Difference Methods for the Numerical Integration of Ordinary Differential Equations," NASA TR R-262 (1967).
55. Lordi, J. A., Mates, R. E., and Moselle, J. R., "Computer Program for the Numerical Solution of Nonequilibrium Expansions of Reacting Gas Mixtures," Cornell Aeronautical Lab., Inc., CAL Rept. no. AD-1689-A-6 (1965).
56. Losev, A. S., and Osipov, A. I., "The Study of Nonequilibrium Phenomena in Shock Waves," Soviet Phys., Trans. 4, 525 (1962).
57. Maillie, F. H., and Hsu, C. T., "Coupled Vibrational and Chemical Relaxation for Harmonic and Anharmonic Oscillators," AIAA J. 6, 564 (1968).
58. Marrone, P. V., and Treanor, C. E., "Chemical Relaxation with Preferential Dissociation From Excited Vibrational Levels," Phys. Fluids, 6, 1215 (1963).
59. Mayer, J. E., and Mayer, M. G., Statistical Mechanics, John Wiley and Sons (1940).
60. McCubbin, T. K., Jr., Darone, R., and Sorrell, J., "Determination of Vibration-Rotation Line Strengths and Widths in CO₂ Using a CO₂-N₂ Laser," Appl. Phys. Letters, 8, 118 (1966).
61. Millikan, R. C., and White, D. R., "Vibrational Energy Exchange between N₂ and CO₂. The Vibrational Relaxation of Nitrogen," J. Chem. Phys., 39, 98 (1963).
62. Montroll, E. W., and Shuler, K. E., "Studies in Nonequilibrium Rate Processes. I. The Relaxation of a System of Harmonic Oscillators," J. Chem. Phys., 26, 454 (1957).

- 62a. Montroll, E. W., and Shuler, K. E., "The Application of the Theory of Stochastic Processes to Chemical Kinetics," *Advances in Chemical Physics* (Interscience Publishers, Inc., N.Y.), 1, 361 (1958).
63. Moretti, G., "A New Technique for the Numerical Analysis of Nonequilibrium Flows," *AIAA J.* 3, 223 (1965).
64. Nikitin, E. E., *Theory of Thermally Induced Gas Phase Reactions*, Indiana University Press, Bloomington and London (1966).
65. Nikitin, E. E., "The Vibrational Relaxation of Diatomic Molecules, *Proc. Acad. Sci., USSR (Phys. Chem. Sec.)* 124, 161 (1959).
66. Osipov, A. I., "The Relaxation of the Vibrational Motion of an Isolated System of Harmonic Oscillators," *Proc. Acad. Sci. USSR (AIP Eng. Tran.* 1960), 130, 523.
67. Osipov, A. I., and Stupochenko, E. V., "Non-Equilibrium Energy Distributions Over the Vibrational Degrees of Freedom in Gases," *Soviet Phys.*, 6, 47 (1963).
68. Pearson, W. E., and Baldwin, B. S., Jr., "A Method for Computing Non-equilibrium Channel Flow of a Multicomponent Gaseous Mixture in the Near-Equilibrium Region," *NASA TN D-3306* (1966).
69. Pearson, Walter E., "Channel Flow of Gaseous Mixtures in Chemical and Thermodynamic Nonequilibrium," *Phys. of Fluids*, 10, 2305 (1967).
70. Pritchard, H. O., "Shock Waves," *The Chem. Soc. London, Quarterly Reviews*, 14, 46 (1960).
71. Pritchard, H. O., "The Dissociation of Diatomic Molecules and the Recombination of Atoms," *J. Phy. Chem.*, 66, 2111 (1962).
72. Reinhardt, W. A., and Baldwin, B. S., Jr., "A Model for Chemically Reacting Nitrogen-Oxygen Mixtures with Application to Nonequilibrium Air Flow," *NASA TN D-2971* (1965).

- 72a. Rice, O. K., "On the Relation Between an Equilibrium Constant and the Nonequilibrium Rate Constants of Direct and Reverse Reactions," *J. Phys. Chem.*, 65, 1972 (1961).
- 72b. Rice, O. K., "Further Remarks on the Rate-Quotient Law," *J. Phys. Chem.*, 67, 1733 (1963).
73. Rich, Joseph William, "Dissociation and Energy Transfer in Diatomic Molecular Systems," Princeton U. Dissertation, Dept. of Aerospace and Mechanical Sciences (1965).
74. Rich, J. W., and Rehm, R. G., "Population Distribution During Vibrational Relaxation of Diatomic Gases," 11-th Sym (International), The Combustion Institute, pg. 37 (1967).
75. Rubin, R. J., and Shuler, K. E., "Relaxation of Vibrational Nonequilibrium Distributions: I. Collisional Relaxation of a System of Harmonic Oscillators," *J. Chem. Phys.*, 25, 59 (1956).
76. Rubin, R. J., and Shuler, K. E., "Relaxation of Vibrational Nonequilibrium Distributions: II. The Effect of the Collisional Transition Probabilities on the Relaxation Behavior," *J. Chem. Phys.*, 25, 68 (1956).
77. Rush, D. G., and Pritchard, H. O., "Vibrational Disequilibrium in Chemical Reactions," 11-th Sym (International) on Combustion, The Combustion Institute, pg. 13 (1967).
78. Russo, Anthony L., "Spectrophotometric Measurements of the Vibrational Relaxation of CO in Shock-Wave and Nozzle Expansion-Flow Environments," *J. Chem. Phys.*, 47, 5201 (1967).
79. Russo, Anthony L., "Importance of Impurities on Vibrational Relaxation Measurements in N₂," *J. Chem. Phys.*, 44, 1305 (1966).
80. Sebacher, Daniel I., "A Correlation of N₂ Vibrational-Translational Relaxation Times," *AIAA J.*, 5, 819 (1967).
81. Shuler, K. E., "Relaxation of an Isolated Ensemble of Harmonic Oscillators," *J. Chem. Phys.*, 32, 1692 (1960).

- 
82. Shuler, K. E., "On the Perturbation of the Vibrational Equilibrium Distribution of Reactant Molecules by Chemical Reactions," 7-th Symp. (Int.) on Combustion, The Combustion Institute, Butterworths, London, pg. 87 (1959).
 83. Shuler, K. E., "Studies in Non-Equilibrium Rate Processes. II. The Relaxation of Vibrational Non-Equilibrium Distributions in Chemical Reactions and Shock Waves," J. Phy. Chem., 61, 849 (1957).
 84. Shuler, K. E., "Vibrational Distribution Functions in Bimolecular Dissociation Reactions," J. Chem. Phys., 31, 1375 (1959).
 85. Snider, Neil S., "On the Theory of Rates of Dissociation and Recombination of Diatomic Molecules," Frick Chemical Lab., Princeton U., Rept. no. TR-5 (1964).
 86. Stupochenko, Ye. V., Losev, S. A., and Osipov, A. I., Relaxation in Shock Waves, Springer-Verlag, N.Y., Inc. (1967).
 87. Taylor, David K., "Theory of the Effects of Electronic Excitation on the Vibrational and Dissociative Relaxation of Diatomic Molecules," U.S. Naval Ordnance Lab., White Oak, Maryland, NOLTR (65-213) (1966).
 88. Taylor, R. L., Camac, M., and Feinberg, R. M., "Measurements of Vibration-Vibration Coupling in Gas Mixtures," 11th Symp. (International) on Combustion, the Combustion Institute, p. 49 (1967).
 89. Tirumalesa, Duvvuri, "Nozzle Flows with Coupled Vibrational and Dissociational Nonequilibrium," University of Toronto, UTIAS Rept. no. 123 (1967).
 90. Treanor, C. E., and Marrone, P. V., "Vibration and Dissociation Coupling Behind Strong Shock Waves," Symposium on Dynamics of Manned Lifting Planetary Entry, Philadelphia, Penn., Oct. 29-31, 1962, John Wiley and Sons, pg. 160 (1963).
 91. Treanor, Charles E., "Vibrational Relaxation Effects in Dissociation Rate-Constant Measurements," Cornell Aeronautical Lab. CAL Rept. no. AG-1729-A-1 (1962).

92. Treanor, Charles E., "Molecular Vibrational Energy Distributions During Exchange-Dominated Relaxation," Cornell Aeronautical Lab. CAL Rept. no. AF-2184-A-1 (1966).
- 92a. Treanor, C. E., Rich, J. W., and Rehm, R. G., "Vibrational Relaxation of Anharmonic Oscillators with Exchange-Dominated Collisions," J. Chem. Phys., 48, 1798 (1968).
93. Treanor, C. E., and Marrone, P. V., "Effect of Dissociation on the Rate of Vibrational Relaxation," Phys. of Fluids, 5, 1022 (1962).
94. Treanor, Charles E., "Coupling of Vibration and Dissociation in Gas-Dynamic Flows," AIAA paper no. 65-29 (1965).
95. Treanor, Charles E., "A Method for the Numerical Integration of Coupled First-Order Differential Equations with Greatly Different Time Constants," Math. Comput., 20, 39 (1966), also CAL Rept. no. AG-1729-A-4 (1964).
96. Tyson, T. J., "An Implicit Integration Method for Chemical Kinetics," Thompson Ramo Wooldridge Inc., Rep. 9840-6002-RU00 (1964).
97. Vincenti, W. G., and Kruger, C. H., Jr., Introduction to Physical Gas Dynamics, John Wiley and Sons (1965).
98. Von Rosenberg, C. W., Jr., "Vibrational Relaxation of Carbon Monoxide in Non-Equilibrium Nozzle Flow," Ph.D. thesis, the U. of Oklahoma Graduate College (1968).
99. Wray, Kurt L., "Shock-Tube Study of the Coupling of the O₂-Ar Rates of Dissociation and Vibrational Relaxation," J. Chem. Phys., 37, 1254 (1962).
100. Zel'dovich, I. B., and Raizer, Yu. P., Physics of Shock Waves and High-Temperature Hydrodynamic Phenomena, vols. 1 and 2, Academic Press (1966).
101. Zelechow, A., Rapp, D., and Sharp, T., "Vibration-Vibration-Translation Energy Transfer Between Two Diatomic Molecules," J. Chem. Phys., 49, 286 (1968).